STUDY OF ZERO-GRAVITY POSITIVE EXPULSION TECHNIQUES

REPORT NO. 8230-933004

JUNE 1963

CR-50,774

FOREWORD

Presented in this report are the results of a study conducted by the Bell Aerosystems Company during the period 16 April 1962 through 15 February 1963. This work was authorized by Contract NAS7-149 for the National Aeronautics and Space Administration under the administration of NASA's Western Operations Office.

Mr. Frank E. Compitello of NASA Headquarters, Washington, D.C., was the Project Manager and Mr. Richard N. Porter of the Jet Propulsion Laboratory was the Technical Manager of the program.

Principal contributors to this report are:

L. Thompson - Analysis and Evaluation of Metallic Devices
I. DePuy - Structural Investigation
V. Daniels - Dynamic Investigation
W. Walters - Permeability

Approved: Kurt Berman
K. Berman
Assistant Chief Engineer
Design and Development/Rockets

R.F. Goerke
R.F. Goerke
Program Manager

SUMMARY

This report summarizes the results of a 10-month program conducted by the Bell Aerosystems Company to fulfill three prime objectives:

(1) To evaluate metallic positive expulsion devices applicable to rocket propulsion systems.

(2) To conduct design and integration analyses of the expulsion device considered to offer the highest potential for application to manned space flight and for which a broad base of engineering design data were lacking and not in the process of being generated under any other known program.

(3) To design, build, and evaluate an apparatus to measure propellant permeation rates through typical non-metallic materials used in positive expulsion devices. The test data, capable of being generated in the apparatus, were to possess direct applicability to conditions existing in positive expulsion tank systems.

A complete evaluation of the state-of-the-art covering all conceivable methods of achieving positive expulsion in zero-gravity or negative-acceleration fields was undertaken by Bell Aerosystems during a previous NASA study effort (NASr-44) and was continued and expanded during the present program (NAS7-149). Work on both contracts was supplemented by an industry-wide survey of expulsion devices. Summary sheets covering the characteristics and the development status of the various devices are included in Appendices I and II of this report. Based upon the investigations detailed in this report, it was established that a substantial body of engineering design and tank integration data were already in existence, or were being gathered both for non-metallic expulsion devices and for non-conventional systems such as those using surface forces, dielectrophoresis, and acoustics. On the other hand, the existing body of engineering data covering metallic expulsion devices was found to be rather meager. However, metallic expulsion devices offer greater potential for manned space flight because of their ability to withstand a wider range of operating temperatures and radiation dosages than non-metallic systems. Moreover, metallic expulsion devices are compatible with almost the complete spectrum of known rocket propellants, with attendant negligible permeation. Metallic bladders, bellows, piston type tanks, and convoluted diaphragms were evaluated from an overall application standpoint. Although, obviously, the optimum system for a given application can be established only when the specific mission requirements are established (for example, whether or not multiple complete expulsion cycles are required), it was concluded that, for the broadest range of applications, positive expulsion systems employing metallic bellows merit primary consideration. Although bellows technology is quite old, the application of bellows in a flight-type positive expulsion device imposes considerations that are completely outside the realm of

established knowledge. The necessity for minimization of weight and optimization of volumetric and expulsion efficiencies requires both minimum bellows metal thicknesses and operation in the plastic deflection range (extended to lengths 10 times greater than the nested length). Superimposed on this is the necessity to integrate the bellows into the tank and to make the unit capable of withstanding mission requirements such as vibration and shock. It was, therefore, decided to conduct analyses and investigations to generate engineering design data for welded bellows and their integration into positive expulsion units. Obviously, the first step in such an undertaking is the establishment of the tools to accomplish this objective and to appraise their adequacy in the light of experimental data. The two primary tools required are (1) a structural program to predict the composite stresses developed during operation so that factors such as convolution leaf shape and thickness distribution can be appraised and (2) a dynamic program to predict vibrational mode characteristics and their effect on stresses, bellows configuration, and integration and assembly characteristics.

During this effort, a structural program based upon Reissner's shell theory was written and brought to operational status. This program is rather unique in that it enables the engineer to analyze rapidly the effects of large geometric deflections on stresses. This program, although applicable also to other positive expulsion devices such as metallic diaphragms, has been specifically related to the study of welded bellows configurations. It is anticipated that, during a scheduled follow-on program, some of the restrictive assumptions such as axisymmetrical loading and operation within the elastic limit can be removed. An analysis to predict the dynamic characteristics of bellows has been established and has been complemented by original experimental data. Also discussed are methods for bellows design which have proved successful in alleviating the deleterious conditions encountered during shock and vibration. A component and assembly investigation was also conducted to establish fabrication and operational characteristics of bellows-type expulsion.

An apparatus for obtaining permeation rates of rocket propellants through typical expulsion device materials was designed, built, and tested. To approximate the conditions of an actual expulsion unit as closely as possible, the total pressure across the material under test in the permeation apparatus is kept constant. Evaluations were made of various types of detectors capable of increasing the measuring sensitivity of the apparatus.

CONTENTS

Section		Page
1	INTRODUCTION	1
2	ANALYSIS AND EVALUATION OF METALLIC DEVICES	3
	A. RELIABILITY	3
	1. Metal Bladder	3
	2. Piston with Metallic Seals	7
	3. Metal Bellows	7
	B. CYCLE LIFE	7
	1. Metal Bladder	7
	2. Piston and Metal Bellows	7
	C. CYCLIC OPERATION	7
	1. Metal Bladder and Piston	7
	2. Metal Bellows	9
	D. WEIGHT	9
	1. Metal Bladder	9
	2. Piston	9
	3. Metal Bellows	9
	E. LEAKAGE	9
	1. Metal Bladder and Bellows	9
	2. Piston	9
	F. VOLUMETRIC EFFICIENCY	10
	1. Metal Bladder	10
	2. Metal Bellows	10
	G. EXPULSION EFFICIENCY	10
	1. Metal Bladder	10
	2. Piston and Metal Bellows	10
	H. Δ P VARIATION	10
	1. Metal Bladder	12
	2. Piston	12
	3. Metal Bellows	12
	I. STORAGE	12
	1. Metal Bladder and Bellows	12
	2. Piston	12
	J. DYNAMICS	13
	K. DISCUSSION	13
3	STRUCTURAL INVESTIGATION	15
4	DYNAMICS INVESTIGATION	31
	A. PURPOSE AND OBJECTIVES	31
	B. LITERATURE SURVEY	31

CONTENTS (Cont)

Section		Page
	C. ACCORDION MODE ANALYSIS	32
	1. Solution for Accordion Modes	32
	2. Development of Stiffness Matrix	34
	D. APPLYING IBM 7090 PROGRAM 1692 TO A BELLOWS	37
	1. Weight Matrix Development	37
	2. Stiffness Matrix Development	39
	E. SIMPLIFIED FREQUENCY DETERMINATION OF ACCORDION MODES	40
	F. SIMPLIFIED FREQUENCY DETERMINATION OF LATERAL MODES	42
	1. Incremental Circumferential Spring Analogy	42
	2. Handbook Formula Adaption	47
	G. CORRECTION OF LATERAL FREQUENCIES FOR AN INTERNAL PRESSURE	48
	H. OTHER RESONANT CONDITIONS INVESTIGATED	51
	I. RESONANT FREQUENCY OF A LEAF	51
	J. LONGITUDINAL LIQUID DISPLACEMENT MODES	54
	K. CALCULATION OF THE 4-INCH BELLOWS RESPONSE DURING VIBRATION	57
	1. Lateral Mode without Pressure	58
	2. Lateral Mode with Increased Internal Liquid Pressure	59
	L. SPRING RATE	60
	M. VIBRATION TESTING OF 4-INCH BELLOWS	64
	1. Sinusodial Vibration Tests	64
	2. Longitudinal Vibration	64
	N. INTERNAL AND EXTERNAL PRESSURE EFFECTS ON ACCORDION MODE RESPONSE	75
	O. ACCORDION MODE ATTENUATION	80
	P. LATERAL VIBRATION OF 4-INCH BELLOWS	80
	Q. VIBRATION TESTS OF 9-INCH BELLOWS ASSEMBLY	85
	1. Longitudinal Vibration Tests	85
	2. Lateral Vibration Tests	91
	3. Discussion of Test Results	91
5	COMPONENT AND ASSEMBLY INVESTIGATION	101
	A. BELLOWS ASSEMBLY DESIGN	101
	B. DIAPHRAGM CONFIGURATION	103
	C. UNSTABLE OPERATION	103
	D. FABRICATION SEQUENCE	105

CONTENTS (Cont)

Section		Page
	E. VOLUME CALCULATION	105
6	PERMEABILITY	109
	A. SYNOPSIS	109
	B. GENERAL	109
	C. THEORY AND BACKGROUND	111
	D. PERMEATION TEST APPARATUS	114
	E. PERMEATION TEST WORK	114
	F. EVALUATION OF ANALYTICAL TECHNIQUES	130
	1. Karmen Type Voltage Breakdown Detector	136
	2. Thermistor or Thermal Conductivity Detector	139
	3. Cross-Section Detector	139
	G. CONCLUSIONS	142
	H. FUTURE WORK	144
7	REFERENCES	147

APPENDIX

I.	Summary of Positive Expulsion Devices	155
II.	Summary of Positive Expulsion Devices (Previous Contract NASr-44)	191
III.	Discussion of Structures Computer Program	265
IV.	Operating Instructions for Bellows-Type Permeation Apparatus	283
V.	Glossary	301

ILLUSTRATIONS

Figure		Page
1	Evaluation of Positive Expulsion/Orientation Devices	4
2	Double Convoluted Metallic Diaphragm	5
3	Four-Mil Electrodeposited Nickel Alloy Bladder	8
4	ΔP Variation	11
5	Typical Bellows for Axial Thrust Solution	18
6	Effect of Number of Finite Points (M) on Longitudinal and Circumferential Stress Calculated with Computer Program 1753	19
7	Effect of Six-Leaf Analyses on Longitudinal Stress of Case I	21
8	Longitudinal Bending Near Fixed Support of Cylinder Under 1 psi Internal Pressure	23
9	Test Case IIP	24
10	7-1/8 Test Bellows Deformation at 16.9 lb Thrust	26
11	7-1/8 Test Bellows Deformation at 0.41 lb/in.^{2} Internal Pressure	27
12	Computed Stresses in 3rd Leaf of 7-1/8 Bellows at 16.9 lb Thrust	28
13	Computed Stresses in 3rd Leaf of 7-1/8 Bellows at 0.41 lb/in.^{2} Pressure	29
14	Mathematical Model of Bellows	38
15	Trapped Liquid in Bellows	39
16	Calculated 7-Inch Bellows Accordion Modes	41
17	Simple Beam	41
18	Pure Moment Applied to Segment of Simple Beam	43
19	Bellows Represented as a System of Concentrated Masses Connected by Massless Springs Around the Circumference	43
20	Pure Moment Applied to Segment of Bellows	43
21	Segments of Bellows Showing Massless Springs	44
22	Segment of Bellows Showing Massless Springs in Deflected Position	45
23	Bellows Distortion with Internal Pressure	50
24	Liquid Displacement Mode	55
25	Lateral Resonant Frequency versus Internal Water Pressure of a 4-Inch Diameter Bellows	62
26	Hysteresis Curve	63
27	Frequency versus Length Curve	65
28	100-Convolution Bellows in Pyrex Pipe	66
29	Center Convolution Response with Head Fixed	67
30	Head Dynamic Pressure with Head Fixed	68
31	Base Dynamic Pressure with Head Fixed	69

ILLUSTRATIONS (CONT)

Figure		Page
32	Center Convolution Response with Head Free	70
33	Head Dynamic Pressure with Head Free	71
34	Base Dynamic Pressure with Head Free	72
35	Head Response with Head Free	74
36	Liquid Displacement Mode of 7-Inch Bellows Compared to Third Harmonic Accordion Model	76
37	7-Inch Diameter Model Bellows	77
38	Fundamental Accordion Mode of 7-Inch Diameter Bellows	78
39	Fundamental Liquid Displacement Mode of 7-Inch Diameter Bellows	79
40	Response of Center Convolution with 3-Ring Baffles Installed Inside Bellows with Head Free	81
41	Installation of Ring Baffles	82
42	Lateral Vibration Setup	83
43	Center Convolution Lateral Response During Vibration with Head Clamped	84
44	Center Convolution Lateral Response During Vibration with Head Free	86
45	Center Convolution Longitudinal Response During Vibration with Head Free	87
46	Longitudinal Vibration Test of 9-Inch Bellows	88
47	Accordion Mode of Bellows	89
48	Fundamental Accordion Mode at 73 cps	90
49	Liquid Displacement Mode at 139 cps	92
50	Low Frequency Vibration Test of 9-Inch Bellows	93
51	Lateral Vibration Test of 9-Inch Bellows	94
52	Deflection-Pressure Curve for 9-Inch Bellows	95
53	Force versus Deflection Curves	102
54	Overlay of Deformation	104
55	Actual Volume versus Calculated Volume	107
56	Permeability Apparatus Assembly	115
57	Upper Bellows Flange	116
58	Mounting Flange	117
59	Top Cover	118
60	Body	119
61	Bottom Cover	120
62	Gaskets	121
63	Permeability Apparatus Mounted on Infrared Unit	122
64	Permeability Apparatus Mounted on Wooden Stand	123
65	Permeability Apparatus Disassembled	124

ILLUSTRATIONS (CONT)

Figure		Page
66	Flow Schematic of Permeation Test Apparatus	125
67	Calibration Curve for $N_2O_4 \rightleftharpoons 2NO_2$	126
68	Total Permeation versus Time	128
69	Permeation Rate versus Time	129
70	Comparison of Permeation Test Data	131
71	Flow Sheet for Test Apparatus	132
72	Sketch of Test Assembly	133
73	Results of Detector Evaluation	135
74	Karmen Detector	137
75	Karmen Voltage Breakdown Detector	138
76	Thermal Conductivity Detector Circuits	140
77	Cross-Section Detector	141
78	Proposed Sampling Techniques for Atmospheric Pressure Analysis	143
79	Proposed Design of Permeation Chamber	145

TABLES

Number		Page
1	Summary of Positive Expulsion Devices	6
2	Vibration Test Results	33
3	Leaf Frequency Summary	53
4	Lateral Frequency Calculation	61

SECTION 1

INTRODUCTION

The requirement for multi-cycle capability of a positive expulsion device has, until recently, been satisfied by employing bladders or diaphragms fabricated from plastics and elastomers. A re-examination of these more classical methods has become necessary due to the stringent operating requirements involved in long-term orbital missions or in spacecraft applications.

These requirements, imposed in a space environment, include operation through a wide temperature range and exposure to high-level radiation. The positive expulsion device must also exhibit low permeation and diffusion rates through the gas-liquid barrier, compatibility with selected propellants, and the reliability associated with manned spacecraft applications, combined with high expulsion and volumetric efficiencies. Selection of an operating device to fulfill these criteria generally precludes the use of organic materials and has prompted this investigation of metallic devices.

Section 2 of this report presents the results of a design study to evaluate the pertinent devices and to select the one considered to have the greatest potential. The selection was based upon a review of the state-of-the-art, supplemented by data available from current programs and a parametric analysis of the three most promising metallic devices within state-of-the-art capability.

As a result of this analysis, the welded metal bellows was selected and a study of the structural and dynamic aspects of this device was conducted. The results of the study are presented in Sections 3 and 4. Supporting data and the computer program developed for the structural analysis are given in Appendix III.

In support of the over-all study of positive expulsion devices, a component and assembly investigation provided a frame of reference by determining size limitations, fabrication processes, and operating characteristics of the bellows device. Results of this study are discussed in Section 5.

Appendix I presents a summary of positive expulsion devices compiled from an extensive survey of the industry and the literature. To enhance the usefulness of this report, the results of a similar survey, previously conducted under Contract NASr-44, are presented in Appendix II.

The permeation work conducted under the present contract is discussed in Section 6. Instructions for operating the bellows-type permeation apparatus designed and fabricated during this program are presented in Appendix IV.

SECTION 2

ANALYSIS AND EVALUATION OF METALLIC DEVICES

A program of analysis and evaluation of metallic positive expulsion devices was conducted to select the device or devices which indicated the greatest potential for manned spacecraft application. This work included a review of the positive expulsion technology at Bell Aerosystems and in the industry. As such, it included a survey of current programs at Bell which could be considered as contributing to the status of this technology. The work was definitized by a parametric comparison resulting from a design study conducted to select the most efficient metallic expulsion device for cylindrical tank application.

With reference to Figure 1, the expulsion devices considered are shown diagramatically with the source program indicated. Model 8173 refers to Air Force contract AF04(611)-8183, Maneuvering Satellite Propulsion System Demonstration, awarded to Bell Aerosystems in May 1962. One of the tasks on this program includes a feasibility study, design, and fabrication of a double-convoluted metallic disphragm for a spherical propellant tank (see Figure 2). A description of this device is included in a summary sheet in Appendix I.

Other devices mentioned in Figure 1 and generally classed as orientation or pooling devices are being studied under Air Force Contract AF04(611)-8200 (Model 8219), awarded to Bell Aerosystems in June 1962. Included in this work are electromagnetic devices, capillary tubes, exploding wires, and foaming plastics. These devices are considered beyond the state-of-the-art and, thus, beyond the scope of this program. The Phase I Progress Report for work accomplished on Contract AF04(611)-8200 was published in December 1962. This report, SSD-TDR-62-172, is entitled "Development of Expulsion and Orientation Systems for Advanced Liquid Rocket Propulsion Systems". Two devices selected for continued study in Phase II of Contract AF04(611)-8200 are the surface force technique and dielectrophoresis. Summary sheets for these methods are included in Appendix I of this report.

The expulsion devices under Model 8500 include the more-classic concepts in metallic devices. The Bell-sponsored work involved a complete design study and analysis. The results of this work are summarized in Table 1, together with an explanation of the parametric comparisons.

A. RELIABILITY

1. Metal Bladder

The establishment of the reliability for a metal bladder is considered poor since the operating life of a collapsing bladder is one cycle. Reliability testing

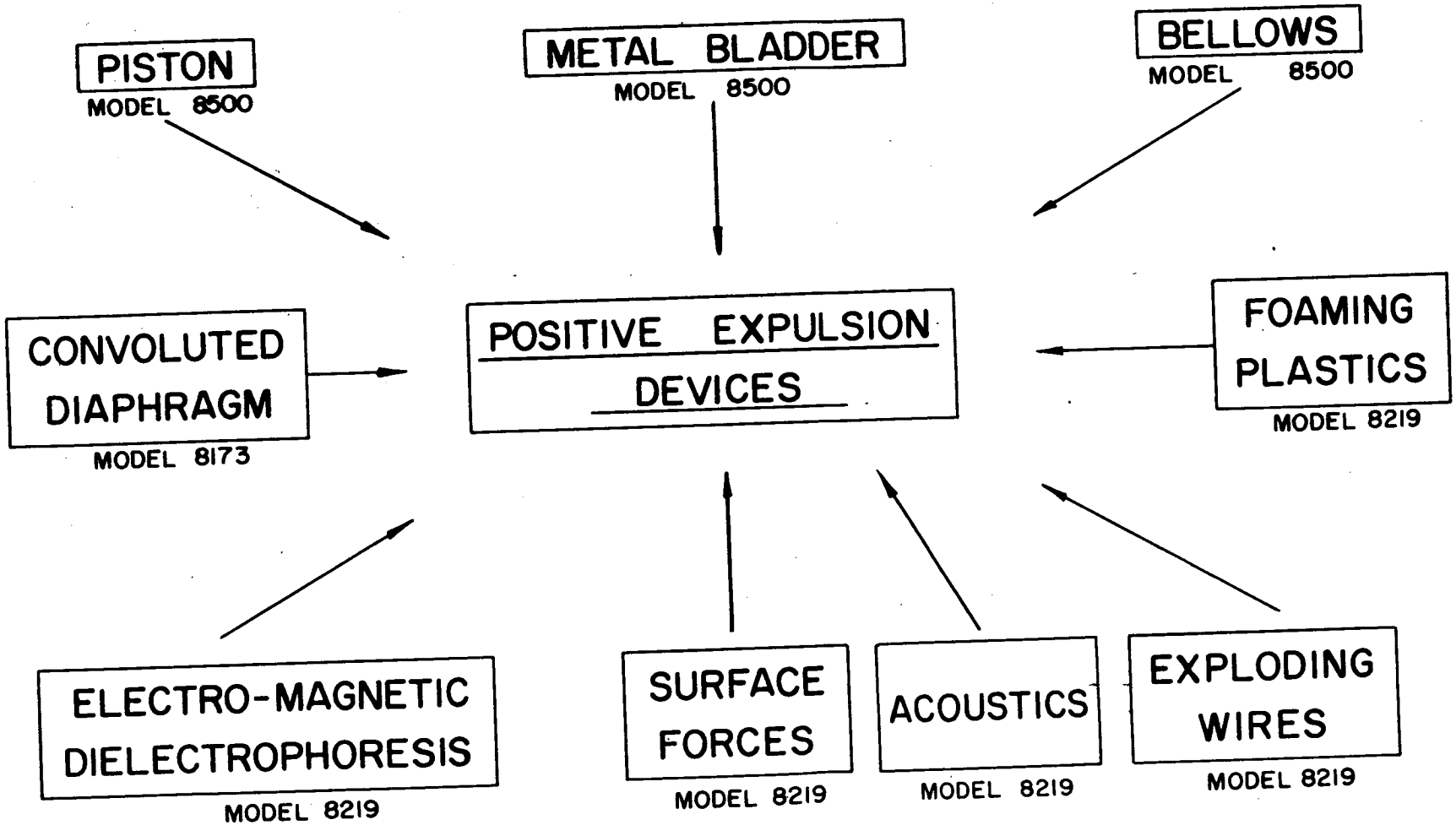

Note: Model 8500 Refers to Bell-Sponsored Programs

Figure 1. Evaluation of Positive Expulsion/Orientation Devices

Figure 2. Double Convoluted Metallic Diaphragm

TABLE 1

SUMMARY OF POSITIVE EXPULSION DEVICES

	METAL BLADDER	PISTON	BELLOWS
Reliability	Poor	Excellent	Excellent
Life Cycles	One	200+	200
Cyclic Operation	Poor	Poor	Good
Weight	13.8	19.3	25.9
Leakage	Zero	High	Zero
Volumetric Efficiency	Good	Good	Good
Expulsion Efficiency	97.5%	98% plus	98% plus
$\triangle P$ Variation	7.5 max.	34 psi (9.25)	3.1 psi
Storage	Good	Poor	Good
Dynamics			
Sinusoidal and Random Vibration (5 to 3000 cps)	Critical	Good	Questionable
Low-Frequency Vibration (Slosh) (0.1 to 10 cps)	Semi-critical	Good	Good
Acceleration	Good	Good	Good
Shock	Good	Good	Good
Pressure Surge	Questionable	Good	Questionable

would be accomplished by performing single expulsions on a series of bladders; however, no testing could be accomplished on the deliverable item to preclude random failures because even partial expulsions will cold-work the material and increase the possibility of leakage in over-stressed areas.

2. Piston With Metallic Seals

An expulsion system incorporating a piston with metallic seals is rated excellent because a piston arrangement is basically a multiple-cycle device. After fabrication, the piston would be installed in the tank and a "run-in" period consisting of a number of expulsion cycles would be necessary to increase sealing efficiency. The use of non-metallic seals would reduce reliability since there is a possibility of "shredding" which could allow excessive leakage.

3. Metal Bellows

The bellows is considered the most reliable device since it can be programmed for multicycle testing on a selected number of units to qualify a design, and then random failures screened out from deliverable units by cycling during acceptance testing.

B. CYCLE LIFE

1. Metal Bladder

The fold pattern assumed by a bladder under the differential pressure required for expulsion causes highly stressed areas at the resulting small bend radii. An attempt to re-cycle these overstressed and work-hardened areas will result in structural failure. Figure 3 shows the fold pattern resulting from one expulsion with an electro-deposited nickel alloy bladder with a 0.4-inch wall fabricated for and tested by the Bell Aerosystems Company.

2. Piston and Metal Bellows

The piston device and the bellows assembly have demonstrated efficient and reliable multicycle operation.

C. CYCLIC OPERATION

Cyclic operation refers to the on-off short-duration expulsions with fast predictable response characteristics; normally a requirement for a reaction control system.

1. Metal Bladder and Piston

Neither the metal bladder nor the piston effectively provide cyclic operation; the bladder is ineffective because of inertia forces resisting collapse and the high differential pressure requirements to collapse compound folds; the piston is

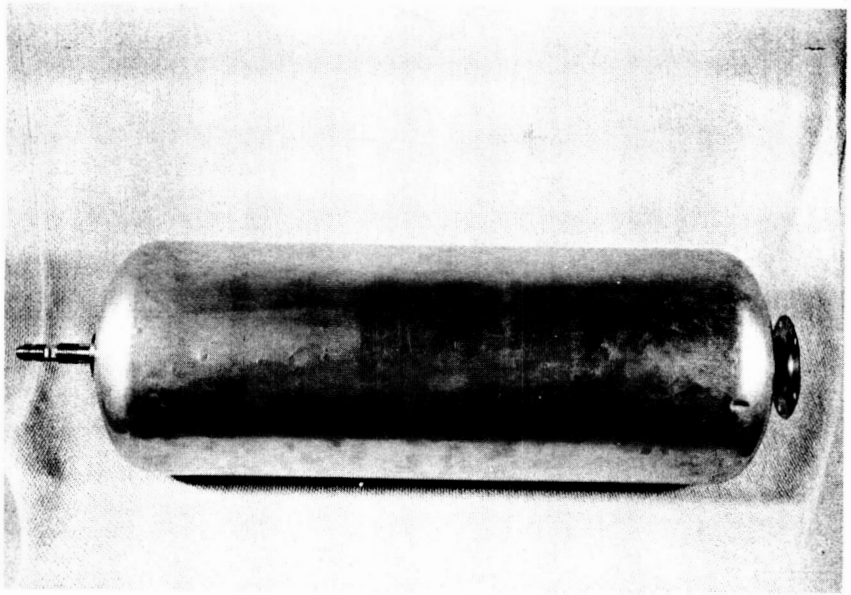

Before Test

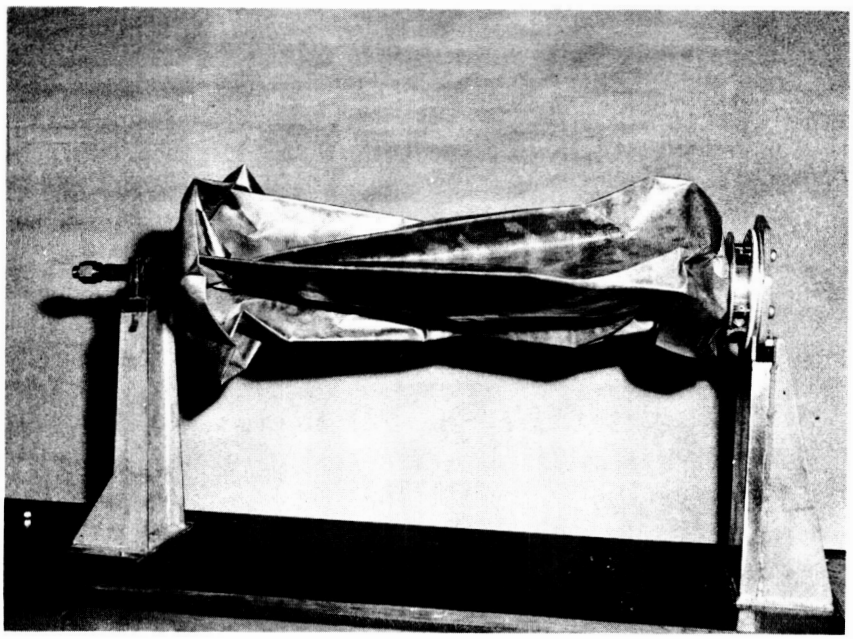

After Test

Figure 3. Four-Mil Electrodeposited Nickel Alloy Bladder

ineffective because of break-away friction between the seals and tank wall resulting in slow response characteristics.

2. Metal Bellows

The bellows has demonstrated response times comparable to a pressurized tank without a positive expulsion device so that cyclic operation is essentially a function of valve operation.

D. WEIGHT

The weight values, shown numerically to give a better comparison, refer to the complete system weight (tank and expulsion device) for a cylindrical tank with a loadable propellant requirement of 2900 cu in., a length of 46 in., and an O.D. of 10 in. maximum.

1. Metal Bladder

Because of its simplicity, the metal bladder device has a considerable weight advantage, even including the necessary diffuser tube. The weight shown is for a 0.004-in., 1100 aluminum alloy bladder.

2. Piston

Because the piston device requires a center guide with additional seals and a greater tank wall thickness for rigidity, it weighs approximately one-third more than the metal bladder system.

3. Metal Bellows

A metal bellows system, fabricated from 0.006-in. 347 stainless steel, has a weight value approximately equal to the piston tank.

E. LEAKAGE

1. Metal Bladder and Bellows

The welded construction design of the metal bladder and bellows devices provides for zero leakage because there are no mechanical seals and no diffusion nor permeation.

2. Piston

Leakage through the piston seals will vary, depending upon the efficiency of the design and the quality of the seals.

The break-away friction of metal seals prevents the piston from floating to compensate for differential pressures. The magnitude of this frictional force, equivalent to 34 psi in this design, would encourage leakage through the seals. With plastic seals, the problem is increased with diffusion and permeability through the plastic material and negates some of the advantages of a metallic device.

F. VOLUMETRIC EFFICIENCY

The volumetric efficiency refers to the loss of tank volume due to the incorporation of the positive expulsion device.

1. Metal Bladder

The volumetric efficiency of the piston tank assembly is reasonably good (about 92%) in comparison to the bladder design.

2. Metal Bellows

The bellows tank assembly, with a design that permits nesting outside of the propellant envelope, has a volumetric efficiency equivalent to the piston design. This is also a function of the number of convolutions and the span.

G. EXPULSION EFFICIENCY

Expulsion efficiency is defined as the ratio of the amount of propellant loaded to the amount of propellant expelled.

1. Metal Bladder

Because of its erratic fold pattern, the bladder tank assembly can trap propellant in folds and will not always exhibit an expulsion efficiency as high as the 97.5 percent shown in Table I. The hollow diffuser tube assembly will always contain propellant that cannot be expelled.

2. Piston and Metal Bellows

Both the piston and bellows assemblies have an expulsion efficiency in excess of the normal requirement of 98 percent. Except for the small amount of propellant trapped in the piston seals and between leafs of the bellows assembly when nested, essentially all propellant can be expelled.

H. ΔP VARIATION

The ΔP variation is a measure of the pressure drop through the tank assembly and is normally measured at the gas inlet port and the propellant discharge port. The numerical values shown are for comparison only and refer to a propellant flow of approximately 0.9 cu ft/min (0.728 lb/sec at S.G. = 0.796). See Figure 4.

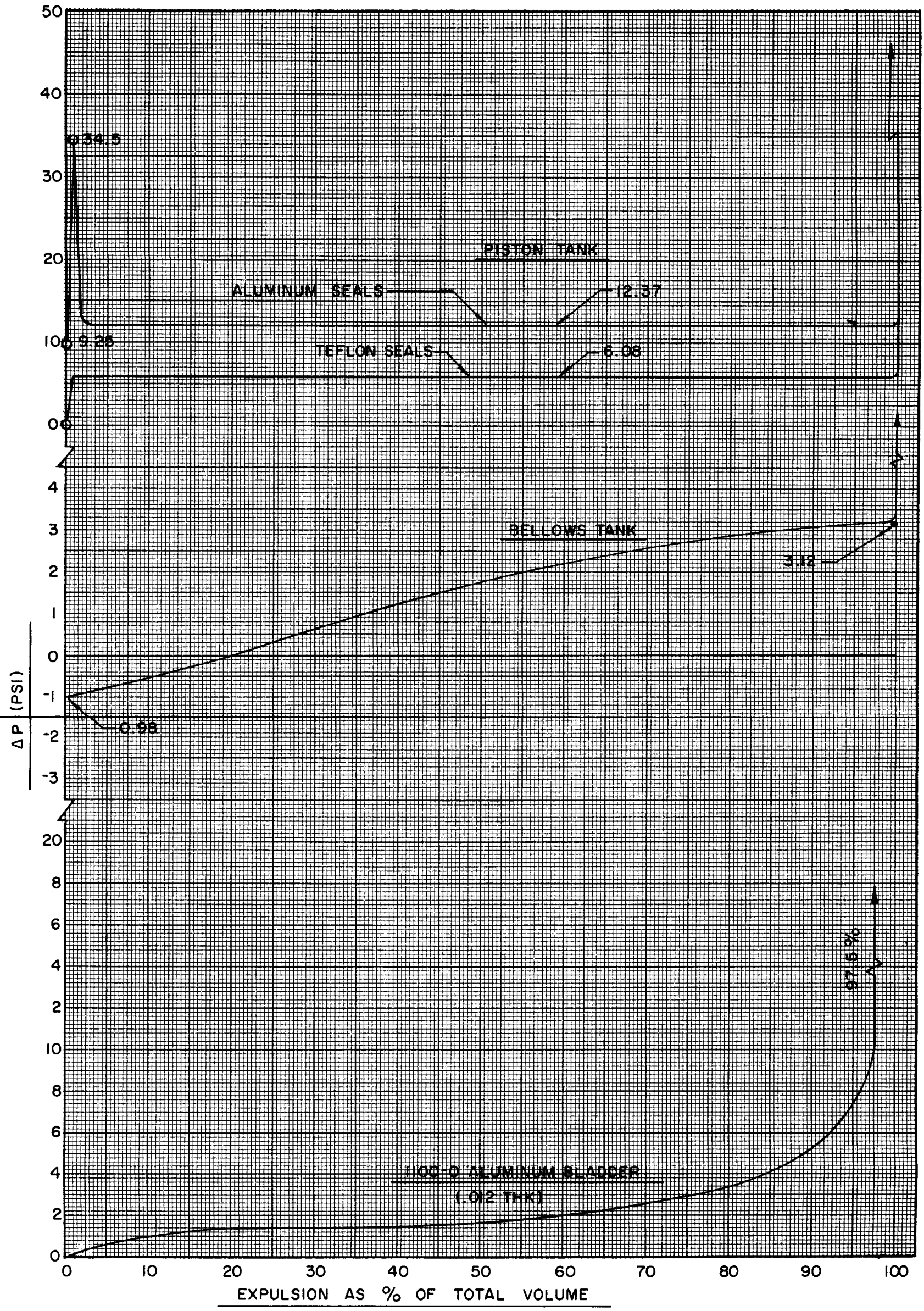

Figure 4. Δ P Variation

1. Metal Bladder

The ΔP curve, when plotted as a function of percent of total propellant expelled for the bladder assembly, exhibits a constant trace for the major portion of the expulsion cycle. As the fold pattern assumes compound shapes, the ΔP rises sharply at approximately 90 percent and continues in an irregular trace to a ΔP equivalent to total tank pressure.

2. Piston

In considering the pressure drop peculiar to a piston tank assembly, the type of seals must be considered separately because the influence of wall friction is great. With metallic seals, the ΔP trace peaks on start because of the high break-away friction encountered, and then drops to a constant trace which continues to complete expulsion. Plastic seals have a lower break-away friction than running friction and, in each case, is lower than the metallic seals.

3. Metal Bellows

The differential pressure trace for the bellows assembly includes the hydraulic drop plus the spring rate of the bellows device. With the liquid loaded inside the bellows, the spring rate will assist the liquid expulsion and, thus, reduce the total ΔP to a value less than zero. At the free length position of the bellows, the spring rate is zero and increases to the value required to nest the bellows at complete expulsion. The spring rate component of the total differential pressure amounts to approximately -2.5 psi at full extension to a +2.5 psi at the nested position.

I. STORAGE

Storage in this concept refers to storage in space with intermittant operation of the system over extended periods of time.

1. Metal Bladder and Bellows

Both the bladder and the bellows assemblies lend themselves ideally to space storage. The zero leakage capability of each assembly provides for unlimited storage life.

2. Piston

The inherent leakage associated with any mechanical seal, together with a wide range of temperature environment, indicates a poor storage capability. Additionally, plastic seals present permeability problems and are susceptible to damage from high-level radiation.

J. DYNAMICS

The characteristics of each device when exposed to dynamic environment are discussed in Section 4 and Appendices I and II. The items for which no supporting test data are available are marked "questionable."

K. DISCUSSION

On the basis of the foregoing summary of the analytical study performed on metallic expulsion devices for cylindrical tanks and supporting test data, the bellows assembly proved to be the preferred method for additional study and development. Its potential as a device with particular application for manned flight is evident when compared with other devices in a parametric analysis. The weight penalty incurred can be partly offset by removal of system safety components such as check valves. This analysis has indicated the welded metal bellows offer distinct advantages in the following areas:

(1) High, reliable cycle life

(2) Low and predictable ΔP

(3) Zero leakage and long storage life

(4) High volumetric and expulsion efficiencies

(5) Excellent response characteristic for cyclic operation.

Additional advantages also include those which are common to all metallic devices of welded construction:

(1) Absence of permeation, diffusion, and seal leakage

(2) Resistance to damage from high-level radiation

There are additional merits to a bellows device that are beyond the scope of this analysis but must be considered in the selection of propellant system. These include costs, ease of fabrication, cleaning, filling and draining methods, and system compatibility. In each of these areas, the bellows system has demonstrated advantages over the other expulsion devices.

The design criteria adhered to in the Model 8500 preliminary designs (see Figure 1) reflect the limitations imposed by the lack of supporting test data to extend the design limits of a bellows device. Recognizing these limitations, the design was optimized to accommodate the required propellant capacity within the specified envelope. The resultant bellows assembly incorporated 6-mil stainless steel diaphragms with a span of 0.5 inches and a design pitch of 0.3 inches. Utilizing a ripple design for the best nesting characteristics provided for a stacked height of 0.018 inches per convolution, with a resultant travel of 0.282 inches per convolution.

SECTION 3

STRUCTURAL INVESTIGATION

The objective of the structural subtask may be defined as the development of an analytical method capable of predicting the stress-deflection relationships for welded bellows. The method must accommodate any bellows geometry forming a surface of revolution. Because of its application to expulsion devices, the method must include the effects of large deflections to a degree that would allow practical study of the effects of geometric variations on stresses and deflections.

Methods that employ the usual text-book formulas based upon small deflection shell or plate theories are not applicable to large deflection. Available computer programs involve the matrix displacement approach to the analysis of discrete element structural idealizations. However, the necessary nonlinearization of such programs, when completed, will produce a program requiring large amounts of computer time.

Because of limitations imposed by the state-of-the-art of stress analysis, certain compromises to the actual expulsion bellows problem are necessary. The nature of the actual problem, as outlined elsewhere in this report, may vary from small elastic deflections for an extended life to large inelastic deflections for limited life. Because of the tendency of the outer diameter of a bellows to be drawn inward during extension, compression hoop stresses are also introduced which may produce any one of several types of structural instability.

When diaphragm deflections are very small (approximately one-half the thickness), stresses are largely due to the bending action. As deflections increase, the diaphragm midplane length changes such that membrane forces become significant and may no longer be neglected. As deflections increase further, the diaphragm undergoes distortion of its original shape to such a degree that this effect must be taken into account in the analysis. The effect of distortion is to change the relationship of load to deflection as deflection changes, producing a load-deflection curve in the elastic range rather than the usual straight-line relationship. In this condition, called geometric nonlinearity, the stress-deflection relationships follow the same curved path during loading and unloading, since the material is still elastic. Conditions of elastic instability may be considered as special cases of geometric nonlinearity.

As bellows deflection is increased still further, some of the bellows material is stressed beyond its elastic limit producing a condition of physical nonlinearity. In this condition, stress-deflection relationships during loading and unloading differ, causing a hysteresis loop (see Figure 24). The more the loading is increased beyond the elastic limit the greater the area of the hysteresis loop. The resulting

cycle life of any structure in a physically nonlinear condition is limited. Life cycle test results on structures in this condition unfortunately contain considerable scatter, making large safety factors on design cycle life necessary. While an analytical method accounting for physical nonlinearity is desireable, it was considered that, to accomplish parametric design studies, such a method would introduce unnecessary complexity. An assumption was made, therefore, that the designs which are superior in the geometrically nonlinear range will also be superior in the physically nonlinear range. A method accounting for geometric nonlinearity was required if accurate computation of stresses and deflections are to be made up to the material elastic limit as well as detection of conditions of elastic instability.

Having decided on the scope of the method to be developed, a search of the literature was conducted and several bellows manufacturers were contacted. Little information was found, either in the available literature or from the manufacturers, which would be directly applicable to bellows analysis except in the region of small deflections.

One analytical approach considered at this time was use of a force-displacement computer program available at Bell Aerosystems. The program solves for compatability loads and moments at the boundaries of discrete elements with known force-displacement relationships.

The discrete elements are selected from a library of elements within the program to approximate the geometric design to be analyzed. This program has an advantage in that each discrete element may be of any size commensurate with accurate approximation of the structure. This method, however, is linear and would require modification to take geometric nonlinearity into account. In the nonlinear range, much of the advantage of using relatively large discrete elements would be lost as each increasing deflection produces distortions requiring redivision into smaller elements. At this time, the program library of elements did not contain shell elements; therefore, force-displacement relationships for the desired shell element would have to be formulated for inclusion in the program library. The alternative to obtaining a shell element would be to approximate the bellows geometry as an assemblage of small plates.

Before proceeding with the necessary modifications and additions to the discrete element program, a more classical approach was sought. If equations describing the large deflections of a bellows could be derived and solved, a shorter method might be obtained. Because of the mathematical complexity of the large deflection theories available, the services of a consultant experienced in this field were sought. Several persons, prominent in the field of shells, were contacted. Through the advice of Dr. E. Reissner, Bell obtained the services of Dr. R. Archer of Case Institute of Technology. Dr. Archer had recently completed work on a paper (Reference 25) in which he had developed a computer program for the solution of Equations III and IV of Reference 32). The program solution was applied to the classic problem of elastic instability of spherical shells. Dr. Archer's results

demonstrate the applicability of Reissner's Equations III and IV to structural shell problems having considerable geometric nonlinearity. These equations will not predict elastic instabilities that are non-axisymmetric such as those producing circumferential buckles. The shell must be a surface of revolution, loaded axisymmetrically and experiencing only the small strains found within the elastic limit.

The computer program developed by Dr. Archer involves a very rapid matrix inversion method dependent on the finite difference approximation assumed for the basic differential equations. Fortunately, the program was written in Fortran language which is accepted by the IBM 7090 computer at Bell Aerosystems; therefore, the basic equation solution part of Dr. Archer's program could be used directly. Modifications were written to describe a bellows geometry, as well as to include compatibility relationships for the inner and outer leaf boundaries.

Hetenyi and Timms (Reference 31) assume that a single leaf may be used to analyze a bellows by considering the leaf fixed at its inner and outer boundaries. It seems logical, however, that only partial radial restraint exists, especially at some distance from bellows end attachments. For this reason, the first bellows program was set up using four bellows leaves (two complete convolutions). At the leaf juncture points, compatibility was established between rotation, deflection, tangential edge moments, horizontal, and vertical forces. The end extremities of the two-convolution bellows were assumed fixed. At this point in the program development, only axial thrust loads were considered. The complexity of considering local pressure effects was left to a later time, since at this point the search was for basic understanding of the problem. The problem considered by the first non-linear program is shown by the solid lines of Figure 5.

Realizing the necessity of checking the program against some known results, a parallel program was written considering only one leaf with various boundry conditions. Case I (Restrained Edges) of Reference 31 was selected as a test case because of the presence of experimental data reportedly taken with extreme care on accurately prepared and measured specimens. Since the program solution involves finite difference approximations, the number of finite points, "M," has important bearing on the accuracy of the results. Results calculated for increasing values of "M" are shown in Figure 6 with the experimental values of Reference 31. At the larger values of "M," the stresses calculated agree closely with those calculated in the referenced paper. Spring rates calculated with the program 1753 vary from 6917 lb/in. at "M" = 20 to 6903 lb/in. at M = 120 and agree with the experimental value of 6920 lb/in. reported. Case II (Simply Supported Edges) of Reference 31 was also calculated using "M" = 20 and the spring rate was found to be 5575 lb/in. by comparison with the experimental value of 5800 lb/in. It would seem that experimental deviations from the complete radial freedom of Case II would have a greater effect on experimental spring rate than would experimental deviations from the

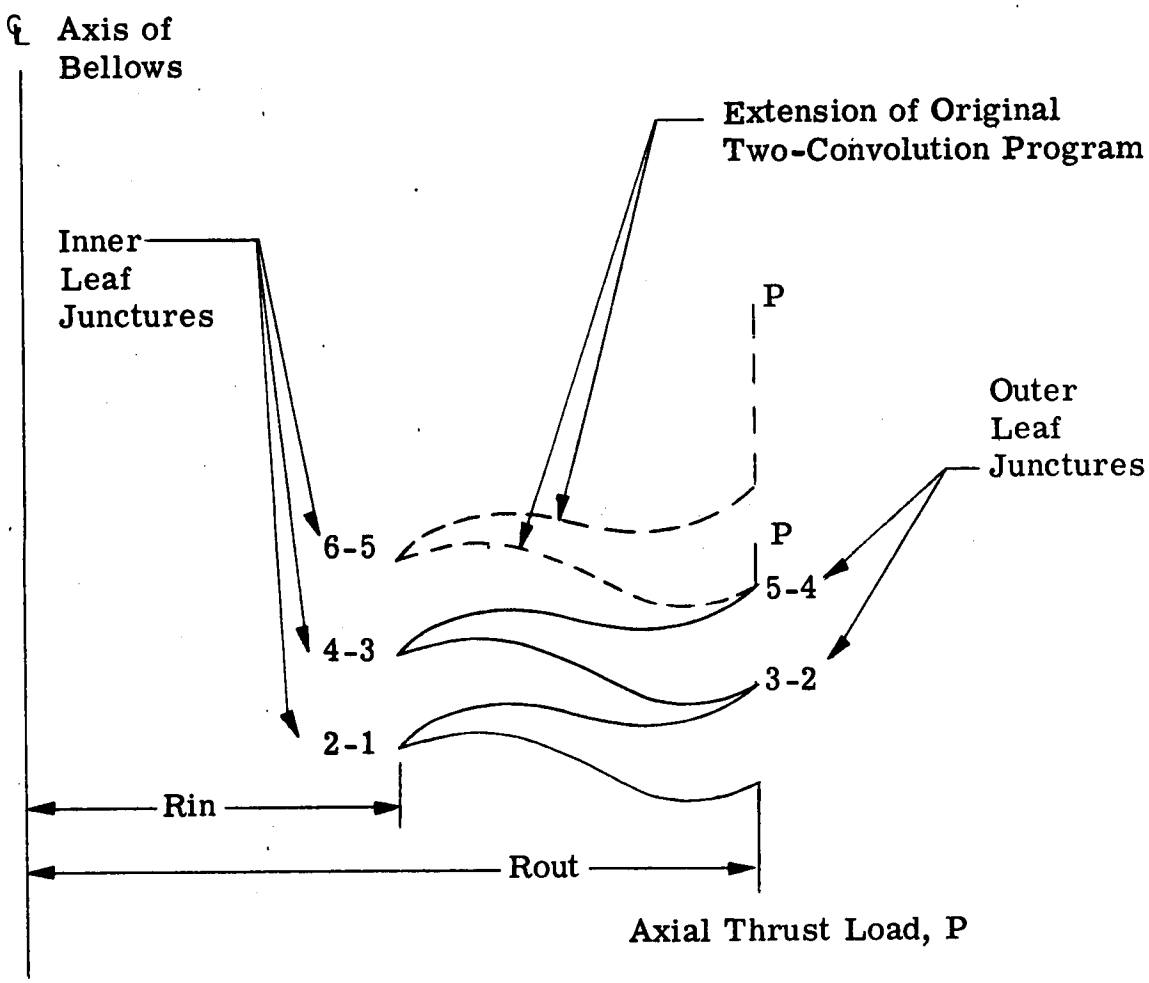

Figure 5. Typical Bellows for Axial Thrust Solution

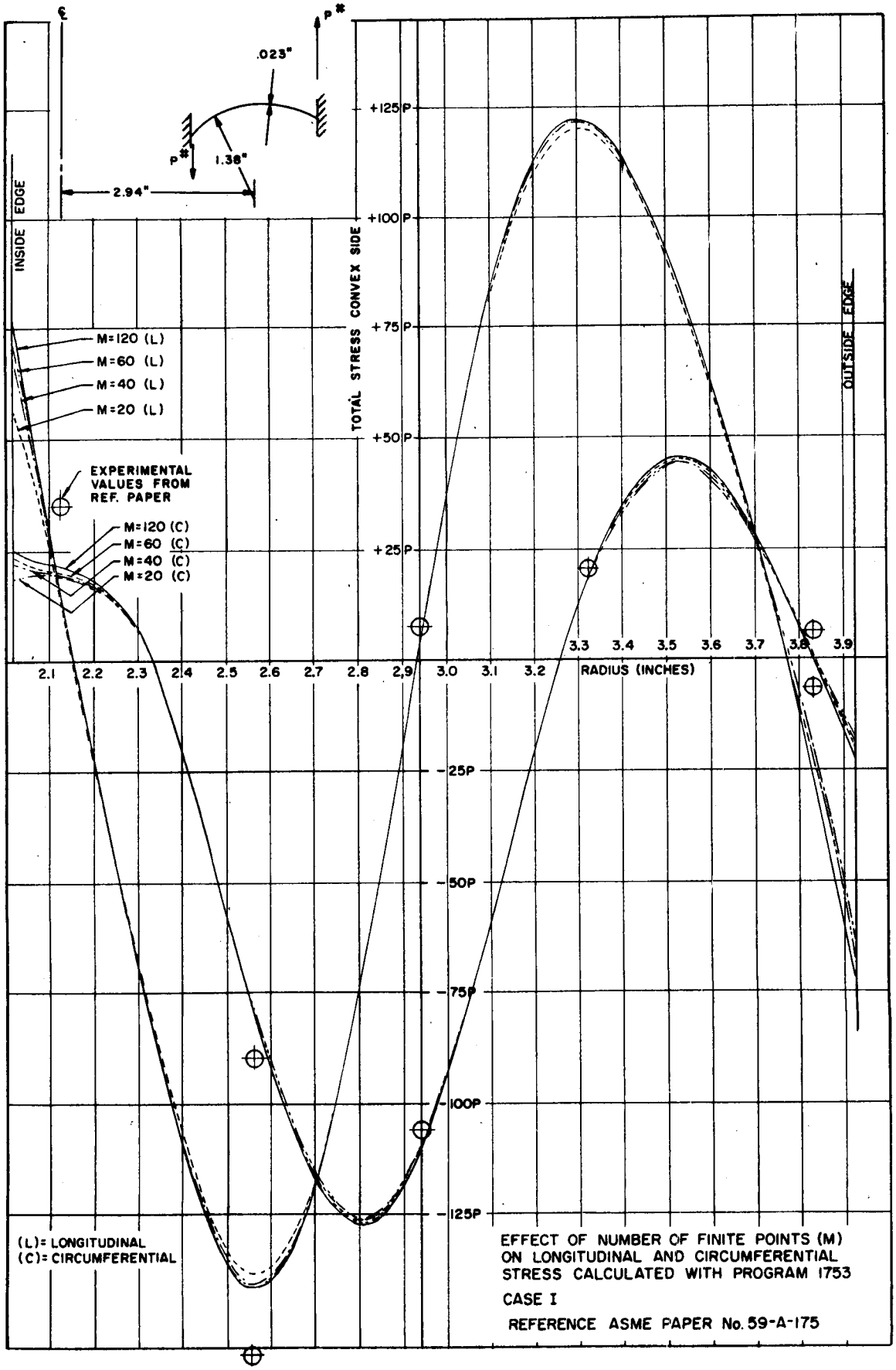

Figure 6. Effect of Number of Finite Points (M) on Longitudinal and Circumferential Stress Calculated with Computer Program 1753

constraint of Case I. The results of these test cases seemed to demonstrate that the Bell Aerosystems program was free of errors in its basic solution.*

While calculating the single-leaf test cases, it was observed that the computer time required was about 20 percent less than that required for comparable calculations made with the two-convolution program. A suitable boundary condition was sought which would allow for parametric studies using only one leaf. Using the two-convolution program, various end boundary conditions were introduced using different leaf geometries. Agreement between computed quantities at the end points and those at junction 3-2 (see Figure 5) is required before that end boundary may be used on a single-leaf solution. When the end boundaries were assumed clamped against rotation but free to move radially and the leaf geometry was conical, perfect agreement was achieved at all three points. When a parabolic leaf shape was introduced, there was no agreement either with the above end boundary assumption or with any other. It was concluded, therefore, that accurate bellows analysis, using a single leaf is obtained only when there is symmetry of neighboring leaves with respect to a plane normal to the axis of the surface of revolution.

During the search for a suitable one-leaf boundary condition, it was noticed that, by changing only end boundaries in the two convolution program, different values were obtained throughout the bellows. This means that more than two convolutions must be considered to calculate the stresses in one complete convolution far from end effects. Consequently, the two-convolution program was extended to three convolutions as shown by the dotted extension in Figure 5. Several cases were computed with varied end boundaries and leaf geometries. It was found that, for any given leaf geometry, identical values are obtained at junctions 3-2 and 5-4 (Figure 5) regardless of end boundary conditions. In fact, an inadvertent programming error introducing illogical conditions at one end resulted in the same values at junctures 3-2 and 5-4 as obtained after corrections of the error. Three complete convolutions, therefore, seems to be the minimum number that will produce accurate computation of the stresses and deflections in one complete convolution far removed from bellows end support effects.

To illustrate the importance of the three-convolution program to accurate stress calculation, the geometry of Case I, Reference 31, was used in a three-convolution problem. The longitudinal stresses in one leaf unaffected by end attachment is compared in Figure 7 with those in a single leaf from Figure 6. The largest stress variation occurs in the area of the weld where experience has shown failures are most likely to occur.

* Hetenyi's experimental results confirm that his assymototic solution is favorable to the geometry selected. The more-exact solution using IBM program 1753, therefore, agrees favorably with Hetenyi's calculated results. This does not necessarily confirm the validity of Hetenyi's solution to any geometry.

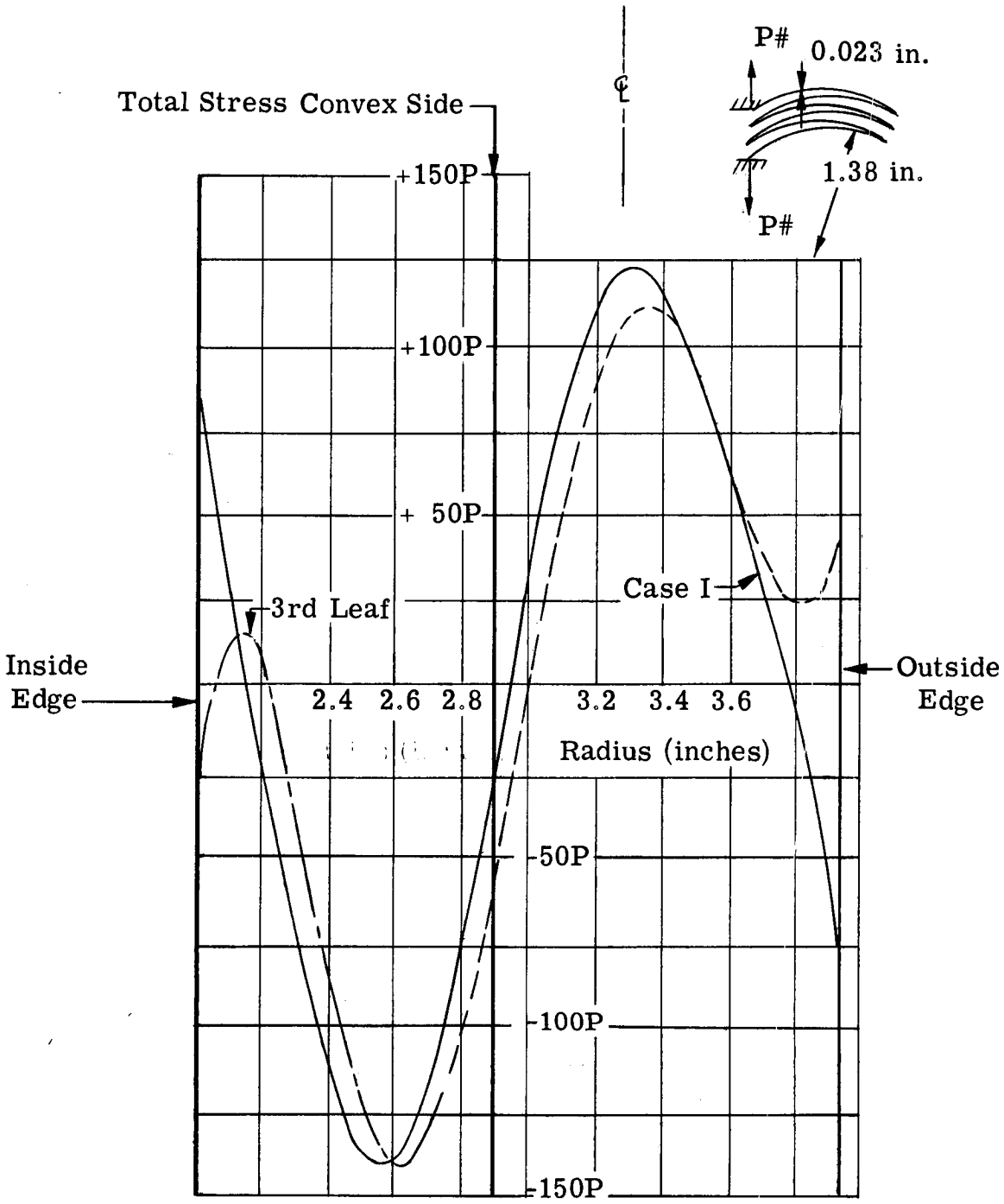

Figure 7. Effect of Six-Leaf Analysis on Longitudinal Stress of Case I, ASME Paper 59-A-175

Although the search for a single-leaf solution applicable to general bellows analysis was unsuccessful, the resulting three-convolution program computing time is still short. For example, computation of stresses and deflections at 481 solution points in a typical three-convolution problem for nine load values required 1.38 minutes.

Because of the success achieved to this point with the nonlinear program, it was decided to hold the discrete element approach in reserve. A linearized solution of the one-leaf program provides the necessary force-displacement relationships for any element of a shell of revolution for the discrete element program library. However, the nonlinearization of the discrete element program would still present a rather large task with greater computation time required per problem than with the existing nonlinear program.

Local pressure effects, previously neglected, were next incorporated into the program. These modifications required many changes and additions to the program. Since the pressure is assumed acting on the deformed surface, the vertical and horizontal components of pressure become dependent upon the finite element rotation, which is one of the unknowns of the basic differential equations. An additional iteration step, therefore, is required to account for local pressure effects.

Because of the necessity of again computing stresses and deflections for some known classic problem to check the local pressure modification, the single leaf program was also modified to include local pressure effects. Two test cases were selected. The first case (I_p) was a cylinder under uniform internal pressure fixed at the ends with axial load reacted externally. The second case (II_p) was a flat circular plate under uniform pressure fixed at its outer diameter. These nearly opposite cases were selected to demonstrate the versatility of the IBM 1753 nonlinear program. The second case was calculated to larger stress values to show results in the non-linear range. The results of case I_p are shown in Figure 8 compared with values calculated by the classical equations of Timoshenko, et al. (Reference 24). The results of case II_p are shown in Figure 9 compared with the data presented by Way (Reference 33). The agreement achieved on these two test cases was considered as sufficient verification of the validity of the modified program including the effects of local pressures. In the computation of test cases I_p and II_p it was noticed that, with local pressure included, values of "M" of at least 200 were required to obtain good agreement with classic results.

A 7-1/8 inch diameter test bellows, used extensively for dynamic testing, was at first considered to be a good test case for the three-convolution program. Casting serious doubt on any computed result, however, was the fact that the exact bellows geometry as delivered was unknown. The leaf shape originally manufactured was known from drawings but the method of manufacture of the finished bellows changes this shape to an unknown degree. The bellows leaves are welded together in the nested position and the bellows is stretched beyond the elastic limit to set the desired free length. With these facts in mind it was decided to compute

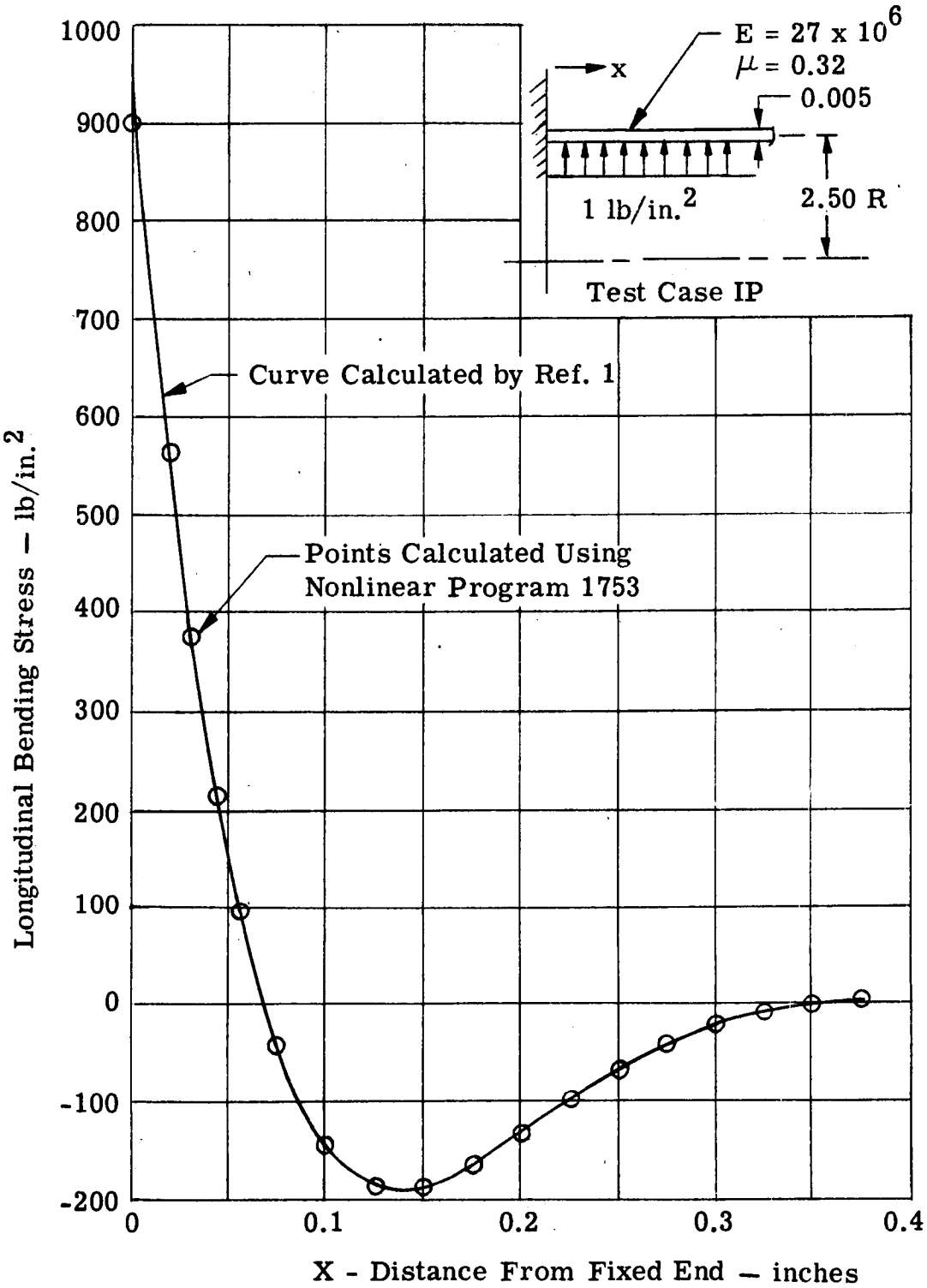

Figure 8. Longitudinal Bending Stress Near Fixed Support of Cylinder Under 1 psi Internal Pressure

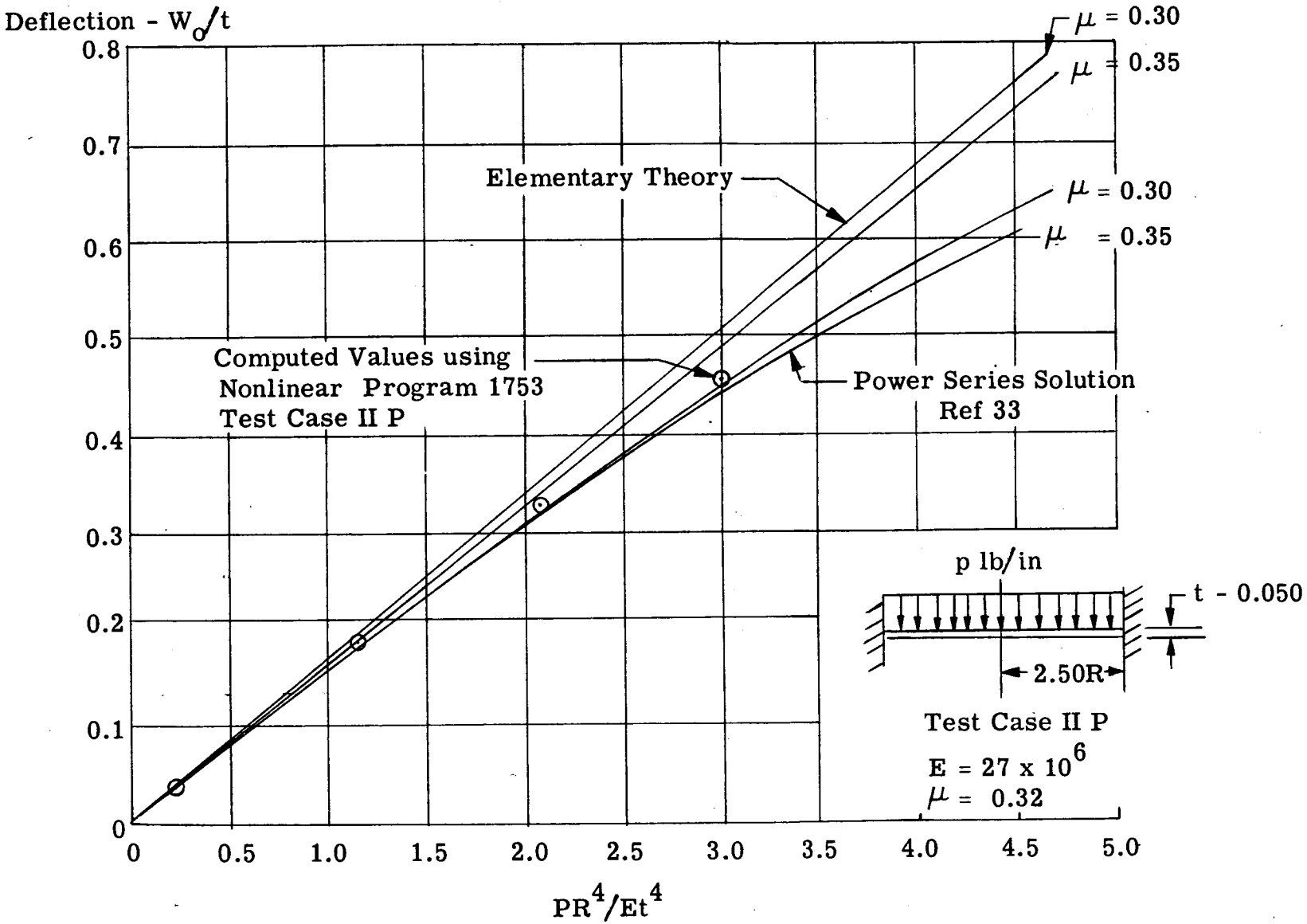

Figure 9. Test Case IIP

the stresses and deflections of the original geometry from a nested position up to elastic limit stress thereby simulating the elastic range distortions occurring when setting the free length. Computations were made for conditions of axial thrust only and for extension under internal pressure only. The distorted leaf shape under axial thrust and internal pressure at a maximum stress of 30,000 psi is shown in Figures 10 and 11 compared with the original shape. The bending and membrane stresses in both the radial and circumferential directions are shown in Figures 12 and 13. Maximum stresses occur in this case at the leaf junctures where experience shows most failures occur.

Because of the difficulty in defining the geometry at zero stress of the 7 1/8 inches diameter bellows or of any bellows available at Bell Aerosystems, no experimental test case is available to check the three-convolution non-linear program. One bellows manufacturer has been contacted to supply geometric information and test results for a bellows constructed with an initial pitch in the zero stress condition. If the actual bellows of this type is manufactured with careful adherence to design drawings, a suitable test calculation can be made of the three-convolution program.

At the conclusion of this contract, the nonlinear IBM program 1753 is restricted to investigation of shells with constant thickness and modulus of elasticity, however, much of the work necessary to allow for consideration of variations in thickness and modulus has been carried out. Because of unexpected delays in making local pressure modifications operational, the IBM cards have not been punched for inclusion of variable thickness and modulus. There is no great difficulty in performing the required modifications, aside from the usual program "debugging" process. It is anticipated that inclusion of variable thickness will be made at an early date and the program again checked against some classic result. These modifications are required to study the effects of local thinning caused by deep forming of certain bellows leaf designs.

After detailed study of the problems involved in the structural analysis and design of welded bellows, it may be concluded that no exact equation for the optimum leaf design is obtainable. However, using the analytical tool developed here, a great many parametric variations may be studied by rapid computer methods to determine the optimum for a given family of shapes. The computer program developed under this contract and included in Appendix III represents an advance in the analysis of bellows, however, much remains to be done. Extension of the program to include the effects of physical non-linearities would be a logical following step and appears to be feasible. Recent work by others also indicate that analysis of certain nonsymmetric instabilities is also possible.

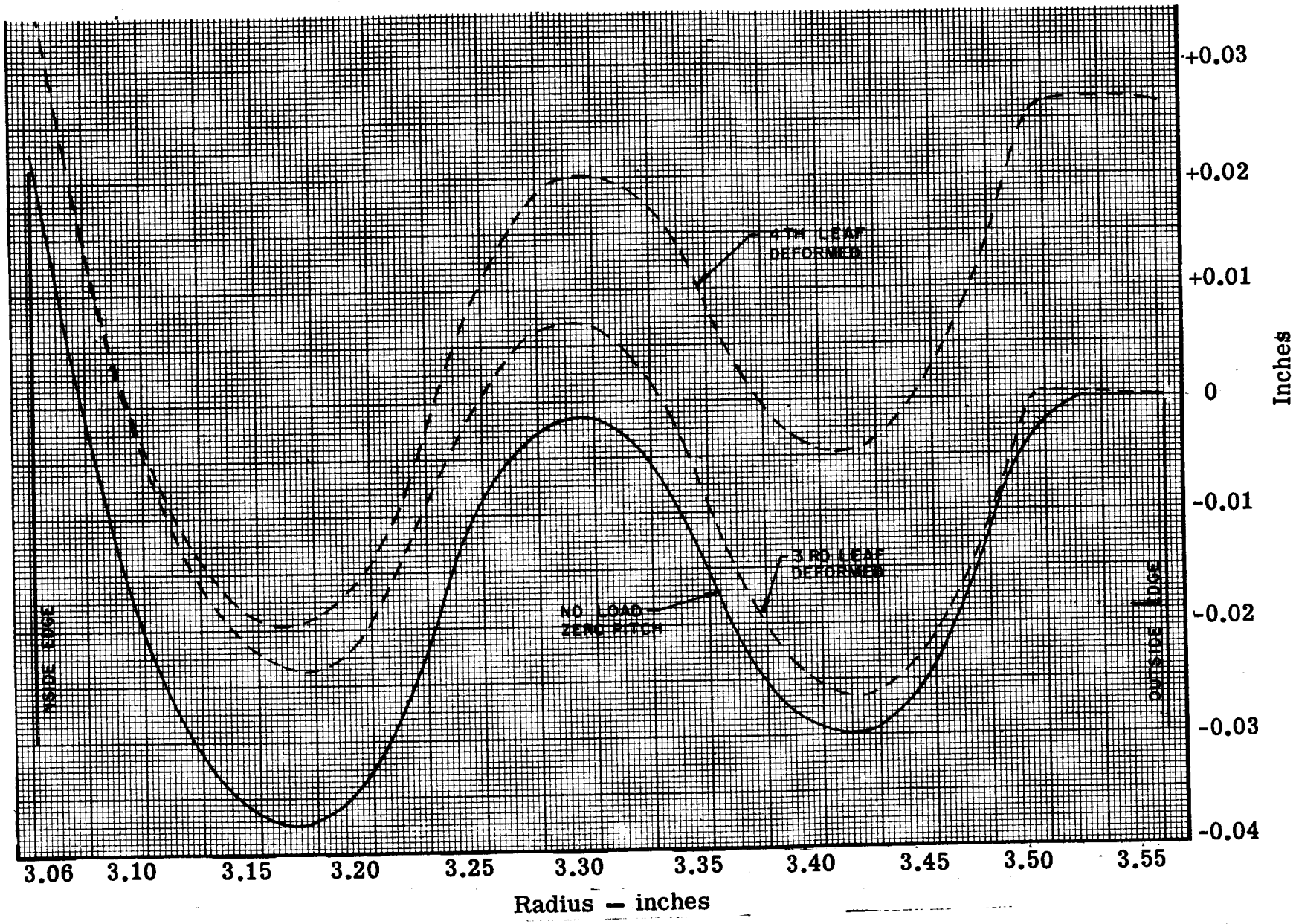

Figure 10. 7-1/8 Test Bellows Deformation at 16.9 lb Thrust

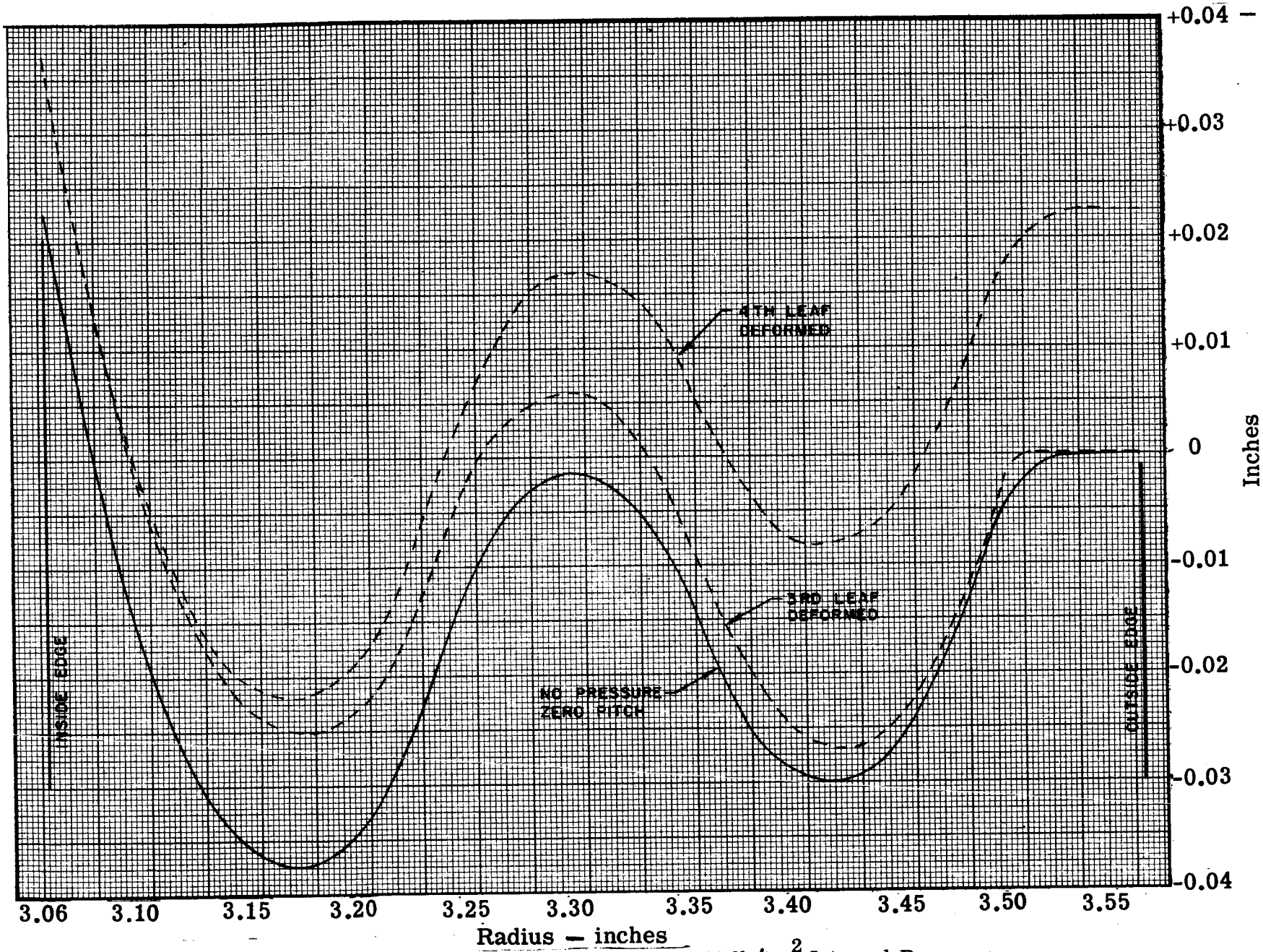

Figure 11. 7-1/8 Test Bellows Deformation at 0.41 lb/in.^{2} Internal Pressure

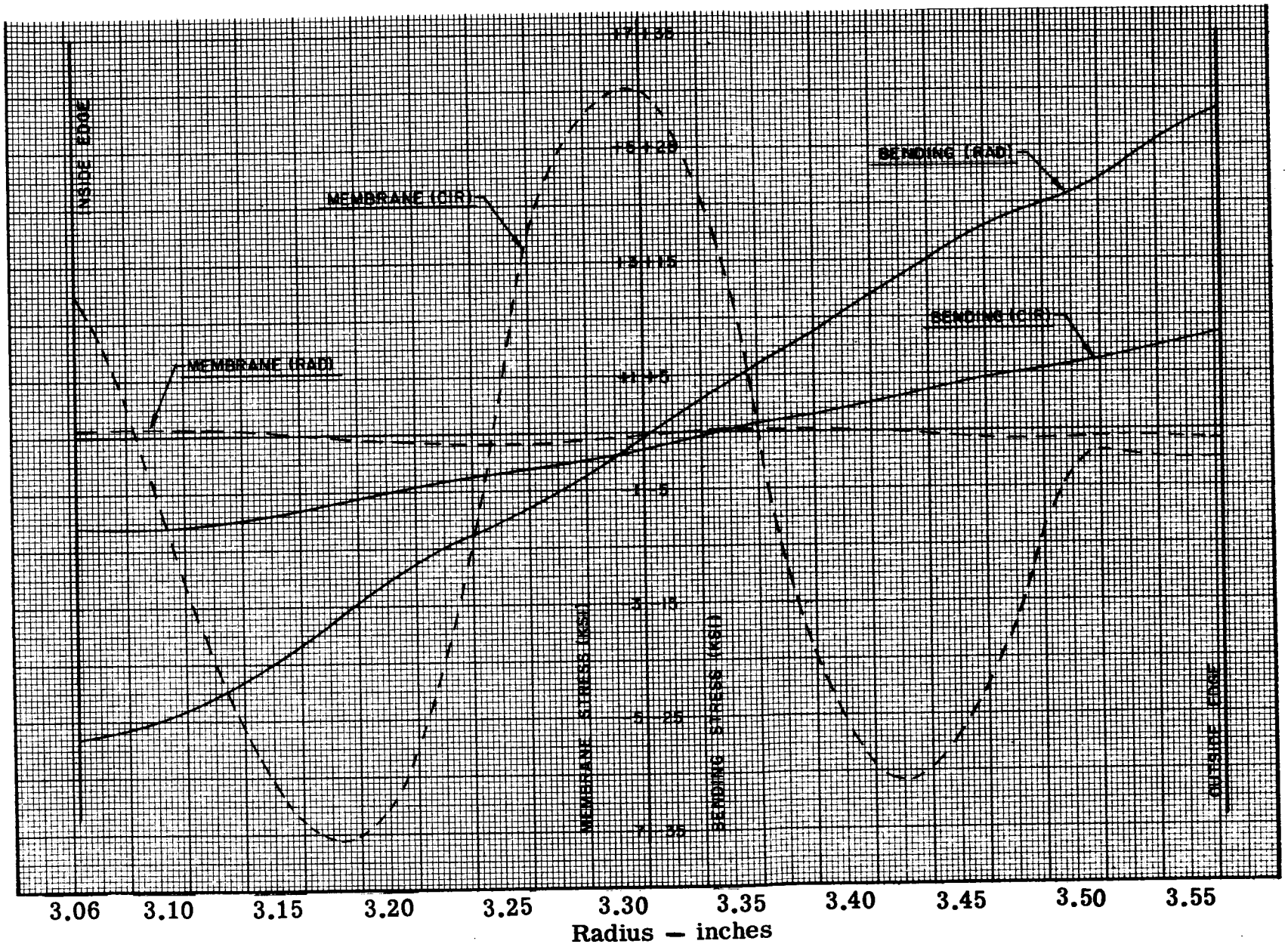

Figure 12. Computed Stresses in 3rd Leaf of 7-1/8 Bellows at 16.9 lb Thrust

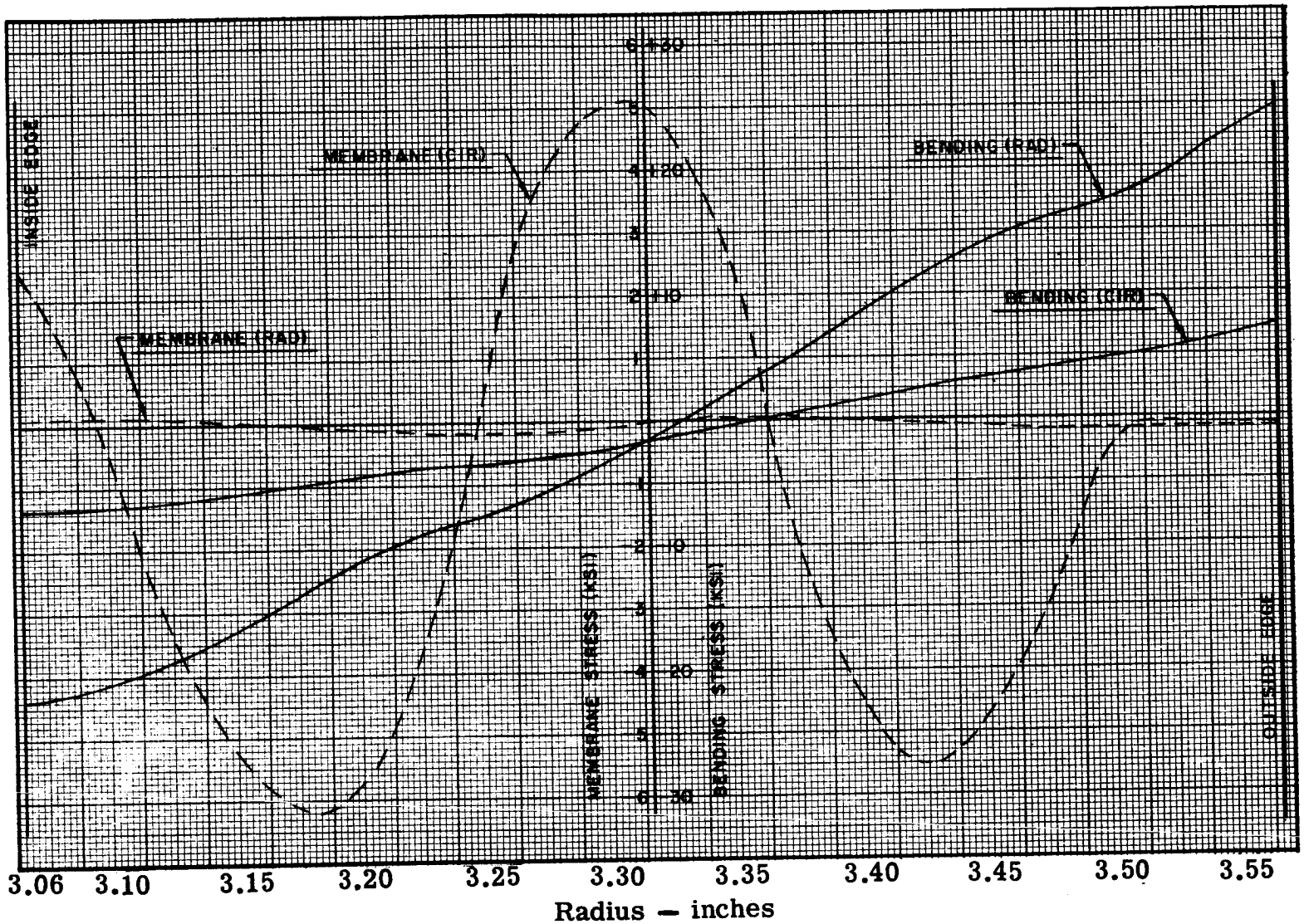

Figure 13. Computed Stresses in 3rd Leaf of 7-1/8 Bellows at 0.41 lb/in.^{2} Pressure

SECTION 4

DYNAMICS INVESTIGATION

A. PURPOSE AND OBJECTIVES

The dynamics investigation was conducted to determine steady-state and/or transient response of a welded bellows when subjected to an applied dynamic environment. The environments of interest included sine/random vibration, shock, and acoustic noise that can occur prior to or during bellows operation.

Emphasis was placed on those parameters considered to have the most influence on bellows response during sinusoidal vibration. These included the physical characteristics of the bellows i.e., leaf mass, head mass and spring rates of the individual leaf and/or assembly plus the fluid effects of viscosity, density and bulk modulus.

Also investigated were variations in differential pressure and the modes associated with the liquid column bounded by the inner weld diameter and the liquid trapped within convolutions. The identification of these modes and the development of a method of analysis for predicting resonant frequencies and possible modes of failure is presented as well as experimental verification of the analytical method.

B. LITERATURE SURVEY

A literature survey was conducted relative to the topic of bellows dynamics. The search revealed references to formed bellows, but apparently welded bellows are of too recent origin to have received much attention.

In answer to a request to the AEC Oakridge Library, two bellows reports were obtained from the Office of Technical Service (OTS) in January 1963. These reports were written in 1954 by D. B. Vail at Knolls Atomic Power Laboratory, Schenectady, New York. Vail calculated approximate natural frequencies of a 4 in. O.D., 10 in. long, 136 convolutions, and 0.019 in. leaf thickness welded bellows. These calculations, which are valid for the elastic range, showed good agreement with sinusoidal vibration test results; the lowest resonances appearing at 19.5 cps longitudinal and 15.7 cps lateral. These bellows were intended for use in a high-temperature submarine liquid sodium system where forcing frequencies from such sources as the propeller, hull vibrations, and pump occur below 32 cps. In addition, it was mentioned that self-excitation of the bellows can occur due to pressure pulsations in the flowing sodium. Mr. Vail, when contacted at the General Electric Co., San Jose, California, stated that this bellows was modified and approved for service after reducing its effective length.

Mr. J. Matt at Thompson Ramo Wooldridge reported failures on welded disc bellows with few convolutions used in conjunction with rotary face seals. Literature from the various bellows manufacturers mentions vibration response of bellows, but does not account for the fluid affects inside a bellows.

Experimental testing for verification of analytical results was conducted on a 4 inch diameter bellows assembly. The operation of this bellows was restricted to elastic motion. An extensive test program was conducted with sinusoidal vibration applied in the longitudinal and lateral directions. During the longitudinal vibration scans, two distinct modes of response were identified. For convenience, the more-common longitudinal bellows mode, wherein the response is similar to that of a prismatic bar or coil spring fixed at each end, was arbitrarily named the accordion mode. This mode was predicted. Rather unexpectedly a second longitudinal mode was found; for convenience this was arbitrarily named the liquid displacement mode. As described elsewhere in this report, both modes occur at a fundamental frequency and odd integer higher harmonic frequencies. Attenuation devices and their damping effect at critical frequencies are described.

During an appreciable portion of this investigation, Bell Aerosystems Company was under contract to develop an operational bellows assembly for a secondary propulsion system (Model 8250). Test results with the Model 8250 bellows assemblies vibrated in the plastic range are reported. These data are presented in Table 2 to corroborate the analytical analysis.

C. ACCORDION MODE ANALYSIS

Longitudinal or axial vibration modes, herein referred to as accordion modes, can be established for nearly any bellows configuration by use of the following matrix iteration technique which neglects damping and bellows head elastic terms. These elastic forces may cause slight coupling with the motion of the last few convolutions attached to the head. However, test results showed little influence on over-all accordion mode motion.

1. Solution for Accordion Modes

The following matrix equation for multi-degree of freedom systems can be found in many standard textbooks on mechanical vibrations.

$$\left[C\right] \left[M\right] \left\{Y\right\} = \frac{1}{\omega_a^2} \left\{Y\right\} \tag{1}$$

Where:

$\left[C\right]$ = a square matrix of flexibility influence coefficients, in./lb

$\left[M\right]$ = a diagonal matrix of mass terms, lb-sec^2/in.

$\left\{Y\right\}$ = a column matrix of deflections, in.

TABLE 4-1

VIBRATION TEST RESULTS

Description	4 in. Bellows			7 in. Bellows			9 in. Bellows		
Actual Outside Diameter, D_o	4.3 in.			7.125 in.			9.0 in.		
Inside Diameter, D_i	3.644 in.			6.125 in.			8.0 in.		
D_o/D_i Ratio	1.18			1.16			1.12		
Length During Vibration	10.7 in.			39.8 in.			5.86 in.		
Nested Length	-			3-3/4 in.			0.50 in.		
Pitch Length	0.107 in.			0.3 in.			0.3 in.		
Free Length After Nesting	-			19.12 in.			2.015		
Free Length After Extension	8.75 in.			29.1 in.			4.61 in.		
Material	410 St. Stl.			321 St. Stl.			347 St. Stl.		
Leaf Thickness	0.004 in.			0.006 in.			0.006 in.		
No. of Convolutions	100			135			20		
Weight of Bellows	1.00 lb			5.18 lb			1.039 lb		
Span	0.328 in.			0.5 in.			0.5 in.		
Leaf Shape	Ripple			Ripple			Modified Ripple		
Weight of Trapped Fluid	0.82 lb			7.6 lb			3.1 lb		
Head Weight	1.47 lb			2.4 lb			0.723 lb		
Test Liquid in Bellows	Distilled water, air, oil, jelled water			Distilled water			Distilled water		
Total Effective Spring Rate	10.8 lb/in			15 lb/in.			103-150 lb/in.		
Spring Rate/Convolution	1080 lb/in.			2025 lb/in.			2060 lb/in.		
	Calc. cps	Test cps	Nodes	Calc. cps	Test cps	Nodes	Calc. cps	Test cps	Nodes
Accordion Modes	23.9	23.75	2	10.3	11	2	59.5-78.4	73	2
	71.7	71.0	4	30.7	34	4			
	119.5	117.5	6	50.6	56	6			
	167.0	178.0	8						
Liquid Displacement Modes		87			39	6		139	2
					111				
					177				
Lateral Frequencies (Zero Internal Pressure)	12.25	16.2	2						
	34.3								
	67.4	61.0	6						

ω_a = the accordion mode frequency in radians/second = $2\pi f_a$

$\frac{1}{\omega_a^2}$ = commonly referred to as the eigen value

In applying Equation (1) to the determination of bellows frequency, the matrix of flexibility coefficients $[C]$ was not immediately available. On the other hand, a matrix of stiffness influence coefficients $[S]$ could be readily established in a manner which will be explained in succeeding paragraphs. Flexibility coefficients were established since,

$$[C] = [S]^{-1} \tag{2}$$

where $[S]^{-1}$ stands for the matrix inverse of $[S]$.

Symbolically $[S]$ can also be given by $k\ [s]$ (3)

Where k is some spring rate value, lb/in., and $[s]$ represents deflections in integers (stiffness matrix of influence coefficients in integers)

Substituting Equation (3) into (2):

$$[C] = [S]^{-1} = (k\ [s])^{-1} = \frac{1}{k}\ [s]^{-1} \tag{4}$$

2. Development of Stiffness Matrix $[s]$

The bellows was assumed to be a set of spring masses which are connected in series. For such a system, an $[s]$ matrix can be formulated in the following manner. Consider a set of five masses connected in series by springs as depicted in the following sketch. Moreover, as is true for the bellows, assume that the spring stiffness is a constant k:

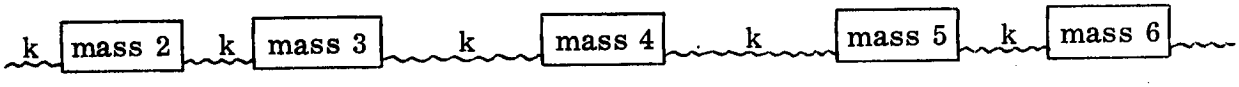

To establish the $[s]$ matrix, consideration will be given to the forces that are acting on each mass as one of the masses is subjected to a unit displacement, all other masses being held fixed. For illustrative purposes, assume that the mass which undergoes a unit horizontal displacement, d, is mass 4, all other masses being held fixed.

The force which mass 4 experiences is $F_4 = 2\ k\ d$, where k is the stiffness of the spring on either side of that mass. The force F_4 consists of two components: a component in compression equal to kd and a component in tension also equal to kd. At the same time (because of the unit displacement, d, of mass 4), mass 5 experiences a force $F_5 = -kd$. Similarly, mass 3 experiences a force $F_3 = -kd$. Note that

the forces experienced by masses 3 and 5 are of opposite sense to that experienced by mass 4, hence the minus sign in the definitions of F_3 and F_5. Moreover, the forces experienced by masses 2 and 6 as a result of the unit displacement, d, of mass 4 would be zero, i.e. $F_2 = F_6 = 0$. What has been said regarding the forces on masses 2 through 6 due to a unit displacement of mass 4 could be stated in a similar manner for unit displacement of any of the masses 2 through 6, all other masses being held fixed. As a consequence of this, the forces experienced by each of the masses due to displacement of any other mass may be written in matrix form as $\{F\} = [k]\{d\}$:

$$\{F\} = \begin{Bmatrix} F_2 \\ F_3 \\ F_4 \\ F_5 \\ F_6 \end{Bmatrix} = \begin{bmatrix} 2k & -k & 0 & 0 & 0 \\ -k & 2k & -k & 0 & 0 \\ 0 & -k & 2k & -k & 0 \\ 0 & 0 & -k & 2k & -k \\ 0 & 0 & 0 & -k & 2k \end{bmatrix} \begin{Bmatrix} d_2 \\ d_3 \\ d_4 \\ d_5 \\ d_6 \end{Bmatrix} \tag{5}$$

where $F_2 \ldots F_6$ are the forces experienced by masses 2, 3, 4, 5 and 6, respectively, correspondingly $d_2 \ldots d_6$ are the displacements which each mass undergoes.

In this matrix equation, if $d_2 = d_3 = d_5 = d_6 = 0$, and $d_4 = d$, (the unit displacement of mass 4 as discussed previously in some detail) then it will be seen that the forces experienced by each mass are:

$$\{F\} = \begin{Bmatrix} F_2 \\ F_3 \\ F_4 \\ F_5 \\ F_6 \end{Bmatrix} = \begin{bmatrix} 2k & -k & 0 & 0 & 0 \\ -k & 2k & -k & 0 & 0 \\ 0 & -k & 2k & -k & 0 \\ 0 & 0 & -k & 2k & -k \\ 0 & 0 & 0 & -k & 2k \end{bmatrix} \begin{Bmatrix} 0 \\ 0 \\ d \\ 0 \\ 0 \end{Bmatrix} = \begin{Bmatrix} 0 \\ -kd \\ 2kd \\ -kd \\ 0 \end{Bmatrix}$$

That is, $F_2 = F_6 = 0$, $F_3 = F_5 = -kd$, and $F_4 = 2kd$.

These are the results previously discussed for a unit deflection in mass 4 while all other masses are held fixed.

It can be seen that k is a common factor in the square matrix just presented. Hence, that matrix could be written as

$$[S] = k \begin{bmatrix} 2 & -1 & 0 & 0 & 0 \\ -1 & 2 & -1 & 0 & 0 \\ 0 & -1 & 2 & -1 & 0 \\ 0 & 0 & -1 & 2 & -1 \\ 0 & 0 & 0 & -1 & 2 \end{bmatrix}$$

Such a matrix is, in fact, the stiffness matrix that was denoted by $[s]$ in Equation (3).

Note that if the springs between masses are not identical, the foregoing basic procedure will still apply. Also, either or both ends of the bellows may be free. In such cases, the $[s]$ matrix diagonal terms will no longer be 2.0 in all cases and the adjacent terms in each row will not always be -1.0.

What has been stated above for a set of 5 masses may be extended to any number of masses connected in series by springs, each of which has a stiffness k. A bellows may be so characterized.

All that needs to be accounted for in setting up the $[s]$ matrix that is new are the end conditions. On the assumption that the ends of the bellows are fixed, so that an infinite force is required to give the end masses a unit deflection, the first element in the first row and the last element in the last row of the $[s]$ matrix will be infinity. In actual practice, however, some very large number is substituted for infinity. Thus for a bellows of 30 spring-connected masses the required $[s]$ matrix for Equation (4) is by elements as follows:

$$\begin{bmatrix} s_{1,1} & s_{1,2} & s_{1,3} & s_{1,4} & s_{1,5} & s_{1,6} \ldots & s_{1,30} \\ s_{2,1} & s_{2,2} & s_{2,3} & s_{2,4} & s_{2,5} & s_{2,6} \ldots & s_{2,30} \\ s_{3,1} & s_{3,2} & s_{3,3} & s_{3,4} & s_{3,5} & s_{3,6} \ldots & s_{3,30} \\ s_{4,1} & s_{4,2} & s_{4,3} & s_{4,4} & s_{4,5} & s_{4,6} \ldots & s_{4,30} \\ s_{5,1} & s_{5,2} & s_{5,3} & s_{5,4} & s_{5,5} & s_{5,6} \ldots & s_{5,30} \\ s_{6,1} & s_{6,2} & s_{6,3} & s_{6,4} & s_{6,5} & s_{6,6} \ldots & s_{6,30} \\ \cdot & \cdot & \cdot & \cdot & \cdot & \cdot & \cdot \\ \cdot & \cdot & \cdot & \cdot & \cdot & \cdot & \cdot \\ \cdot & \cdot & \cdot & \cdot & \cdot & \cdot & \cdot \\ s_{30,1} & s_{30,2} & s_{30,3} & s_{30,4} & s_{30,5} & s_{30,6} \ldots & s_{30,30} \end{bmatrix}$$

Where: $s_{1,1} = s_{30,30} = 1 \times 10^7$, (large number, but not infinite)

$$s_{2,2} = s_{3,3} \cdots\cdots s_{29,29} = 2.0$$

$$s_{1,2} = s_{2,1} = \cdots\cdots = s_{28,29} = s_{29,28} = -1$$

And all other elements are zero.

Equation (1), as it stands, is a subcase of a general equation by which the natural modes of a structure may be calculated. This more general equation has been written in Fortran language for solution on an IBM 7090 digital computer. This program carries Bell Aerosystems Program No. 1692. The program employs an iterative procedure to solve Equation (1), i.e., a normalized deflection shape $\{Y\}$ is assumed on the left-hand side of the equation. This deflection shape is multiplied by the matrix product $[C]$ $[M]$ and a new column matrix is obtained which, when normalized, is given by the right-hand side of Equation (1), namely, $\frac{1}{\omega_a^2}\{Y\}$. The eigen value $\frac{1}{\omega_a^2}$ represents the quantity divided out of the newly obtained column matrix to normalize that matrix. The newly obtained column matrix is substituted into the left-hand side of Equation (1) and the procedure outlined above is repeated. The process is continued until the output normalized column matrix equals the input normalized column matrix. The final eigen value is solved and the frequency f_a in cps is printed out along with the normalized deflections for the fundamental and its higher harmonic modes.

D. APPLYING IBM 7090 PROGRAM 1692 TO A BELLOWS

1. Weight Matrix Development

Figure 14 shows the lumped mass representation of the 135 convolution 7-inch bellows whose accordion mode was predicted by IBM Program 1692.

For analysis purposes, the mass is assumed to be lumped together into 30 segment masses to cut down on the volume of input data. Regardless of how many actual convolutions are present in the physical bellows, the mass can be distributed into a finite number of masses, in this case 30 segment masses. The 30 segment masses can be further classified as the head mass M_1, the convolution segment masses M_2 to M_{29} inclusive and the head mass M_{30}.

The meaning of each segment mass can be best understood by comparing the mathematical model to an actual bellows (refer to photo in Figure 23). The base mass M_1 which is physically the flange or base of the bellows does not enter into the calculation other than as a very large but not infinite number in the weight matrix.

The segment mass, M_{15}, which is typical of all masses from M_2 to M_{29} inclusive, contains the combination of leaf metal weight W_m and trapped liquid weight W_t. To calculate the W_m portion of M_{15} divide the total weight of the bellows convolutions by 28, the number of convolution segments.

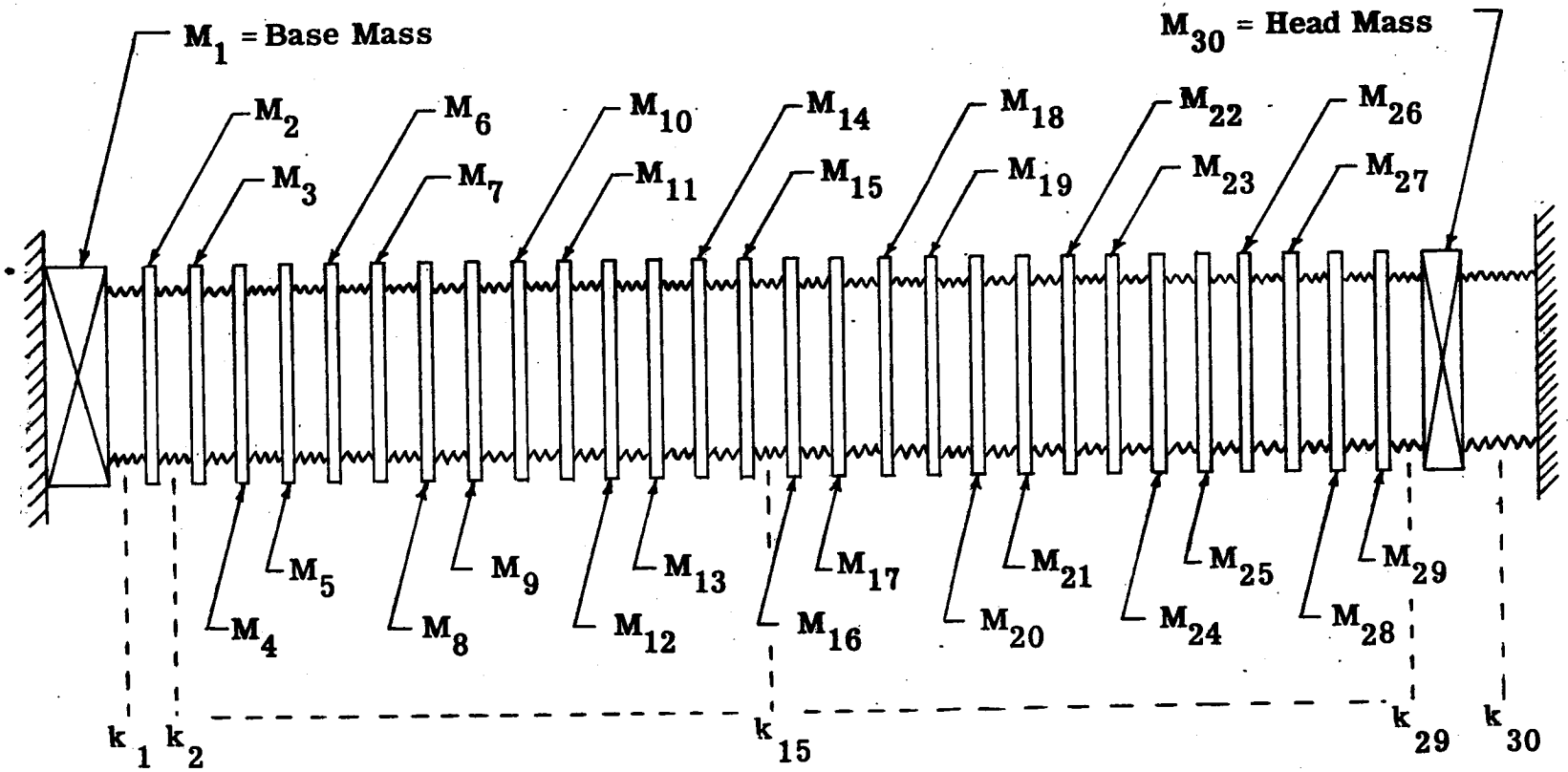

Figure 14. Mathematical Model of Bellows

To calculate W_t, divide the total amount of fluid trapped in all convolutions by 28, for each convolution segment. This trapped fluid can be approximated as follows:

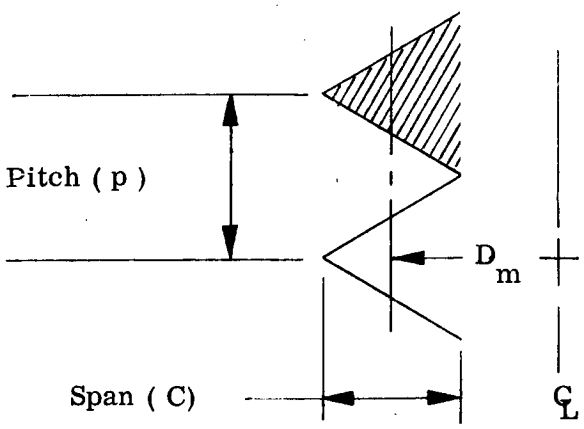

$$W_t = \frac{(\text{Pitch})\,(\text{Span})\,(\pi)\,(D_m)^2\,(\rho)}{(28)} \tag{135}$$

where

D_m = Mean diameter of bellows, inch

ρ = Density of liquid lb/in.^{3}

(6)

Figure 15. Trapped Liquid in Bellows

Note that if a 4-inch diameter bellows has 100 actual convolutions, the mathematical convolutions segment M_{15} is equivalent to 100/28 = 3.57 convolutions; if a 7-inch diameter bellows has 135 actual convolutions the mathematical convolution segment M_{15} is equivalent to 135/28 = 4.83 convolution, etc.

The head mass M_{30}, the moveable end of the bellows, does not enter into the calculation other than as a very large but not infinite number in the weight matrix. This is obvious when the bellows head is fixed or bearing against the inner wall of the shell enclosing the bellows. When the head is free from the shell, due to the ullage distance or partial expulsion, again head mass may generally be neglected due to fluid influences; i.e., the effective spring rate or bulk modulus of a liquid is very high as compared with leaf spring rates. Head response during sinusoidal vibration tests with free and fixed heads showed identical frequency responses at the center convolution. It appears that the bellows convolutions shear the liquid column near the inside diameter weld. Only the convolution metal and the trapped fluid is moving at acceleration amplitudes greater than the input acceleration amplitudes at the base of the bellows.

2. Stiffness Matrix Development

For analysis purposes, in Figure 14 the stiffnesses are assumed to be lumped together in a manner similar to the 30 masses.

The base stiffness k_1 and the head stiffness k_{30} are considered to be very large but not infinite, i.e., - in the [S] matrix $k_{1,1}$, $k_{30,30}$, $s_{1,1}$, and $s_{30,30}$ are very large. The base attaches to an armature head of a vibrator in the laboratory and to tank shell/vehicle structure in service while the bellows head is in contact with the fluid column.

Convolution segment stiffness at mass fifteen, k_{15}, which is again typical of all stiffnesses from k_2 to k_{29} inclusive is represented by an influence coefficient of 2 in the stiffness matrix [S] i.e., $k(s_{2;2})$ as previously explained. The numerical value of the k in front of the stiffness matrix can be obtained by dividing the overall bellows spring rate by 28, the number of springs.

The IBM Program 1692 was used to predict the response of three bellows sizes referred to in this report as 4-in., 7-in., and 9-in. bellows. Bellows description results of IBM calculations, and actual vibration test results are shown in Table 2. Figure 16 shows calculated mode shapes for the 7-inch bellows.

E. SIMPLIFIED FREQUENCY DETERMINATION OF ACCORDION MODES

The exact method shown in Paragraph C.1. can predict mode shape as well as frequency for any combination of springs and masses in series. However, a very good approximation of the frequency can be obtained for a system of uniform springs and masses by using formulas developed in Reference 18 for elastic bodies, as shown in the following. The location of the nodes for the various normal modes can be found in any table for uniform beams such as Table 7-3 of Reference 22.

Consider the case of a uniform beam clamped or fixed at both ends:

$$\omega_a = \eta \pi \sqrt{\frac{AE}{\mu_1 L^2}} \quad , \quad \eta = 1,2,3 \tag{7}$$

where: ω_a = accordion mode resonant frequency, radians/sec = $2\pi f_a$

A = area of beam (bellows), in.^{2}

E = modulus of elasticity, psi

L = length of beam (bellows), in.

μ_1 = mass per unit length, lb-sec^2/in.^{2}

By Hooke's Law $\delta = \frac{PL}{AE}$ δ = Deflection, inches

$\delta_1 = \frac{L}{AE}$ δ_1 = Deflection for unit load, in./lb.

$K_a = \frac{AE}{L}$ $K_a = \frac{1}{\delta_1}$ = Longitudinal total effective spring rate (beam), or accordion mode (bellows) lb/in.

also $\mu_1 = \frac{M}{L} = \frac{W}{gL} = \frac{W}{386L}$

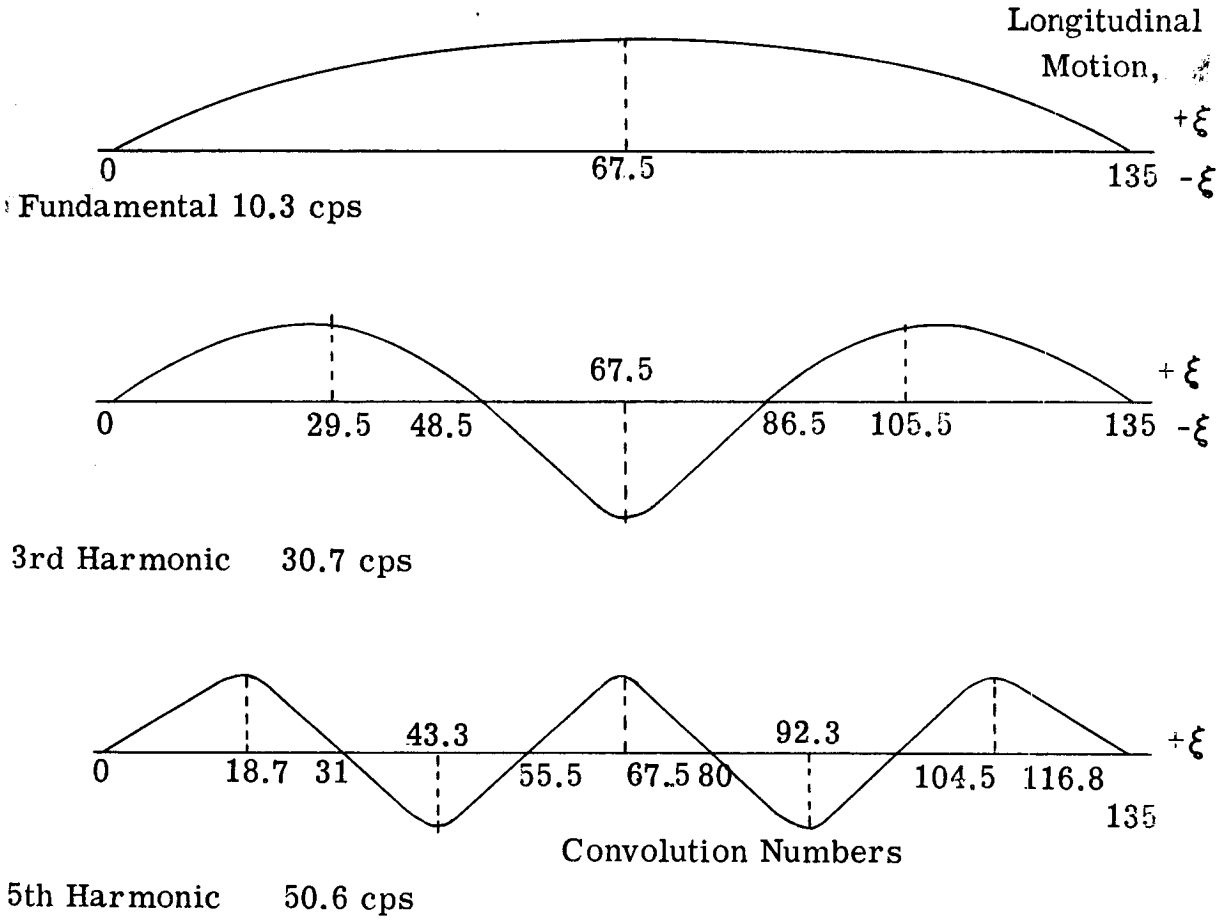

Figure 16. Calculated 7-Inch Bellows Accordion Modes

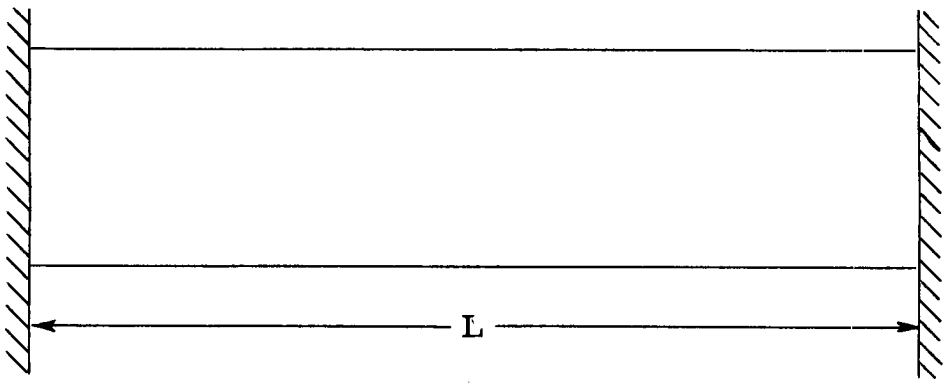

Figure 17. Simple Beam

Therefore, substituting in formula (7) for n = 1

$$f_a = \frac{\pi}{2\pi} \sqrt{(K_a)\left(\frac{1}{L}\right)\left(\frac{L}{M}\right)}$$

$$f_a = \frac{1}{2} \sqrt{\frac{K_a}{M}} = \frac{1}{2} \sqrt{\frac{386}{W} K_a} \tag{8}$$

for fundamental accordion mode.

F. SIMPLIFIED FREQUENCY DETERMINATION OF LATERAL MODES

1. Incremental Circumferential Spring Analogy

For a uniform beam clamped or fixed at both ends and neglecting the axial forces, the following formula in Reference 18 is usually used to calculate beam lateral frequencies,

$$\omega_1 = A_n \sqrt{\frac{EI}{\mu_1 L^4}} \tag{9}$$

where A_n = numerical constant which depends on manner of constraint, for the clamped-clamped beam the values for successive modes are 22.0, 61.7, 121.0, 200.0, 298.2, etc.

EI = bending stiffness in the lateral direction, lb-in.^{2}

μ_1 = mass per unit length, lb-sec^2/in.^{2}

L = length of beam (bellows), in.

E = modulus of elasticity, lb/in.^{2}

I = moment of inertia, in.^{4}

To apply Equation (9) to a bellows, it is necessary to express bellows elasticity in terms of the simple beam elastic parameter EI. To accomplish this, consider a simple beam (Figure 17) of a length L equal to the bellows length (Figure 19). The bellows has been represented as n masses connected in series by n springs. If K_A is the longitudinal total effective or compressive stiffness of the complete bellows, then the longitudinal stiffness of one segment is $k = K_A (n)$.

The elastic equivalence of the bellows and the simple beam has been established in terms of the angular deflections, θ, resulting from the application of a pure moment T to a segment of a simple beam and a bellows segment. (Figures 18 and 20).

For the case of the simple beam increment, the relationship between the segment moment T and resulting angular deflection θ is well known as:

$$\frac{T}{\theta} = \frac{EI}{l}$$

where l is the length of the segment (one or more convolutions).

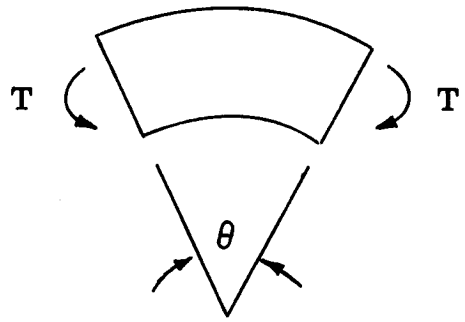

Figure 18. Pure Moment Applied to Segment of Simple Beam

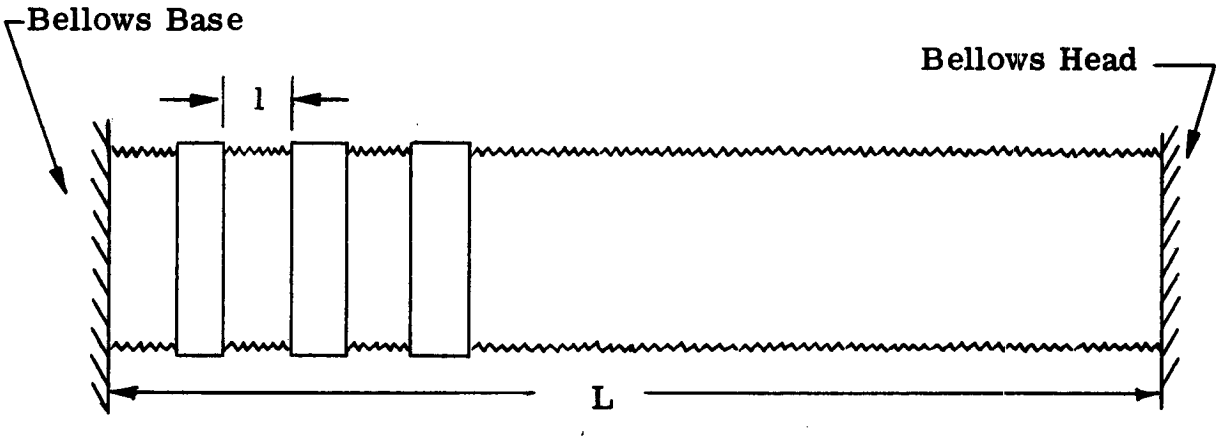

Figure 19. Bellows Represented as a System of Concentrated Masses Connected By Massless Springs Around the Circumference

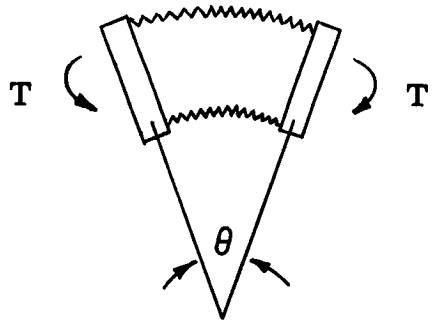

Figure 20. Pure Moment Applied to Segment of Bellows

For bellows segments of equal length, we may define $\frac{T}{\theta} = \frac{k_\theta}{l}$, where k_θ is the angular spring rate,

then $\left(\frac{T}{\theta}\right)_{\text{simple beam segment}} = \left(\frac{T}{\theta}\right)_{\text{bellows segment}}$

so that $$(EI)_{\text{bellows}} = k_\theta = \left(\frac{T}{\theta}\right) l_{\text{bellows}} \tag{10}$$

Thus to find the effective EI for the bellows, it is necessary only to determine the ratio of the applied moment T to the resulting deflection θ per unit length of bellows. This is accomplished in the following development.

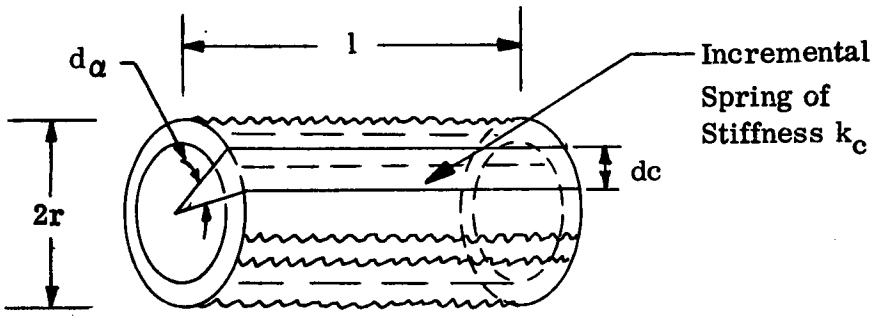

Figure 21. Segment of Bellows Showing Massless Springs

Figure 21 represents the bellows segment with stiffness k in the longitudinal direction, r is the effective radius of the bellows, assumed as the mean radius of the convolutions. Since the spring extends around the circumference of the segment, the longitudinal stiffness per unit length along the circumference c will be the same value.

$$k_c = \frac{k}{c} \quad \text{lb/in./in. circumference} \tag{11}$$

If a moment T is applied to the bellows segment as indicated in Figure 22, each increment $\overline{dc}$ of spring along the circumference will undergo either an extension or contraction. The incremental springs above the center line extend. Those below the center line contract. As shown by Figure 22, a given incremental spring at a distance h above the center line will experience a change in length y due to application of the moment T. The <u>force</u> experienced by the incremental spring will be given by:

$$F_{dc} = k_c \, (\overline{dc})y \tag{12}$$

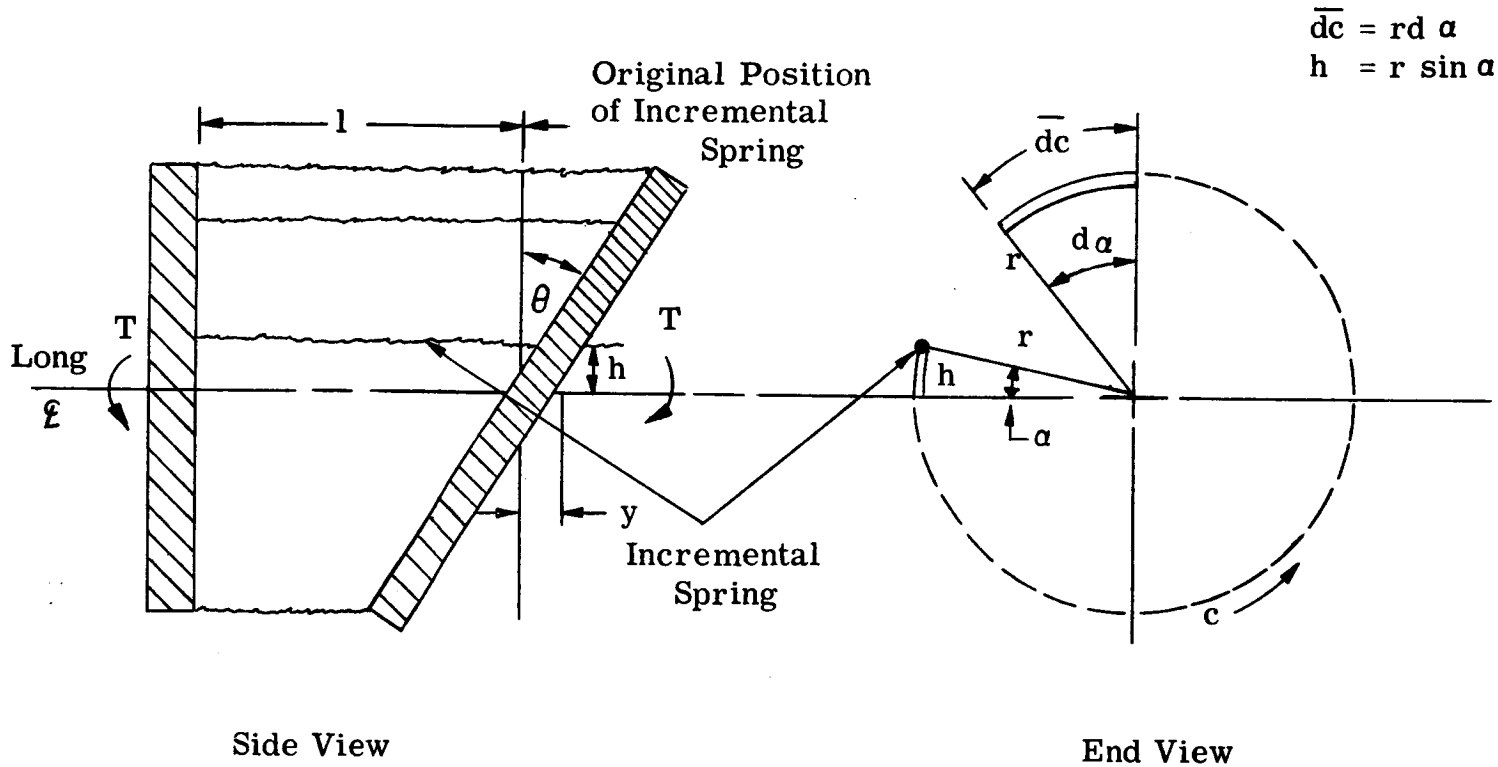

Figure 22. Segment of Bellows Showing Massless Springs in Deflected Position

For small θ , $y = h\,\theta$

Thus, Equation (12) becomes:

$$F_{dc} = k_c \quad (\overline{dc})\ (h)\ (\theta) = \frac{k}{c}\ (\overline{dc})\, h\theta \tag{13}$$

Moreover, the <u>moment</u> about the centerline will be:

$$T_1 = F_{dc} \quad h = \frac{k}{c}(\overline{dc})h^2\,\theta \tag{14}$$

Referring to Figure 22, it becomes apparent that:

$\overline{dc} = rd\ \alpha$ while $h = r \sin \alpha$. Making these substitutions into Equation (14), the following equation will evolve:

$$T_{dc} = \theta\ \frac{k}{c}\ r^3(\sin^2 \alpha)\ \ d\,\alpha \tag{15}$$

The moment T will be the integral of the moments around the circumference with respect to d :

$$T = \int_0^{2\pi} \theta \frac{k}{c}\ r^3(\sin^2 \alpha)\ \ d\,\alpha \tag{16}$$

Since $c = 2\pi r$ (while k, r, and θ are constants), Equation (16) may be written as:

$$\frac{T}{\theta} = \frac{kr^2}{2\pi} \int_0^{2\pi} (\sin^2 \alpha)\, d\ \alpha \tag{17}$$

Since $\displaystyle\int_0^{2\pi} (\sin^2 \alpha)\ d\,\alpha = \left[\frac{1}{2}\alpha - \frac{1}{4}\sin(2\alpha)\right]_0^{2\pi} = \pi$

Equation (17) becomes:

$$\frac{T}{\theta} = \frac{kr^2}{2\pi}\ (\pi) = \frac{kr^2}{2} \tag{18}$$

Applying Equation (18) to Equation (10):

$$(EI)_{Bellows} = \left(\frac{kr^2}{2}\right)\ l \tag{19}$$

where k is the stiffness of one bellows segment and l is the length of the segment. However, notice that Equation (19) assumes that the spring rate k for each convolution is the same and that k_c around the circumference is also the same. In a physical

bellows, this may not be true because each leaf is formed separately and two leaves are welded to form a convolution separately.

If there are n segments (n masses),

$$\text{then } k = K_A(n) \tag{20}$$

$$\text{and } l = \frac{L}{n} \tag{21}$$

Using Equations (20) and (21) in Equation (19):

$$EI = \frac{K_A r^2 L}{2} \tag{22}$$

Moreover, on the basis of Equation (22), Equation (9) may be written:

$$\omega_1 = A_n \sqrt{\frac{K_A r^2 \frac{L}{2}}{\mu_1 L^4}} = A_n \sqrt{\frac{K_A r^2}{2 \mu_1 L^3}} \tag{23}$$

2. Handbook Formula Adaption

A second method was also used to develop an equivalent EI in terms of the longitudinal total effective spring rate K_A, lb/in.

$$\omega_1 = A_n \sqrt{\frac{EI}{\mu L^4}}$$ Den Hartog formula for lateral vibrations (9)

$$\delta = \left(\frac{1}{384}\right) \cdot \left(\frac{WL^3}{EI}\right)$$ Clamped - clamped beam with uniform load, Reference 19, page 108.

$$\delta_1 = \left(\frac{1}{384}\right) \left(\frac{L^3}{EI}\right)$$ Deflection for unit load $\frac{\delta}{W}$ (24)

$$K_L = \frac{384\ EI}{L^3}$$ K_L = lateral spring rate lb/inch $= \frac{1}{\delta}$ (25)

And, transposing for EI:

$$EI = \frac{L^3 \quad K_L}{384} \tag{26}$$

By Hooke's Law, as shown before:

$$K_A = \frac{A\,E}{L}$$

or

$$E = \frac{K_A\,L}{A} \tag{27a}$$

by substitutine Equation (27) into Equation (25):

$$K_L = \left(\frac{384I}{L^3}\right) \cdot \left(\frac{K_A L}{A}\right) = \frac{384\ I\ K_A}{L^2 A}$$

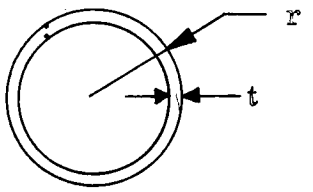

Assume bellows is a thin cylinder of thickness t

Area of Cylinder: $A_C = 2\ \pi\ r\ t$

Inertia of Cylinder: $I_C = \pi\ r^3\ t$ (Reference 19, page 72)

$$K_L = \frac{(384)\ (\pi\ r^3 t)\ (K_A)}{L^2\ \ 2\ \pi\ (rt)} = \frac{384\ r^2\ K_A}{2L^2}$$

Substituting K_L into Equation (26):

$$EI = \left(\frac{L^3}{384}\right) \cdot \left(\frac{384\ r^2\ K_A}{2\ (L)^2}\right) = \frac{K_A\ \ r^2\ L}{2}$$

which agrees with Equation (22).

G. CORRECTION OF LATERAL FREQUENCIES FOR AN INTERNAL PRESSURE

The lateral resonant frequency decreases with increases in internal pressure. This fact was also reported in Reference 20 which states:

> "The effect of differential pressure upon the lateral stability of bellows is similar to the axial loading of columns or to the stability of springs with an axial load. The analytical solution for the stability of bellows with axial load may be treated in a manner similar to that shown in 'Vibration Problems in Engineering' by Timoshenko or in 'Mechanical Springs' by Wahl. The critical buckling is a function of the end condition and the effective physical properties of the bellows. The applied load is a function of the applied differential pressure and the effective area. Where the internal pressure is higher than the external pressure, i.e., for a negative pressure differential, a decrease in

the lateral frequency will occur. The effect of either a positive or a negative pressure differential will be negligible upon the longitudinal resonance of the bellows."

From Timoshenko (Reference 21), the following expression is obtained for a column simply supported under axial loading:

$$f_p = f_1 \sqrt{1 + \frac{P}{n\, P_{CR}}} \tag{27b}$$

where (+) is used for negative pressure differentials, and (-) for positive pressure differentials

P_{CR} = critical column buckling force, lb

P = axial force (tension positive, compression negative, lb)

f_1 = natural frequency, cps

f_p = corrected natural frequency, cps

n = mode number 1, 2, 3

$$P_{CR} = \frac{4\pi^2 EI}{L^2} \quad \text{for a beam with clamped ends} \tag{27c}$$

(Note: the value 4 may be too high for most practical cases)

Both the test data shown in Reference 20 and the test data obtained at Bell Aerosystems Company on the 4-inch diameter bellows indicate that the lateral frequency decreases with increases in internal pressure. Tests, described later, on the same 4-inch bellows show that positive pressure differentials of 200 psi and negative pressure differentials of 6 psi had no affect on the longitudinal accordion mode frequencies. A negative pressure differential with no vibration at 10 psi (24.7 psia internal pressure) created a compression force sufficient to cause snaking of the bellows (see Figure 23). Lateral frequencies decreased with negative pressure differentials of 2 to 6 psi because of slight distortion of the bellows due to internal pressures. Resonant frequencies obtained for any pressure condition were the same whether the input vibration was applied during increasing or decreasing frequency sweeps thus indicating bellows linearity at fixed extensions. The fundamental lateral mode decreased from 16.2 cps with zero internal pressure to a value of 9.7 cps with 6 psi internal pressure. The third harmonic decreased from 61 cps to 53.7 cps when 6 psi was applied.

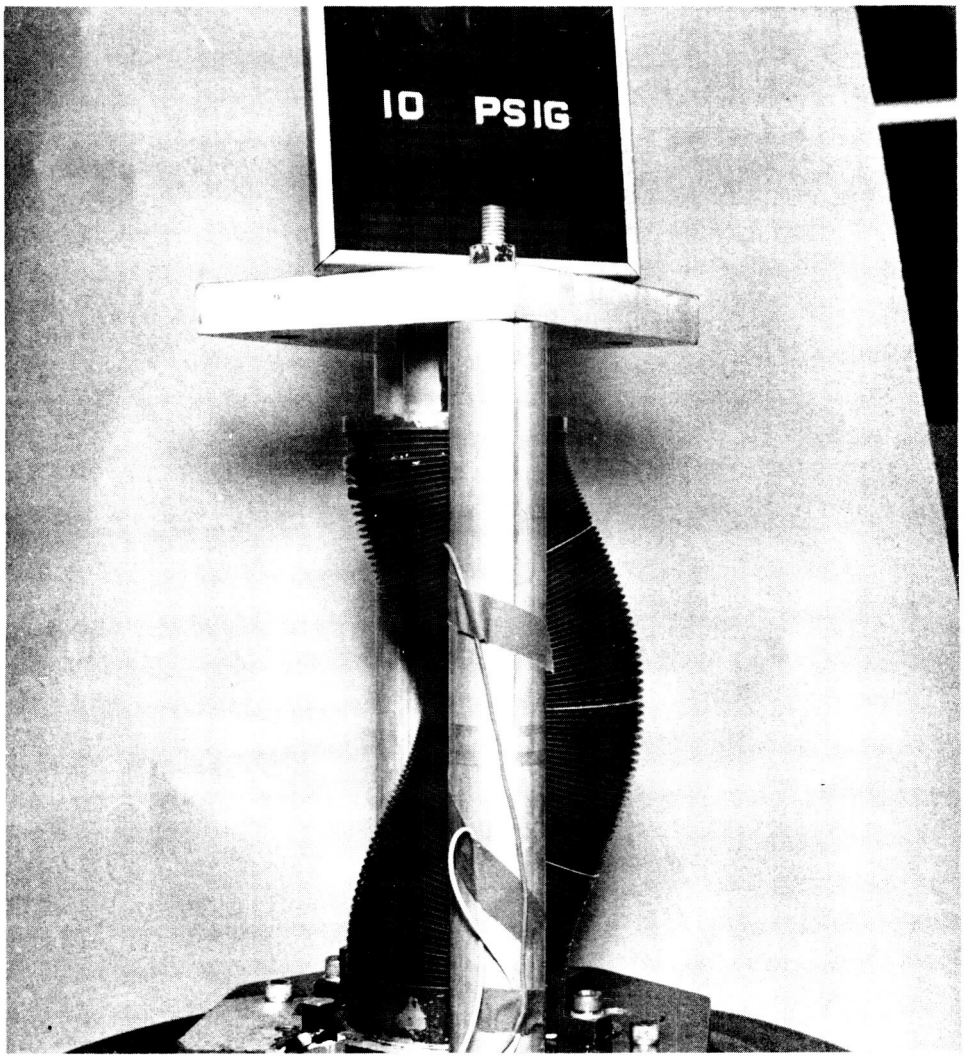

Figure 23. Bellows Distortion with Internal Pressure

H. OTHER RESONANT CONDITIONS INVESTIGATED

As stated in the introduction, only those areas considered significant dynamically were investigated in detail during this program. One particular area of initial concern was local resonance of a leaf since vibratory strains superimpose on static strains. In addition, each leaf which is welded at the outer and inner diameters should be designed such that local leaf resonance will not be excited during service environments. Further, if local leaf resonance occurs the leaf could "flip" back and forth which is again an undesirable condition. This phenomenon of "flip" is not clearly understood; further investigations are warranted for optimization of leaf design.

The following calculations will show that, because of the combined factors of high spring rate of each leaf, short spans and low mass, resonance will only occur at frequencies much higher than the conventional 3000 cps limit presently in use in this country. In addition, the liquid inside the leaves will have the tendency to dampen out this resonance. These calculations are based upon the assumption that a flat thin leaf behaves quite similar to a single sweep leaf contour or nesting design.

I. RESONANT FREQUENCY OF A LEAF

A procedure for calculating the lowest natural frequency of an annular plate, analogous to the resonant frequency of a bellows leaf, is presented in Reference 23. The method allows either of two mounting conditions to be investigated:

(1) Inner and outer edges clamped

(2) Inner and outer edges simply supported or free

The plate to be considered is the first of the two cases:

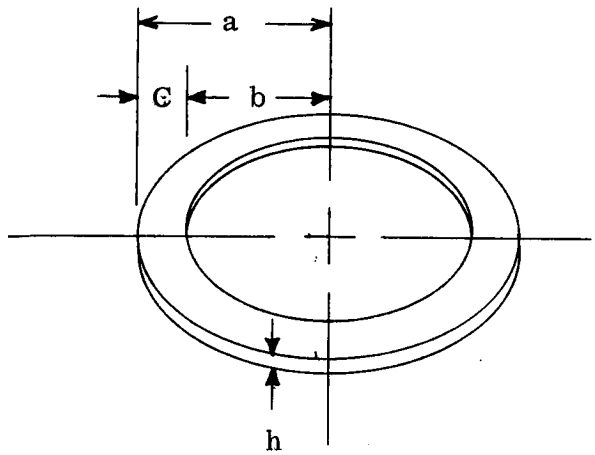

(Figure 1 from Reference 23)

The formula for determining the frequency f_c of such a plate is given in Reference 23 as:

$$f_c = q\, u^2 \left(\frac{h}{b^2}\right) \sqrt{\frac{E}{\rho m}} \tag{28}$$

where h = thickness of the plate (same as thickness for a bellows leaf), in.

b = inside radius of plate (bellows), in.

ρm = mass density, slugs/in.^{3}

E = Young's modulus of elasticity, lb/in.^{2}

q = dimensionless factor dependent upon Poisson's ratio, ν

u = parameter which is a function of a/b and the type of restraint

C = plate span (bellows), in.

a = outside radius of plate (bellows), in.

The parameter u was determined from an eigen value analysis involving Bessel functions. Graphs of u vs a/b for a clamped-clamped plate, as well as q vs u, are presented in Reference 23, Figure 2. These graphs only give data for $\frac{a}{b}$ ratios down to 2.2. On the 4-in., 7-in., and 10-in. bellows shown in Table 2, these ratios are 1.18, 1.16, and 1.12, respectively.

Equation (28) was evaluated for a steel annular plate for constant C = 0.5 inch which is a representative value for leaf spans under consideration and various a/b = J. The results are summarized in Table 3.

As a comparative study, it was decided to investigate the fundamental frequency of a representative wedge of the annular plate by using Den Hartog's formula for a clamped-clamped plate. The frequency formula (9) in this instance is

$$f_1 = \frac{22.0}{2\pi} \sqrt{\frac{EI}{\mu_1 L^4}} \tag{33}$$

f_1 being equivalent to f_c in this application and,

$I = \frac{dh^3}{12}$ where d and h are dimensions of the wedge shown by the dashed lines in Reference 23, (Figure 1).

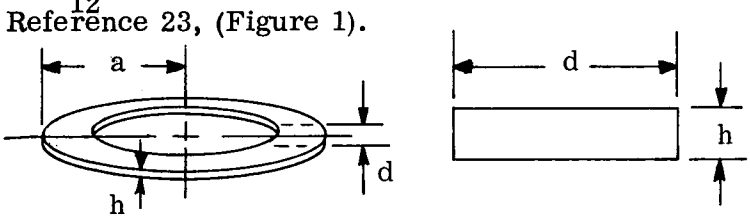

d = unit distance of 1 in.
h = 0.006

$$I = \frac{(1)\,(0.006)^3}{12}$$

TABLE 3

LEAF FREQUENCY SUMMARY

For steel, $\nu = 0.3$, $q = 0.04815$ (from Figure 2 of Reference 6)

$E = 30 \times 10^6$ psi $\qquad h = 0.006$ in.

$\rho_m = 0.000733$ lb-sec^2/in.^{4}

Let: $\frac{a}{b} = J \qquad (29)$

$a-b = C = 0.5 \qquad (30)$

then $a = \frac{CJ}{N-1} \qquad (31)$

$b = \frac{C}{J-1} \qquad (32)$

J = a/b	u	b (in.)	a = (b + 0.50) (in.)	f = 58.5 (u/b)^2 (cps)
20	0.25	0.026	0.526	5280
10	0.50	0.0566	0.556	4725
6	0.925	0.1000	0.600	5000
4	1.530	0.166	0.666	4920
3	2.300	0.250	0.750	4940
2.8	2.580	0.278	0.778	5040
2.6	2.900	0.311	0.811	5060
2.4	3.300	0.356	0.856	5000
2.2	3.900	0.417	0.917	5125

$I = 0.018 \times 10^{-6}$ in^4; $E = 30 \times 10^6$ lb/in.^{2} so that $EI = 0.540$ lb-in.^{2}

The mass per unit length of circumference $\mu_1 = dh\,\rho_m$

where $\mu_1 = 0.044 \times 10^{-4} \dfrac{\text{lb-sec}^2}{\text{in.}^2}$. Substituting in Equation (33):

$$f_c = \frac{22.0}{2\pi L^2}\sqrt{\frac{0.540}{0.044 \times 10^{-4}}} = \frac{12.5 \times 10^2}{L^2}$$

If L is set equal to C = 0.5 in. (span from the previously discussed calculations), then f = 5000 cps, which agrees favorably with frequencies previously determined by the method of Reference 23. Thus, it appears that this latter approach to frequency determination is as acceptable as the method of Reference 23.

Further, it appears that the 7-in. and 10-in. bellows tested with 0.5 in. spans would have local leaf resonances of approximately 5000 cps because increasing the outer diameter has only a second order affect on the leaf resonant frequency, especially as the $\frac{a}{b}$ ratio approaches unity.

J. LONGITUDINAL LIQUID DISPLACEMENT MODES

In addition to convolution movement in the accordion mode, there exists another mode of response during vibration which is herein arbitrarily named the liquid displacement mode. In this mode, considerable longitudinal bellows head displacement was observed in contrast to the negligible head motion during the accordion modes. Also, measurements of the liquid pressures inside the bellows have indicated the presence of finite pressure oscillations. A phase angle change of 180 degrees between base input acceleration and internal dynamic pressure exists at a fundamental frequency and at approximately each odd integer multiples of this fundamental. Longitudinal convolution motion is also present; however, the mode shape depends upon several things, one of which is the relative location of the liquid displacement mode to its adjacent accordion modes. Lateral motion is also present during these modes especially when the bellows is extended to large L/D ratios.

Observations of the free liquid surface were also made while sinusoidal vibration was applied to the head and base of the 4-in. diameter bellows in a inverted position (Figure 24). Considerable liquid spray was present when vibrating at the fundamental liquid displacement mode frequency of 87 cps. To minimize the free surface spray, a jelling agent was added to the liquid and thin wooden sticks placed in the free surface of the resulting jelled liquid mass. The longitudinal axes of the sticks were parallel to the longitudinal axis of the bellows. This allowed the motion of the liquid free surface to be studied under stroboscopic light. The bellows-jelled liquid system was vibrated at the fundamental liquid mode frequency. All sticks were seen to move longitudinally and in phase with each other. This

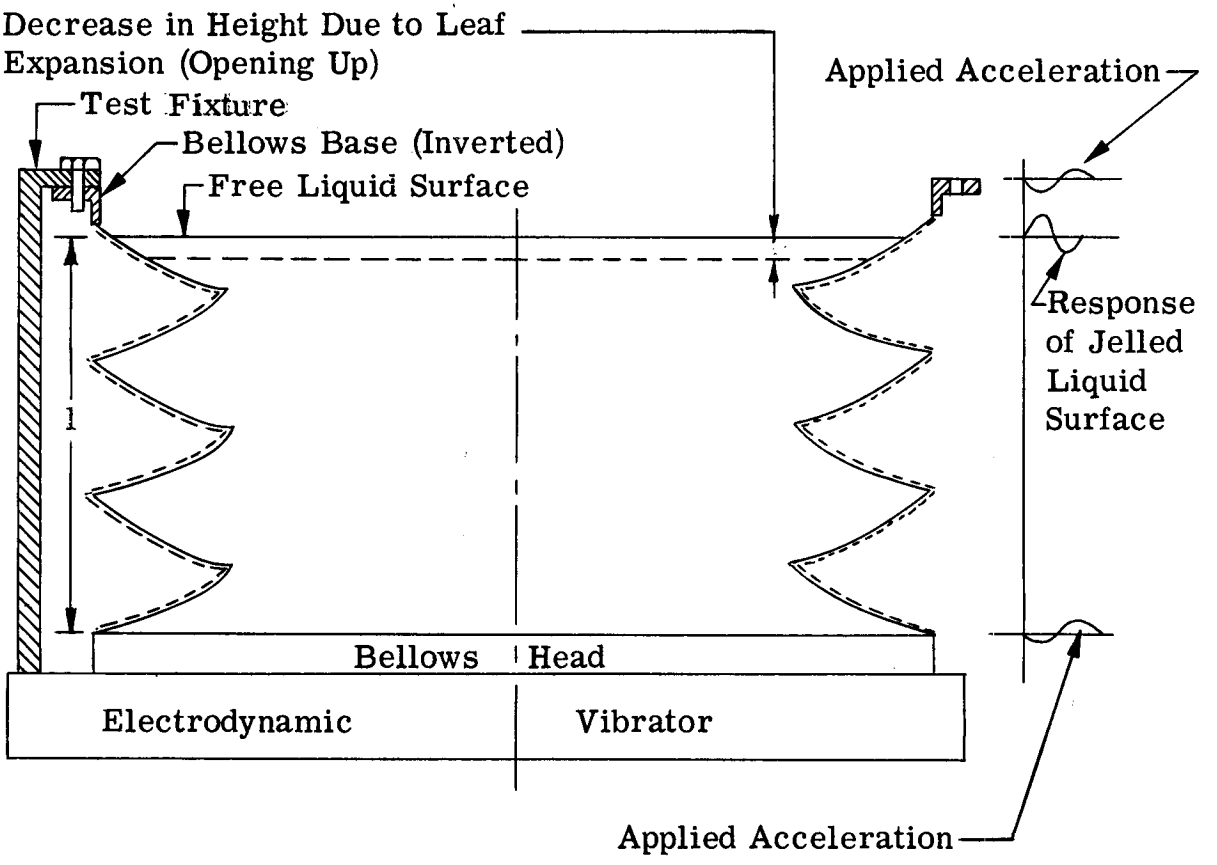

Figure 24. Liquid Displacement Mode

appears to indicate that each 'slab' of jelled liquid remains within a plane. However, the fundamental frequency was observed to be slightly higher than that of the unjelled liquid. This increase in frequency was probably due to the viscosity of the jelling agent or slight change in bellows end restraint.

With the exception of the research study presented in NASA report No. 7129-933003 by B. B. D'Ewart (Reference 10) no mention of the above phenomena was found in the available literature on bellows. Mr. D'Ewart's explanation of a thin wall vessels "breathing" mode could be considered analogous, to the liquid mode phenomenon experienced by the bellows. However since this phenomon is not completely understood a further investigation is warranted.

Mr. D'Ewart found that a liquid filled plastic container would "breathe," that is, expand radially when subjected to longitudinal vibrations. This mode exists as a result of the elastic deformation of a tank and is a function of the tank size, material, skin gages and fluid density. He showed that the experimental "breathing" mode frequency was within 5 percent of the computed frequency. This mode is similar to the extensional mode shown in Reference 22, Table 7-11 for circular rings whose thickness in a radial direction is small compared to the radius.

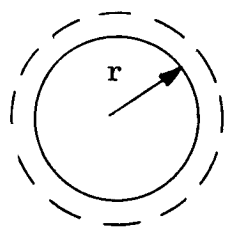

Sketch A. Shell or Ring Extensional (Radial or "Breathing" Mode)

The mode in Sketch A is quite different from the mode shown in Sketch B which represents flexure in plane of ring with n complete wave lengths in circumference.

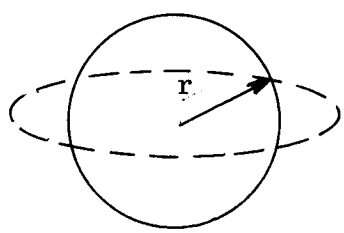

n=2

Sketch B - Shell or Ring Flexure Mode

The deformation of the tank shell (loop strains) due to radial liquid motion can be equated to stored potential energy and is analogus to a simple spring in a single degree of freedom system. An outward radial movement of the shell to the dotted

position shown in Sketch (A) causes the free liquid surface to decrease in height. The natural frequency ω_d of the tank radial mode was given in Reference 10 as:

$$\omega_d = \frac{1.11}{l} \sqrt{\frac{Et}{\rho_m r}} \qquad \text{radians/sec}$$

where E = the cylinder modulus of elasticity, lb/in.^{2}

t = cylinder wall thickness, in.

ρ_m = fluid mass density, lb-sec^2/in.^{4}

r = cylinder radius, in.

l = distance from the bottom of the cylinder to the free surface, in.

The elasticity of the plastic cylinder in Reference 10 can be compared to the elasticity of each bellows leaf. The potential energy will be stored as additional leaf membrane and bending strains.

Figure 24 shows how the expansion of the leaves can produce a lowering of the free surface. Conversely, a contraction of the leaves produces a raising of the free surface. If a bellows head is attached to the top leaf, this head will fall and rise similar to that observed on the sinusoidal vibration tests previously mentioned. Eventually it is hoped that the leaf membrane and bending strains will be supplied as an output of the IBM Program No. 1753 discussed in Section 3. These strains must be added to those produced by the accordion mode response. With these strains, a formula to predict the natural frequency of the liquid displacement mode should be possible.

K. CALCULATION OF THE 4-INCH BELLOWS RESPONSE DURING VIBRATION

A bellows spring rate of 10.8 lb/in. was obtained by two experimental methods. Section 4, L, discusses analytical methods used to determine spring rate.

The first method was to obtain head deflection measurements with a dial gage versus increasing amounts of internal pressures. Multiplying the ΔP times bellows effective area gave force which was divided by the deflection to give spring rate. The second method was to attach a massive weight and velocity pickup to the bellows head and slightly displace the head such that a decay amplitude at constant frequency, f, was displayed on a Brush recorder.

Substitution of the frequency into the following expression (Reference 18) gave the longitudinal total effective spring rate K_A:

$$f = \frac{1}{2\pi} \sqrt{\frac{K_A}{M + \frac{m}{3}}} \qquad M = \frac{W}{g}; \; m = \frac{w}{g} \tag{34}$$

where: f = frequency of decay signal, cps

W = attached weight, bellows head weight, velocity pickup weight, and attachment hardware, lb

w = weight of bellows convolutions, lb

1. Accordion Mode Frequencies:

$$f_{a_1} = \frac{n}{2} \sqrt{\frac{K_A}{M}} \qquad n = 1, 3, 5, 7 \tag{8}$$

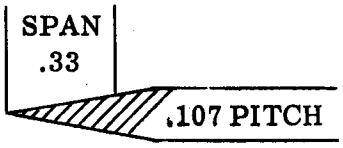

$$f_{a_1} = \frac{n}{2} \sqrt{\frac{K_A \; g}{W_t + W_m}}$$

$$f_{a_1} = \frac{1}{2} \sqrt{\frac{10.8\ (386)}{1.85}} \qquad p = \frac{10.7 \text{ in.}}{100} = 0.107 \text{ PITCH}$$

f_{a_1} = 23.9 cps $\qquad W_t = \frac{1}{2} C\ p\ \pi\ ND_m\ \rho$ (6)

f_{a_3} = 71.7 cps $\qquad W_t = 1/2\ Cp\ \pi . N\ D_m\ \rho$

f_{a_5} =119.5 cps $\qquad W_t = (1/2)(0.33)(0.11)(\pi)(100)(3.97)(0.0362) = .82$ lb

f_{a_7} =167.0 cps

W_m = bellows weight = 1.00
W_t = trapped water = 0.82
1.82 lb

2. Lateral Mode Without Pressure

$$\omega_1 = A_n \sqrt{\frac{K_A\ r^2}{2\mu\ L^3}} \tag{23}$$

$$f_1 = \frac{A_n}{2\pi} \sqrt{\frac{K_A\ r^2}{2\ \mu_1\ L^3}} = \frac{A_n}{2\pi} \sqrt{\frac{K_A\ r^2\ g}{2(W_t + W_m + W_i)L^3}}$$

$$f_{l_1} = \frac{22.0}{2\pi} \sqrt{\frac{(10.8)(1.986)^2\ (386)}{(2)\ \ (5.84)\ \ (10.7)^3}}$$

$$f_{l_1} = 12.25 \text{ cps}$$

$$f_{l_2} = \frac{61.7}{22}\ (12.25) = 34.3 \text{ cps}$$

$$f_{l_3} = \frac{121}{22.0}\ (12.25) = 67.4 \text{ cps}$$

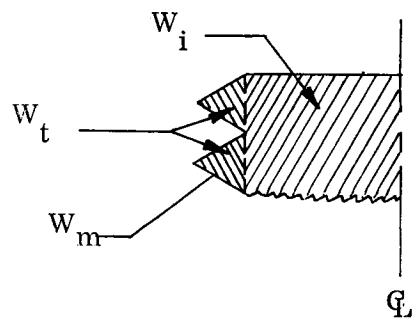

W_i = Weight of water inside bellows

$= (0.7854)(3.644)^2\ \ (10.7)(0.0362)$

$= 4.02$ lb

$W_t = 0.82$

$W_m = 1.00$

$W_i = \frac{4.02}{5.84}$ lb

3. Lateral Mode with Increased Internal Liquid Pressure

The above lateral frequencies will now be adjusted using EI values calculated in Reference 20 and by using equivalent EI values established in this report.

From Reference 20:

$$E_{EFF} = \frac{K_A L}{A} = \frac{(10.8)(10.7)}{4.06} = 28.5 \text{ lb/in.}^2 \tag{27a}$$

$$A_{EFF} = 0.7854(D_o^2 - D_i^2$$

$$= 0.7854\ (4.30^2 - 3.64^2) = 4.06 \text{ in.}^2$$

$$I_{EFF} = 0.7854 \left[\left(\frac{D_o}{2}\right)^4 - \left(\frac{D_i}{2}\right)^4 \right] = 8.14 \text{ in.}^4$$

$$P = A_{EFF} \text{ (pressure)}$$

$$P = (4.06)\ (-2) = -8.12 \text{ lb}$$

$$P_{CR} = \frac{4\pi^2\ E_{EFF}\ I_{EFF}}{L^2} \tag{27c}$$

$$P_{CR} = \frac{4\pi^2}{10.7^2}\ E_{EFF}\ I_{EFF}$$

$$P_{CR} = 0.345\ E_{EFF}\ I_{EFF}$$

$$P_{CR} = (0.345)\ (28.5)\ (8.14) = 80.0 \text{ lb (Reference 20 method)}$$

However,

$$P_{CR} = 0.345\ K_A\ r^2\ \frac{L}{2}$$

$$= 0.345\ (10.8)\ (1.986)^2\ \left(\frac{10.7}{2}\right)$$

$$= 78.6 \text{ lb (Using Equation (22) substitution for EI)}$$

Table 4 shows the detailed calculations using the second method. Figure 25 compares the calculated frequencies with the test results obtained from the 4-in. bellows vibration test.

L. SPRING RATE:

Previous experience on other vibration problems indicated that it would be necessary to establish a spring rate for each leaf and then, somehow, combine these springs to obtain the over-all equivalent spring rate.

From the literature search, the only formula that appears to apply to welded-disc bellows is in Reference 14 (Stevens, Sealol):

K_A = longitudinal total effective spring rate, lb/in.

$$K_A = \frac{\pi E D_m}{N} \cdot \frac{h^3}{C^3}$$

where: E = Young's modulus, lb/in.^{2}

D_m = Mean Diameter, in.

N = number of convolutions

h = convolution thickness, in.

C = span, in.

Although this approximate formula does not take into account spring rate changes due to leaf shape, pressure, etc., it nevertheless provides a spring rate in the elastic range to start an analysis. This spring rate would be on the increasing strain portion of the hysteresis curve shown in Figure 26.

The spring rate for bellows extensions beyond the linear elastic range at the present time in this country must be obtained by experimental means. It is hoped,

TABLE 4. LATERAL FREQUENCY CALCULATION

Lateral Resonant Frequency for Fundamental Mode where n = 1

$$f_p = f_1 \sqrt{1 + \frac{P}{n^2 P_{CR}}}$$

p	P	$\frac{P}{(1)\ P_{CR}}$	$1 + \frac{P}{(1)\ P_{CR}}$	$\sqrt{1 + \frac{P}{(1)\ P_{CR}}}$	f_p
0	0	0	1.0	1.0	16.0
2	-8.12	-0.103	0.897	0.945	15.12
4	-16.24	-0.207	0.793	0.890	14.23
5	-20.30	-0.258	0.742	0.860	13.75
6	-24.36	-0.310	0.690	0.830	13.28

Lateral Resonant Frequency for Third Mode where n = 3

$$f_p = f_1 \sqrt{1 + \frac{P}{n^2 P_{CR}}}$$

p	P	$\frac{P}{9\ P_{CR}}$	$1 + \frac{P}{9\ P_{CR}}$	$\sqrt{1 + \frac{P}{9\ P_{CR}}}$	f_p
0	0	0	1.0	1.0	60.5
2	-8.12	-0.011	0.989	0.994	60.1
4	-16.24	-0.023	0.977	0.987	59.7
5	-20.30	-0.029	0.971	0.985	59.5
6	-24.36	-0.034	0.966	0.982	59.4

The lateral resonant frequency as calculated by the method of Reference 20 is essentially the same as that calculated previously since the difference between the value of P_{CR}, as calculated by both methods, is small.

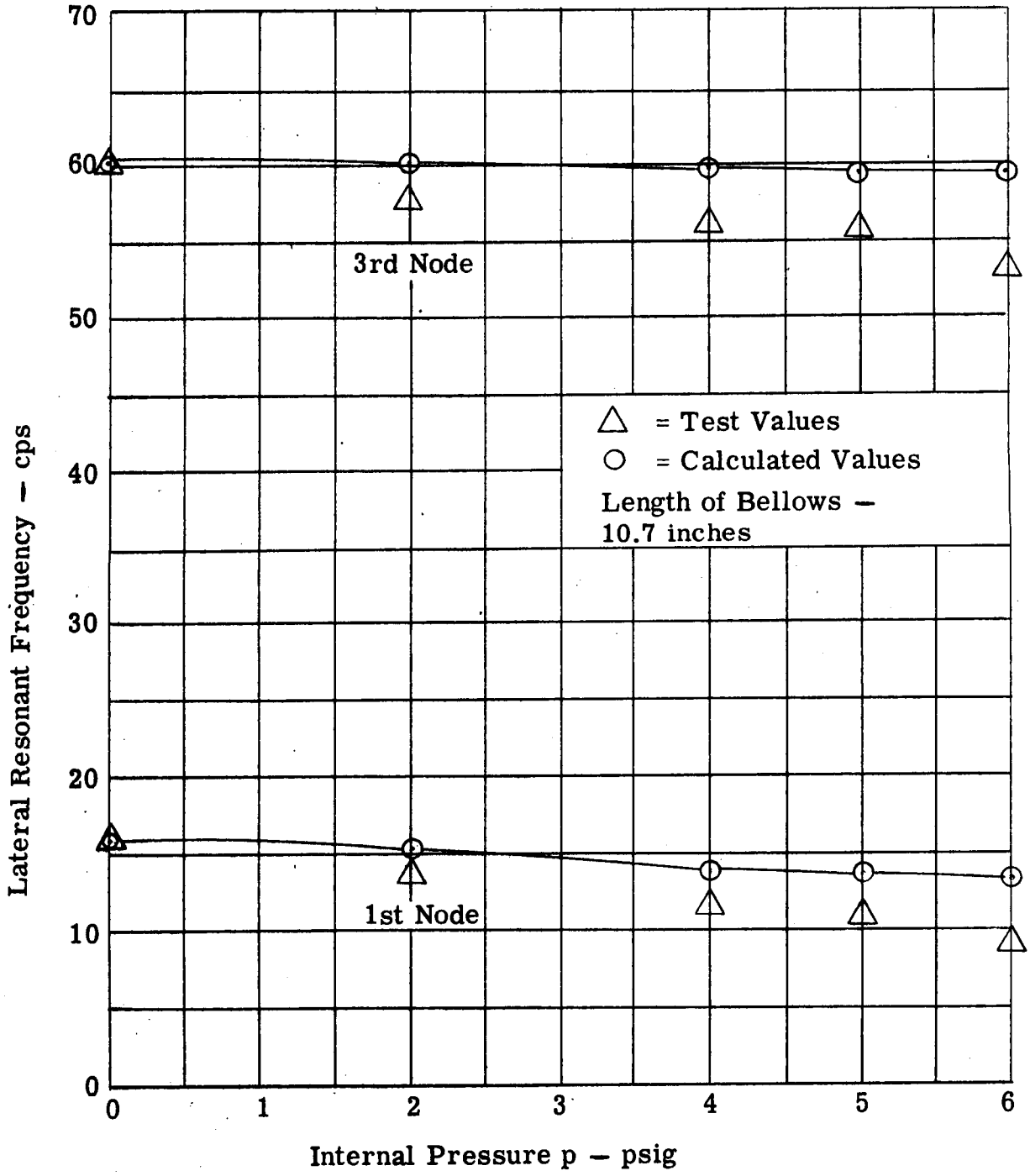

Figure 25. Lateral Resonant Frequency Versus Internal Water Pressure of a 4 Inch Diameter Bellows

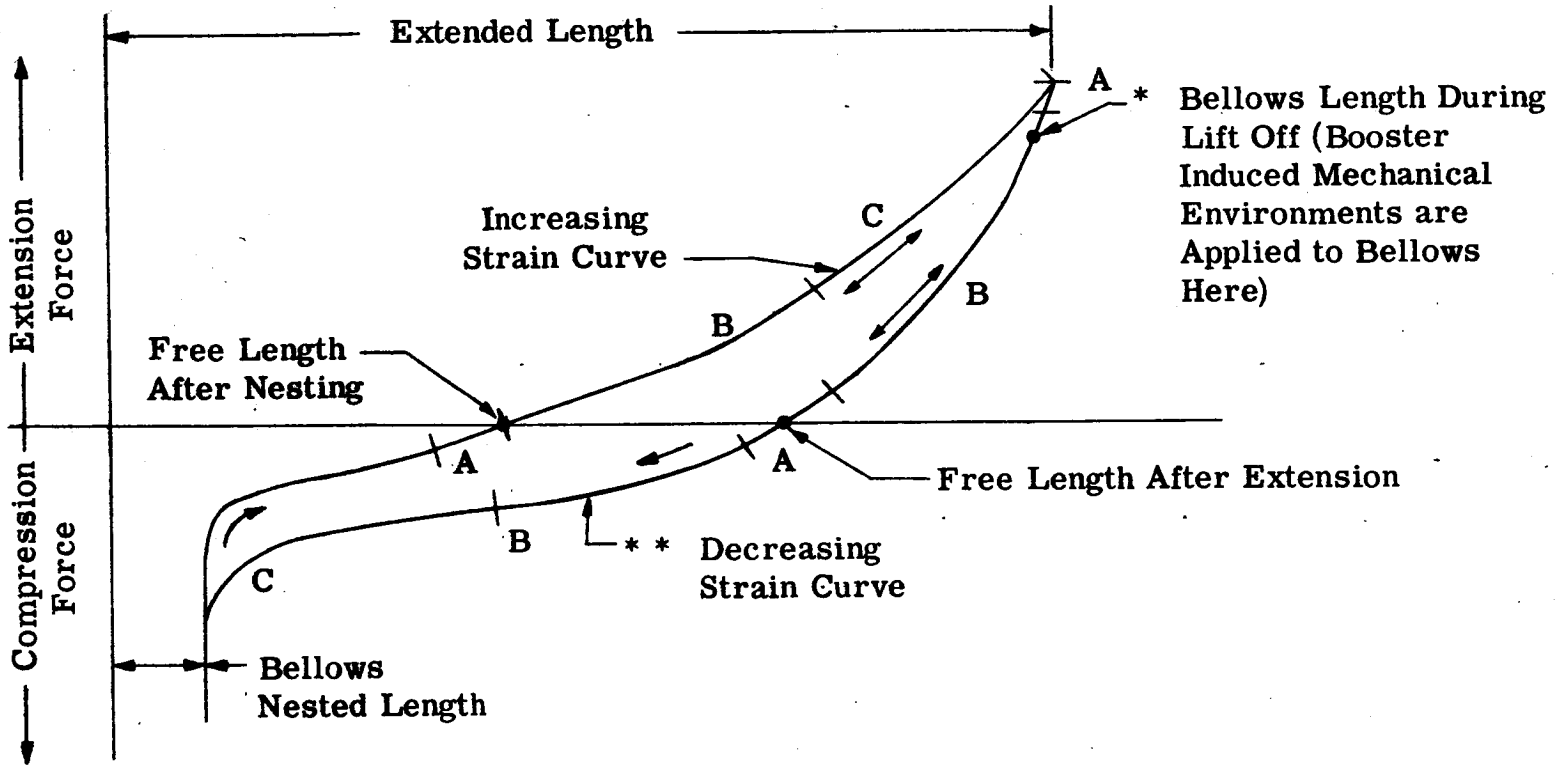

A - Linear Elastic (straight and reversible)

B - Geometric Non-linearity (curved and reversible)

C - Physical Non-linearity (curved and irreversible)

* - Represents fully loaded position. Maximum bellows capacity at extended length less ullage volume allowance for propellant temperature compensation.

** - Vibration always occurs along this curve when bellows are extended beyond linear elastic range. Because motions are relatively small during vibrations, the spring rate usually remains constant at any fixed bellows extended length.

Figure 26. Hysteresis Curve

however, that IBM program 1753 discussed in Section 3 can be expanded to compute digitally this data for a bellows dynamic analysis. Either a load-deflection technique or a decay amplitude technique can be used. Both methods are described elsewhere in this report. If a prototype bellows is not available, these techniques can be used to determine the spring rate per convolution on a test capsule and this value divided by the number of convolutions in the prototype.

It should be emphasized that because of the variation in spring rate for different bellows extensions (static pitches) and associated effective masses, the resonant frequencies will vary throughout a missile flight as propellant is consumed. Figure 27 shows how the longitudinal and lateral fundamental frequency varies at different bellows positions. Test experience to date has also shown that the amplification factor at resonance in each mode tends to increase with decreasing bellows extension. This may be due to different amounts of viscous damping present at various extensions, caused perhaps by having the internal weld head shearing the stagnant liquid column.

M. VIBRATION TESTING OF 4-INCH BELLOWS

1. Sinusoidal Vibration Tests

Sinusoidal vibration tests were conducted on the 4-in. bellows periodically throughout the contract period to obtain visual proof of the various calculated modes of response. This 4-in. bellows was donated by the Sealol Corporation, Providence Rhode Island and is shown mounted for vibration in Figure 28. Written descriptions of these modes, X-Y plots, pulse camera movies, still photographs, etc, were recorded at time of test. Movies of this bellows are being submitted to NASA simultaneously with the submittal of this report. All vibration tests were conducted in the elastic range with a bellows length of 10.7 in. measured from the first to the 100th convolution.

2. Longitudinal Vibration

During sinusoidal longitudinal vibration, at each frequency the response acceleration of the convolution tips was divided automatically by the input acceleration at the bellows base. This true transmissibility system, developed at Bell Aerosystems Company, reflects the absolute value of Q at a specified convolution versus input frequency; Q is defined as normalized acceleration, i.e., output acceleration divided by input acceleration. The dynamic range of this equipment is set at 20 to 1; thus a Q response of less than 1 will usually be plotted as 1 and peaks over 20 will be flat. Figures 29, 30, and 31, respectively, show the center convolution acceleration, dynamic pressure at head, and dynamic pressure at the bellows base during vibration with the head fixed to the vibration fixture at zero psig liquid pressure (fixture same as used for lateral tests in Figure 4-24). Dynamic pressure during vibration is defined herein as the pressure variation about the absolute static pressure. Figures 32, 33, and 34 show the same information with the head restraint fixture removed, at 2 3/4 psig liquid pressure, this pressure is necessary to

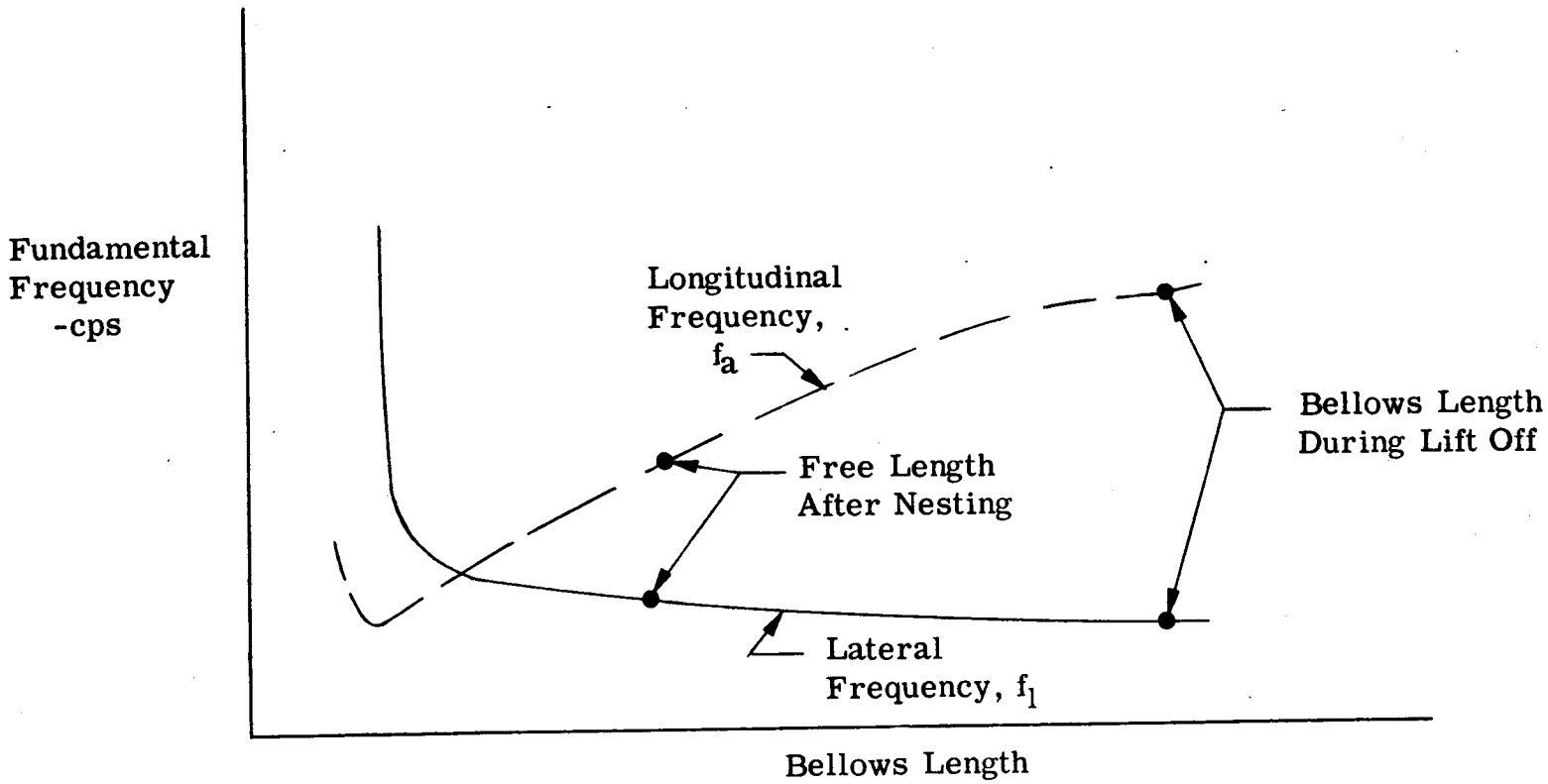

Figure 27. Frequency versus Length Curve

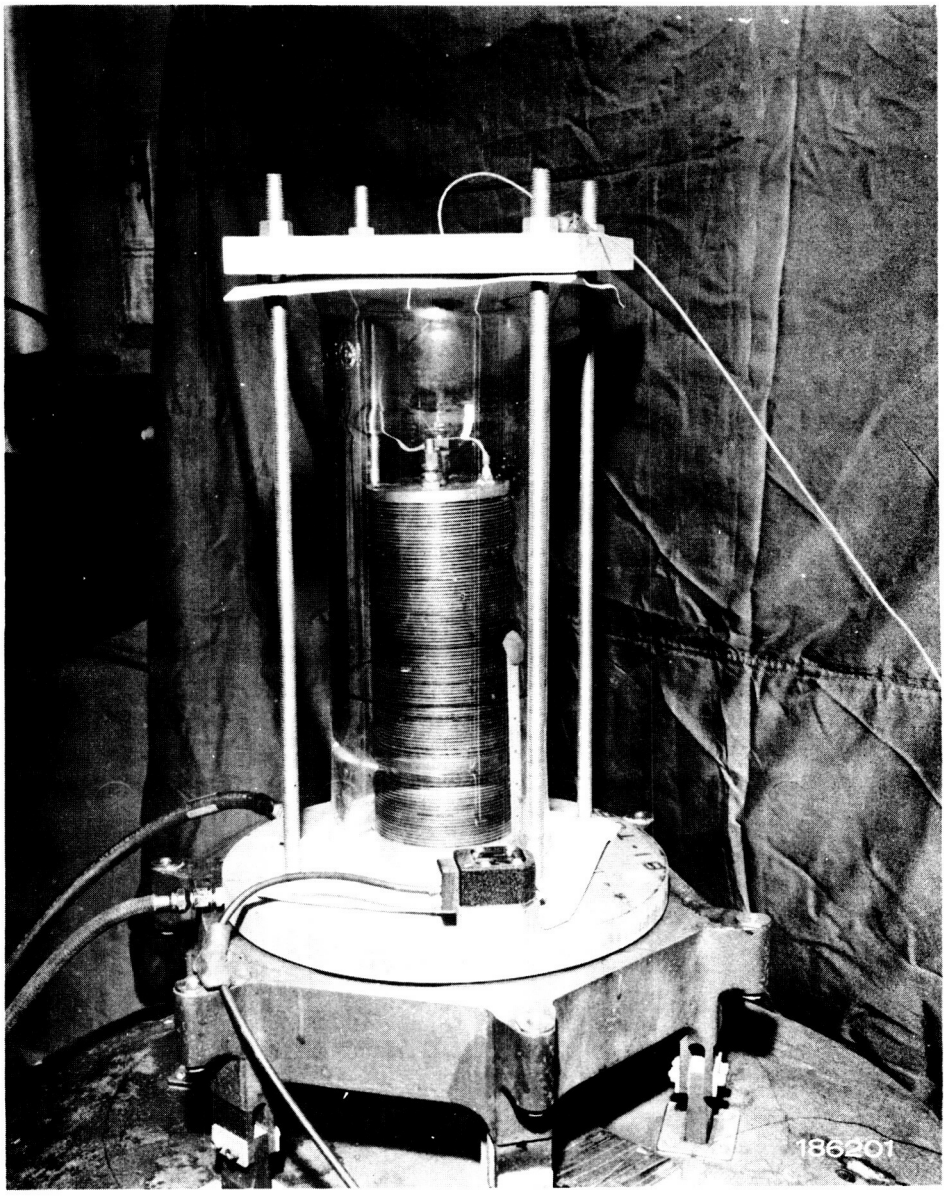

Figure 28. 100-Convolution Bellows in Pyrex Pipe

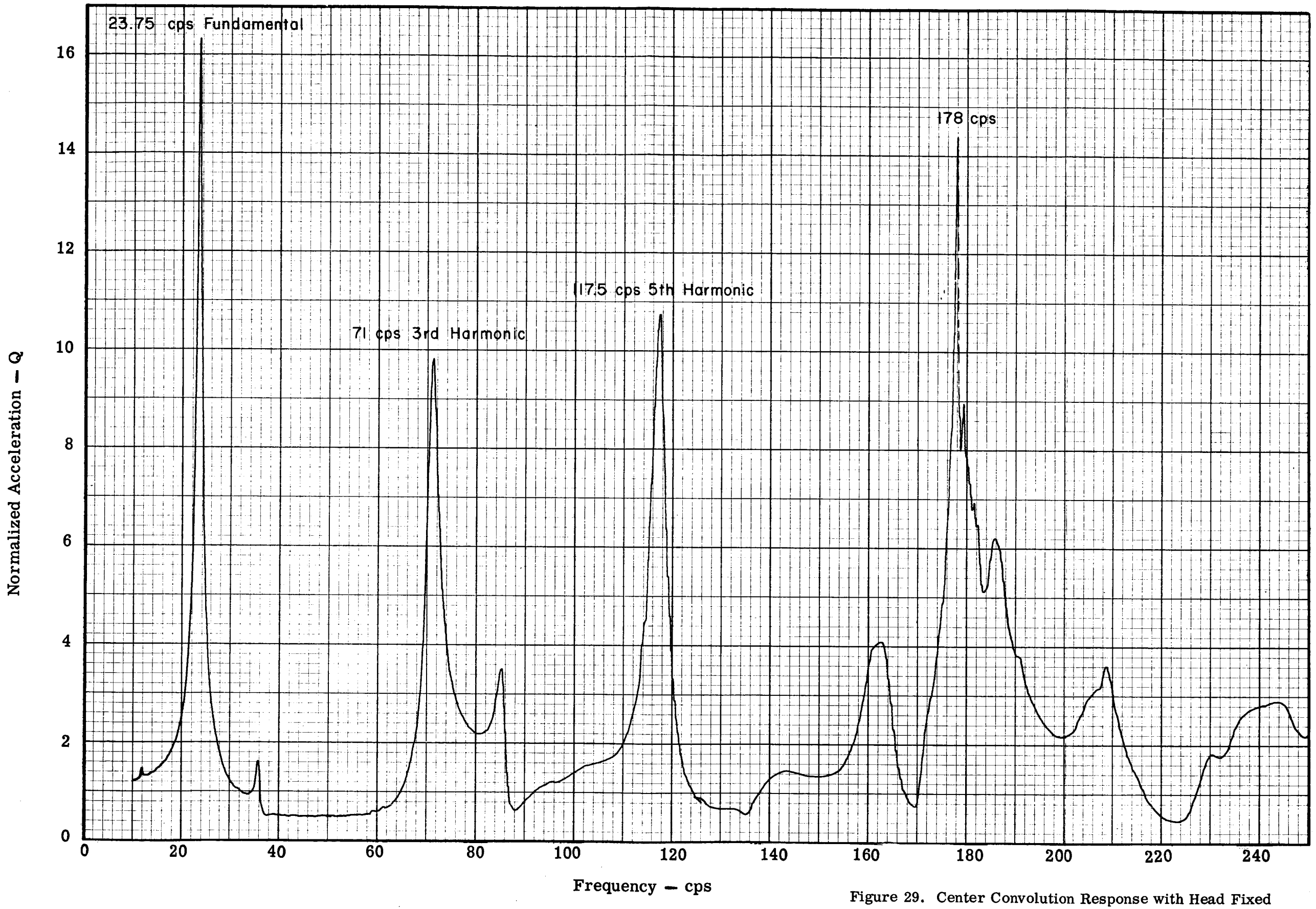

Figure 29. Center Convolution Response with Head Fixed

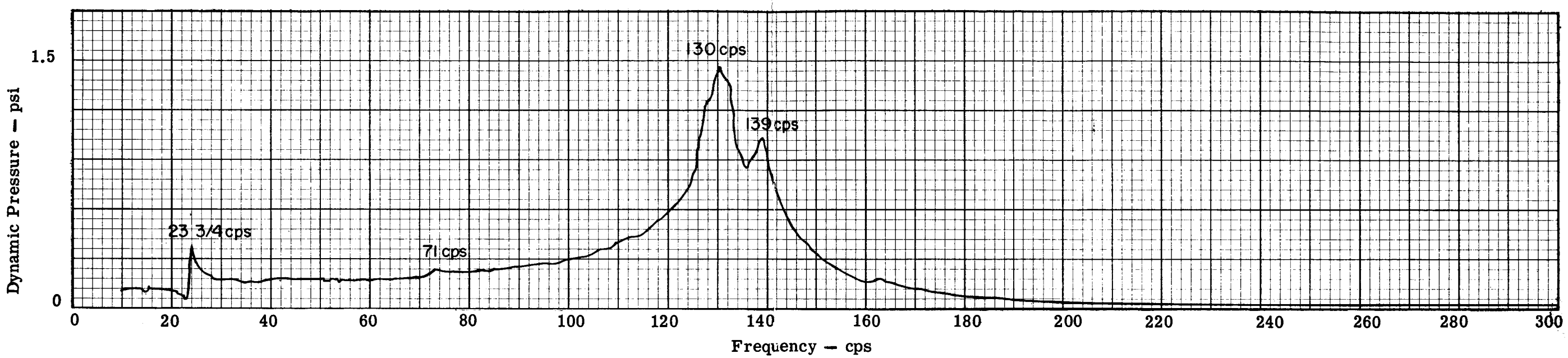

Figure 30. Head Dynamic Pressure with Head Fixed

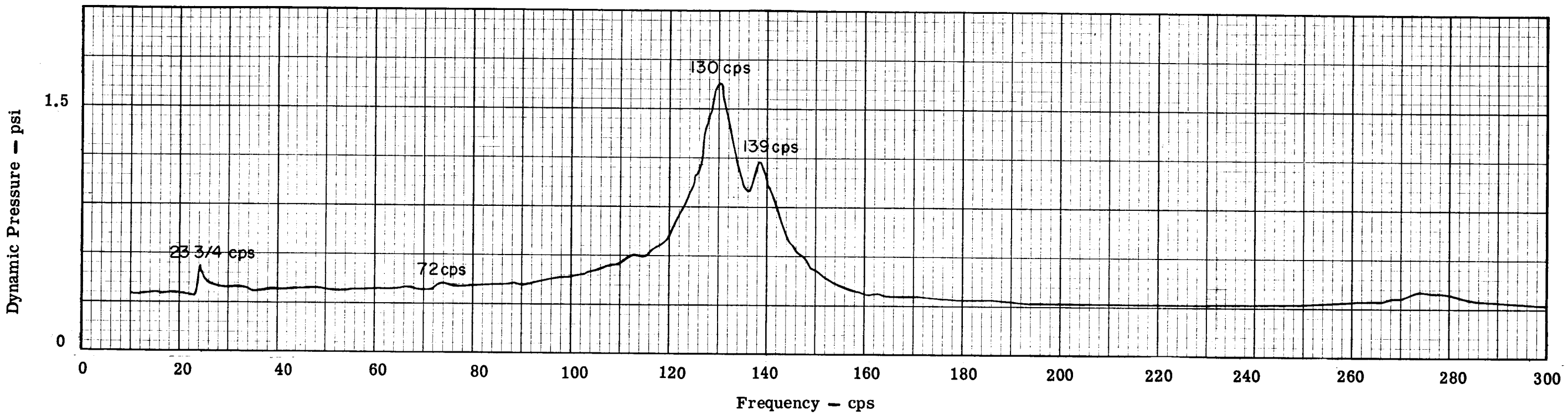

Figure 31. Base Dynamic Pressure with Head Fixed

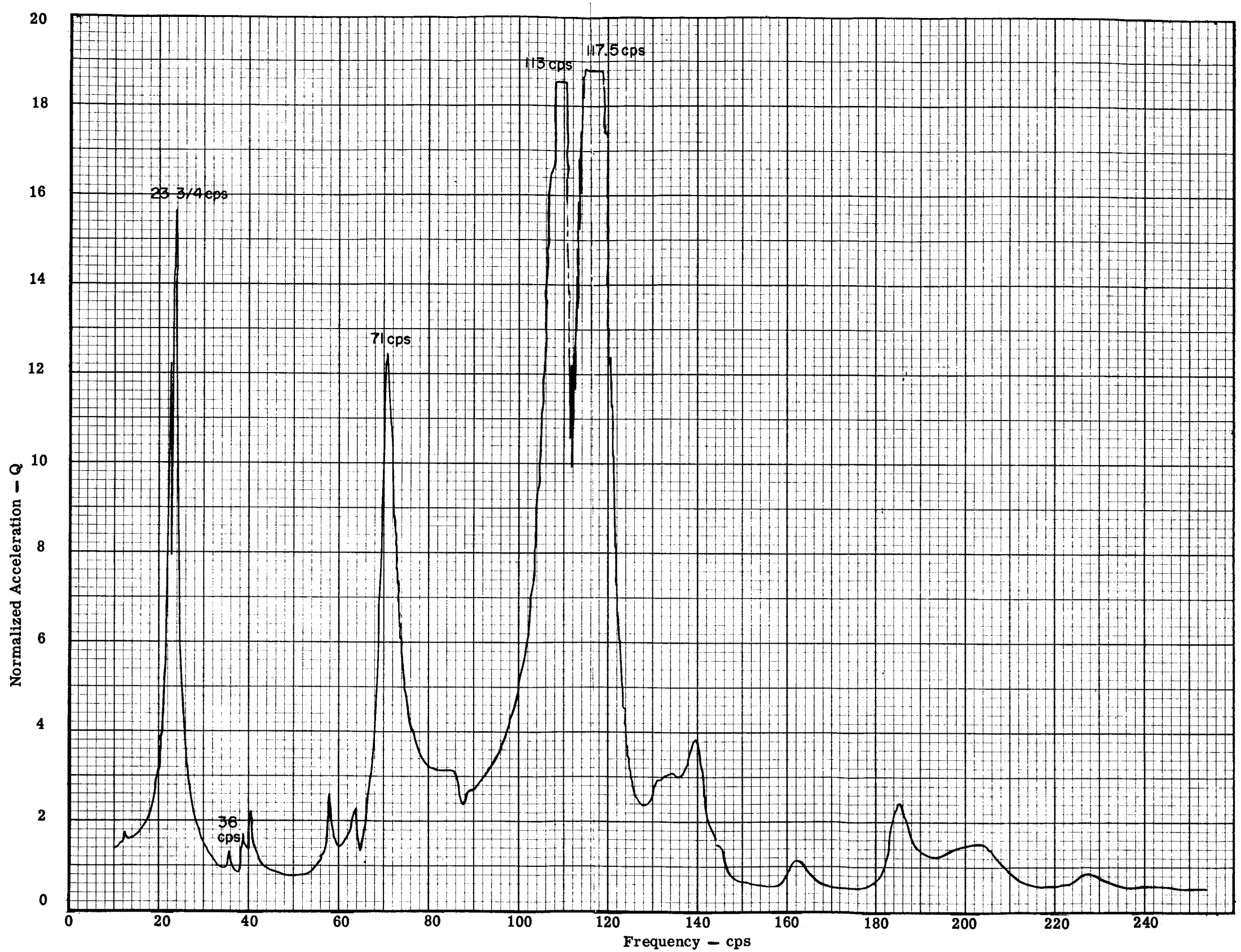

Figure 32. Center Convolution Response with Head Free

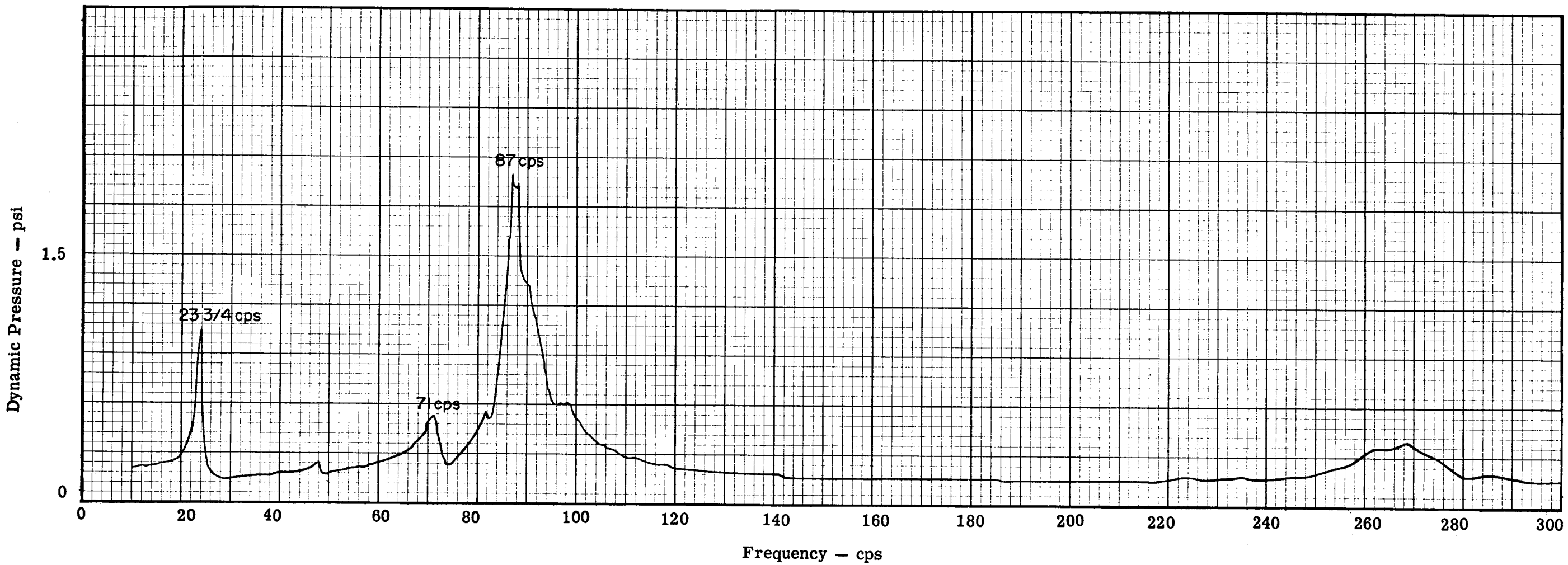

Figure 33. Head Dynamic Pressure with Head Free

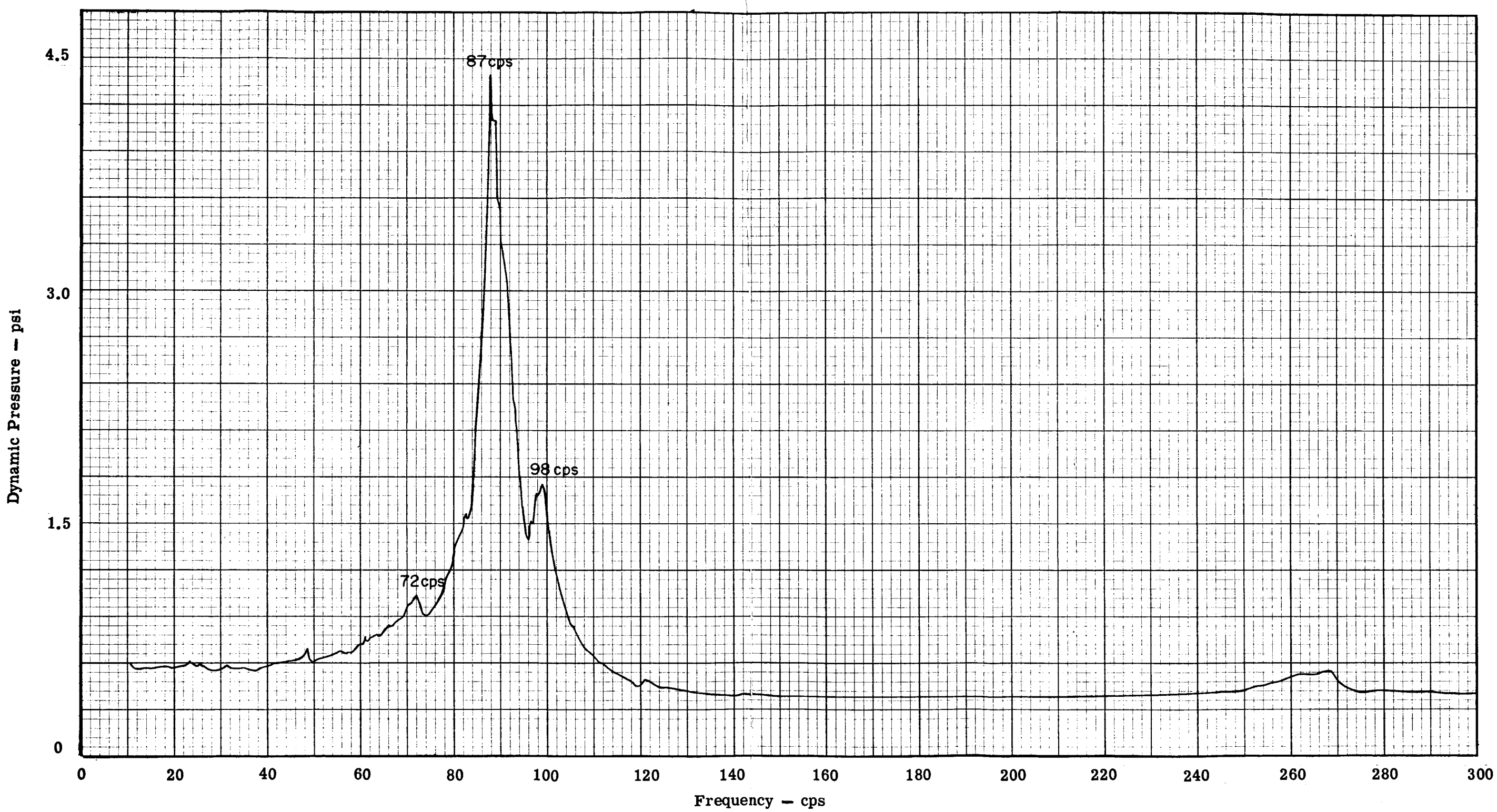

Figure 34. Base Dynamic Pressure with Head Free

maintain the bellows length of 10.7 in. Figure 35 shows head acceleration with head free.

When in service, the bellows head will be a small distance from the tank shell head. This provides an ullage space to compensate for propellant expansion.

Response identification is as follows:

(1) Figures 29 and 32 - Bellows center convolution.

		Number of Nodes
23 3/4 cps	Fundamental accordion mode nodes at base and head.	2
36 cps	Minor lateral model	-
71 cps	3rd harmonic accordion mode.	4
117.5 cps	5th harmonic accordion mode.	6
178 cps	7th harmonic accordion mode.	8

(2) Figure 35 - Head response.

23 3/4 cps and 71 cps	Minor reaction to accordion mode response.
87 cps	Fundamental liquid displacement mode.

(3) Figures 30 and 33 - Dynamic pressure at bellows head.

Figures 31 and 34 - Dynamic pressure at bellows base.

23 3/4 and 71 cps	Minor reaction to accordion mode response.
130 cps	Liquid displacement mode with head fixed.
87 cps	Liquid displacement mode with head free.

From these data and response of the other convolutions, the following conclusions are made:

At the Accordion Modes

(1) The resonant frequencies of each convolution is not affected by head restraint, i.e., the same frequency can be obtained with the head fixed or free; only a slight change in amplitude of response was measured.

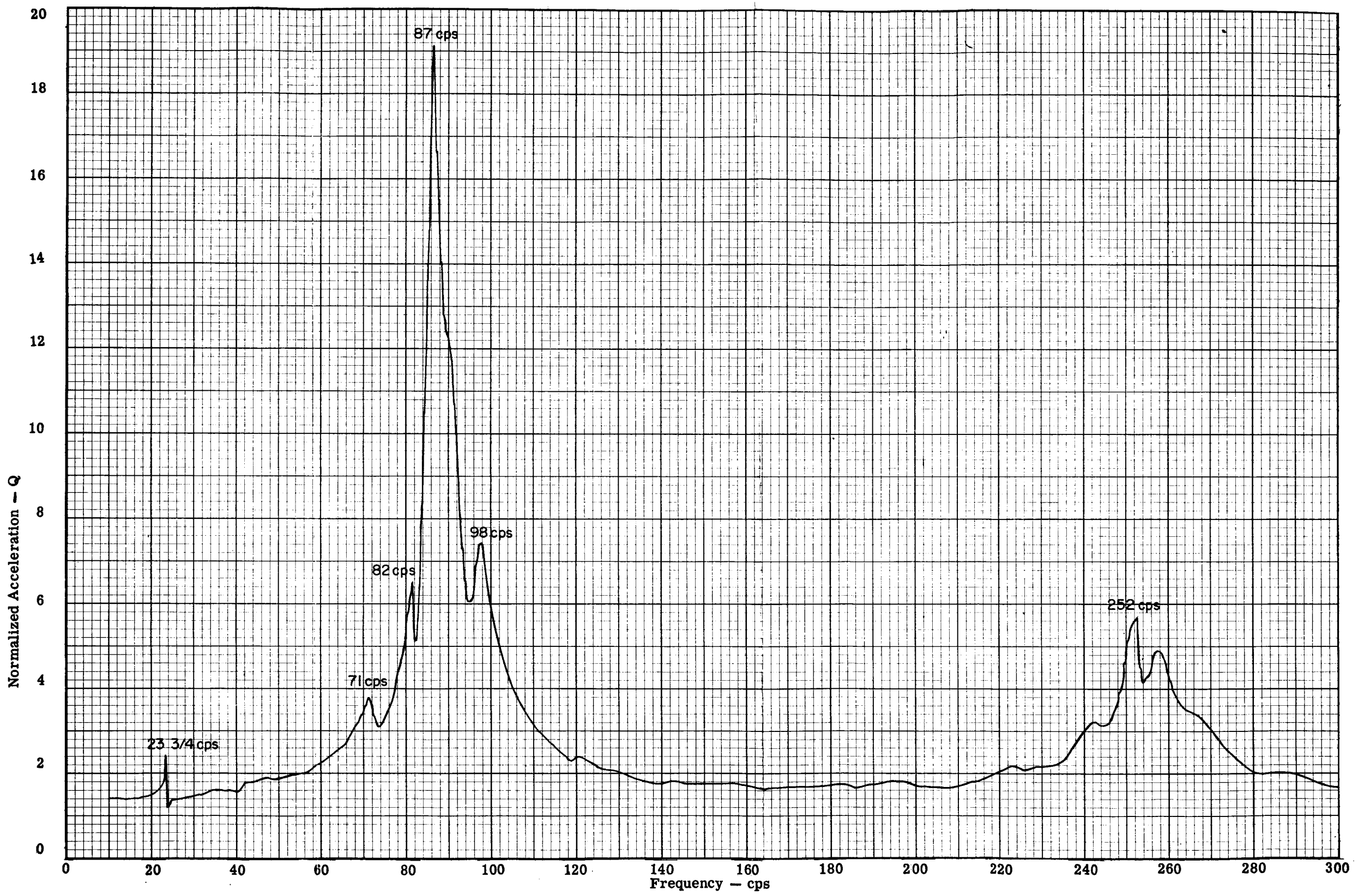

Figure 35. Head Response with Head Free

(2) Little or no head motion is present.

(3) It appears that the inside diameter weld beads are shearing the stagnant internal liquid column.

(4) No response at fractional multiples of the fundamental frequency occurs during vibration.

(5) Little or no cross-coupling of longitudinal and lateral modes of vibration occurs.

At the Liquid Displacement Mode

(1) Both frequency and amplitude of dynamic pressure response vary with the degree of head restraint.

(2) Head motion is present only when these modes are excited.

(3) From item (2), it follows that the total trapped volume of fluid inside the convolutions increases when the head is moving toward the base.

(4) Dynamic pressure resonance occurs at the base and head even if both ends of the bellows is restrained during vibration.

(5) For the free head case the pressure rise is greater at the bellows base.

(6) Both longitudinal and lateral motions are present.

Additional sinusoidal vibration tests conducted on the 7 inch bellows more-clearly defined accordion and liquid displacement modes of response. Figures 36 through 39 describe convolution motion at the first and third accordion modes and fundamental liquid displacement mode. Figure 39 also compares the fundamental liquid displacement mode with the fundamental accordion mode.

N. INTERNAL AND EXTERNAL PRESSURE EFFECTS ON ACCORDION MODE RESPONSE

Figure 28 shows the vibration set-up used to evaluate the effect of external gas pressure on the accordion modes. Resonance of the center convolution was held at 23 3/4 cps while increasing the pressure to 200 psig. Observations of the motion under stroboscopic light revealed that external pressure did not affect the fundamental accordion mode.

The Pyrex pipe was removed and 6 psig was applied to the water contained inside the bellows. Accelerometer plots made of the center convolution revealed that internal pressure did not affect the fundamental accordion mode.

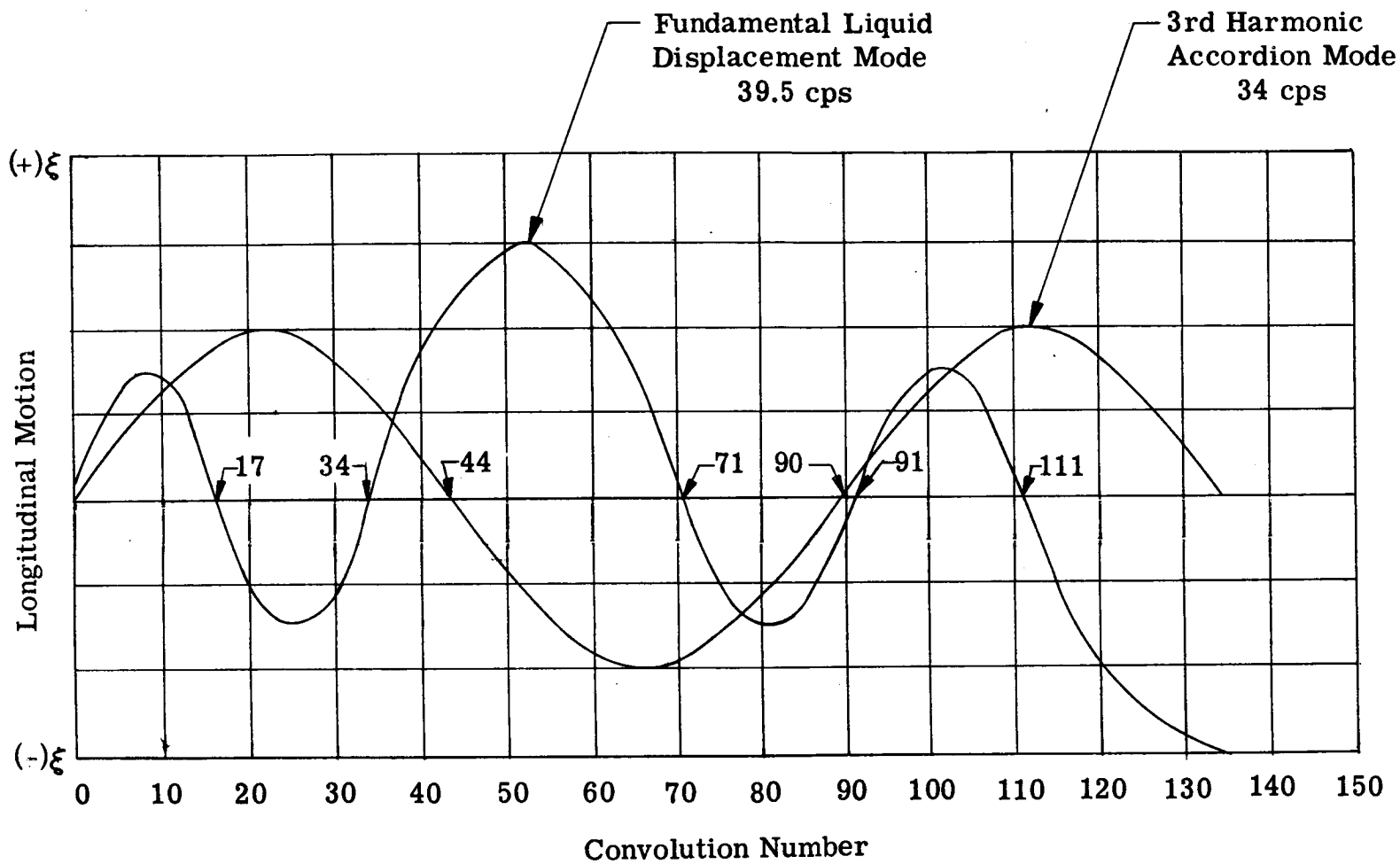

Figure 36. Liquid Displacement Mode of 7 Inch Bellows Compared to Third Harmonic Accordion Mode

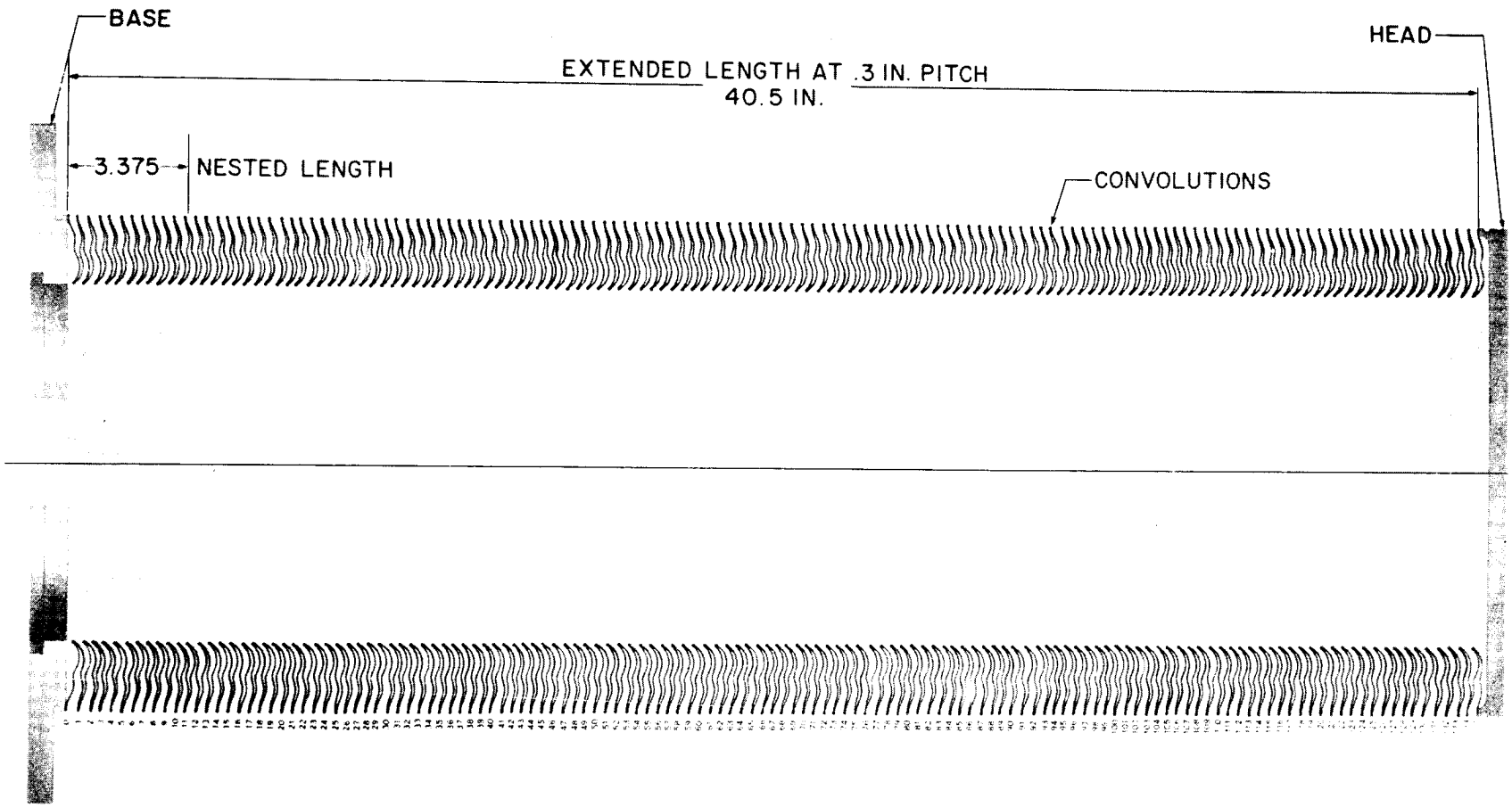

NO. OF CONVOLUTIONS	135
LEAF THICKNESS	.006
SPAN	1/2 IN.
MATERIAL	321 ST. STL

WEIGHTS	
CONVOLUTIONS	5.18 LB
HEAD	2.40
TOTAL FLUID	51 LB
TRAPPED FLUID	7.6 LB

Figure 37. 7-Inch Diameter Model Bellows

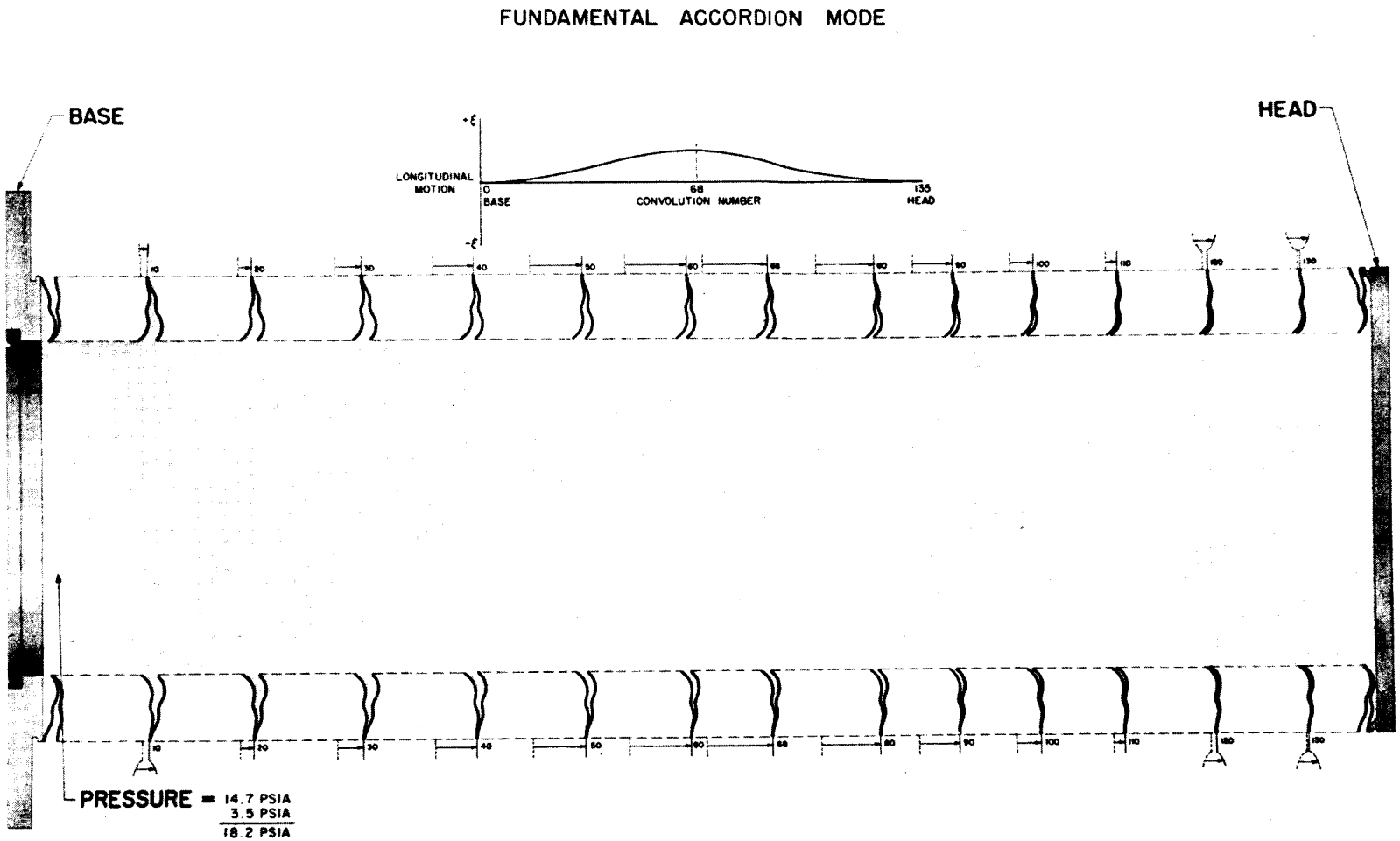

DESCRIPTION

1. HEAD STATIONARY
2. CENTER COLUMN OF FLUID STAGNANT
3. NO DYNAMIC PRESSURE RISE
4. LONGITUDINAL CONVOLUTION TIP MOTION
5. NO LATERAL CONVOLUTION TIP MOTION
6. TRAPPED FLUID VOLUME REMAINS CONSTANT

Figure 38. Fundamental Accordion Mode of 7-inch Diameter Bellows

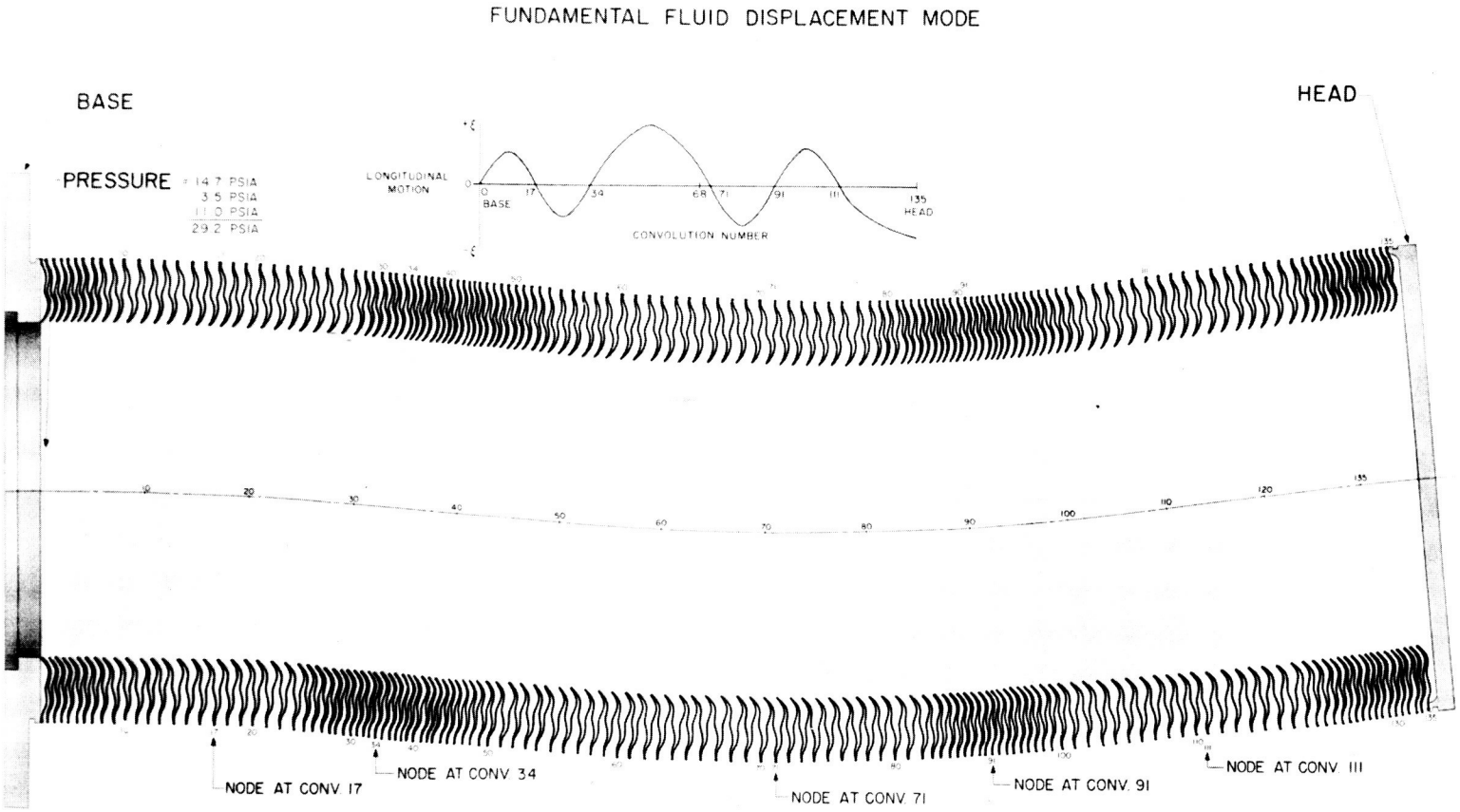

DESCRIPTION: ACCORDION MODE

1. HEAD STATIONARY
2. CENTER COLUMN OF FLUID STAGNANT
3. NO DYNAMIC PRESSURE RISE
4. LONGITUDINAL CONVOLUTION TIP MOTION
5. NO LATERAL CONVOLUTION TIP MOTION
6. TRAPPED FLUID VOLUME REMAINS CONSTANT

DESCRIPTION: FLUID DISPLACEMENT MODE

1. LONGITUDINAL AND LATERAL HEAD MOTION
2. CENTER COLUMN OF FLUID IN MOTION
3. APPRECIABLE DYNAMIC PRESSURE RISE
4. LONGITUDINAL CONVOLUTION TIP MOTION
5. LATERAL CONVOLUTION TIP MOTION
6. TRAPPED FLUID VOLUME INCREASES

Figure 39. Fundamental Liquid Displacement Mode of 7-inch Diameter Bellows

O. ACCORDION MODE ATTENUATION

If a bellows service environment is such that only one discrete forcing function is present, often a bellows can be designed such that its resonance will not coincide with the forcing frequency. This can be accomplished by variation of such design parameters such as leaf thickness, shape, and effective length.

In most missile applications where the design is optimized in terms of available envelope and weight, the design must provide the capability to operate under conditions of environmental shock, acoustic and random vibration inputs. Thus, dampening methods must be considered. One general method used successfully includes coulomb damping devices.

Coulomb damping by frictional devices can be designed to exert small forces on the external weld bead, internal weld bead, or the leaves only. These include close fitting metallic or nonmetallic sleeves, bands, helical springs, and springs between tank shell and leaves. These frictional damping devices often are successful as a quick fix; however, in the long run, these usually prove to be unreliable.

Another method of accomplishing damping is by means of viscous forces. This appears to be a more desirable method of attenuating bellows motion. During this program, limited analysis and experiments were conducted on the 4-inch diameter bellows to suppress accordion mode convolution motion.

A method which successfully supplied viscous damping and/or convolution clamping was to install ring baffles at anti-nodes of bellows response. Figure 40 shows the response of the center convolution with and without ring baffles installed inside the bellows at the 25th, 50th, and 75th convolutions. Notice that the fundamental accordion mode has dropped to 16 cps and the higher harmonics have essentially been completely dampened out. No attempt was made to optimize baffle geometry or location. The fact that high motion attenuation was obtainable is considered very significant. These baffles protruded 0.4 inch into the liquid beyond the inside weld bead line on the only configuration tested although even this much may not be necessary. The ring baffles installed in the bellows can be seen in Figure 41.

P. LATERAL VIBRATION OF 4-INCH BELLOWS

Figure 42 shows the bellows mounted for lateral vibration. Motion of the bellows head was restrained by clamping it at the eight screw locations shown on the photograph. Convolution motion was sensed by the miniature crystal accelerometer shown mounted at the center convolution. The "true transmissibility system" divided the center convolution response by the input accelerometer signal. The input accelerometer was cemented to the base of the bellows, as shown.

Figure 43 presents the response of the center convolution with the head fixed and zero internal gage pressure. The applied input was 0.2g from 5 to 30 cps and

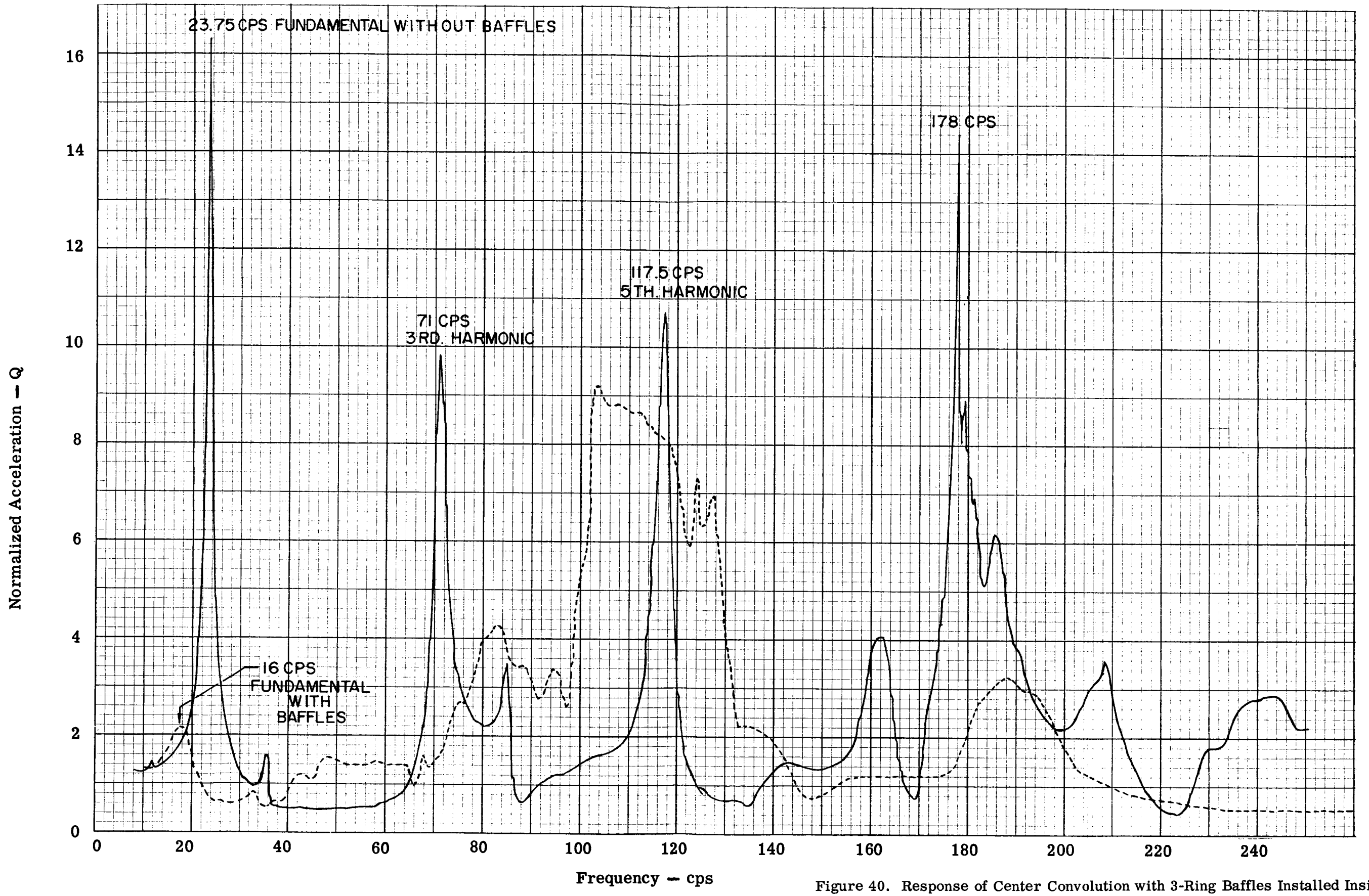

Figure 40. Response of Center Convolution with 3-Ring Baffles Installed Inside Bellows with Head Fixed

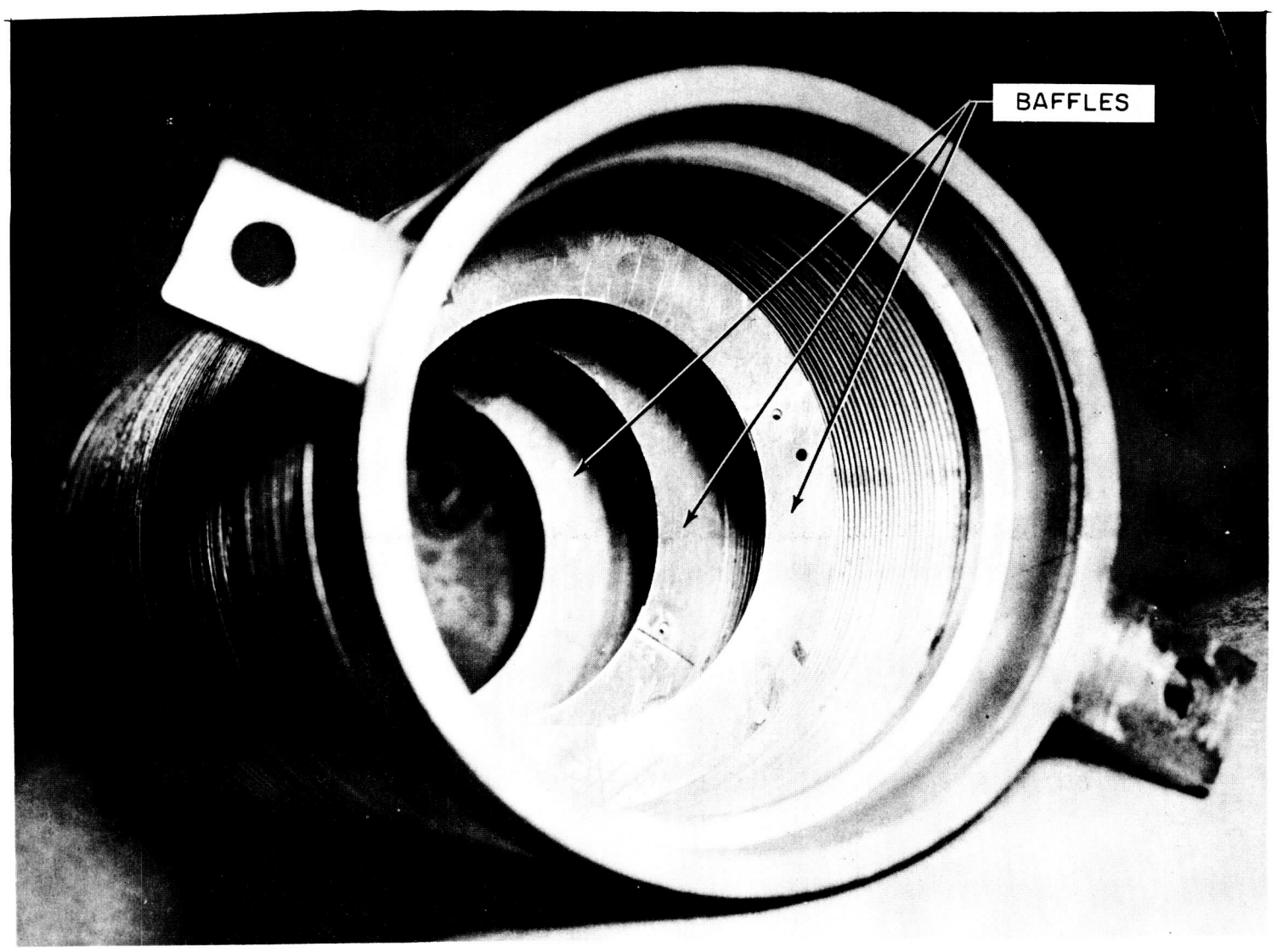

Figure 41. Installation of Ring Baffles

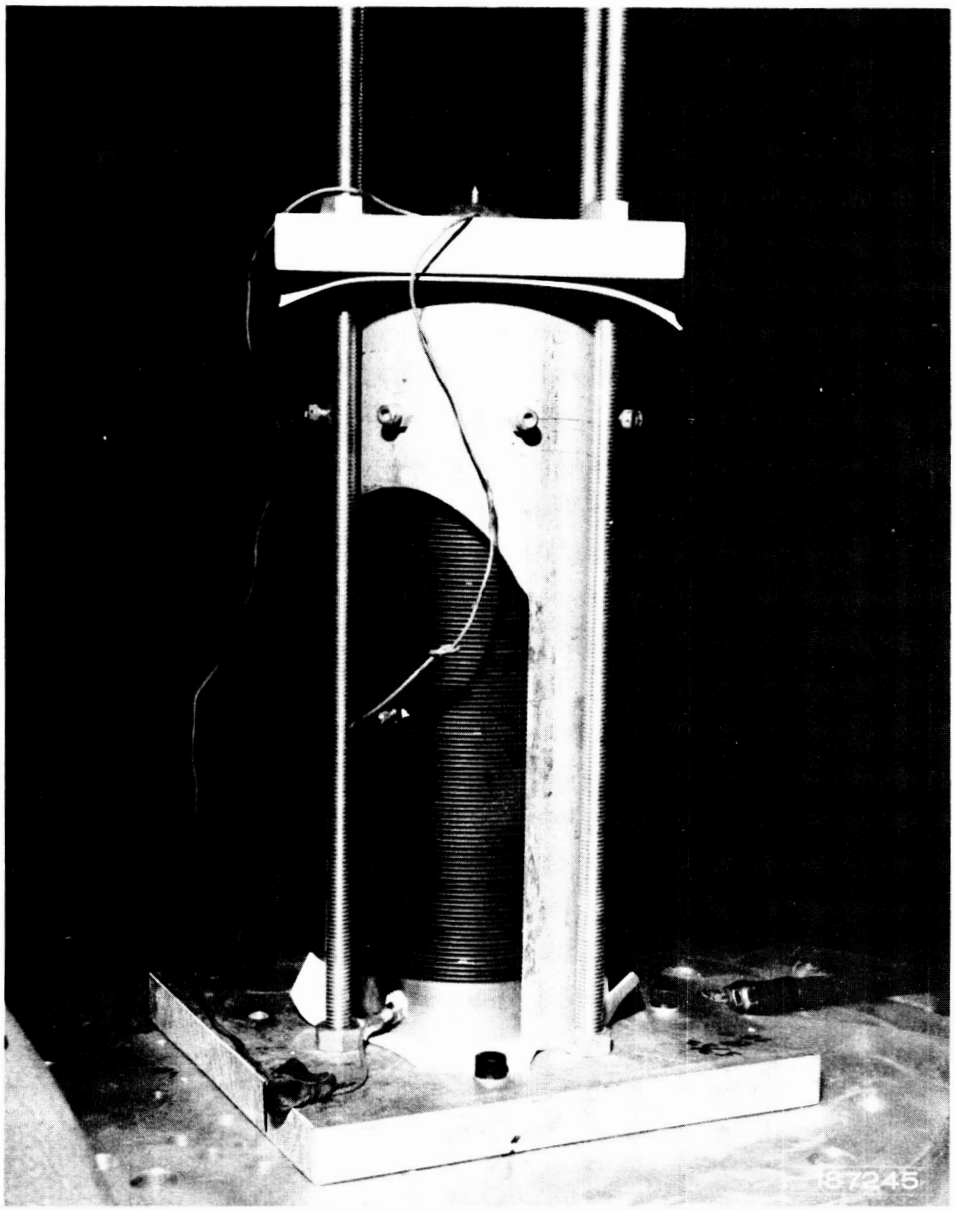

Figure 42. Lateral Vibration Setup

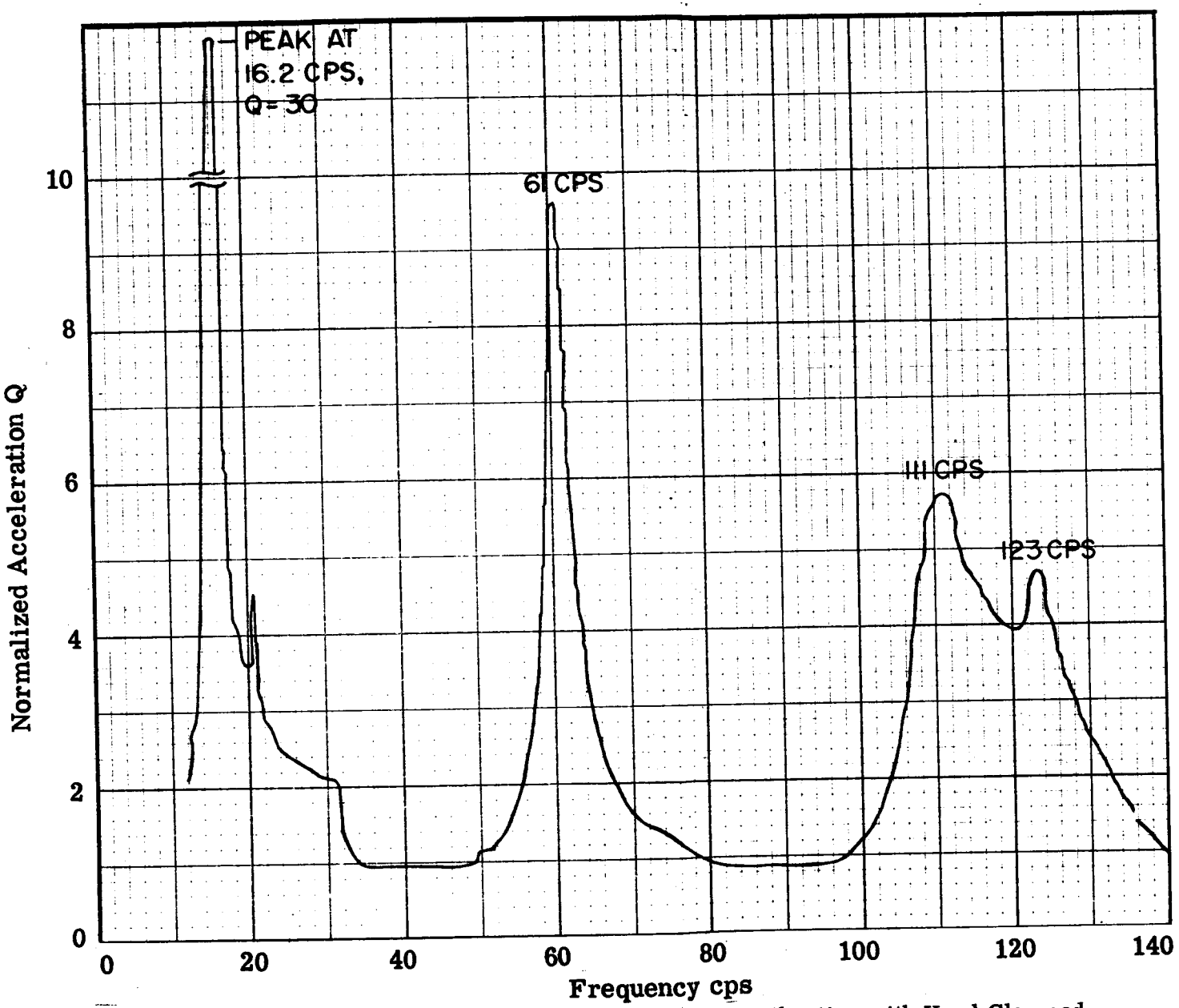

Figure 43. Center Convolution Lateral Response During Vibration with Head Clamped

1g from 30 to 140 cps. The resonance at 16.2 cps was identified as the fundamental lateral mode whereas the third harmonic occurred at 61 cps. These compare with calculated values of 12.25 and 67.4 cps. Broad-band resonance from 100 to 140 cps was attributed to a lateral response from the liquid displacement mode. A minor lateral mode also exists at 36 cps; response at this mode is evident on transmissibility plots taken at 90 degrees coordinates around the bellows.

The test fixture has a radial clearance of 0.10 inch on each side of the bellows. This would simulate a tank shell clearance. The actual design clearance of the bellows-tank assembly should consider several factors. To minimize damage during operation, the clearance should be held to a few thousandths of an inch. A small clearance results in small acceleration forces, since this force is directly proportional to the lateral motion of the convolution tips. However, from a practical viewpoint, the minimum clearance will be dictated by manufacturer's tolerances on the tank shell and bellows leaf size. Hence, fabrication problems such as shell concentricity, axial alignment, and internal weld bead tolerance will dictate the design clearances.

Figure 44 shows lateral response; Figure 45 shows longitudinal response with the head free at 2 3/4 internal gage pressure. The only new frequency, not mention in prior longitudinal and lateral frequency discussions, occurred at 41 cps. The 41 cps response is probably due to cross-coupling affects. It is emphasized that this condition simulated a bellows mounted in a shell with substantial radial clearance. Vibrations under conditions of small clearances results in the convolution tips striking on the shell which causes nonlinear bellows response.

Q. VIBRATION TESTS OF 9-INCH BELLOWS ASSEMBLY

1. Longitudinal Vibration Tests

All longitudinal sinusoidal vibration tests were conducted in the bellows plastic strain region at a length of 5.860 inches (0.3 inch pitch). Several surveys were made in the low-frequency range from 0.1 to 10 cps at 1/2-inch double amplitude using a hydraulic slosh machine designed by Bell Aerosystems. The motion of the convolutions was at all times in phase with the input motion of the bellows base. The maximum motion amplification from bellows head to base was 1.25 to 1. Applying 15 psig gas pressure outside the bellows did not change the dynamic response. From these tests, it is concluded that the lowest natural frequency is above 10 cps.

Several surveys were made in the high-frequency range from 5 to 500 cps at inputs from 1 to 4g using a MB C-25 Shaker (Figure 46). Resonance of the convolutions was apparent at 73, 139, and 200 cps. Up to the lowest natural frequency of 73 cps, motion of the convolutions was in phase with the induced motion at the base. At 73 cps, the center convolution was oscillating back and forth at greater double amplitude displacements than the base and head, (Figure 47).. The relative motion of each convolution was scaled from enlarged photographs and presented in Figure 48..

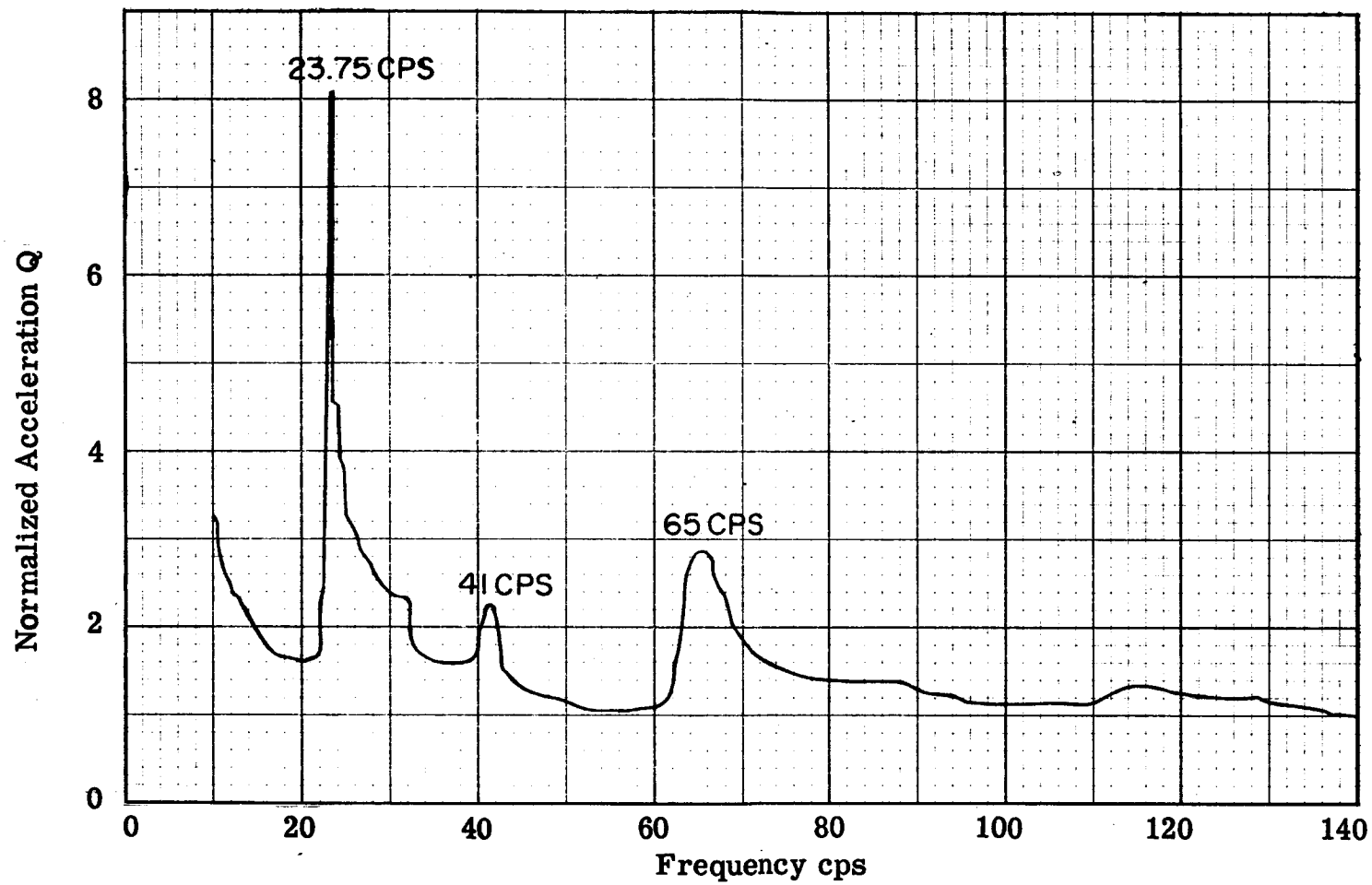

Figure 44. Center Convolution Lateral Response During Vibration with Head Free

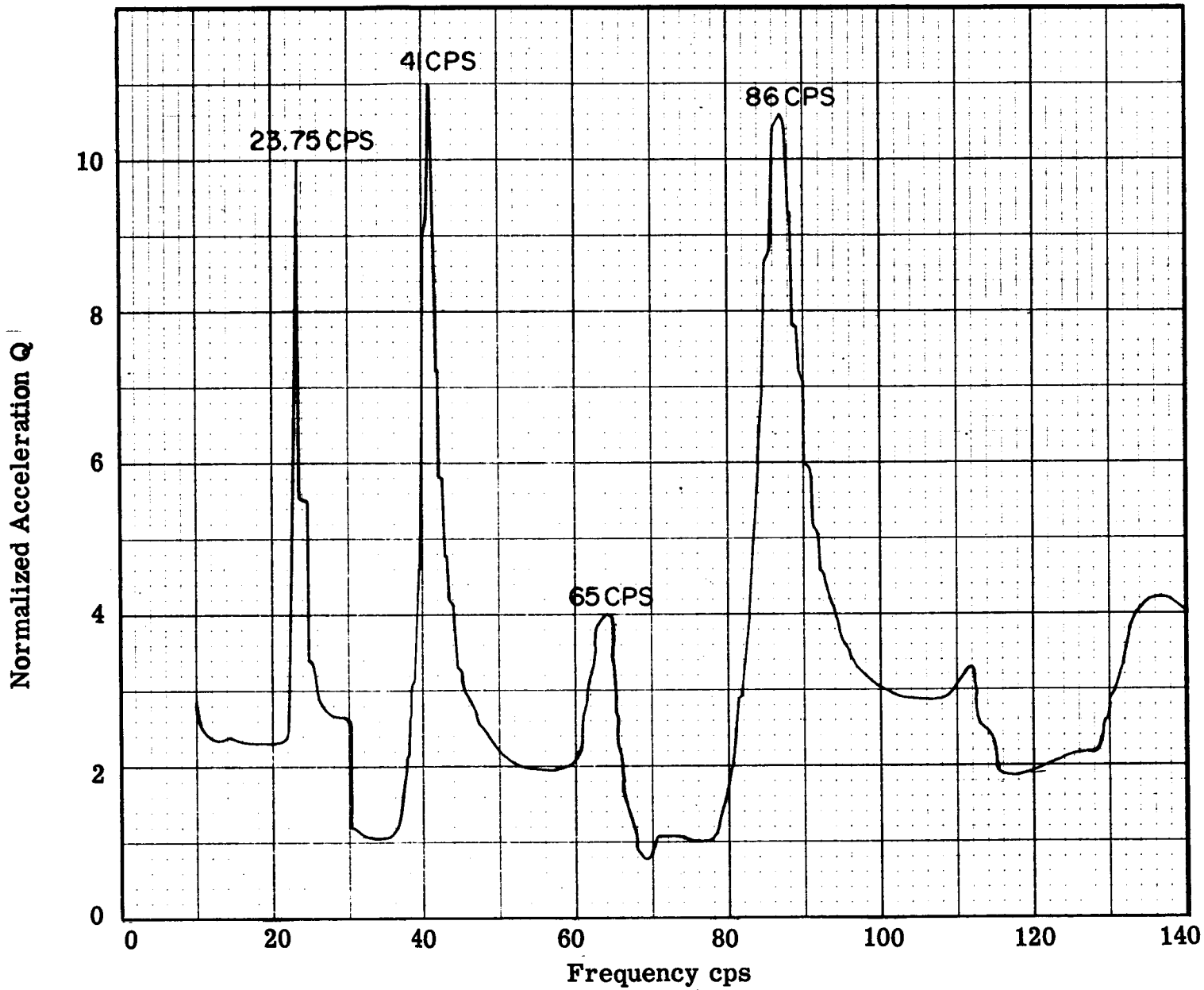

Figure 45. Center Convolution Longitudinal Response During Vibration with Head Free

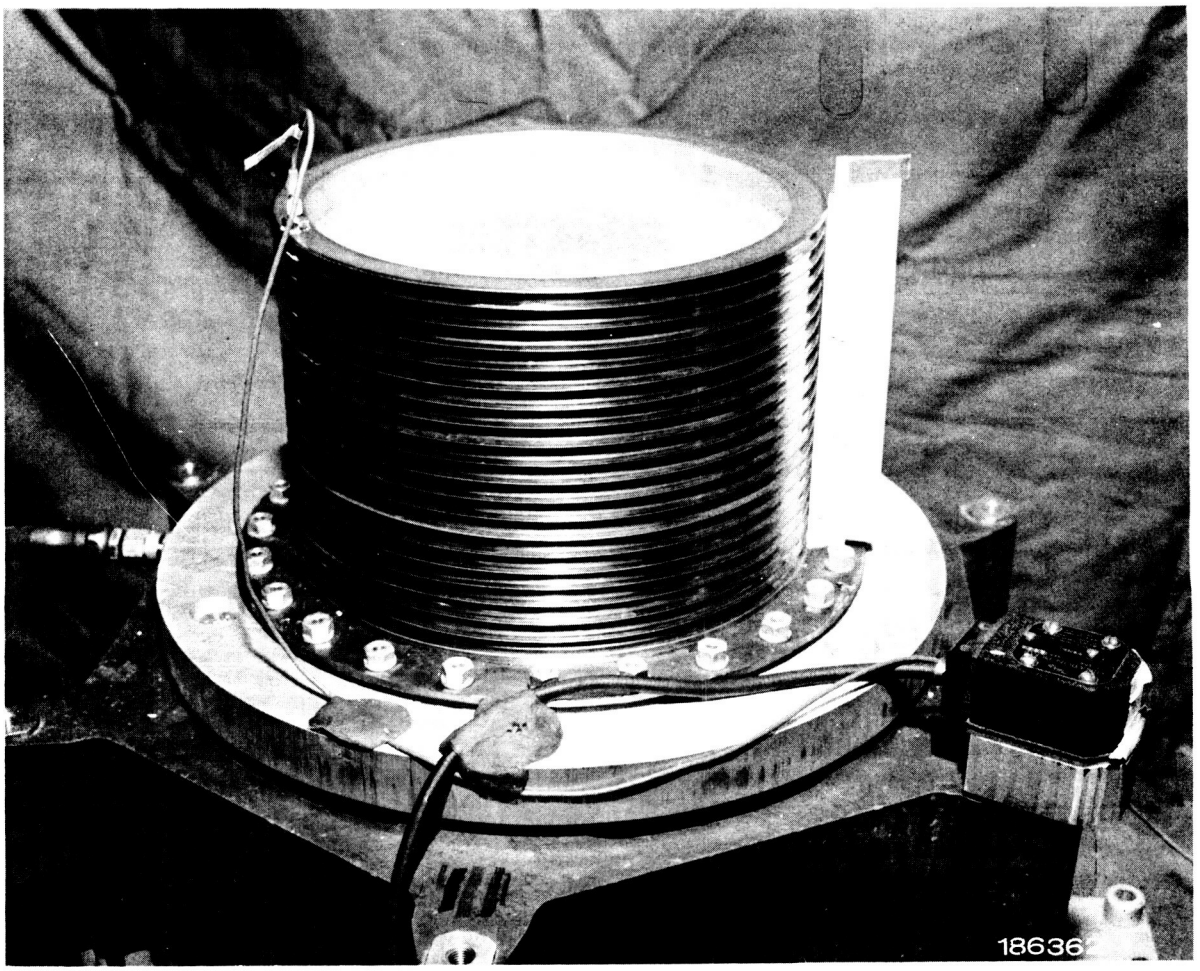

Figure 46. Longitudinal Vibration Test of 9 Inch Bellows

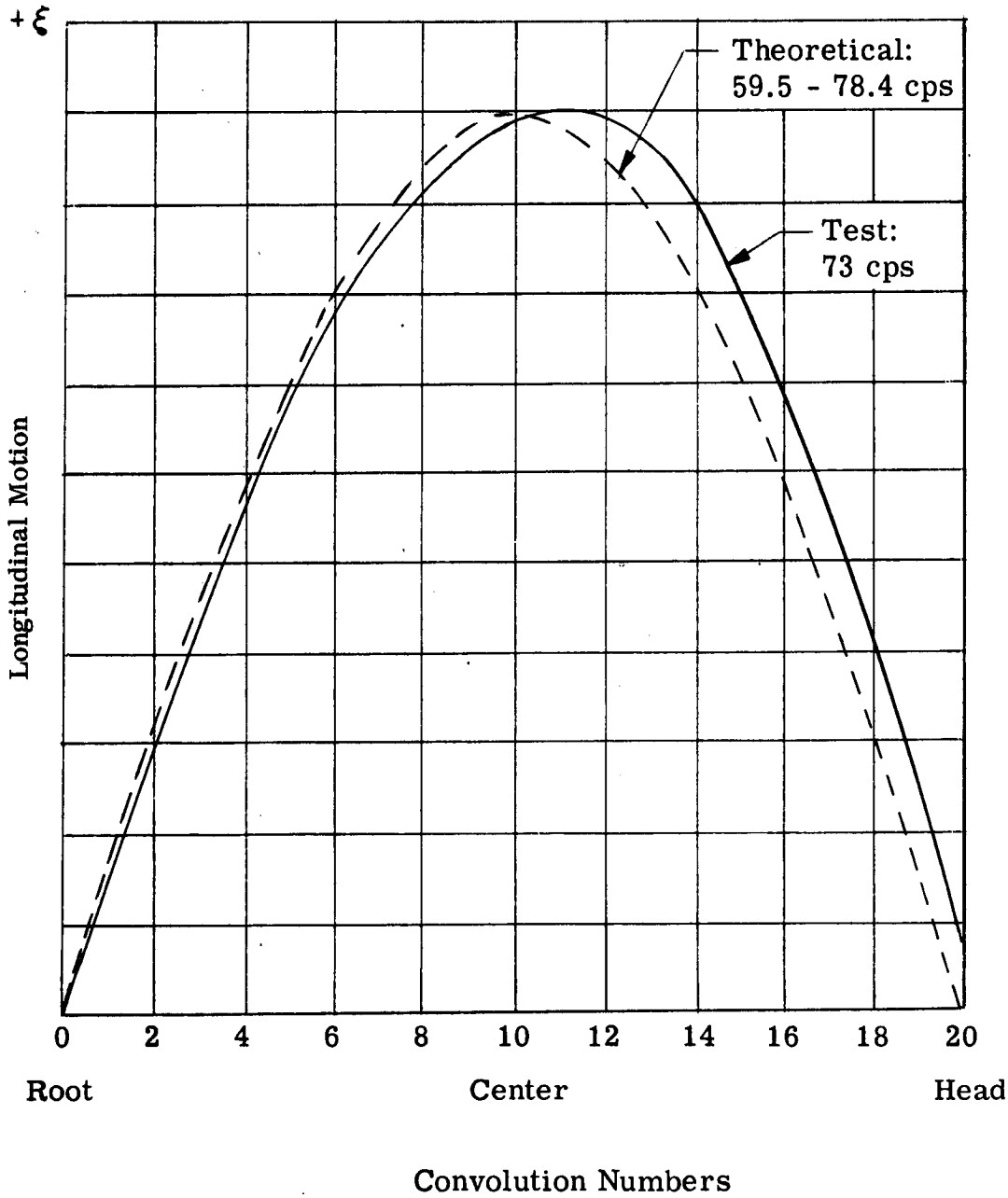

Figure 47. Accordion Mode of Bellows

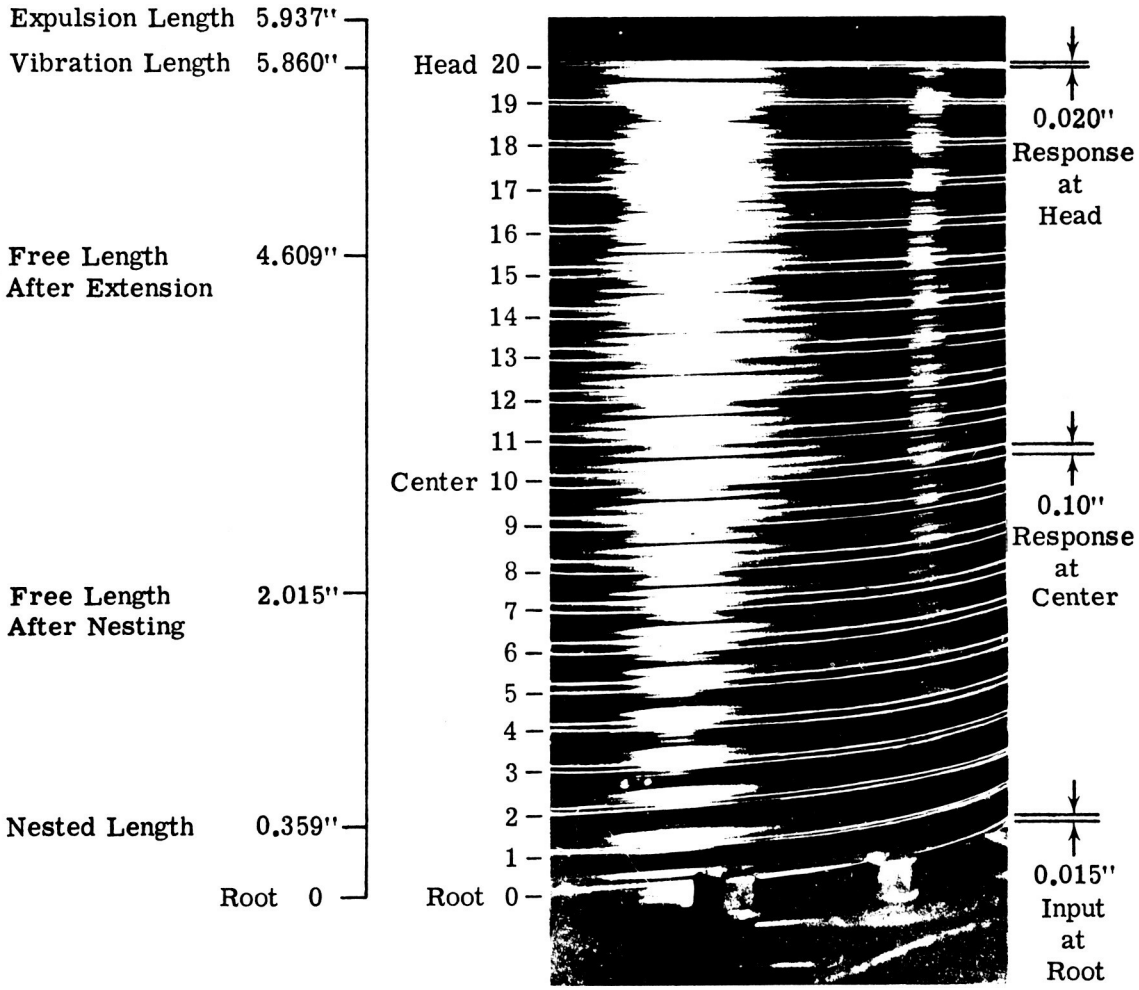

Fundamental Accordion Mode at 73 cps. Water Filled 9" O.D. Bellows Extended 1 1/4" From Free Length. Note That the Center Convolution Moves 0.10" D.A. (27g) With an Applied Root Movement of 0.015" D.A. (4g).

Figure 48. Fundamental Accordion Mode at 73 cps

This longitudinal mode of vibration has been referred to as the fundamental accordion mode of vibration. At 73 cps, the double-amplitude displacement at the center convolution was 0.10 inch (27g) with a 0.015 inch double-amplitude (4g) input at the base. This corresponds to a motion or acceleration amplification of 6.7 to 1. At the same instant of time, the head had an amplification of 1.3 to 1. This was probably due to the skirt of the liquid displacement mode of 139 cps.

The next resonant frequency of the bellows was 139 cps. At this frequency, the center convolution is stationary but the head is oscillating violently as shown in Figure 49. In addition to convolution motion, the flat thin head on the bellows was "oil canning." Graphite powder poured on the head quickly gathered at the nodal ring. Since considerable head motion and flexing was present due to presumed liquid column displacements, this mode was arbitrarily named the fundamental liquid displacement mode.

2. Lateral Vibration Tests

Several surveys were made in the lateral direction with the bellows in the attitude shown in Figure 50 in the low frequency range of 0.1 to 10 cps. Some rocking of the head was seen, but a full resonant condition was not reached.

The bellows fixture assembly was then attached to a slip plate and vibrated in the lateral direction as shown in Figure 51. A frequency survey between 5 and 36 cps was made and lateral resonance of the convolutions was apparent at 19.2 and 29.9 cps.

3. Discussion of Test Results

The natural frequencies found during these tests depend upon the bellows extended height during test. Measurements made on S/N-2 bellows presented in Figure 52 shows that the total effective spring rate in the 0.3 inch pitch extended position (plastic strain region) is several times greater than the free length position (elastic strain region). Spring rates noted in Figure 52 reasonably agree with the value of 31.3 to 35.8 lb/in. measured by the manufacturer.

Although meager spring rate data in the 0.3 inch pitch extended position (length during vibration) is available, a limited comparison was made. An average longitudinal spring rate of 119 lb/in. from the decreasing strain curve was substituted into a square stiffness matrix considering 20 degrees of freedom. The weight of the leaves and various amounts of trapped fluid between leaves were substituted into a diagonal mass matrix. Using an iterative process, the IBM 7090 Digital Computer produced the frequency and mode shape shown in Figure 47. Reasonable correlation was obtained for both frequency and mode shape.

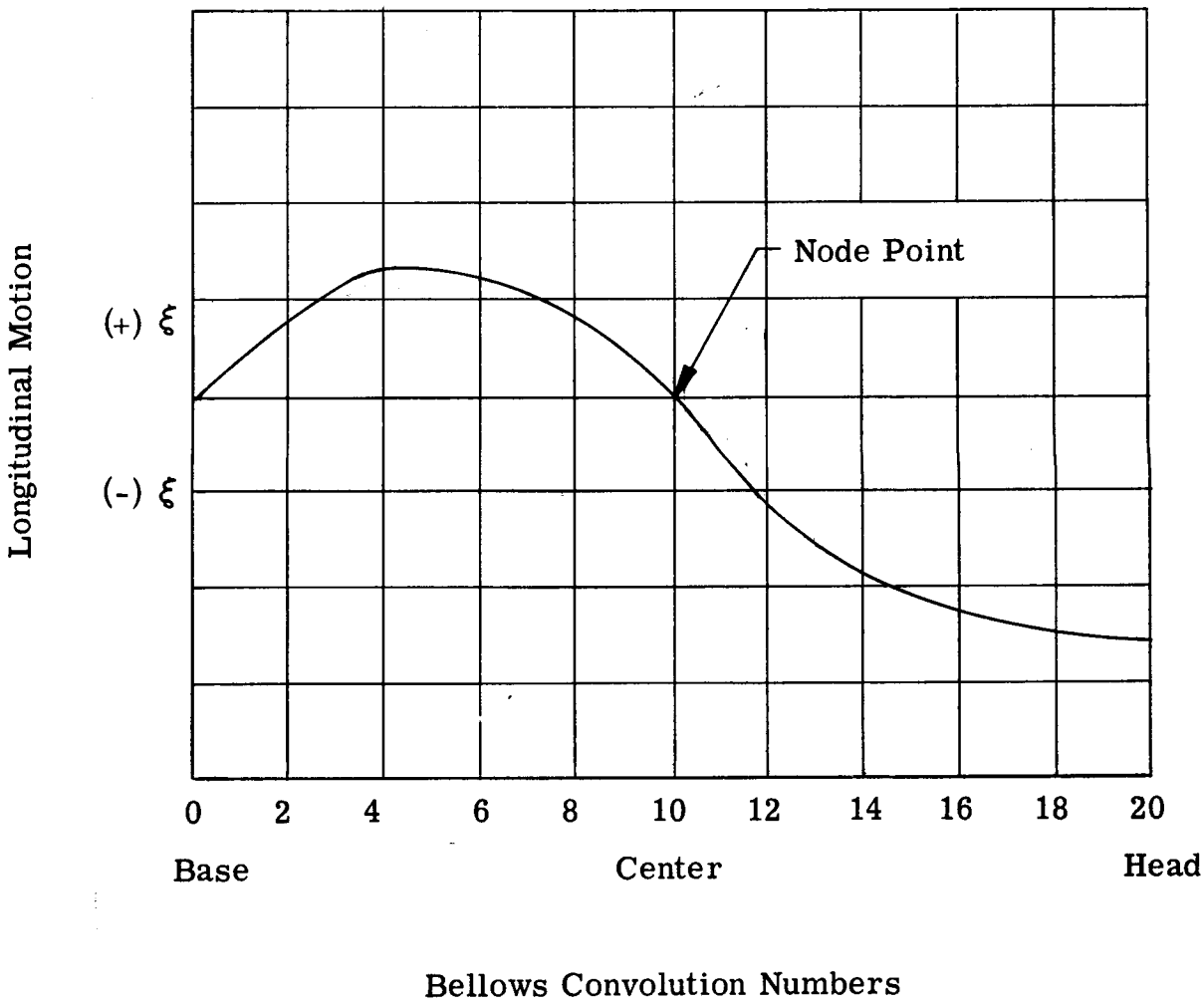

Figure 49. Liquid Displacement Mode at 139 cps

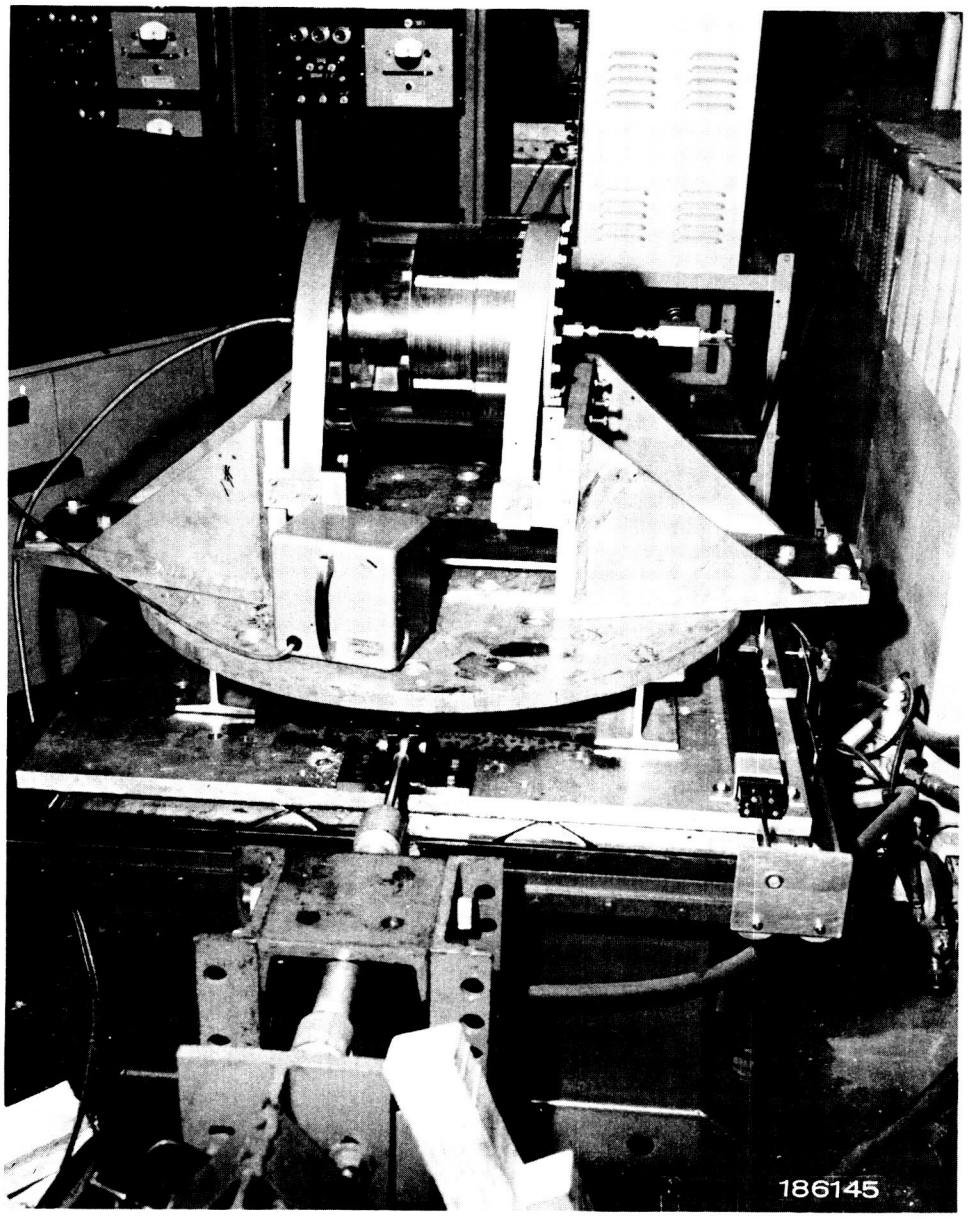

Figure 50. Low Frequency Vibration Test of 9 Inch Bellows

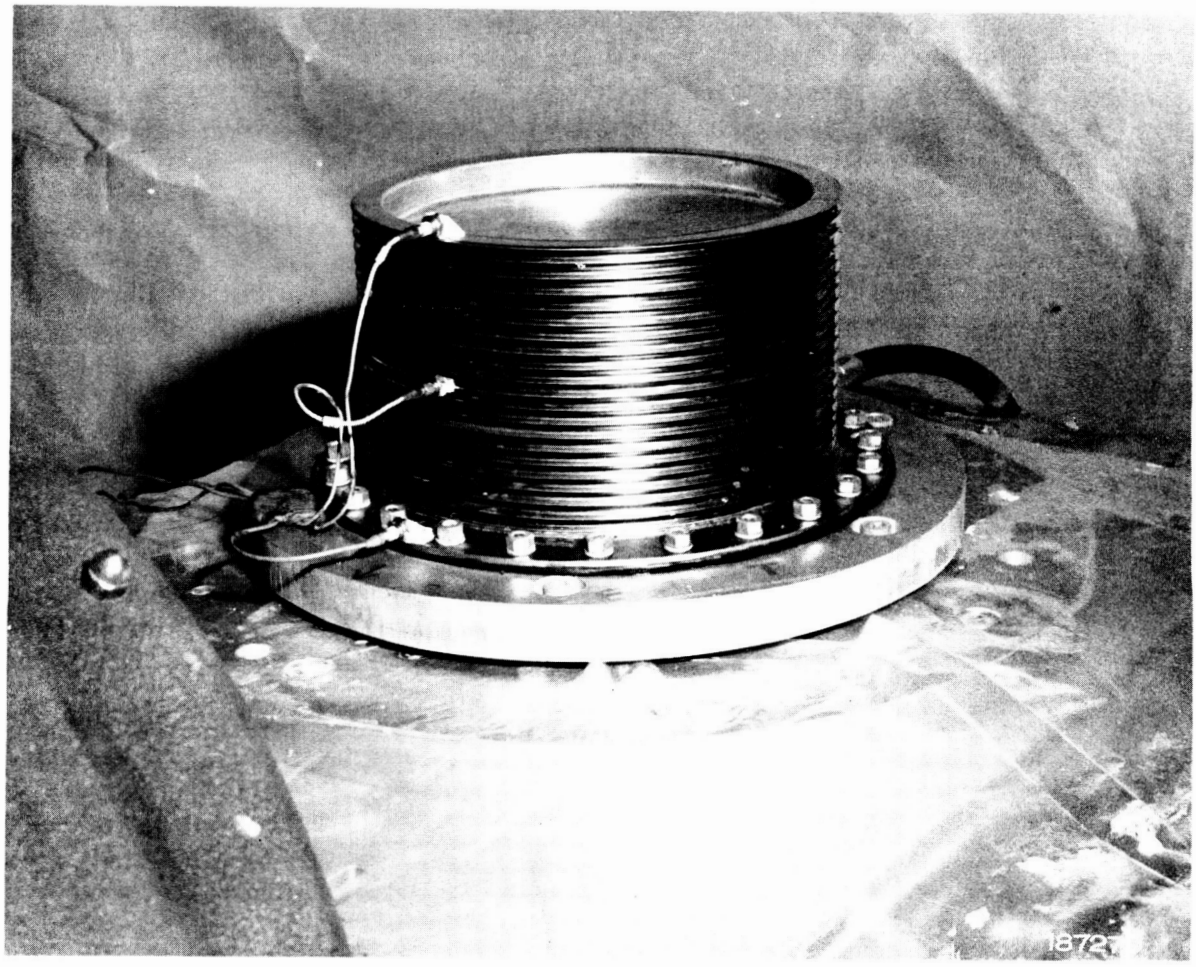

Figure 51. Lateral Vibration Test of 9 Inch Bellows

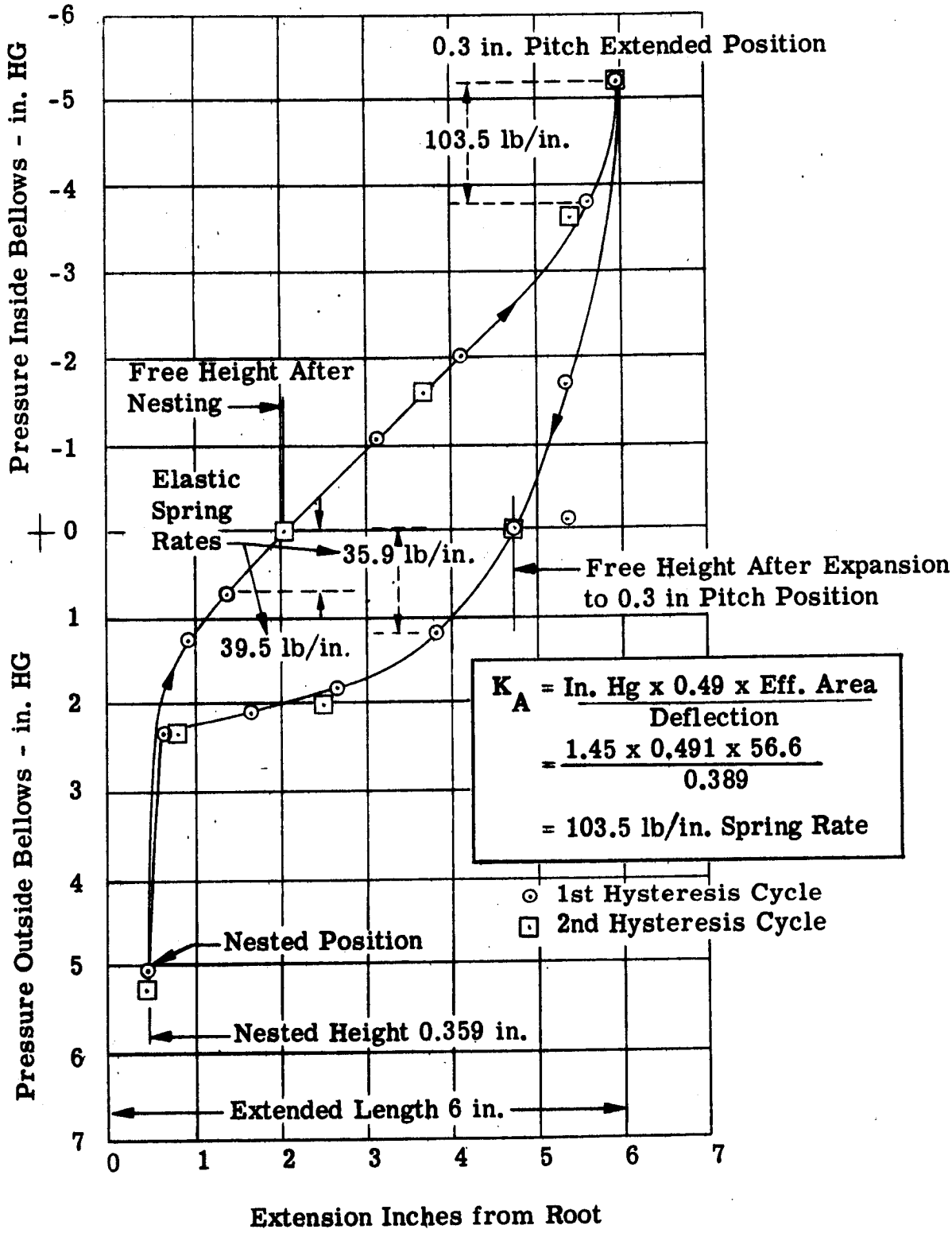

Figure 52. Deflection-Pressure Curve for 9-Inch Bellows

CONCLUSIONS RELATIVE TO DYNAMICS INVESTIGATION

There are three types of bellows vibration modes identified in this report. Common longitudinal modes, arbitrarily named the accordion modes; a second class of unusual longitudinal modes, arbitrarily named the liquid displacement modes; and, lastly, the lateral modes.

The accordion modes are recognized by large longitudinal convolution tip motion at the center and negligible head motion. In these modes the bellows was found to shear the liquid at the inner diameter convolution tips. Motion of the center convolution can be over 15 times greater than the applied motion at the base. The liquid displacement modes have both lateral and longitudinal convolution tip motion and considerable head motion. Measurements made of the liquid pressure inside the bellows indicate the presence of small pressure oscillations when longitudinal vibration is applied in the liquid displacement modes.

Both longitudinal (accordion) modes and lateral modes of vibration can be predicted by substituting bellows effective spring rates and masses into formulas developed in this report for bellows with uniform leaf geometries. A matrix of stiffness influence coefficients was also developed for digital computation of bellows frequency and mode shape for both uniform and non-uniform leaf geometries in accordion modes. Agreement between results of an IBM 7090 Digital Computer program and the accordion mode formula was obtained for four uniform leaf shape bellows. Vibration test data also agreed with the predicted results in both the elastic and plastic strain regions.

Local resonance of each leaf was also determined for bellows of 4-in., 7-in., and 9-in., outside diameter; however, because of the high spring rates of the individual leaf and its low mass, resonance was calculated to occur over 3000 cps for all three bellows.

Experimental means must be used to obtain an exact effective longitudinal spring rate of any prototype bellows design, The spring rate varies with static pitch of the bellows. Reasonable approximations can be made for a spring rate on test capsules containing 10 to 20 convolutions and these scaled up to bellows with larger number of convolutions. Effective masses can be established knowing the bellows geometry and fluid density.

Bellows response in the accordion mode was attenuated by installing ring baffles between the inner leaves and extending into the stagnant liquid column. Maximum attenuation can be obtained if these baffles are installed at anti-nodes of the fundamental accordion mode and odd interger multiple thereof.

The lateral frequency formula for bellows requires substitution of both the modulus of elasticity and moment of inertia. An equivalent EI was established for a bellows which utilizes the experimentally obtained longitudinal spring rate. The

same equivalent expression $\frac{K_A r^2 L}{2}$ was developed by two distinct methods. The calculated lateral frequency must be altered to account for internal fluid pressure whereas the longitudinal frequency need not be altered.

S. SYMBOLS USED IN THE TEXT

a = outside radius of plate (bellows), in.

A = cross-sectional area of bellows, in.^{2}

A_c = area of cylinder, in.^{2}

A_{EFF} = effective area, in.^{2}

A_n = numerical constant

b = inside radius of plate (bellows), in.

c = circumference of bellows, in.

C = plate (bellows) span, in.

d = distance, in.

D_i = inside diameter of bellows, in.

D_m = mean diameter of bellows, in.

D_o = outside diameter of bellows, in.

E = modulus of elasticity, lb/in.^{2}

E_{EFF} = effective modulus of elasticity, lb/in.^{2}

EI = bending stiffness in lateral direction, lb-in.^{2}

f = frequency of decay signal, cps

f_a = longitudinal or axial frequency, herein called the fundamental accordion mode frequency, cps

f_c = resonant frequency of a bellows leaf, cps

f_l = lateral frequency, cps

f_p = corrected lateral natural frequency, cps

F_{dc} = force experienced by incremental circumferencial spring, lb

g = acceleration of gravity, 386 in./sec^2

h = distance, in.

I = moment of inertia, in.^{4}

I_c = moment of inertia of cylinder, in.^{4}

I_{EFF} = effective moment of inertia, in.^{4}

J = a/b, dimensionless ratio of plate (bellows)

k = longitudinal spring rate of bellows segment of length 1 (several leaves); spring rate, lb/in.

k_c = stiffness of incremental spring, lb/in./in. circumference

k_θ = angular spring rate, lb-in.^{2}

K_A = longitudinal total effective spring rate of all convolutions, lb/in.

K_L = lateral spring rate, lb/in.

l = length of segment, one or more convolutions; distance, in.

L = length of bellows from base-convolution junction to head-convolution junction; length of a beam, in.

m = bellows convolution mass, lb/sec^2/in.

M = mass, lb/sec^2/in.

n = integer

N = number of convolutions

p = convolution pitch, in.

P = applied unit force at end of beam (bellows), lb

P_{cr} = critical column buckling load, lb

q = dimensionless parameter dependent upon Poisson's ratio

Q = normalized acceleration, i.e. output acceleration/input acceleration, non-dimensional

r = effective radius of bellows; cylinder radius, in.

t = thickness of equivalent cylinder wall, in.

T = segment moment, in.-lb

T_1 = moment, in.-lb

T_{dc} = applied incremental moment, in.-lb

u = parameter which is a function of a/b and type of leaf restraint

w = weight of bellows convolutions, lb

W_i = weight of liquid inside of bellows, lb

W_m = weight of leaf(s), lb

W_t = weight of liquid trapped in convolution(s), lb

y = distance, in.

α = angle in general

δ = deflection, in.

δ_1 = deflection for unit load, in.

θ = angular deflection, rad

ρ = density of fluid; bellows, lb/in.^{3}

ρ_m = mass density of fluid, lb-sec^2/in.^{4}

μ_1 = mass per unit length, lb-sec^2/in.^{2}

ν = Poisson's ratio

ξ = longitudinal displacement of convolution tip along bellows length, in.

ω_a = axial or longitudinal frequency, herein called the fundamental accordion mode resonant frequency, rad/sec

ω_d = natural frequency of tank radial mode, rad/sec

ω_1 = lateral frequency, rad/sec

$\frac{1}{\omega_a^2}$ = eigenvalue, 1/(rad/sec)^2

$[C]$ = square matrix of flexibility influence coefficients, in./lb

$\{d\}$ = column matrix of displacements, in.

$\{F\}$ = column matrix of forces, lb

$[k]$ = square matrix of spring stiffness coefficients, lb/in.

$[M]$ = diagonal matrix of mass terms, lb-sec^2/in.

$[s]$ = square matrix of stiffness influence coefficients, integers

$[S]$ = square matrix of stiffness influence coefficients, lb/in.

$[W]$ = diagonal matrix of weight terms, lb

$\{Y\}$ = column matrix of deflections, in.

SECTION 5

COMPONENT AND ASSEMBLY INVESTIGATION

To establish a practical envelope as a basis for the structural and dynamic investigations, surveys of the literature and industry were conducted. These surveys were initiated to provide the relationship between propulsion system requirements and present fabrication capability.

Supplementing these surveys, the incorporation of bellows devices into two current programs at Bell Aerosystems provided an opportunity to evaluate development hardware. Vendor contacts during procurement phases of these programs also afforded a better opportunity to discuss design procedures and fabrication methods. These discussions, handicapped by proprietary restrictions in both design and fabrication, produced little specific information. The restrictions, which are intended for self-protection, also result in concealment of areas, particularly in bellows design, where there is a definite need for analytical effort.

General design information from published literature is available for approximate solutions and is included with this report. Bellows manufacturers have supplemented these data with empirical relationships from experimental testing. These empirical equations, tailored for specific requirements, are used in fabrication of test units. Test results are then evaluated and experience dictates the changes in parameters (thickness, shape, etc.) found necessary to provide for operation within the required tolerance.

A. BELLOWS ASSEMBLY DESIGN

An effort was made to correlate the general solution proposed by Freely and Goryl (Reference 58) with experimental test results obtained with a test bellows. The equations used assumed a flat plate diaphragm shape and, in addition, neglected the influence of boundary conditions at the inner and outer weld joint.

Figure 53 shows graphically a comparison of an experimentally determined "Force versus Deflection" curve with one calculated from the relationship shown in Reference 58.

$$F = \pi E \; D_m \frac{t^3}{w} \; \frac{\Delta}{N}$$

where F = axial force, lb

E = Young's modulus

D_m = mean diameter

t = thickness

w = span

This reduces to:

$F = C \; \Delta$ for the particular application in Figure 53.

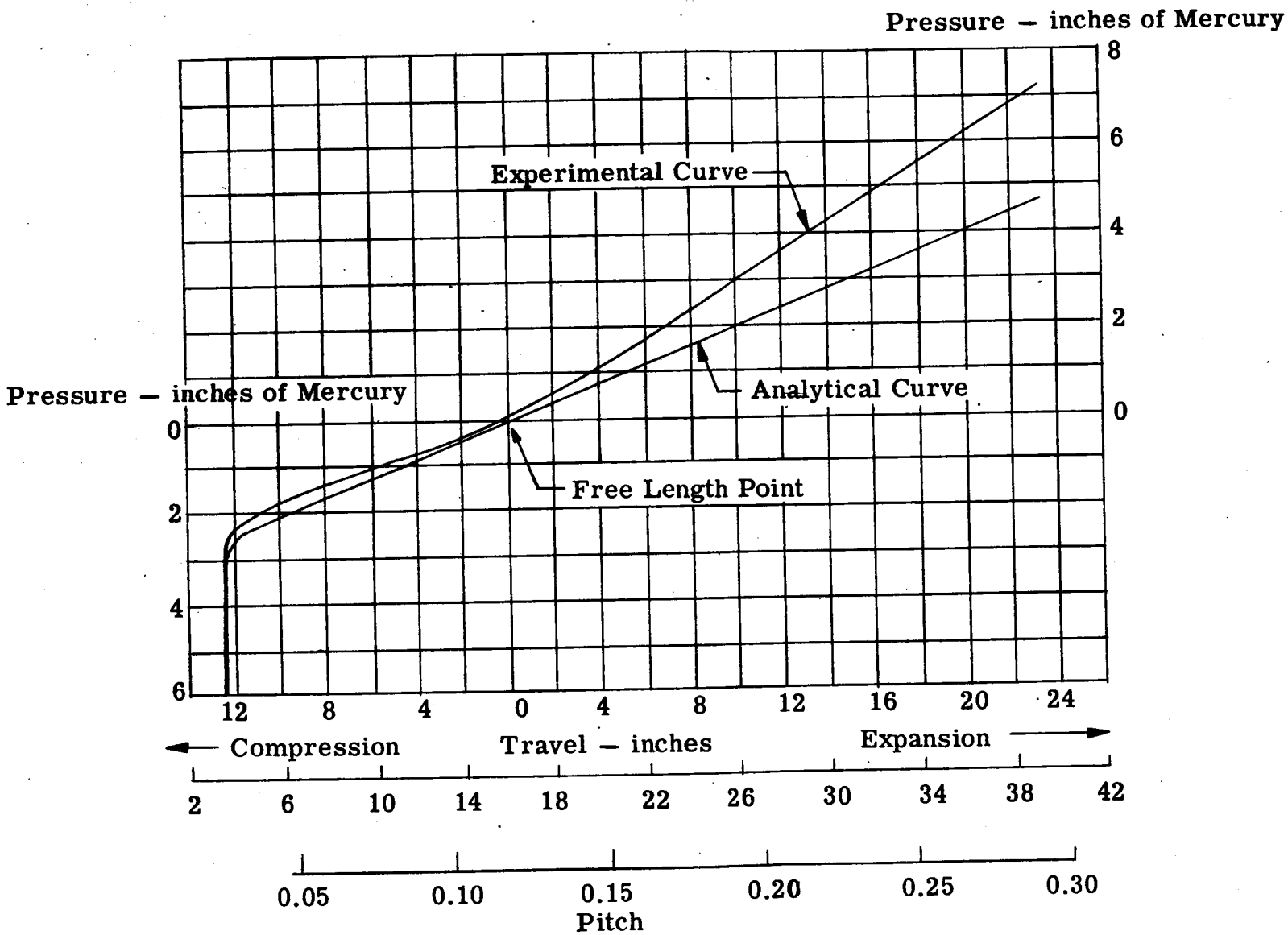

Figure 53. Force Versus Deflection Curves

Δ = deflection

N = number of plates

C = constant

B. DIAPHRAGM CONFIGURATION

The diaphragm shape or ripple configuration are two general patterns. One is a series of ripples of constant radii at a constant depth. The other, called a tapered ripple, has a constant radii of varying depth. The number of ripples is another design variable. In the absence of a precise method of stress calculation, the intent is to provide the maximum amount of material in a given span. This maximum is controlled by the depth of draw possible without excessive metal thinning, the nesting properties of the assembly, and the effect on spring rate.

Bellows fabricators are standardizing several configurations for better accumulation of empirical data on shape factors.

It appears from the position of the respective curves in Figure 53 that the use of this general solution provides a comfortable design margin. This involves another assumption; i.e., that this relationship of shape factor to joint efficiency extends to all designs.

Test observations with the same bellows assembly indicate this to be a questionable assumption. Bellows assemblies deflected with enough plastic extension to cause permanent deformation were mounted in plastic and sectioned. Three samples of varied extensions all showed that permanent set occurred in only one diaphragm of each convolution. This resulting set is represented in the enlarged sectioned convolution shown in Figure 54. The unequal stress distribution is evident from the selective distortion.

C. UNSTABLE OPERATION

Three forms of instability were investigated in this phase of the program. The most common type, called flipping, results from the selective distortion caused by unequal stress distribution or overpressurization, or a combination of both. This unstable condition is evidenced by an erratic diaphragm motion normally in the compressive stroke.

Snaking is an assembly instability resulting from the local flipping of a series of convolutions. This unstable condition, caused by overpressurization, is shown in Figure 54.

The final condition encountered, called buckling, is a failure caused by exceeding the hoop strength of the assembly. This results from overextension or excessive external pressure, or a combination of both.

Solid Line Indicates Nested Position.
Dotted Overlay Indicates 0.300 Pitch.

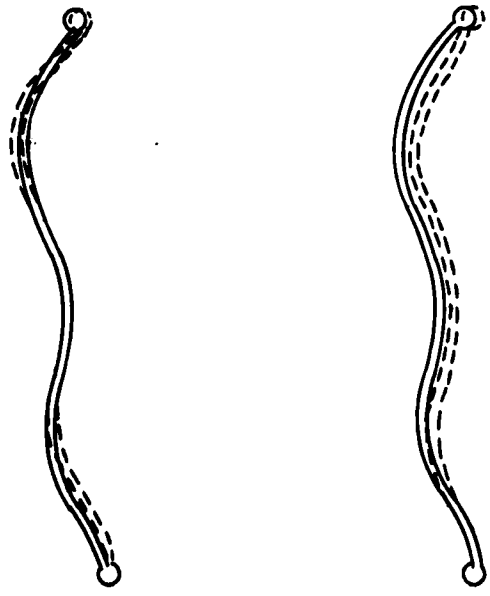

Figure 54. Overlay of Deformation

Except for buckling, the other forms of instability are not necessarily destructive malfunctions. They do, however, seriously limit the life cycle capability of an assembly.

Failure is normally a fatigue crack in a circumferential direction in the heat-affected zone adjacent to the weld head.

D. FABRICATION SEQUENCE

Fabrication sequence becomes important, both from a quality control standpoint and, significantly for this program, from the determination of a method compatible with the structural analysis program.

Two methods of fabrication in general use vary greatly, but only in the forming process. One method employs separate dies for forming the upper and lower diaphragms in a convolution (mirror-image diaphragms). When formed, the separate diaphragms are fusion-welded at the inside diameter using the T.I.G. method (thoriated tungsten electrodes with an inert atmosphere of argon). A sufficient number of convolutions are joined at the outside diameter to form an assembly. In a bellows assembly fabricated in this manner, the free length is a function of the fabricated pitch set in the forming dies.

The second method consists of forming all diaphragms from the same forming dies. These are assembled in the same manner. However, when assembly is completed, the free length is in the nested position. The diaphragms are separated only by the weld beads, although there may be some spacing caused by slight distortion of diaphragms when chill rings are inserted during the welding operation. To set a free length, the assembly is extended until it has yielded and then compressed, removing some of the plastic set. When released, the assembly assumes a free length which defines the elastic operating range. It is obvious that the former method adapts itself more readily to the computer program presented herein (Appendix III) for structural analysis. The geometry of the diaphragm is changed in the latter method with the plastic deformation required to set the free length.

E. VOLUME CALCULATIONS

The calculation of useable volumes within a bellows assembly also involves an assumption that bellows are assembled from flat plates.

A quick, approximate method with fairly good accuracy in small-diameter bellows involves the calculation of a cylindrical volume with a diameter equivalent to the mean diameter of the bellows assembly.

Method I – $V = \frac{\pi}{4} \left(D_o^2 - D_i^2 \right) L$

or

$V = \frac{\pi}{4} D_m$

V = volume

D_o = outside diameter

D_i = inside diameter

D_m = mean diameter

L = bellows travel

A method showing better agreement with actual hardware calibrations in larger size bellows utilizes the volume equation for a frustum of a cone.

Method II – $V = \frac{\pi}{12} (L) (D_o^2 + D_i D_o + D_i^2)$

A graphical representation of actual volumes versus calculated volumes using Method II is shown in Figure 55.

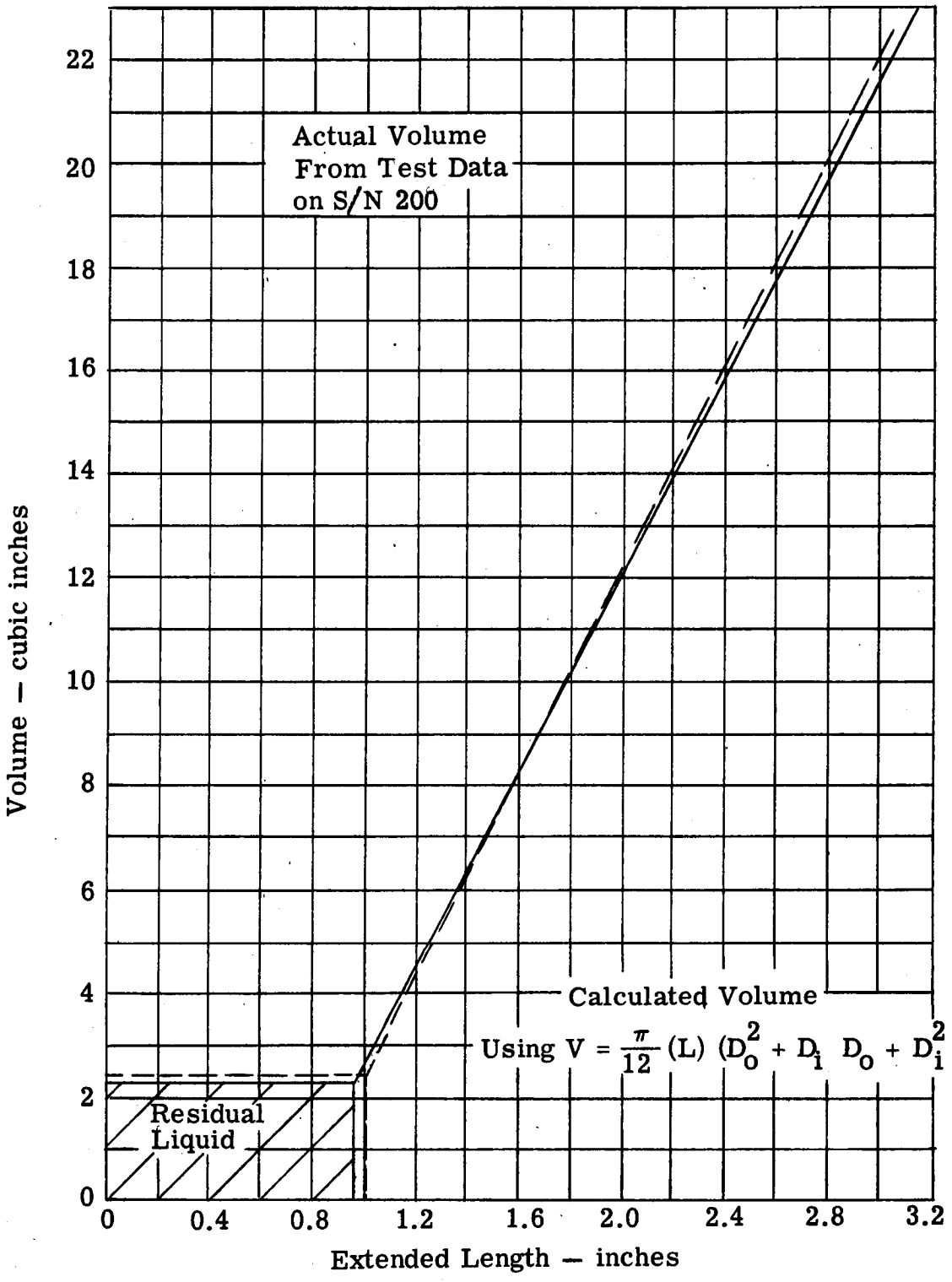

Figure 55. Actual Volume Versus Calculated Volume

SECTION 6

PERMEABILITY

A. SYNOPSIS

The basic concepts of permeation are reviewed briefly to show how the operating conditions in a positive expulsion device (tank/bladder type) affect propellant losses due to permeation. It is shown that permeation of propellant into a closed ullage space will stop when the ullage space becomes saturated with propellant at a given temperature. An apparatus is described for conducting tests under conditions simulating those that exist in a positive expulsion device; data are presented for the permeation of oxides of nitrogen that may be used for design purposes. The test work presented establishes the validity of the basic design of the permeation chamber. Various methods of detecting the permeant have been reviewed; three methods that appear to be applicable to the test conditions are:

(1) Karmen voltage-breakdown detector

(2) Thermistor-type thermal conductivity detector

(3) Cross-section detector

The basic criteria for choosing these detectors, in addition to their small size, are their ability to detect diatomic, as well as polyatomic molecules, and their high sensitivity (10^{-7} mole concentration or better). There are no test data for these detectors that are directly applicable to the test conditions; the exact choice depends mainly on the over-all range of detection desired. Areas requiring additional work are also discussed in the following paragraphs.

B. GENERAL

There are several "standard" tests for determining the permeation of plastics and elastomers to liquids and gases. These tests, including the ASTM test (D1434-58), are similar at least in principle. They do not, however, provide data that are directly useful for the design engineering of a positive expulsion system. It was, therefore, recognized that a need existed for a new "standard" test that will provide useful data for design engineering.

A program was established to study permeation technology and to devise a test that might be accepted as a new standard. The objectives of this program were:

(1) To design an apparatus that could be used as a standard for permeation testing of both storable and cryogenic propellants.

(2) To build the apparatus and conduct tests to prove reliability of the design concept, using storable propellants.

(3) To determine the optimum analytical techniques for measuring permeation rates.

(4) To establish procedures for determining:

   (a) The accumulation of propellant due to permeation under temperature cycling conditions.

   (b) The permeation of cryogenics.

To accomplish these objectives, it was necessary to determine what methods existed for permeation testing. Therefore, an extensive literature survey was conducted to determine what test methods and conditions have been used elsewhere. The sources reviewed are listed in References 61 through 109.

It was learned during this literature search that all procedures and equipment in use have several basic features in common:

(1) The test permeant is usually in the vapor state, although some tests have been conducted with liquids.

(2) The test permeant is generally at atmospheric pressure, although a few tests at elevated pressures are reported.

(3) The downstream side of the test membrane is usually evacuated (for example, ASTM test), although some investigators have conducted tests at atmospheric pressure; in any case, the difference in partial pressure across the membrane is kept constant at approximately one atmosphere (where the downstream side is maintained at atmospheric pressure, the permeant is continuously swept out with an inert gas).

(4) The test time is generally short, 2 to 4 hours.

A typical positive expulsion system will have a tank containing a bladder which in turn holds the liquid to be expelled. The bladder will be made of a flexible plastic or elastomeric material. A pressurizing gas, usually inert, will be contained between the tank wall and bladder. When a valve on the liquid side is opened, the gas expanding against the flexible bladder expells the liquid. Over a period of time, some of this liquid may be lost due to permeation through the bladder into the pressurizing gas space.

Most positive expulsion devices, and particularly the permeation problems encountered with these devices, have the following features in common:

(1) The bladder (or diaphragm) is in contact with a liquid.

(2) The pressure over the liquid is the same as the gas pressure, with the bladder merely acting as boundary layer between the liquid and gas phases.

(3) The gas space (the ullage space) is closed; the liquid that permeates into the ullage space is not removed but accumulates.

(4) The contact time, or mission life, of the space system may be days, months, or even years.

Comparing these features with those of the standard permeation tests listed previously shows an incompatibility between the test conditions and the conditions existing in a positive expulsion device under which permeation occurs. The overall objective, therefore, for this program was to develop a relatively simple and inexpensive apparatus which would produce accurate, reproducible, permeability data for a variety of propellant/pressurizing gas combinations under operating conditions simulating those in a positive expulsion device; and to determine the optimum analytical techniques for determining these permeation rates under simulated operating conditions. Before discussing these objectives further, a brief review of the theory of permeation is presented.

C. THEORY AND BACKGROUND

Many articles have been written over the decades describing diffusion (or permeation), its theory, mathematical treatments, etc. Some of the more elucidative articles of recent vintage have been written by G. J. Van Amerongen (References 61, 62, and 68), R. M. Barrer (Reference 67), W. E. Brown (Reference 65), and W. Jost (Reference 69). Graham, in 1866, presented the first theory on permeation. He postulated that permeation (the over-all process of transfer of a material from one side of a membrane to the other) is a phenomenon involving solution of the gas or vapor into a membrane, diffusion of the permeant through the membrane, and evaporation (or desorption) of the permeant away from the downstream side of the membrane. This theory still stands today, supported by much experimental data.

The process of diffusion of a species through the crystalline structure of a membrane is usually much slower than the process of solution and evaporation and is, therefore, controlling. The diffusion process is described by Fick's Law:

$$\frac{\delta c}{\delta t} = - \frac{\delta}{\delta x} \left(-D \cdot \frac{\delta c}{\delta x}\right) \tag{28}$$

Derivation of this equation can be found in texts describing thermodynamics of natural phenomena (for example see Reference 70).

In the vast majority of applications of plastic and elastomeric films, where permeation might be a problem, a steady-state or equilibrium condition is quickly established. Such applications include the food packaging industry, bottling of

liquids in plastic containers for commercial and consumer markets, and the transport of liquids and gases through plastic pipe and tubing.

In these various areas, the material that permeates through the membrane (wrapper, bottle, pipe wall, etc.) is quickly swept away from the area by air currents. Consequently, the difference in concentration across the membrane becomes constant and $\delta c / \delta t = \theta$. Under these conditions, a steady-state relation can be derived:

$$n = D(C_1 - C_2) \frac{A}{d} t \tag{29}$$

where: n = number of moles of material that diffuse in time t

D = diffusion coefficient

A = area of membrane

d = thickness of membrane

$C_1 - C_2$ = difference in molar concentration across membrane

If it is assumed that Henry's law governs the solubility of permeant in the membrane (not too inaccurate an assumption at low solubilities), then Equation (29) can be written in terms of the solubility coefficient, S, and partial pressure difference of the permeant across the membrane:

$$n = DS(p_1 - p_2) \frac{A}{d} t \tag{30}$$

It is reiterated here that the text refers to the diffusion process within the structure of the membrane, so p_1 refers to the in-going surface and p_2 refers to the surface at the downstream side. As previously stated, the third step in the permeation process is evaporation of the permeant away from the membrane. If evaporation does not occur, then p_2 will increase from zero initially to a value equal to p_1, so that $p_1 - p_2$ becomes zero and diffusion stops; hence, the over-all process of permeation stops.

Evaporation will continue only as long as the partial pressure of the permeant in the vicinity of the downstream side of the membrane is less than the vapor pressure of that permeant at the given temperature. As these molecules leave the surface of the membrane they will collide with molecules of the pressurizing gas and with the wall of the test chamber. Many of these molecules will be reflected back to the surface of the membrane. Since the mean free path of travel of molecules at the test temperature and pressure are in the sub-micron range, collisions between molecules will be many and frequent. A detailed description of these phenomena, including the diffusion of the permeant through the gas space (this is usually quite rapid), is beyond the scope of this report, but can be found in texts on the kinetic theory of gases. It is sufficient to say that initially, when the concentration of

permeant in the gas is essentially zero, the rate of evaporation will be high, decreasing as the concentration of permeant increases.

The over-all permeation, Q, of a molecule of liquid through a membrane to a point a finite distance, m, away from the membrane, could then be described as the permeation, n (Equation 30), through the membrane times evaporation rate, Ev, at time, t, where:

$$Ev = f\left[D', (C_2 - C_m), t\right] \tag{31}$$

The prime refers to the gas side of the membrane. However, $D' >> D$, particularly when m is small so that diffusion through the membrane is still controlling. In other words, at the moment molecules of permeant first reach the downstream side (surface 2) of the membrane, $(C_2-C_m) = C_2$, and they evaporate rapidly to position m. Some of these molecules will be reflected back to surface 2 so that $(C_2-C_m) \rightarrow 0$; C_2 however is still less than C_1. In the meantime, more molecules reach surface 2, so that again $C_2 > C_m$; these diffuse to m, so that again $(C_2-C_m) \rightarrow 0$. Some of these are also reflected back to surface 2, so that $C_2 \rightarrow C_1$. This continues until $(C_2 - C_m) = 0$ and evaporation can no longer occur. At the same time, $(C_1 - C_2)$ becomes equal to zero and permeation stops. A plot of the mass of permeant that reaches m versus time, t, will be an exponential curve (see Figure 68).

In the usual type permeation test, C_m is maintained at essentially zero during the test, so that Ev is at a maximum; consequently, C_2 or p_2 is essentially zero during the test and permeation proceeds at a maximum rate. A plot of n versus t would give a straight line after the steady state is reached. Barrer in Reference 67 shows that, if the straight-line portion of the graph is extrapolated back to the time axis, the time lag, θ, is related to the diffusion coefficient, D, and thickness, d, by:

$$D = d^2/6\theta \tag{32}$$

Since the permeation rate, n, is the product of D and S (Equation 30), it can be seen that, by measuring the permeation rate and determining the diffusion coefficient by use of Equation 32, the solubility coefficient for a given membrane can be calculated.

In a positive expulsion device, it is necessary to know the shape of the curve of n versus t to determine what problems may be encountered during the mission of the vehicle. The maximum amount that will permeate can be calculated from the vapor pressure data, ullage volume, etc., since by definition permeation will stop when the partial pressure of the permeant in the vapor space is equal to the vapor pressure of the permeant at the existing temperature. Since mission times vary from several hours to several months, it is sometimes necessary to know how fast this maximum value will be reached. Tests under conditions simulating actual operating conditions will provide these data. An apparatus for conducting such tests was developed under this contract.

D. PERMEATION TEST APPARATUS

The apparatus designed for this program consists essentially of a stainless steel cylindrical chamber containing a bellows. The one end of the bellows is sealed to the top cover of the chamber and the other is closed with the test membrane. The test liquid is placed in the bellows. The flexibility of the bellows permits some volumetric changes to occur without imparting a pressure differential across the specimen. (Actually the unit is designed for a maximum ΔP of 0.7 psig across the specimen.) Figure 56 is a cross-sectional view of the chamber, and Figures 57 through 62 are detailed drawings of the component parts.

To avoid the requirement for removing samples from the test apparatus for analysis, a Perkin Elmer (Catalog No. 186-0026) high-pressure gas cell having a 5mm path length is attached directly to the two ports on the bottom of the permeation chamber. The arrangement is such that the mounting plate of the gas cell will slide into the bracket at the entrance slit of the Perkin-Elmer Model 421 Infrared Grating Spectrophotometer. Figure 63 is a photograph of the apparatus mounted on the infrared unit.

Figure 64 shows the apparatus on its wooden stand; Figure 65 shows the disassembled apparatus; and a flow schematic of the apparatus is shown in Figure 66..

Because of the reactivity of oxides of nitrogen (used for the test work) with sodium chloride, the gas cell was modified by replacing the standard sodium chloride windows with silver chloride windows 1mm thick. Each of the windows is protected from the high internal cell pressure by a 0.125-in. thick stainless steel disc in which slits of the same dimensions as the spectrophotometer entrance slits are milled. For protection against corrosion, all components of the cell in contact with the silver chloride are silver plated.

E. PERMEATION TEST WORK

To determine quantitatively the amount of permeant that accumulates on the gas side of the membrane, it was necessary to calibrate the gas cell. A limited number of calibration points were established using a 60mm high-pressure gas cell. (The calibrations were made while actual tests were in progress. The concentration of permeant is inversely proportional to the path length at a given absorbance.) A calibration curve was prepared by making successive dilutions of a known N_2O_4/ nitrogen mixture. Since the partial pressures estimated in this manner are not highly accurate, a linear regression equation for the experimental data (calibration data) was calculated:

$$y = 0.024 + 0.0168\ x \tag{33}$$

where y is the theoretical absorbance and x is the partial pressure in mm of Hg. The coefficient of correlation is 0.96 compared with 1.0 for a perfect fit. The resultant calibration curve is shown in Figure 67.

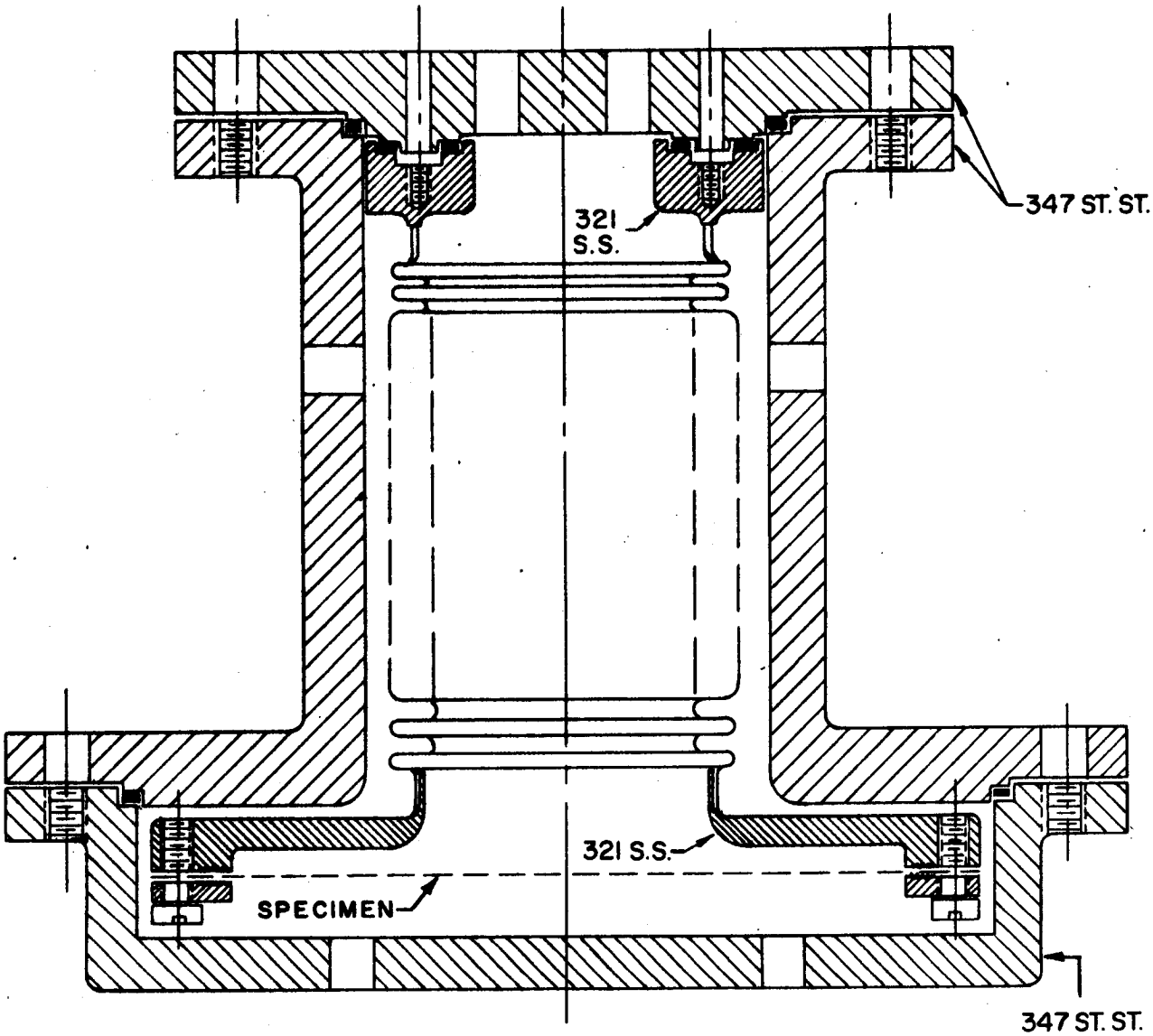

Notes: Approximated Full-Scale.
All Machined Surfaces 63 RMS or Better.

Figure 56. Permeability Apparatus Assembly

Scale 2:1 Approx.
Material: 321 Stainless Steel

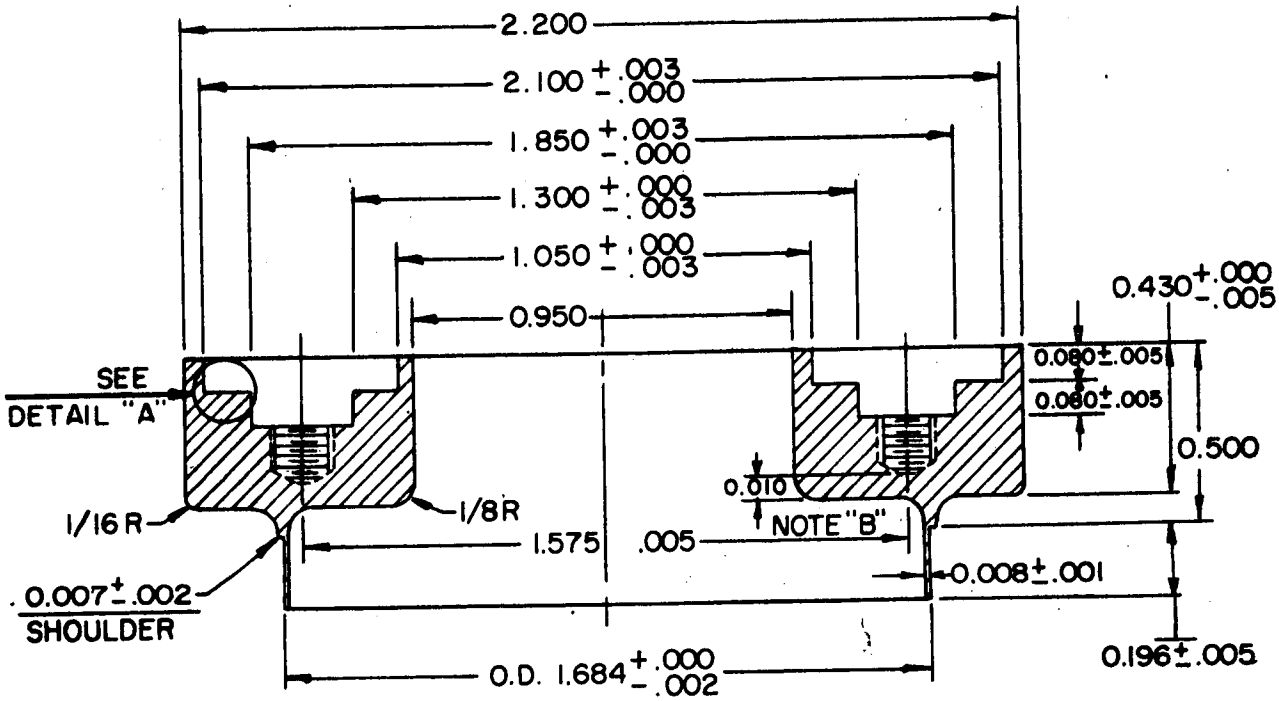

Detail "A"

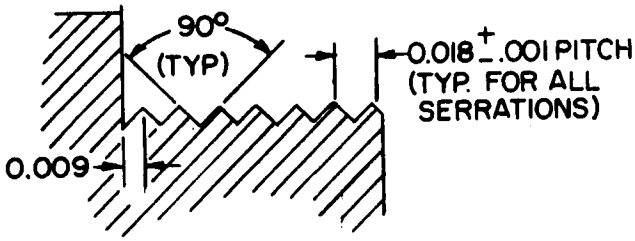

Note "B"
Drill and tap 12 holes
No. 8-36 thread
Leave 0.010 inch well at bottom of hole

Both serrated surfaces controlled to 0.005 inch max. flat crest of serrations in plane which is flat within 0.001 T.I.R. for full diameter

Figure 57. Upper Bellows Flange

① 12 holes 8-36 thread
② 12 holes No. 19 drill

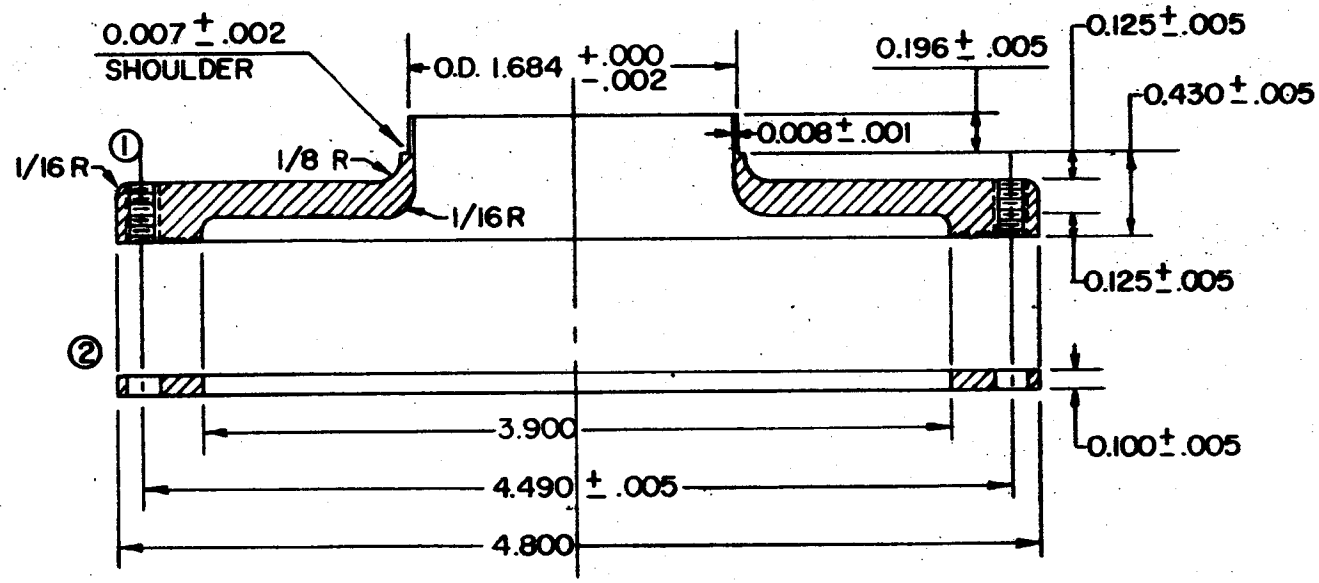

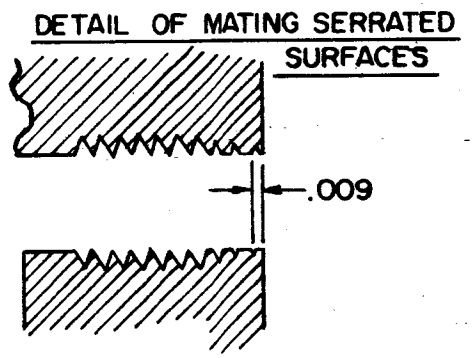

Crest of serrations in plane which is flat within 0.001 T.I.R. for full diameter. Depth of cut for 3rd serration 75% of full cut; for 2nd, 50%; and for first, 25%.

Figure 58. Mounting Flange

① 2 holes 1/4 in. diameter
② 12 holes No. 19 drill
③ 12 holes 7/32 drill

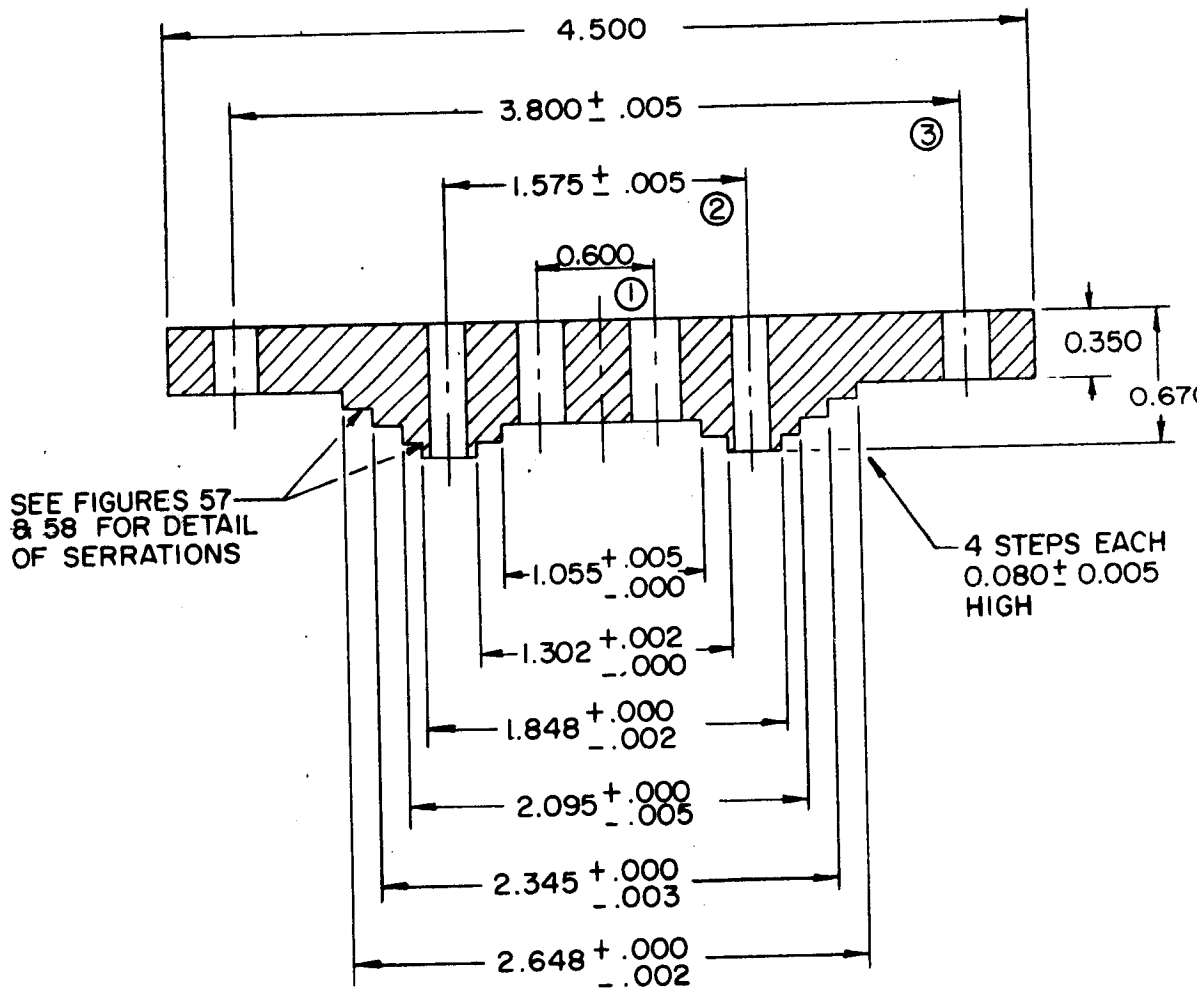

Figure 59. Top Cover

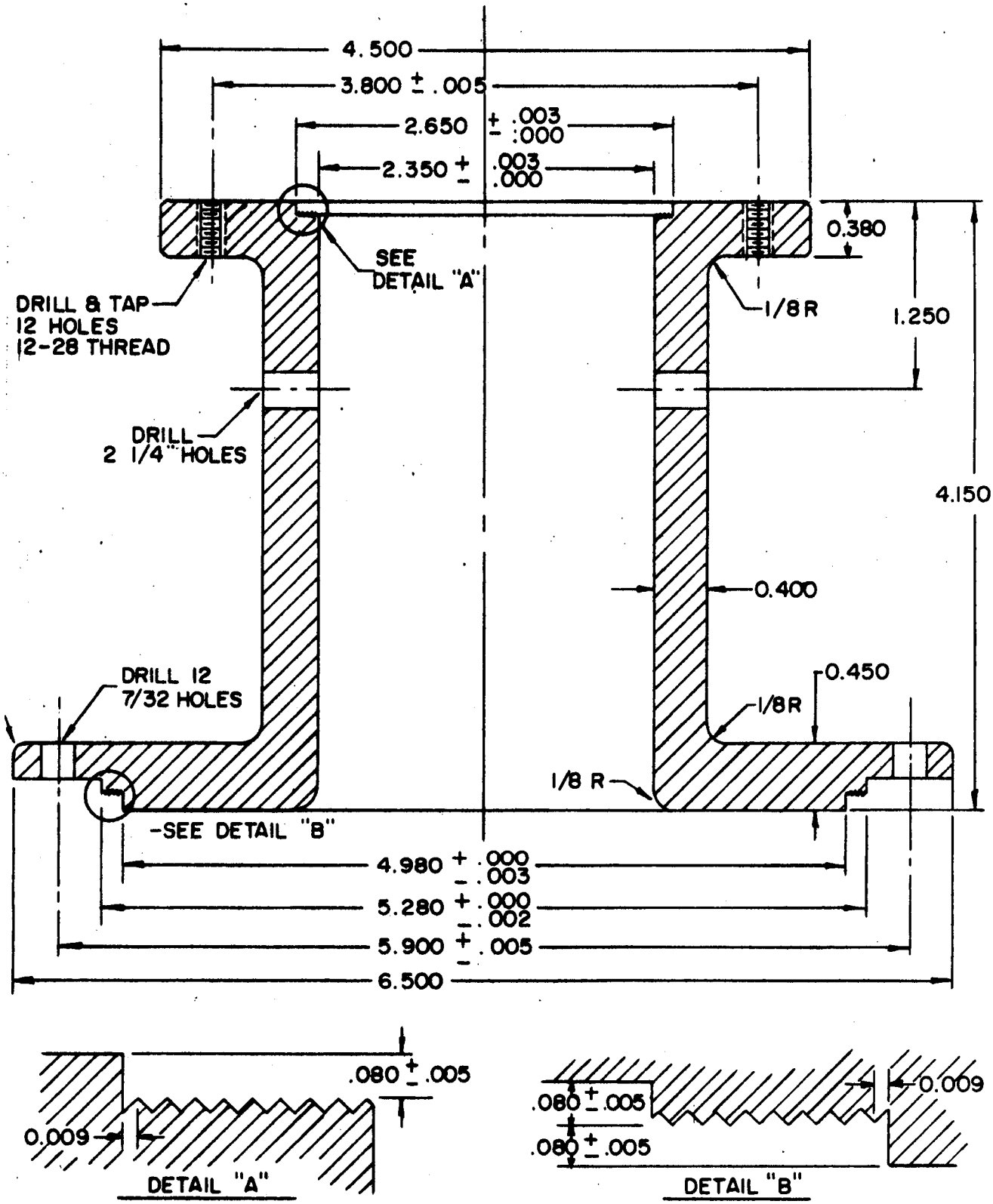

Figure 60. Body

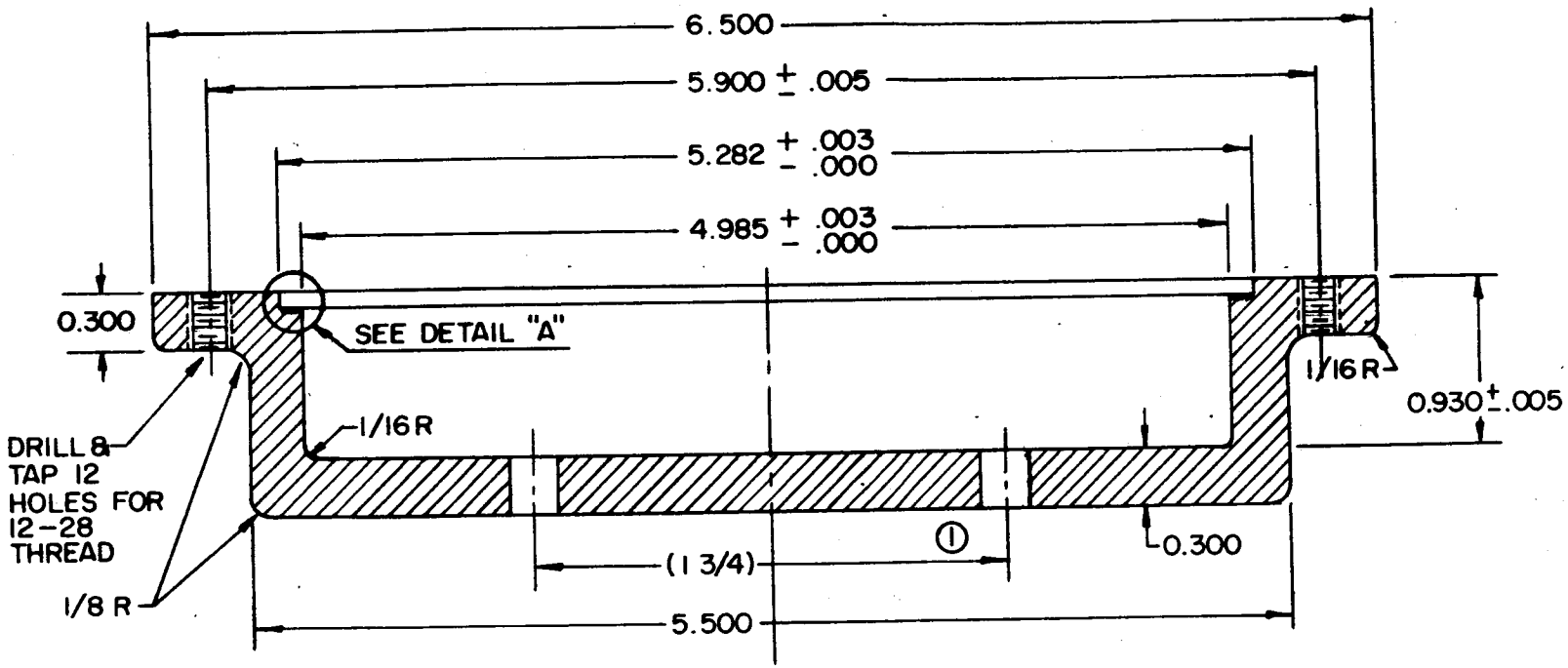

1 Drill 2-1/4 in. holes; before drilling contact W.H. Walters for exact distance between holes

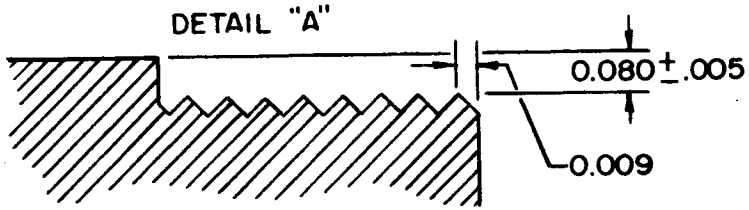

Figure 61. Bottom Cover

Make three sets

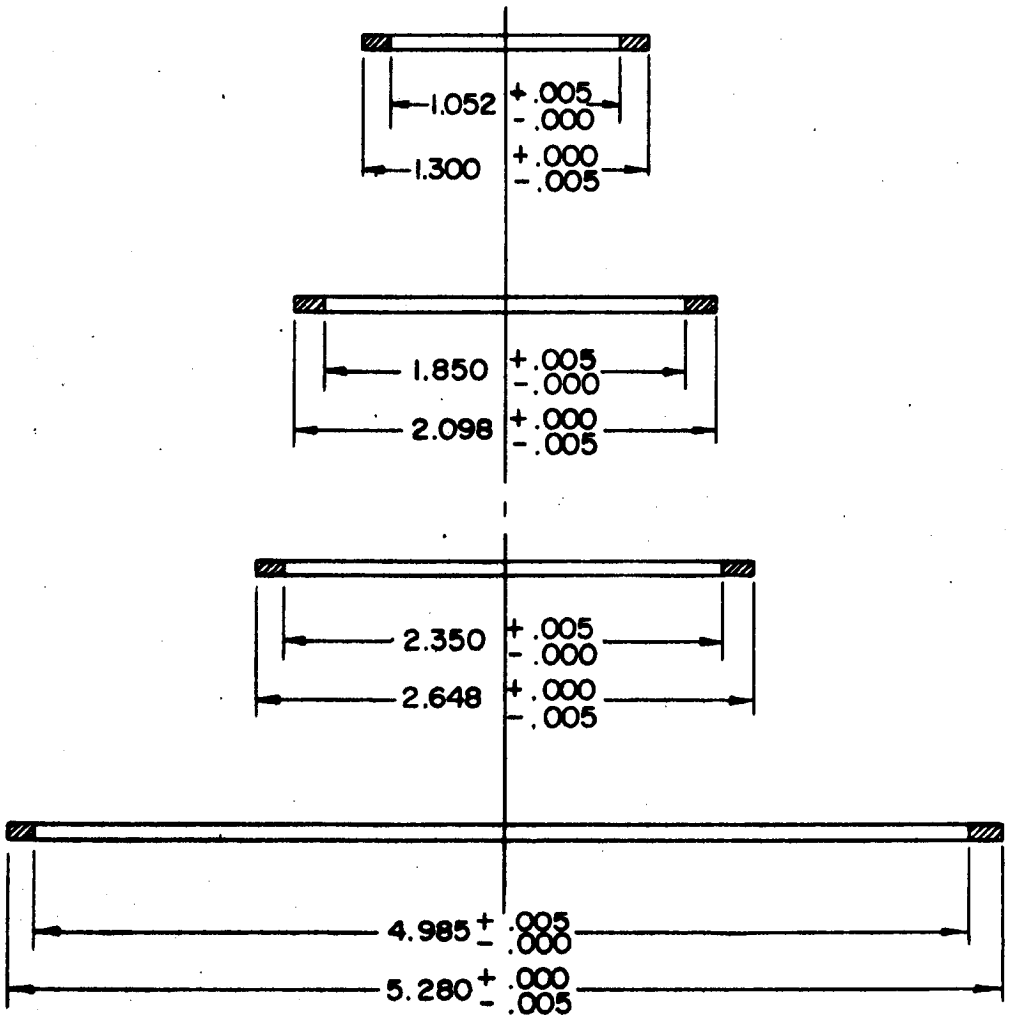

Note: All gaskets 0.060 in. thick teflon

Figure 62. Gaskets

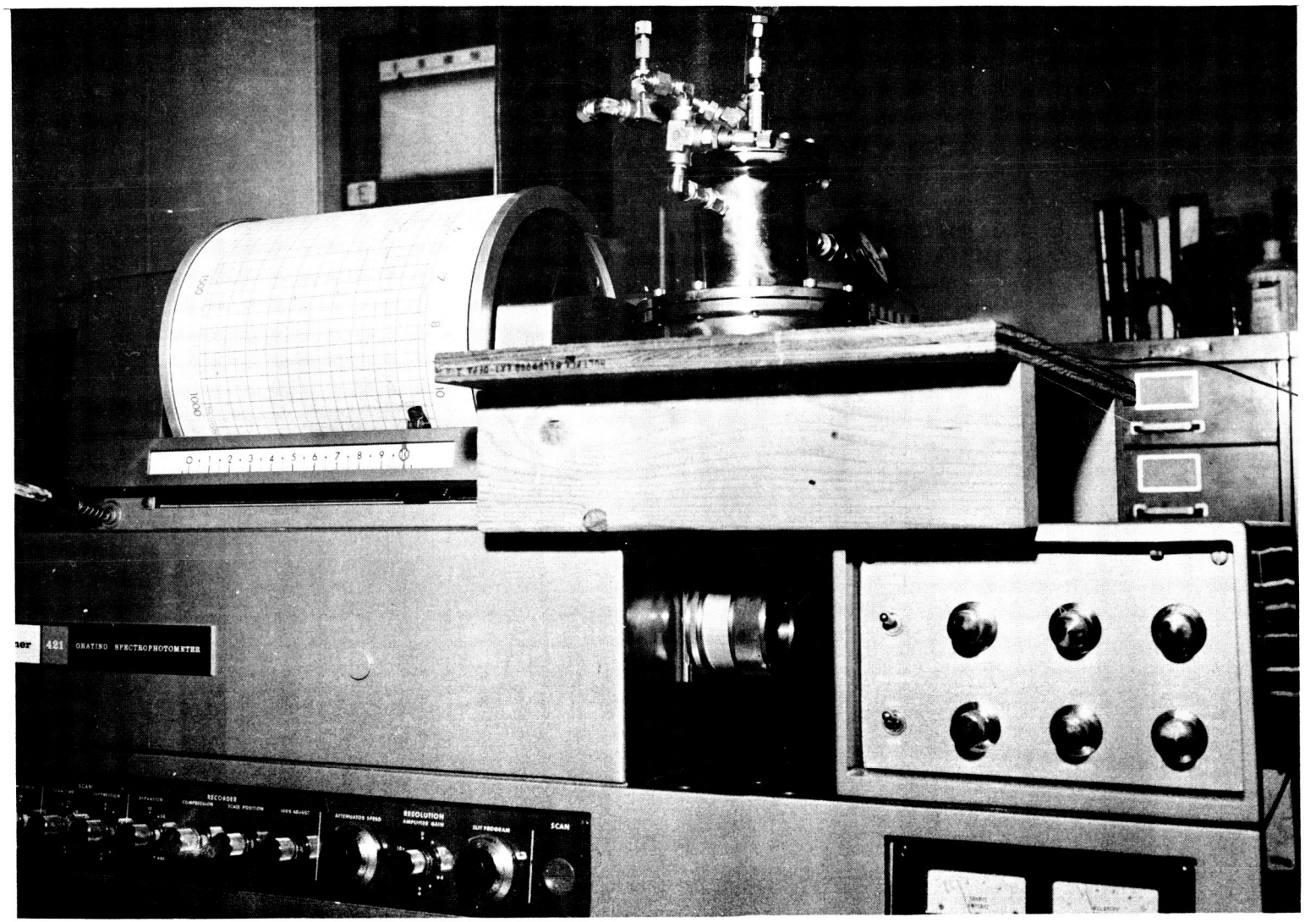

Figure 63. Permeability Apparatus Mounted on Infrared Unit

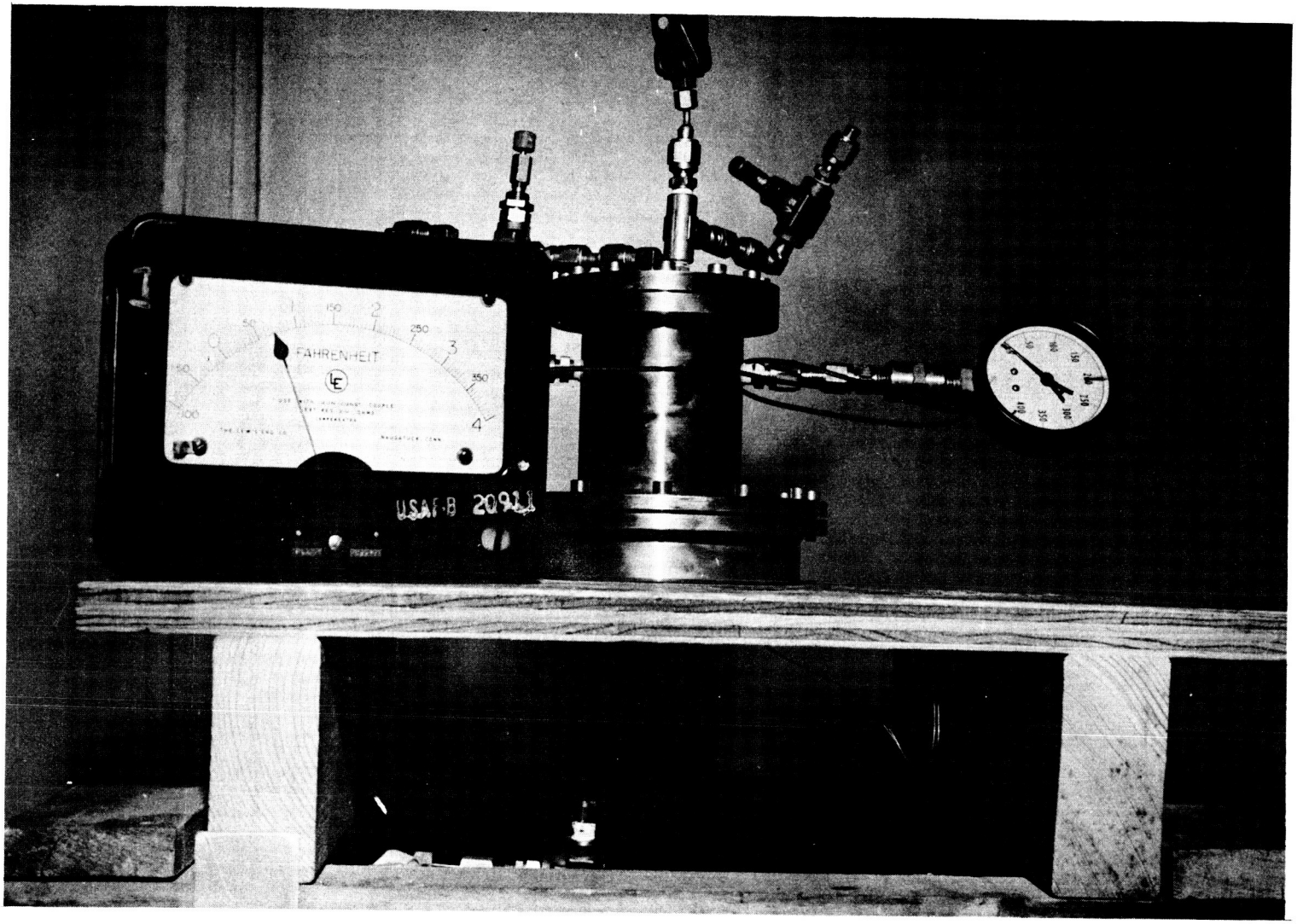

Figure 64. Permeability Apparatus Mounted on Wooden Stand

Figure 65. Permeability Apparatus Disassembled

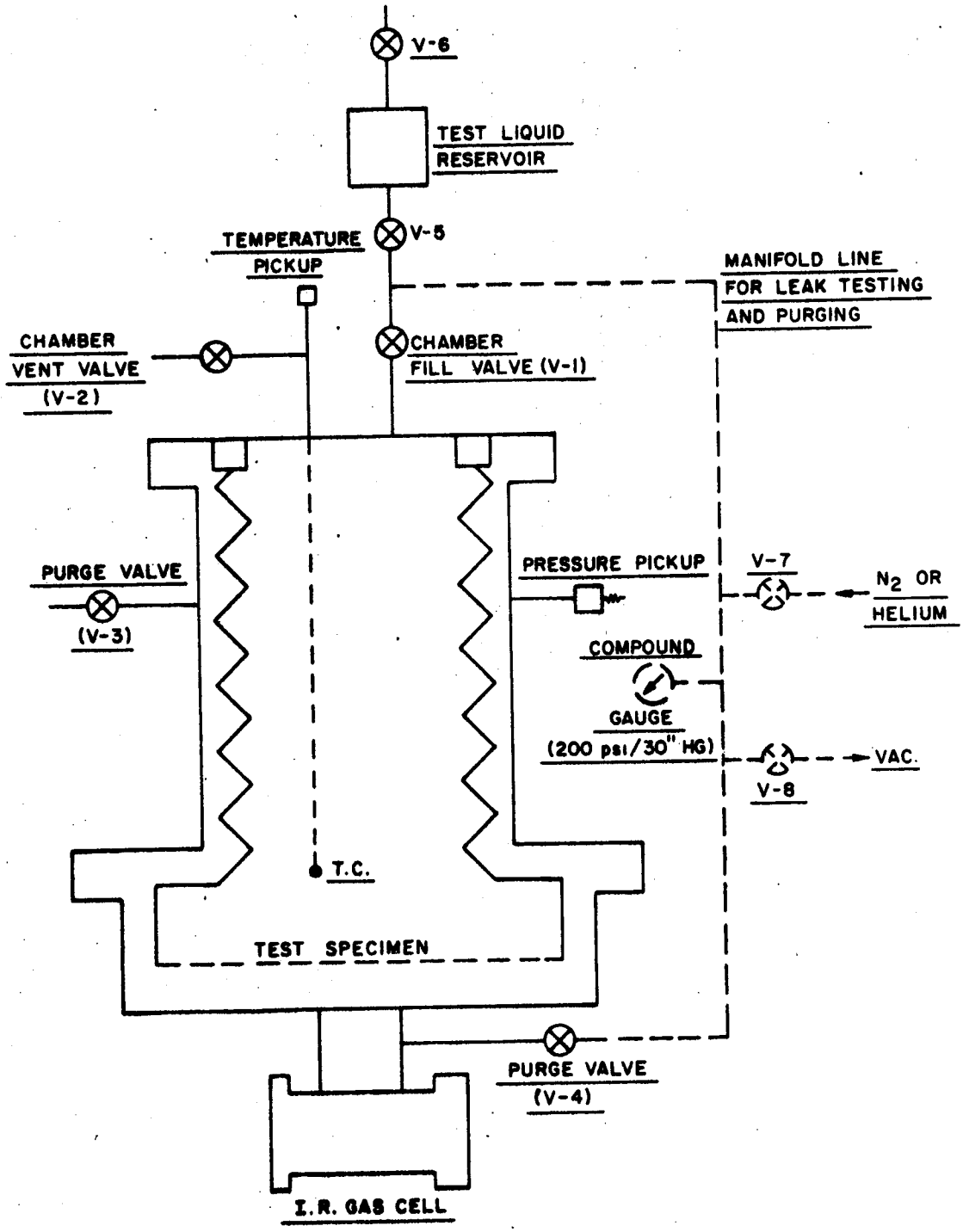

Figure 66. Flow Schematic of Permeation Test Apparatus

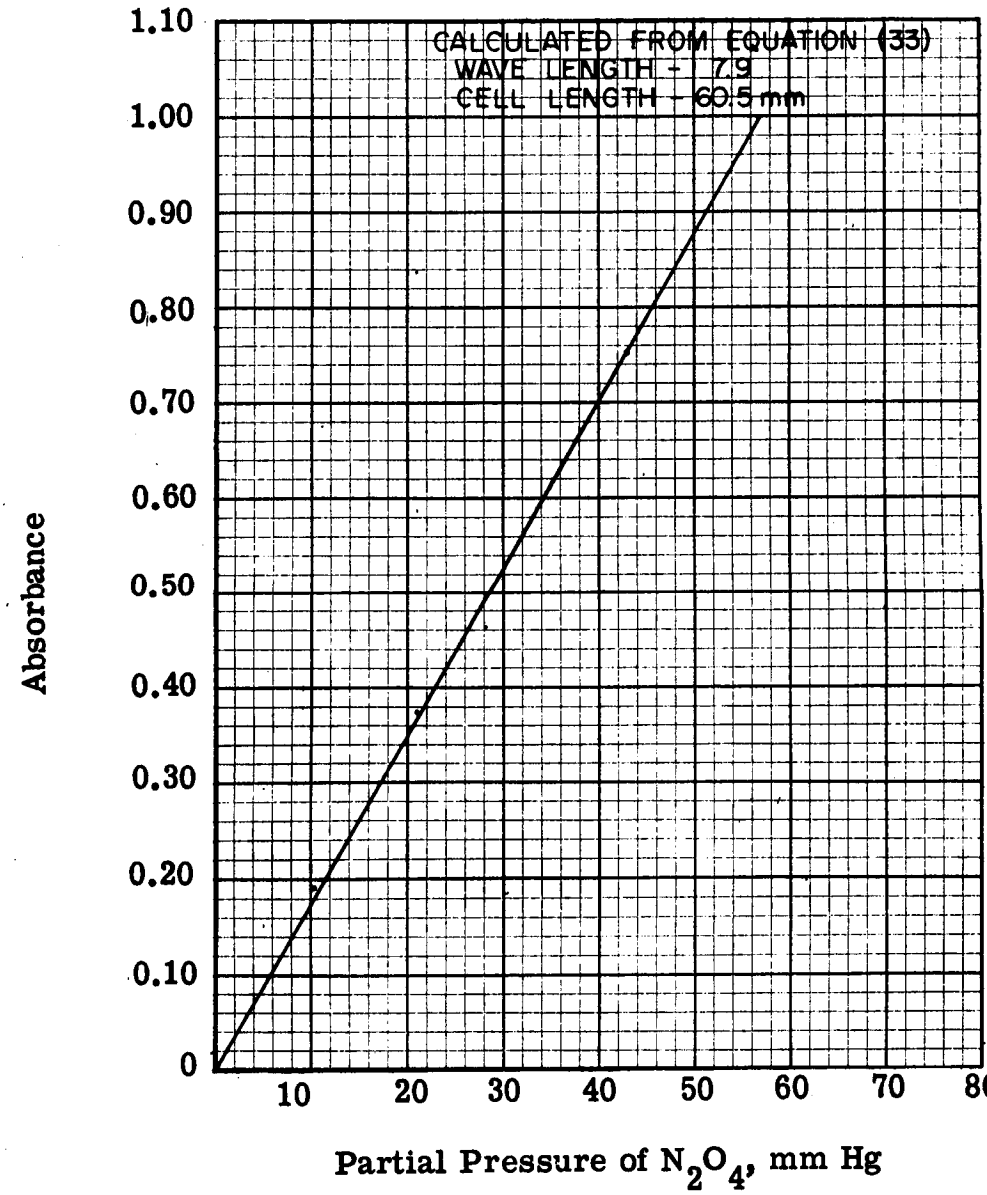

Figure 67. Calibration Curve for $N_2O_4 \rightleftharpoons 2NO_2$

Absorbance measurements (for calibration runs) made at total pressures of one atmosphere and 14.8 atmospheres showed that the absorbance was not measureably affected by pressure.

Nine tests were conducted. In the first four tests, several operating difficulties were encountered. The two main problems were the presence of gas pockets on the liquid side and the lack of temperature control during loading and unloading.

In the first two tests, a differential pressure cell was attached across the gas and liquid sides of the apparatus. This was for the purpose of determining if the specimen flange seated up or down during loading and unloading. This was to be indicated by a ΔP in excess of 0.7 psi. The complexity of the cell and lines, however, was a source of gas pockets on the liquid side. It was removed after the second test.

The other problem was temperature control. If the vapor pressure of the liquid exceeds 0.7 psi (approximately) at the loading temperature, then the specimen can be forced into the lower part of the chamber and damaged. This problem existed particularly with mixed oxides of nitrogen (MON) which boil at +40°F. One criterion for operation, therefore, was that the temperature of the apparatus had to be below the boiling point of the test liquid during loading and unloading.

Following these preliminary tests with their associated operating problems, and before conducting additional tests, detailed operating instructions were prepared. They are included in Appendix IV. The flow schematic for the apparatus, which is included with these operating instructions, is also shown in Figure 66. Five tests were conducted using these operating instructions: for tests Nos. 5 and 6, MON was used; for tests Nos. 7, 8, and 9, N_2O_4 was used. In all tests, only the N_2O_4 molecule was calculated from the infrared spectrum. (The NO fraction of MON generally did not show up on the spectrum during the relatively short time of the tests. This agreed with results from earlier tests conducted at Bell Aerosystems).

The data from the several tests are presented graphically in Figures 68 and 69. Figure 68 presents the total permeation (as determined by the infrared spectrum) versus time for the several tests. Figure 69 presents the calculated permeation rate versus time. These curves converge and approach zero at infinite time. (This can be readily seen from the fact that each point represents the permeation rate at that particular time. If the difference, or change, in total permeation was plotted versus time, then the curve would approach zero at the same time as the curves in Figure 68 approach saturation.)

As predicted from Equations (30) and (31), the amount of material that permeates approaches a maximum value (or $\Delta n \longrightarrow 0$ with time) which can be calculated from a knowledge of the vapor pressure of the permeant, and volume of the gas, or ullage space. What cannot be predicted is the shape of the curve before equilibrium is reached. This will vary with the membrane being tested and to a much lesser extent with the geometry of the system. The three different lots of 6-mil

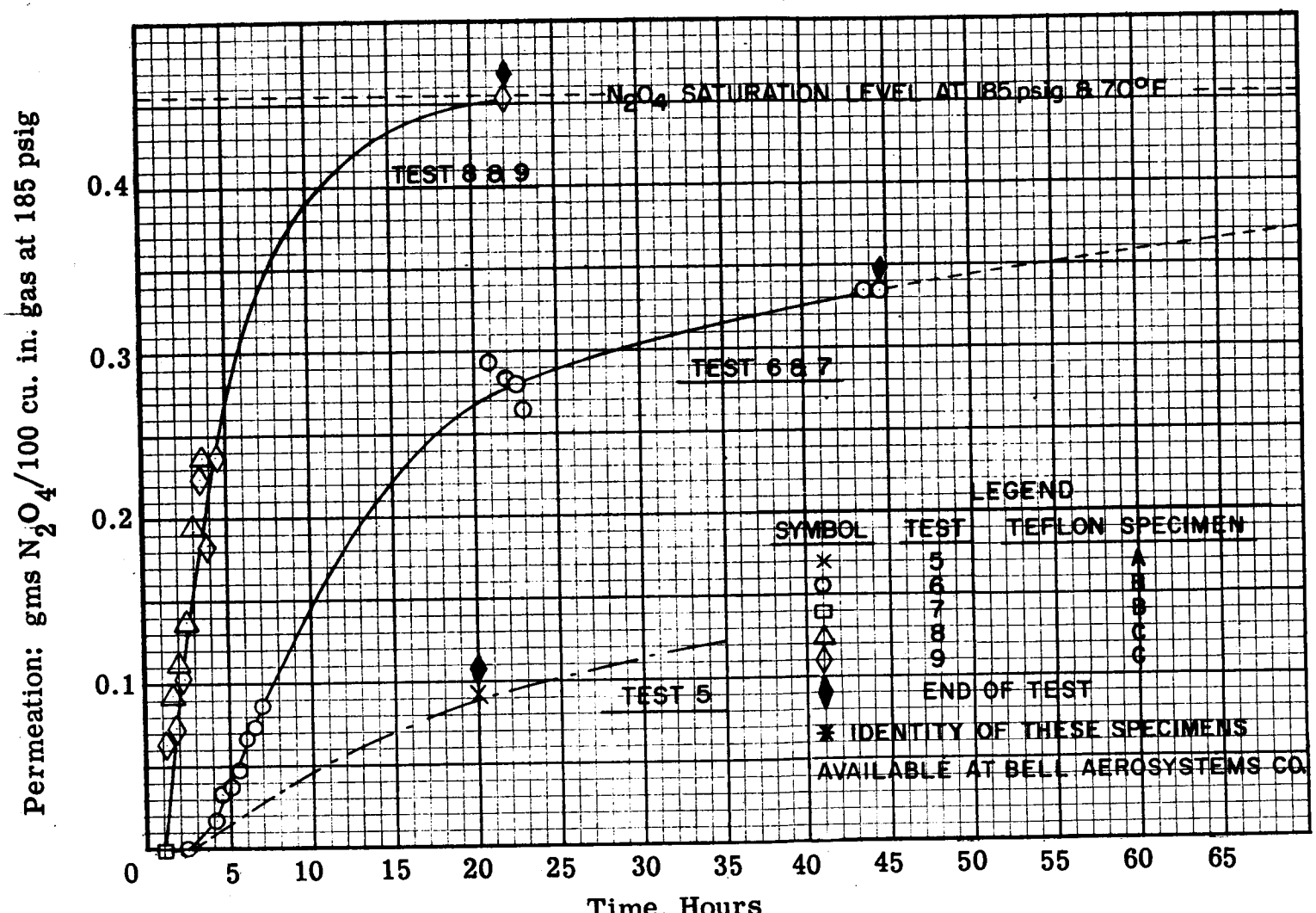

Figure 68. Total Permeation versus Time

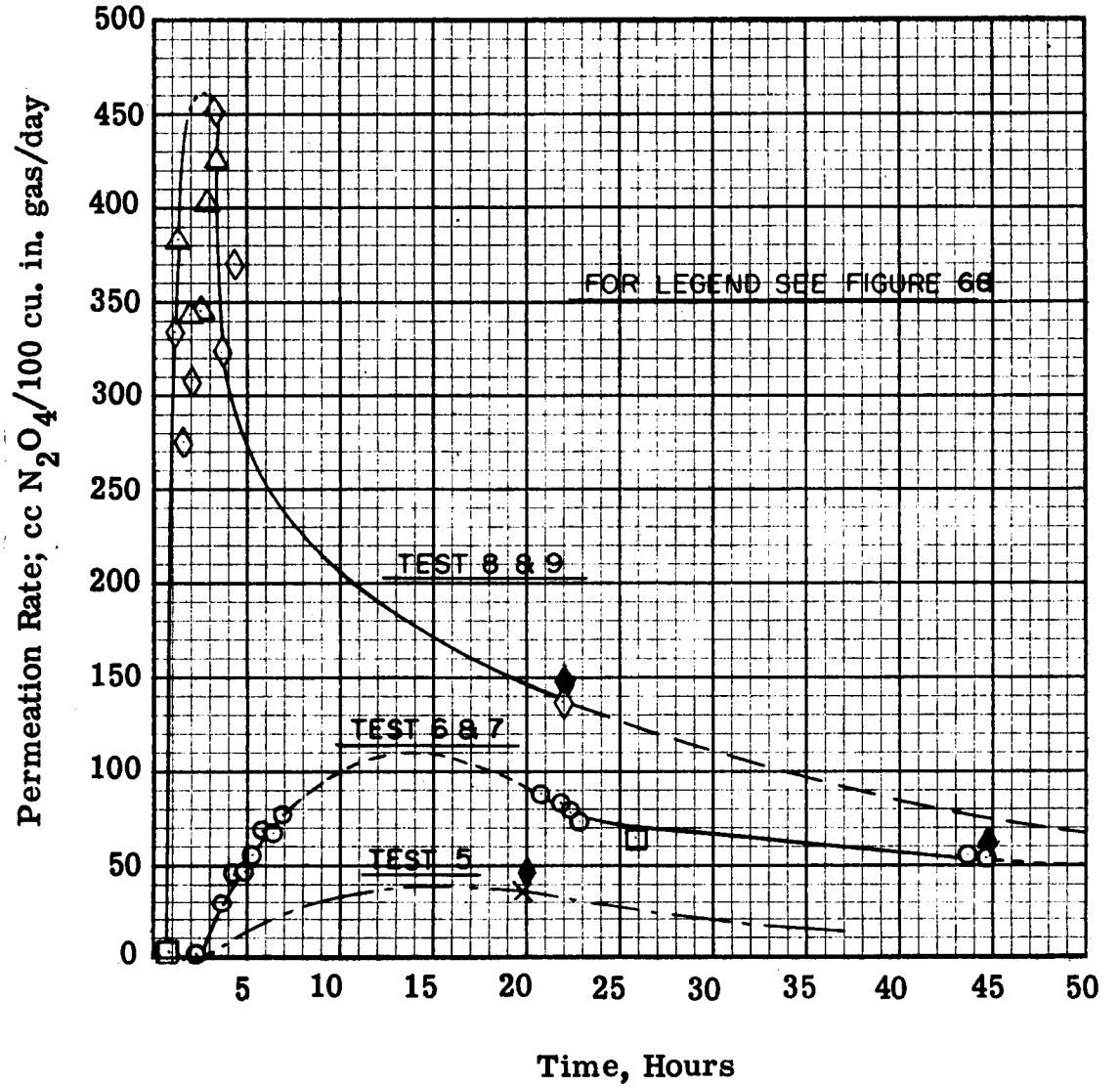

Figure 69. Permeation Rate Versus Time

Teflon used for these tests were tested on an ASTM apparatus (ASTM D1434-58) for gas transmission of MON. Note the comparative position of the curves in Figure 68 and 69, with these different tabulated ASTM rates:

Teflon Type A - 77.3 cc MON/100 sq in./day

Teflon Type B - 414.8 cc MON/100 sq in./day

Teflon Type C - 664.2 cc MON/100 sq in./day

By modifying the apparatus using a different analytical detection device, to be described, it will be possible to generate datum points continuously and automatically from start to saturation. There will be no wide gaps between groups of points as noted in Figures 68 and 69, and hence the exact shape of the curve will be more accurately determined. If the degree of saturation of the ullage space is important and/or critical for a particular mission then it will be possible to predict the extent of the problem and choose a membrane for the bladder with an initial slope such that saturation may or may not (as the case may be) be reached during the mission life of the particular vehicle.

As a matter of interest, earlier permeation work at Bell Aerosystems Company (under other contracts, Reference 109) is summarized in Figure 70 with the test data from current tests. This early work made use of a "Zero Δ P Apparatus" in which zero differential pressure was maintained across a test membrane by manipulating complex valving and piping, and adjusting nitrogen pressure on either side of the membrane as required. Figure 71 is a flow sheet for this apparatus. In addition, there were two tests using a full scale tank and bladder assembly. Figure 72 is a sketch of the test assembly. Analyses were conducted with the Zero Δ P Apparatus after 1, 4, and 10 days. The first analyses with the two tank tests were after 6.8 and 12.5 days, respectively, as noted in Figure 70. Because of the gap between the current data and earlier data, a dotted line is used to join the two. The Bell/NASA data permit a more-accurate extension of the curve approaching zero time. Saturation is reached in approximately 25 days; if the data for tests Nos. 6 and 7 in Figure 68 are extrapolated, the data reach saturation in approximately 25 days. (The data in Figures 68 and 69 are corrected to 185 psig, whereas the data in Figure 70 are at the pressure at the time of analysis.)

F. EVALUATION OF ANALYTICAL TECHNIQUES

As previously stated, one of the objectives of this program was to determine optimum analytical techniques for measuring permeation rates.

The ideal analytical detector would have the following capabilities:

(1) Static operation at pressures to 200 psi.

(2) Stable operation for a couple of weeks over a temperature range of, for example, +140°F down to cryogenic temperature.

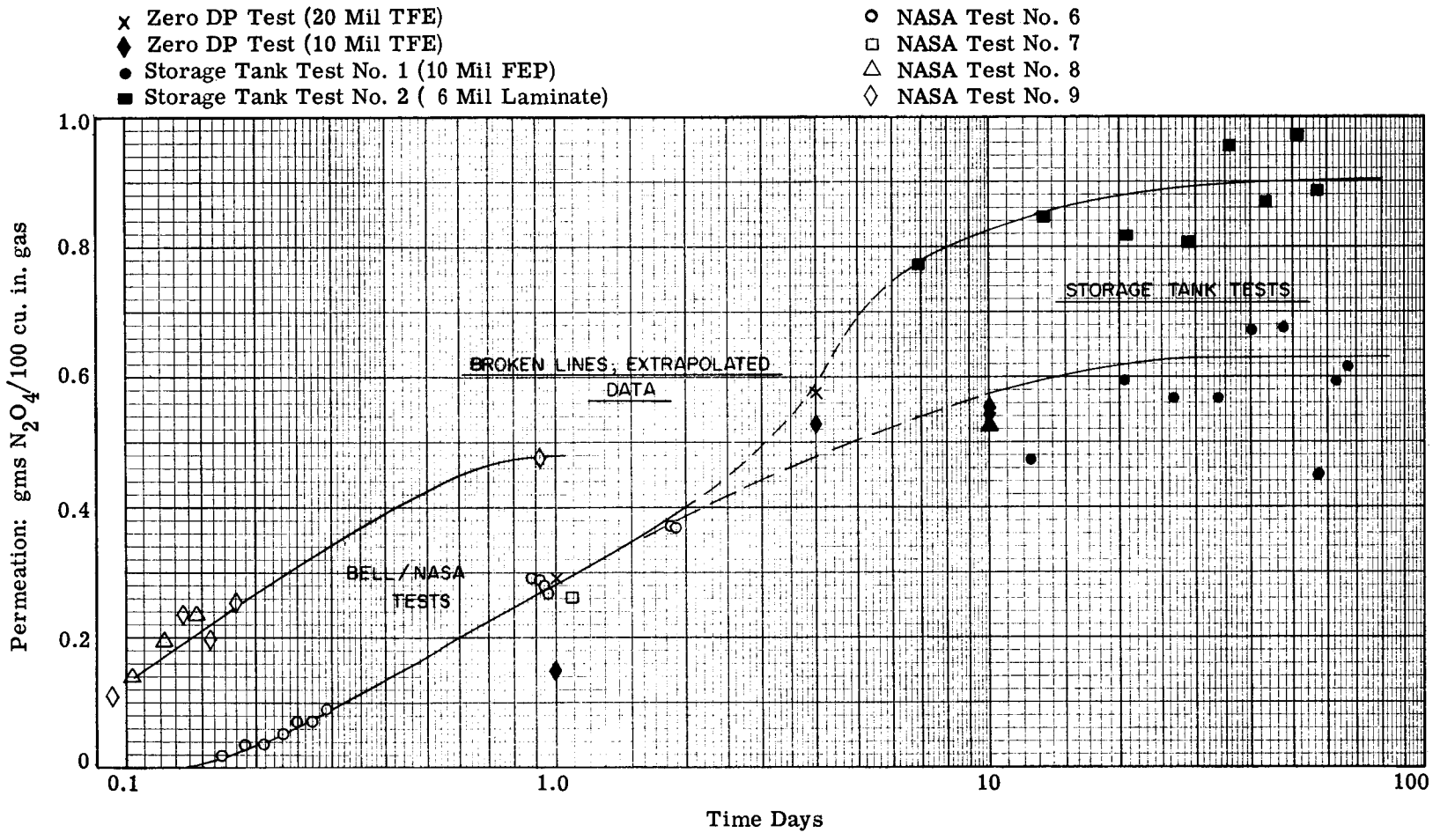

Figure 70. Comparison of Permeation Test Data

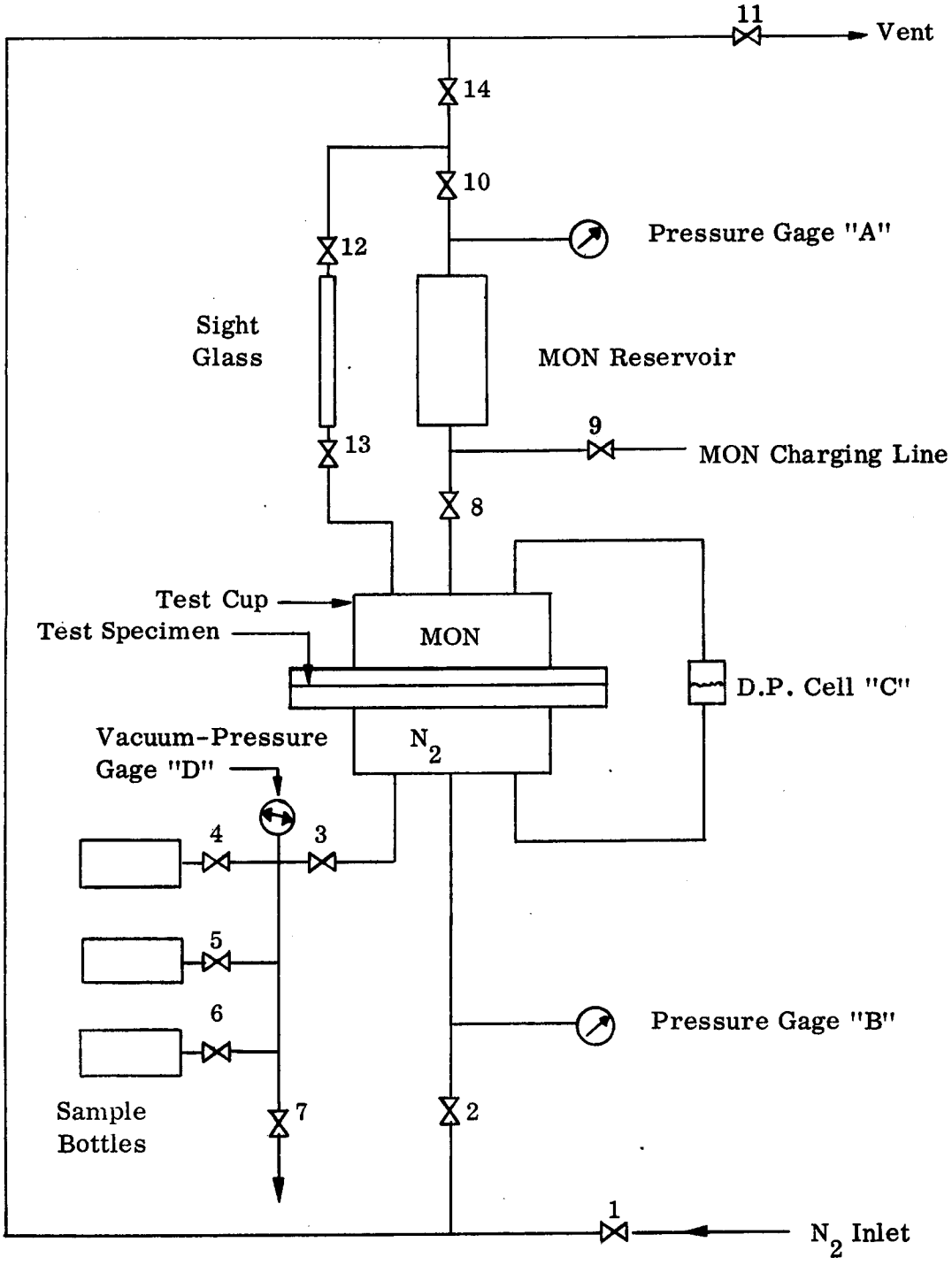

Figure 71. Flow Sheet For Test Apparatus

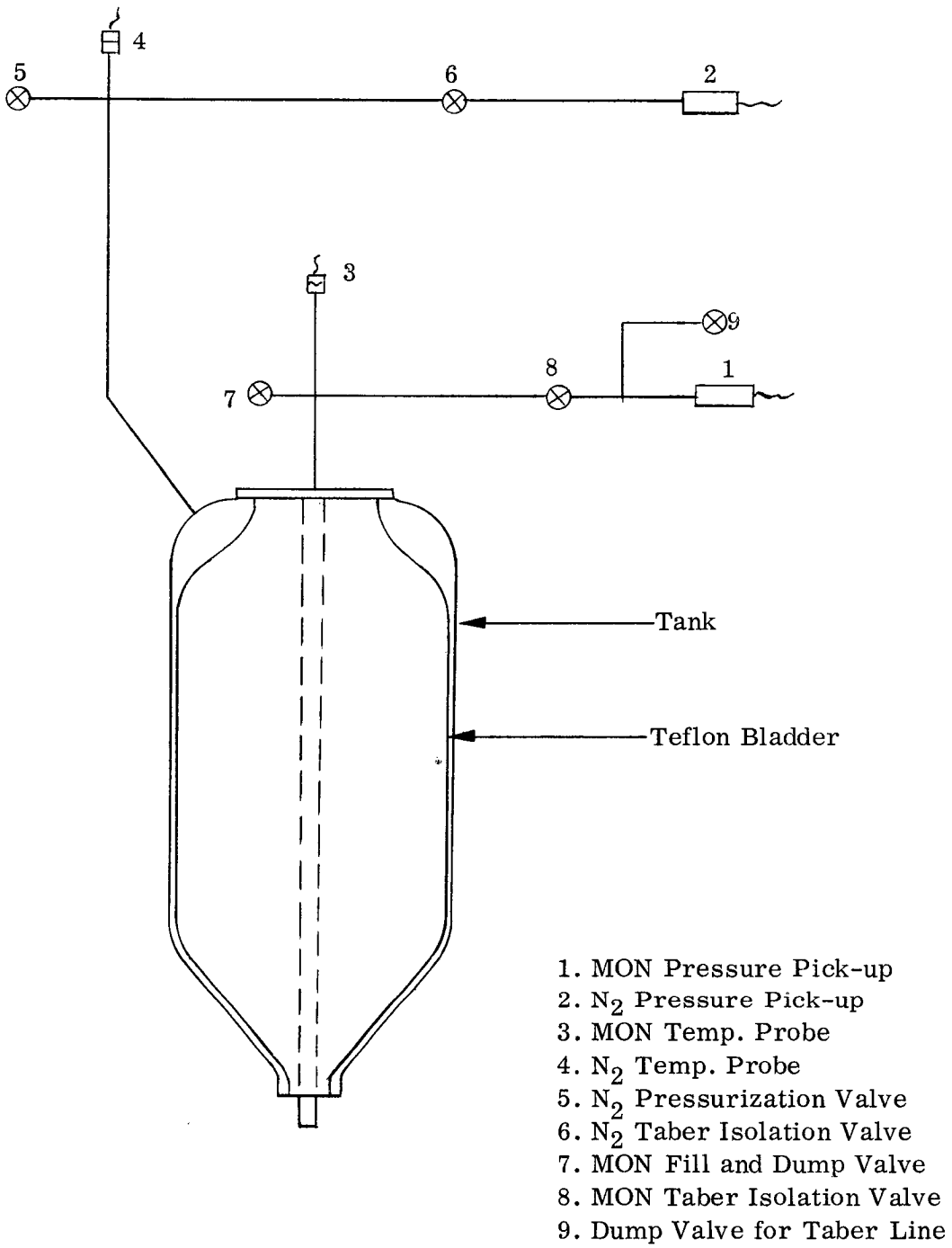

Figure 72. Sketch of Test Assembly

(3) Sensitivity in the ppm to ppb range.

(4) Non-specific, i.e., capable of detecting monatomic, diatomic, and polyatomic molecules.

(5) Relatively small and compact.

(6) Reasonably economical.

There are two general types of detectors that might be considered for this application where an initially pure pressurizing gas is contaminated by an increasing concentration of a second gas or vapor.

The first type would respond to and measure the concentration of the contaminant species. A detector of this type would be extremely sensitive. Typical examples might be the use of radioisotopes, optical absorption, or chemo-electric detectors. Such detectors would by nature be highly specific, and not particularly suitable for the immediate application. Furthermore, the equipment would be expensive and not very small and compact.

The second type of detector would respond to a change in some property of the pure pressurizing gas caused by the introduction of the contaminating species. Such properties might be the thermal conductivity and ionization constant. The most widespread utilization of such sensitive non-specific detectors as these which might be suitable for our application is in the field of gas chromatography.

For this reason the literature on detectors for gas chromatography was carefully reviewed for data on detector performance and characteristics. It was found that detector technology is in a state of constant change and new developments are being disclosed in the literature at a rapid pace. A partial list of published information that has been reviewed is included in the List of References. In addition to the literature survey, direct inquiries including visits were made to Beckman Instruments, Inc., Jet Propulsion Laboratories, and the Perkin-Elmer Corporation.

As this investigation progressed it became increasingly evident that our operational requirements are quite unique and that detector characteristics have not previously been investigated over a broad enough range of conditions to permit a definite selection, at this time, of a particular detector for inclusion in an ultimate design of a standard permeation apparatus. In addition, most of the available data on detector characteristics are reported with complete chromatographic systems as the frame of reference. When it is possible to distinguish the effects due to other components of such systems, for example, column bleed, etc., it is found that such characteristics as base line stability of the detectors is quite good.

Not withstanding these problems with the detector review and evaluation, an attempt was made to compare a number of detectors and the results are tabulated in Figure 73. The results of this preliminary evaluation have focused attention on three types for more thorough investigation. These detectors are discussed in the following paragraphs:

Detector	Operational Capability								
	Item								
	1	2	3	4	5	6	7	8	9
Type I (Responds to and measures conc. of contaminant)									
(1) Radio Chemical*									
(a) Tagged Propellants	C	E	E	E	D	B	A	B	B
(b) Radio Active Clathrates	B	E	E	E	A	B	A	B	B
(c) Neutron Activation	E	E	E	E	A	B	C	B	B
(2) Optical Absorption									
(a) Ultraviolet	A	C	C	A	A	B	D	B	B
(b) Infrared	A	C	C	A	D	B	D	B	B
(c) Chemo. Optical	B	A	B	B	A**	B	D	B	B
(3) Chemo. Electric**									
(a) pH	D	A	D	D	A	B	A	A	A
(b) Conductivity	D	A	D	D	A	B	A	A	A
(4) Miscellaneous									
(a) Mass Spectrometer	B	D	D	E	A	B	D	B	B
(b) Contact Potential 01 factometry	E	E	E	E	A	B	A	E	A
Type II (Responds to change in property)									
(1) Thermal Conductivity									
(a) Hot wire	E	E	E	E	D	A	A	A	A
(b) Thermistor	E	E	E	E	A	A	A	A	A
(2) Gas Density	B	E	E	E	D	A	A	C	C
(3) Electrical									
(a) Flame ionization	B	E	E	E	A	B	A	A	A
(b) Electron Capture* (Cross Section)	C	E	E	C	A	A	A	A	B
(c) Ionization (Break down voltage)	C	E	C	C	A	A	A	D	A

Desirable Detector Capabilities

Item

1. Static operation at pressures up to 200 psi
2. Stable operation over a period $\geq$ 2 weeks
3. Stable operation at constant temperature over a range of -320°F to +140°F
4. Predictable operation under temperature cycling conditions. (-40°F to +140°F)
5. Sensitivity in ppm to ppb range
6. Nonspecific, i.e., capable of response to any change in gas composition
7. Relatively small and compact
8. Reasonably economical
9. Requires no specialized accessories

A Yes

B No

C Probable

D Questionable

E Unknown

* Requires AEC License

** Require scrubbing large gas volume with suitable reagent.

Figure 73. Results of Detector Evaluation

(1) Karmen type voltage breakdown detector.

(2) Thermistor, or thermal conductivity, detector.

(3) The cross-section detector.

1. Karmen Type Voltage Breakdown Detector

When an electrostatic field across a gas is gradually increased the gas will abruptly become conductive. The value of the field strength (voltage) at which this conduction takes place is unique for a given gas composition, temperature, pressure, and detector cell geometry when the current is limited between approximately 0.1 and 10 microamperes.

The detector, as described by Karmen (Reference 106), consists of a hollow cylinder one inch long, 3/8 inch I.D., as the cathode and an anode 1/16 inch in diameter mounted along the axis of the cathode cylinder. Various other configurations were tried and tested at Beckman Instrument Company for Jet Propulsion Laboratories under contract 950/60 and little if any gain in performance was found in departing from Karmen's original design. Beckman, however, made one modification to improve reproducibility of breakdown by including a low-level radioactive source to insure the presence of sufficient primary electrons. In the final design the anode was plated with Nickel 63. A sketch of the Karmen detector is shown in Figure 74 and the electrical hook-up in Figure 75.

The voltage-current characteristics of the discharge are similar to that of a glow-discharge voltage regulator tube, i.e., the voltage drop across the discharge remains almost constant. Because of this voltage regulator action, applied voltage variations do not cause instability in the potential drop across the discharge eliminating the need for an expensive regulated high voltage power supply.

Beckman Instruments Company has found that the rare gases, organics, fixed gases, and nitrogen compounds produce substantial signals with this detector. They have shown that the detector operates satisfactorily over a temperature range of -30°F to +220°F and between 4 psia and 61 psia. The breakdown voltage increases 17 volts per psi in helium, which means that at an operating pressure of 200 psi the voltage requirement for helium would be about 3900 volts. For nitrogen the voltage is expected to be considerably higher. This will probably be a disadvantage for this detector (although not an insurmountable problem). Beckman also reported that this detector is capable of detecting as low as 10^{-10} gram of organic compound to 100 percent concentration. The maximum concentration will be limited by the voltage capabilities of the apparatus. Stability runs using this detector on a gas chromatograph showed day-to-day variation of ±2 percent. However, a significant portion of this error was attributed to the chromatograph and its sample valve.

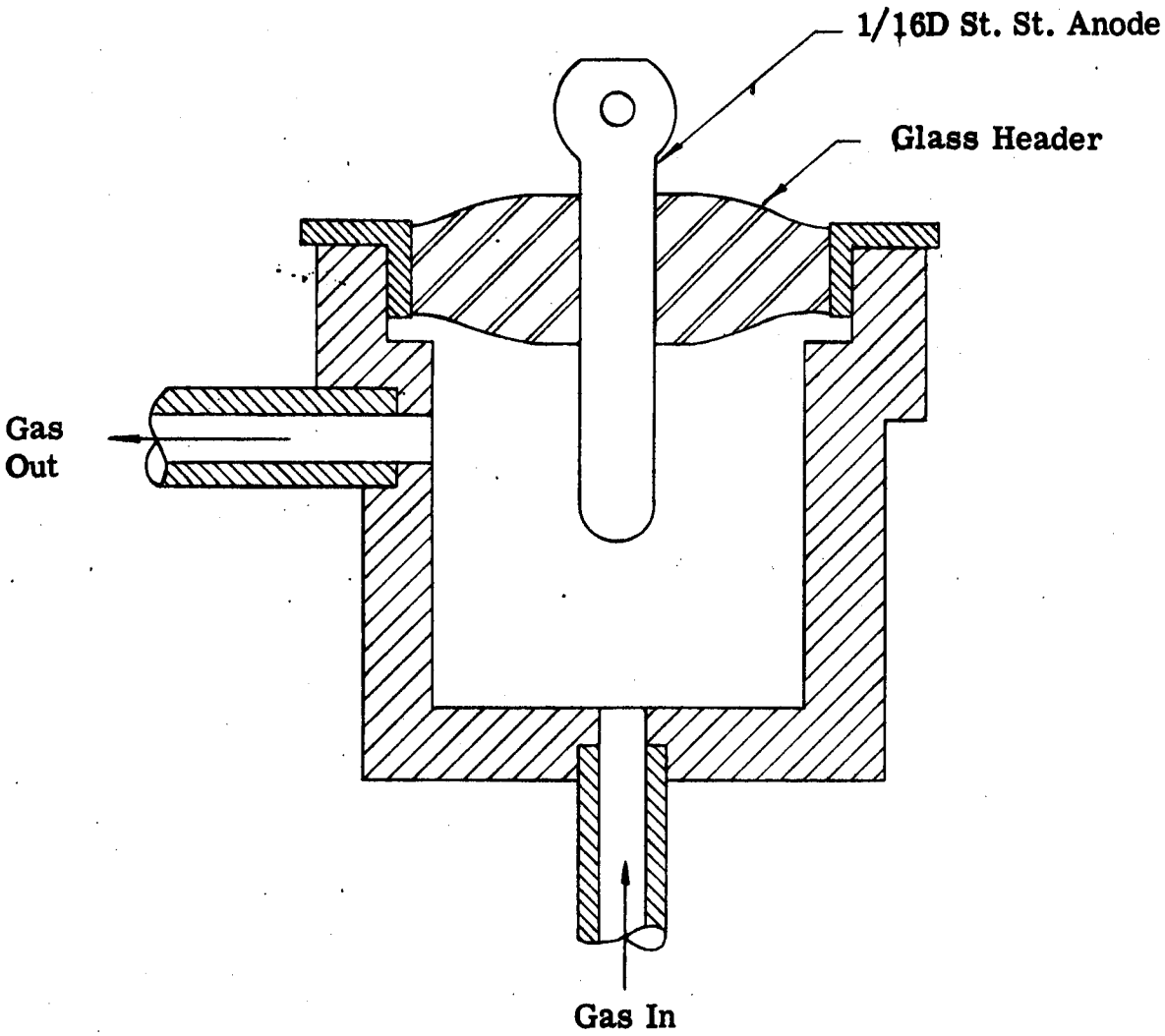

Figure 74. Karmen Detector

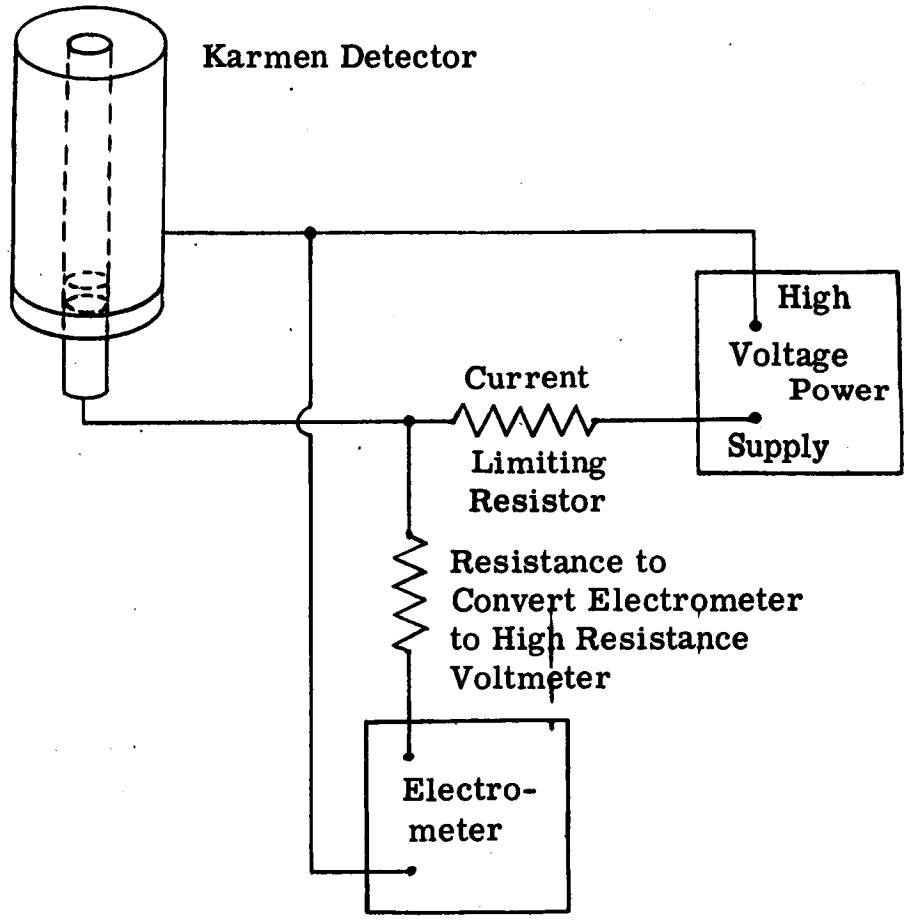

Figure 79. Karmen Voltage Breakdown Detector

Beckman suggested that because of the high voltages required at elevated pressures it may be desirable to take samples of the gas and expand it to atmospheric pressure for analysis. This will be discussed in more detail.

2. Thermistor or Thermal Conductivity Detector

Thermal conductivity detectors operate in the following manner. Changes in thermal conductivity of a pressurizing gas due to the presence of a foreign gas causes a change in the rate of heat removal from the thermistor sensor, thereby changing the temperature of the sensor. The resistance of the sensor varies with its temperature and this resistance change is indicated as an unbalance signal from a Wheatstone bridge circuit. A calibration of unbalance signal versus concentration for a particular pressurizing gas and contaminant can be made. The response is approximately linear with concentration in helium so that a single calibration point, other than zero, would be sufficient for a wide range of concentration. The sensitivity of these detectors is a little lower than the Karmen voltage breakdown detector. Sketches of typical bridge hook-ups are shown in Figure 76.

Thermal conductivity cells have been in existance for a long time. The most common type is a metal block, 2 to 3 inches on a side, containing drilled passages for the standard and unknown gas flows. The sensors are located in appropriate cavities with electrical leads terminating at a terminal block on top of the cell. The advent of the thermistor permits smaller, more compact units. (The thermistor can be about the size of a pin-head). It is anticipated that a thermistor could be inserted (properly insulated) directly into the bottom of the permeation chamber in the gas atmosphere. A second thermistor, as a standard, could be placed in a similar chamber containing only the pressurizing gas.

3. Cross Section Detector

This type of detector is new and, consequently, there is little published data on its operation and performance. The basic response mechanism, however, is as follows: A radioactive source produces bombardment of gas molecules which results in a primary ion current; this current is proportional to the effective cross-sectional area of the gas molecule. By choosing a carrier gas of small cross-section (of the molecule) contaminants of larger cross-section lead to larger ion currents. The voltage applied is sufficient to complete collection of ions without multiplication due to ionization by primary electrons; i.e., the electric field is just sufficient to attract the ions created by the radioactive bombardment, but not strong enough to induce ionization as in the case of the voltage breakdown detector. The response of this detector is perfectly linear from the detection limit to 100 percent of sample. A typical instrumentation set-up for the cross-section detector is shown in Figure 77.

The relative sensitivities of the three detectors just described, in terms of the change in magnitude of the primary effect (ionization constant, thermal conductivity, etc.) per ppm sample in the carrier gas are as follows:

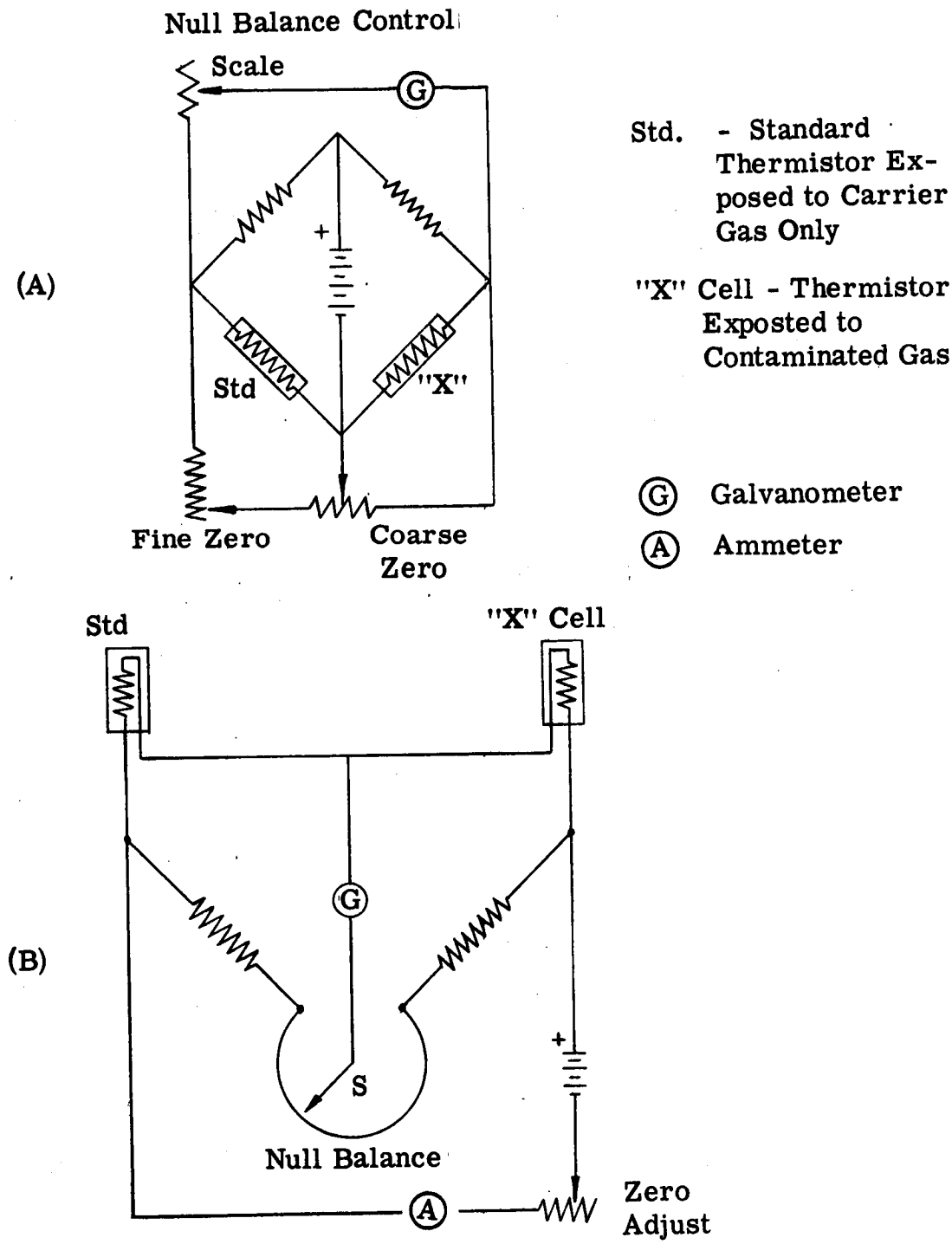

Figure 76. Thermal Conductivity Detector Circuits

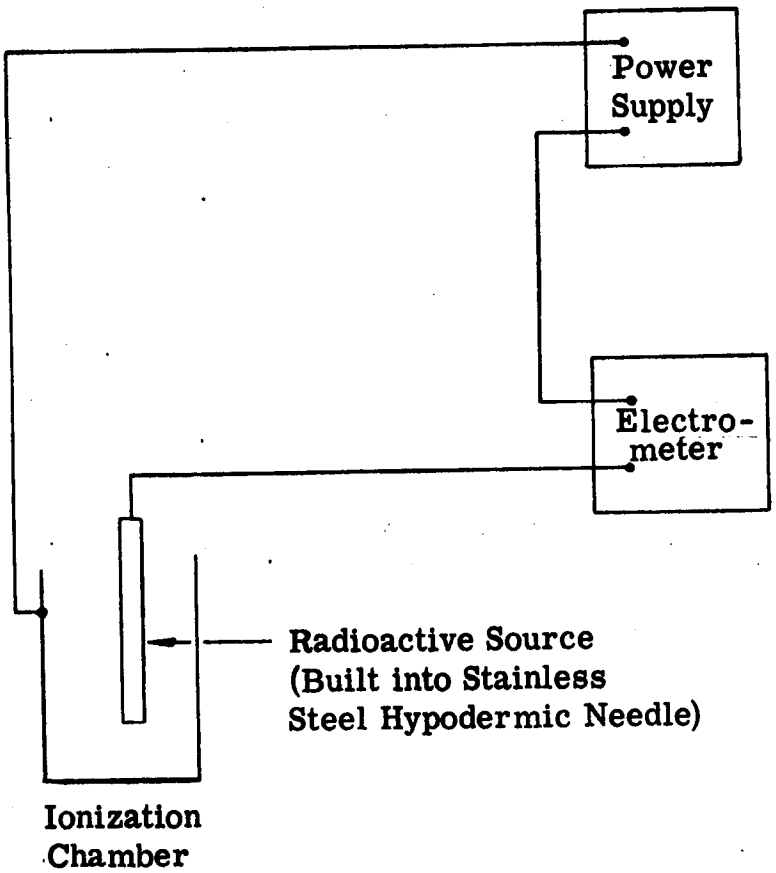

Figure 77. Cross-Section Detector

Karmen Voltage Breakdown	2×10^{-7} change
Thermal Conductivity	5×10^{-7} change
Cross-Section	10^{-5} change

These values will, of course, be modified by the read-out devices used to indicate the change in magnitude of the primary effect. Considering over-all system sensitivities, detector, and read-out devices, the Karmen voltage breakdown technique has the greatest sensitivity, and the thermal conductivity and cross-section techniques have comparable sensitivities.

The consideration in the above discussion of the three detectors has been to build the unit into the permeation chamber. This creates several unknown factors. None of these detectors has been operated at pressures in the range of 200 psi and none has operated in a static atmosphere where the concentration of contaminant is changing with time, at least insofar as our investigations have disclosed. The usual application is with a flow of carrier gas which periodically carries a contaminant with it; between times, pure carrier gas is flowing and a zero point can be reestablished. Also, test time is usually short - a few hours - thus minimizing the chance of zero shift during test.

To circumvent these problems, Beckman suggested taking samples from the chamber periodically and expanding it to atmospheric pressure at the site of the detector. Between samples, the detector can be purged with pure pressurizing gas to reestablish the zero point. Since these detectors are small, it is believed that a complete permeation curve can be generated with the removal of only a small percentage of the total gas volume (e.g., removing 1/4 cc at 200 psi and expanding it to one atmosphere would remove 5 cc in 20 samples, or 2.7 percent of the gas volume of the present apparatus).

The gas sample could be removed by a cavity in a rotary ball valve, or oscillating piston type valve, as shown in the sketches in Figure 78.

G. CONCLUSIONS

An apparatus was designed and built under this program for permeation testing under simulated operating conditions as related to positive expulsion devices. A limited number of tests were conducted. In addition, a review of analytical techniques was conducted to find the method, or methods, most suitable for an optimum permeability apparatus.

Based on this work, the following conclusions are made:

(1) The apparatus as built and tested, using infrared spectroscopy, is limited to polyatomic molecules, i.e., it cannot detect oxygen, hydrogen, nitrogen, etc.

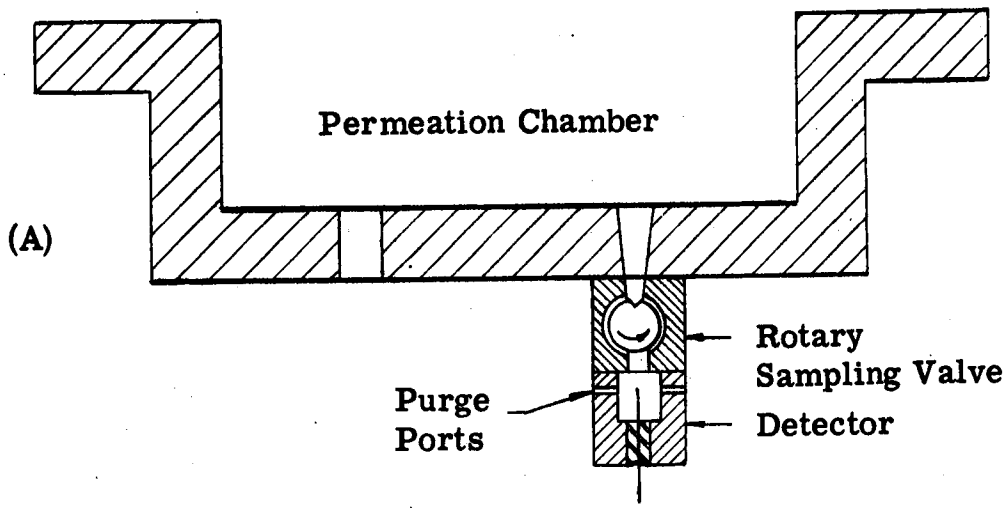

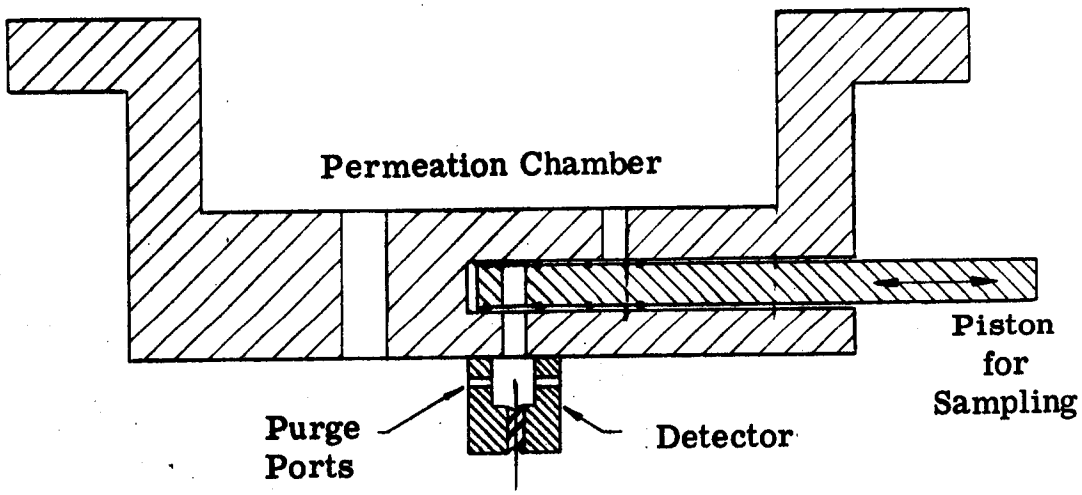

Figure 78. Proposed Sampling Techniques for Atmospheric Pressure Analysis

(2) With the current apparatus, the test temperature is limited to the temperature at which the infrared spectrophotometer operates, generally at +70°F. Temperature cycling tests could be conducted, however, the analysis would have to be made when the temperature is at +70°F.

(3) The apparatus as constructed has to be loaded and unloaded at a temperature below the boiling point of the test liquid to preclude pressure buildup in the chamber that could damage the specimen. This restriction could be eliminated by developing a technique for supporting the specimen during loading and unloading, either mechanically, or with gas pressure. To use pressure would require the use of a differential pressure cell and delicate control of a gas pressurizing valve to balance the pressure across the specimen at less than 0.7 psig. To accomplish the same thing mechanically would require a plate or disc, that could be raised to contact the specimen during loading and lowered during test. One possible design for such a device is shown in Figure 79.

Closely related to the loading and unloading problem is the very limited movement of the free end of the bellows (holding the specimen) in the current apparatus. This limitation has also been eliminated in the design in Figure 79.

(4) Detailed operating instructions have been prepared for the currently designed apparatus and are included in the Appendix. These instructions form a complete document for conducting tests with storable propellants. To conduct tests with cryogenics, a different analytical technique will be required. Any one of three methods can detect diatomic gases: (1) Karmen-type voltage breakdown detector, (2) thermal conductivity detector, and (3) cross-section detector, Because these methods are new, there is insufficient data to evaluate them and design an apparatus for cryogenic testing. (This will be discussed further under section H, Future Work.)

(5) The basic concept at the beginning of this program was to develop a test that would be capable of testing a multitude of propellants under a wide variety of test parameters - a truly universal permeation tester. Such a test would be desirable, but now appears beyond practical conception. The more practical goal then would be to develop a test with as broad a list of capabilities as practicable which after much testing may be accepted as a standard in the industry. It is believed that the test work and apparatus conceived and developed under this contract approaches this latter, more practical, goal.

H. FUTURE WORK

The basic design concept of using a bellows for flexibility in the permeation chamber appears sound and practical based upon the test work accomplished under this contract. Some refinements in design, however, appear desirable; these have been previously mentioned, including a modified design shown in Figure 79.

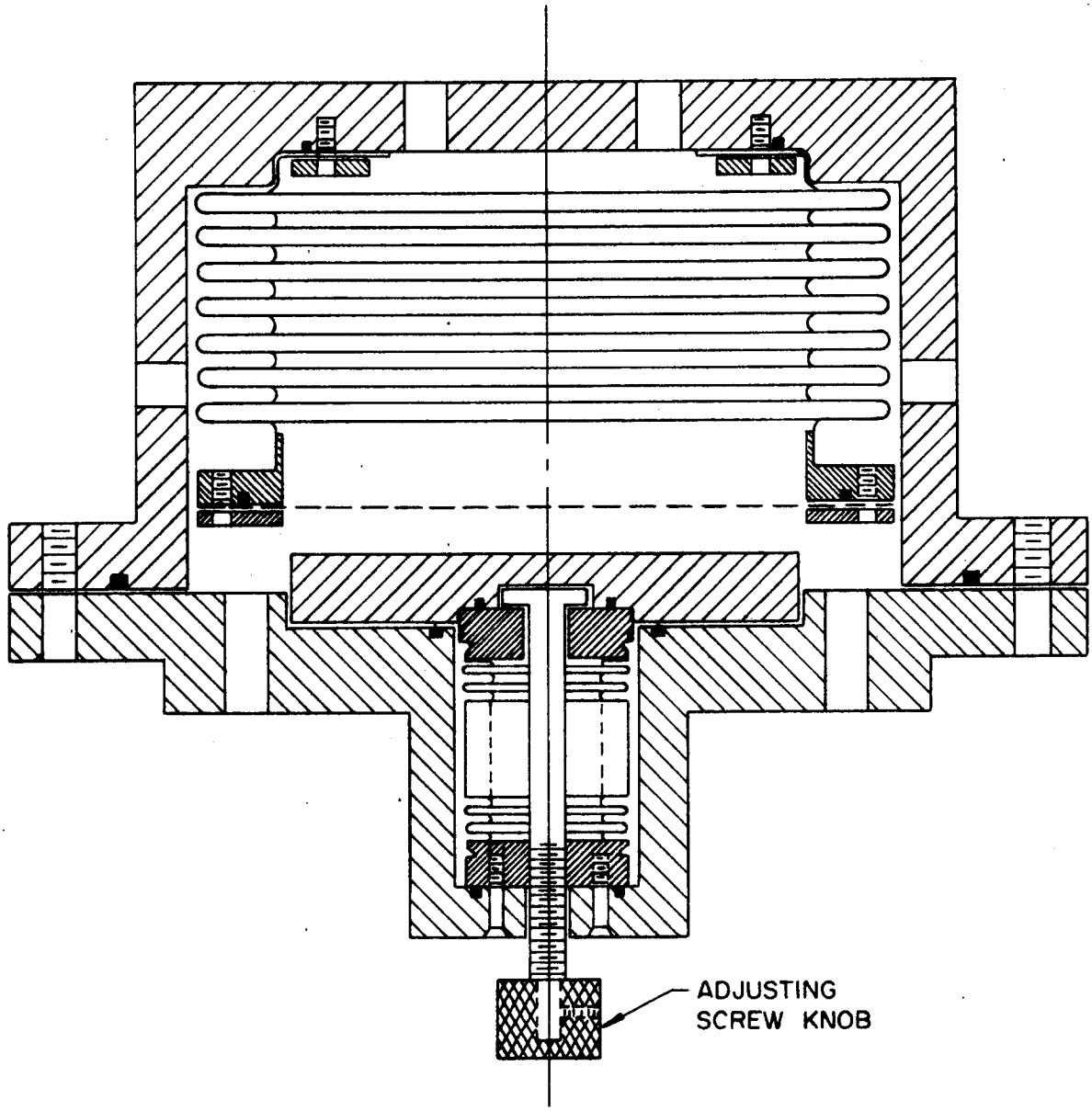

Figure 79. Proposed Design of Permeation Chamber

The major area for further development, therefore, is the analytical technique to be used for permeation studies. There are three methods that appear to be most satisfactory for this application. Before a particular method can be decided upon, several development tests will be required. These tests will be designed to furnish the following information:

(1) Long-term stability: tests to determine if base reference (zero) will remain constant over, say, 3 weeks, or will some compensating schemes be required.

(2) Sensitivity: tests using known concentration to determine range of detection of propellants of interest.

(3) Environmental effects: tests to determine effects of pressure and temperature on stability and sensitivity of system.

Available data indicate the Karmen voltage-breakdown detector is the most sensitive of the three being considered, but it may be limited to concentrations considerably less than saturation. In this case, it would be necessary to revert to a second detector for the high end of the permeation curve. These capabilities and limitations must be determined and correlated with the desired upper and lower limits of detection.

An additional capability that must be determined by experiment is operation of these detectors at cryogenic temperatures. There are no data indicating this capability with any of the detectors studied. The detector would be an integral part of the permeation chamber and consequently it, as well as the chamber, would be submerged during test in a pool of cryogenic having a boiling point equal to or lower than the cryogenic being tested; e.g., a pool of L-N_2 could be used to cool the apparatus for testing LOX; to test L-H_2, a pool of L-He would be required and to keep L-He losses at a minimum a heat shield of L-N_2 would be used. The pool of cryogenic would be contained in a stainless steel Dewar with additional insulation on the outside. As stated in the previous section the overall design of the apparatus is dependent on the type of detector to be used.

Another area recommended for future effort is testing under temperature cycling conditions. It is conceivable that, if the ullage space becomes saturated while the vehicle is in the period of high temperature, condensation may occur as the vehicle enters the decreasing temperature part of the cycle. If this liquid does not reevaporate due to localized entrapment between the tank and bladder when the temperature rises, the loss of propellant due to permeation could be much higher than determined under isothermal conditions because the gas space would no longer be saturated at the higher temperature and a driving force would again exist causing permeation to occur. An additional condition that may cause increased loss of propellant is the probable condensation of vapor on the tank wall during cooling, thus lowering the level of saturation in the ullage space; permeation would continue. If during the heating cycle propellant does not permeate back through the bladder an increased loss of propellant could occur. Further studies including a heat transfer study would be required to determine the susceptibility of the system to this hypothesis.

SECTION 7

REFERENCES

1. Seide, Paul; "The Effect of Pressure on the Bending Characteristics of an Actuator System;" ASME Series E - Sept. 1960 Comments in March 1961 Section E; Space Technology Laboratories, Inc.

2. Daniels, C.M.; "Designing for Duct Flexibility with Bellows Joints;" Machine Design 31:146-55 0 15 1959; Rocketdyne.

3. Vivian, C.H.; "Bellows, Forerunner of the Compressor;" Comp. Air Mag. 64-19-22 May 1959.

4. Preston, J.; "Bellows Operated Water Switch;" J. Sci Inst. 36:98 F 1959.

5. Raskhodoff, M.; "Phase-Adjusting Coupling;" El. Manuf. 64:178 S 1959.

6. "High Precision Barometric Bellows;" Engineering 185:709 JE 6 1958.

7. Turner, C.E. and Ford, H.; "Stress and Deflection Studies of Pipeline Expansion Bellows;" Inst. of Mech. Eng. Proc. 171 No. 15:526-44, Disc 544-50, Reply 551-2 1957.

8. "Tests on Large Stainless Steel Bellows;" Engineer 205:181-2 Ja 31 1958.

9. "Bellows is Redesigned for Welding;" Prod. Eng. 27:161 D 1956.

10. Krivetsky, A.; "Research on Zero-Gravity Expulsion Techniques;" Final Report on Contract NASr-44; Report No. 7129-933003; March 1962; Bell Aerosystems Company

11. Matt, J. and Eichelberger, T.S.; "High-Temperature Metal Bellows Seals for Aircraft and Missile Assemblies;" TM-2883-93; Thompson-Ramo Wooldridge Cleveland, Ohio.

12. Kesko, Wm.; "A Theoretical Analysis of the Buckling of an Internally or Externally Pressurized Bellows and the Actuation Forces Required to Deflect It;" TM 3011-93 (Formed Bellows).

13. Turner, C.B.; "Stress and Deflection Studies of Expansion Bellows;" Mech. Eng. Sci V. 1 N2 Sept. 1959, pp. 130 to 143.

14. Stevens, Justice B.; "Bellows-Type Axial Mechanical Seals;" Machine Design Seals Book, 19 January 1961.

15. Dugundji, John,; "On the Calculation of Natural Modes on Free-Free Structures;" Readers Forum Journal Aerospace Sciences; 11 January 1960, February 1961.

16. Matheny, James D.; "Bellows Spring Rate for Seven Typical Convolution Shapes;" Machine Design, 4 January 1962; General Dynamics/Astronautics.

17. McKinney, G.E.; Mech. Engr. June 1957.

18. Den Hartog, J.P.; "Mechanical Vibration;" 4th Edition, 1956 Appendix.

19. Roark, R.J.; "Formula for Stress and Strain;" 3rd Edition, 1954; condition 33, p. 108; condition 11, p. 72.

20. Vail, D.B.; Reports KAPL-M-DBV-3, KAPL-M-DBV-4, DF54A0584, DF53A0586; Period January 1954 through May 1955; Knolls Atomic Power Laboratory, Schenectady, N.Y.

21. Timoshenko, S.; "Vibration Problems in Engineering;" 3rd Edition, pp. 374-377.

22. Harris, C.M., et al; "Shock and Vibration;" Handbook 1961, Table 7.11, p. 7-36.

23. Orthwein, W.C.; "A Shortcut Procedure for Calculating Natural Frequency of an Annular Plate;" Machine Design, March 1961, pp. 121-122.

24. Timoshenko and Woinowsky-Krieger; "Theory of Plates and Shells;" McGraw-Hill Book Co., Inc.; 1959.

25. Archer, R.; "On the Numerical Solution of the Nonlinear Equations for Shells of Revolution;" Journal of Mathematics and Physics; Vol. XLI,, No. 3; September 1962.

26. Mushtari and Galimor; "Nonlinear Theory of Thin Elastic Shells;" The Israel Program for Scientific Translations; 1961.

27. Reissner, E.; "On the Theory of Thin Elastic Shells;" H. Reissner Anniversary Volume, Contributions to Applied Mechanics, J.W. Edwards, Ann Arbor, Mich.; 1949.

28. Almen and Laszlo; "The Uniform Section Disk Spring;" Trans. ASME Vol. 58 - 1936 p. 305.

29. Stein and Degepth; "Analysis of Partly Wrinkled Membranes;" NASA TN D813.

30. Iberall, A.S.; "Characteristics of Slack Diaphragms;" ASME Paper No. 59-A-175.

31. Hetenyi and Timms; "Analysis of Axially Loaded Annular Shells with Applications to Bellows;" ASME Paper No. 59-A-175.

32. Reissner, E.; "On Axisymmetric Deformation of Thin Shells of Revolution;" Proc. Symp. on Applied Math. 3, 1950 p 32.

33. Way, S.; "Bending of Circular Plates with Large Deflection;" Trans. ASME Vol. 56 1934 p 267.

34. Haringx; "Design of Corrugated Diaphragms;" Trans. ASME 1957, p 55.

35. Sturns, R.G.; "A Study of the Collapsing Pressure of Thin-Walled Cylinders;" University of Illinois Engineering Experimental Station Bulletin No. 329, 1941.

36. Bijllard, P.P.; "Buckling Under External Pressure of Cylindrical Shells Evenly Stiffened by Rings Only;" Bell Aerosystems Company Report No. 02-941-002, April 1954.

37. "On the Design of Formed Bellows;" Thompson-Ramo Wooldridge, Inc. TM-3011-93, 13, July 1961.

38. "High Temperature Metal Bellows Seals for Aircraft and Missile Accessories;" Thompson-Ramo Wooldridge, Inc. Report No. TM-2883-93, 28 March 1961.

39. "First Stage Bellows Capability Demonstration;" Thompson-Ramo Wooldridge, Inc., Report No. ER-4234, 14 Jan 1961.

40. Northdurft, H.; "Eigenshaften von Metallbaelgen;" Engineer Report No. V-205, N-5223, 31 Jan 58. pp 181-182.

41. Howard, J.H.; "Designing with Metal Bellows;" Machine Design - Report No. V-26, n-1, Jan 1954, pp 137-148.

42. "Automatic Welding S.S. Bellows;" Industry and Welding Report No. V-27, N-4, April 1954, pp 44-46, 48, 88, 89.

43. Dickinson, , T.A.; "Resistance Welding Bellows;" Sheet Metal Industries, Report No. V-31, n-330, Oct 1954, pp 854, 855.

44. "Resistance Welding Bellows;" Welding Engineer Report No. V-39, N-10, Oct 1954, pp 47, 53.

45. Hicks, R.; "Reinforced Annular Plates;" Engineering - Report No. V-177, N-4598, 12 Mar 1954, pp 335-336.

46. Hoppmann, W.H.; "Bending of Orthogonally Stiffened Plates;" Am. Soc. of Mech. Engrs. Report No. N-54, A-31, Dec 1954.

47. Sachs, G.; "Fundamentals of the Working of Metals;" Per Gamon Press, Ltd., 1954.

48. "Electron Beam Welds Pay Off for Bellows Maker;" Steel - Report No. 149, 6 Mar 1961, pp 78, 79.

49. "Producing and Testing Bellows Joints;" Engineering - Report No. 190 - N-25-60, pp 732-733.

50. Iskower, R.I.; "Calculates Large Deflections in Discs;" Product Engr. Report No. 32:81, 24 Apr 1961.

51. Daniels, C.M. and Fenton, R.E.; "Pressure Loss Factors for Internally Linked Bellows Joints;" Mech. Design - Report No. 33, 14 Sept 1961, pp 187-189.

52. Turner, C.E.; "Stress and Deflection Studies of Flat-Plate and Torodial Expansion Bellows;" Journal of Mech. Eng. Science Report No. V-1, N-2, Sept 1959, pp 130-143.

53. Swift, H.W.; "Plastic Bending Under Tension;" Engineering Vol. 166, Oct 1948, pp 333-335.

54. Gerard, G.; "Effect of Bend Width upon Minimum Bend Radii;" Journal of Aero Science Vol. 13, 1946, pp 161-170.

55. Shaffer, B.W. and Unger, E.E.; "Mechanics of the Bending Process;" Journal of Applied Mechanics Vol. 27, March 1960, pp 34-40.

56. Shroeder, W.; "Mechanics of Sheet Metal Bending;" Trans. ASME Vol. 65, 1943, pp 817-827.

57. Lubahn, J.D. and Sacks, G.; "Bending of an Ideal Plastic;" Metal Trans. ASME Vol. 72, 1950, pp 201-208.

58. Feely and Goryl; "Stress Studies on Piping Expansion Bellows;" Journal of Applied Mechanics, June 1950.

59. Wahl, A.M. and Lobo, G.; "Stresses and Deflections in Flat Circular Plates with Central Holes;" Trans. ASME Vol. 50, 1930.

60. Haringx, J.A.; "Instability of Bellows Subjected to Internal Pressure;" Philips Research - Report No. 7, 1952.

61. Van Amerongen, G.J.; "The Permeability of Different Rubbers to Gases and its Relation to Diffusivity and Solubility;" J. Appl. Phys., Vol. 17, 1946 pp 972-84.

62. Van Amerongen, G.J.; "Influence of Structure of Elastomers on their Permeability to Gases;" J. of Poly. Sc., Vol. V, No. 3, June 1950, pp 307-32.

63. Binning, R.C.; et al; "Separation of Liquid Mixtures by Permeation;" Ind. & Engr. Chem., Vol. 53, No. 1, Jan 1961.

64. Schuman, A.C.; "Apparatus for Measuring the Gas Permeability of Film Materials of Low Permeability;" ibid, Anal. Ed. Vol. 16, Jan 1944 pp 58-60.

65. Brown, W.E. and Sauber, W.S.; "Gas Transmission by Plastic Films;" Modern Plastics, Vol. 36, Aug 1959 pp 107 ff.

66. Edwards, J.D. and Pickering, S.F.; "Permeability of Rubber to Gases;" Sc. Papers of the Bur. Stds., Paper No. 387, 12 July 1920.

67. Barrer, R.M.; "Diffusion in and Through Solids;" Cambridge Univ. Press, 1951.

68. Houwink, R. (Editor); "Elastomers and Plastomers, Vol. 1, General Theory;" Elsevier Publishing Co., 1950.

69. Jost, W.; "Diffusion in Solids, Liquids, Gases;" Academic Press, Inc., New York, 1952.

70. Denbigh, K.G.; "Thermodynamics of the Steady State;" Methuen & Co., Ltd. (London), John Wiley & Sons, N. Y., 1951.

71. Koch, E.F., Porter, R.N., Stanford, H.B., and Weiner, R.S.; "Advanced Liquid Propulsion System;" Propulsion Div. of Space Programs Summary No. 37-15, Vol. IV, Jet Propulsion Lab., Pasadena, Calif., 30 June 1962.

72. Walker, R.E., and Westenberg, A.A.; "Molecular Diffusion Studies in Gases at High Temperature. I, The 'Point Source' Technique;" J. of Chem. Phys., Vol. 29, Nov 1958 pp 1139 ff.

73. Warren, J.E., et al.; "Evaluation of the Significance of Permeability Measurements;" J. of Pet. Tech., Vol. 13, Aug 1961, pp 739-44.

74. Rogers, E.C., Stannett, V., and Szwarc, M.; "The Sorption, Diffusion, and Permeation of Organic Vapors in Polyethylene;" J. of Poly. Sc., Vol. XLV, 1960, pp 61-82.

75. Van Amerongen, G.J.; "Solubility, Diffusion, and Permeation of Gases in Gutta Percha;" ibid, Vol. II, 1947, p 355 ff, 381-86.

76. Long, F.A. and Thompson, L.J.; "Diffusion of Water Vapor in Polymers;" ibid, Vol. XV, 1955, pp 413-426.

77. Carson, F.T.; "A sensitive Instrument for Measuring the Air Permeability of Paper and Other Sheet Materials;" J. of Res., Bur. Stds., Vol. 12, 1934, p 567.

78. Carson, F.T.; "Effect of Experimental Conditions on the Measurement of Air Permeability of Paper;" ibid, p 587.

79. Cartwright, L.C.; "Measurement of the Gas Permeability of Sheet Materials;" Anal. Chem., Vol. 19, June 1947, p 393 ff.

80. Brubaker, D.W. and Kammermeyer, K.; "Apparatus for Measuring Gas Permeability of Sheet Materials;" ibid, Vol. 25, 1953, pp 424-426.

81. Park, W.R.R.; "Semicro Gas Permeability Apparatus for Sheet Material;" ibid, Vol. 29, Dec 1957, pp 1897-1899.

82. Reamer, H.H. and Sage, B.H.; "The Measurement of Diffusion Coefficients in Gases and Liquids at Elevated Pressures;" Amer. Rocket Soc., Paper 473-57 presented at Sec. Biennial Gas Dynamics Symposium, Evanston, Ill., 26-28 Aug 1957.

83. Jorgensen, F. and Watts, H.; "The Determination of Vapor Diffusion Coefficients: A Modified Technique;" Chem. & Ind., Vol. 36, 9 Sept 1961, p 1440.

84. Taylor, R.L., Hermann, D.B., and Kemp, A.R.; "Diffusion of Water Through Insulating Materials: Rubber, Synthetic Resins, and Other Organics;" Ind. & Engr. Chem., Vol. 28, No. 11, Nov 1936, pp 1255-1263.

85. Pinsky, J.; "Theoretical Study of Polyethylene Permeability;" Modern Plastics, Vol. 34, April 1957, p 145 ff.

86. Pinsky, J., Nielsen, A.R., and Parliman, J.H.; "Investigation of the Shelf Life of Liquids in Polyethylene Bottles;" WADC Report TR-53-133 (4 Parts), Wright Air Development Center, Wright Patterson Air Force Base, Dayton, Ohio, June 1954.

87. Carson, F.T. and Worthington, V.; "Apparatus for Determining Water-Vapor Permeability of Moisture Barriers;" Natl. Bur. Stds., Circular No. C453, 1946.

88. Cutler, J.A. and McLaven, A.O.; "Permeation Through and Sorption of Organic Vapors by High Polymers;" Tappi, Vol. 36, 1953, pp 423-425.

89. Galbraith, A.D. and Kitchen, E.A.; "Permeability Theory vs. Practice in Packaging Liquid Products;" Tappi, Vol. 45, No. 2, Feb 1962, p 173 ff.

90. Daynes, H.A.; "Permeability of Rubber and Methods for Testing It;" Trans. Inst. of Rubber Ind., Vol. 3, 1928, pp 428-453.

91. Stanford Research Institute; "Investigation of the Space Storability of Pressurizing Gases;" SRI Project No. PSU-4000, NASA Contract No. NAS7-105, Quart. Prog. Rpts. 1, 2, and 3, 1962.

92. Brenner, N., and Cieplinski, E.; "Gas Chromatographic Analysis of Mixtures Containing Oxygen, Nitrogen, and Carbon Dioxide;" Annals of the N.Y. Ac. of Sc., Vol. 72, Art. 13, 20 March 1959, pp 705-713.

93. Pierson, R.H., Fletcher, A.N., and Gantz, E.S.; "Catalogue of Infrared Spectra for Qualitative Analysis of Gases;" Anal. Chem., Vol. 28, No. 8, Aug 1956, p 1218 ff.

94. Lindsay, A.L., and Bromley, L.A.; "Thermal Conductivity of Mixture of Gases;" Ind. & Engr. Chem., Vol. 42, No. 8, Aug 1950, p 1508 ff.

95. Keulemans, A.J.M.; "Gas Chromatography;" Reinhold Publishing Co., N.Y., 2nd Ed., 1960.

96. Sternberg, J.C., Foster, R.A., and Said, A.S.; "Principles of Operation of Argon Ionization Detectors for Gas Chromatography;" Paper presented at the 12th Pittsburgh Conf. on Anal. Chem. & Appl. Spect., Feb 1961.

97. Perkin-Elmer Corp.; "Comparative Characteristics of Four Perkin-Elmer Detectors for Gas Chromatography;" Instrument Div., Norwalk, Conn.

98. Thermistor Manual, Fenwal Electronics Inc., Framingham, Mass.

99. Therma Bridge Sensing Detector, Industrial Instruments, Inc., Cedar Grove, N. J.

100. Schmauch, L.J., and Dinerstein, R.A.; "Response of Thermal Conductivity Cells in Gas Chromatography;" Anal. Chem., Vol. 32, 1960, p 343 ff.

101. Littlewood, A.D.; "Sensitivity of Catharometers in Gas Chromatography and the Thermal Conductivity of Binary Gas Mixtures;" Nature, Vol. 184, 1959, p 1631 ff.

102. Dimbat, M., Porter, P.E., and Stross, F.H.; "Gas Chromatography - Apparatus Requirements for Quantitive Application of Gas-Liquid Partition Chromatography;" Anal. Chem., Vol. 28, 1956, p 290 ff.

103. Madan, M.P.; "Simple Bridge Method for Measurement of Thermal Conductivity of Gases and Gas Mixtures;" J. Franklin Inst., Vol. 263, 1957, p 207 ff.

104. Littlewood, A.D.; "Compensated Bridge Circuit for Gas Chromatography;" J. of Sc. Instr., Vol. 37, 1960, 185 ff.

105. Lovelock, J.E.; "Ionization Methods for the Analysis of Gases and Vapors;" Anal. Chem., Vol. 33, 1961, p 162 ff.

106. Karmen, A., and Bowman, R.; "A D.C. Discharge Detector for Gas Chromatography;" Gas Chromatography, Third International Symposium 1962, Academic Press, N.Y.

107. Deal, C.H., Otvos, J.W. Smith, V.M. and Zucco, P.S., "Radiological Detector for Gas Chromatography;" Anal. Chem., Vol. 28, 1956, p 1958 ff.

108. Beckman Instruments, Inc., Space Engr. Group (Article on Karmen Voltage Breakdown Detector), J.P.L. Monthly Progress Report, Contract No. 950160, 14 Nov 1961.

109. Walters, W.H.; "Report on the Investigations of Permeation of Propellants Through Bladders;" Bell Aerosystems Co., Report No. 8101-910030, 15 May 1962.

APPENDIX I

SUMMARY OF POSITIVE EXPULSION DEVICES

APPENDIX I

SUMMARY OF POSITIVE EXPULSION DEVICES

(Contract NAS7-149)

An industry-wide survey was conducted by the Bell Aerosystems Company to determine the state-of-the-art in the field of zero-gravity positive expulsion. Questionnaires, in the form of Summary Sheets, were mailed to 50 companies and agencies in an effort to gather data for this survey. Of the 50 companies solicited, 24 replies were received, but only 8 companies contributed useful information. The contributors in this survey are as follows:

Aerojet-General Corporation
Bell Aerosystems Company
Curtiss-Wright Corporation
Hycon Manufacturing Corporation
Jet Propulsion Laboratory
The Martin Company
NASA-Lewis Research Center
United Technology Corporation

The data gathered during the survey are presented in the following Summary Sheets.

CONTENTS

(Appendix I)

Page

POSITIVE EXPULSION DEVICES

Metallic Bellows 157
Teflon Bladder. 159
Collapsing Teflon Bladder - Seamless Construction 161
Surface Force 163
Dielectrophoresis. 165
Metal Welded Bellows – Accumulator-Type. 167
Metal Welded Bellows 169
Convoluted Diaphragm. 171
Expulsion Bladder – Mariner A Spacecraft 173
Expulsion Bladder – Ranger 3/Mariner A Spacecraft 176
Metallic Expulsion Bladder – Curtiss-Wright 179
Expulsion Bladder – Curtiss-Wright 181
Positive Expulsion Tank 183
Pneumatically Actuated Positive Expulsion Device 185
Cryogenic Expulsion Bladder 187
Squeeze Tank 189

SUMMARY OF POSITIVE EXPULSION DEVICES

Contractor's Name and Address:

Aerojet-General Corporation
P. O. Box 296
Azusa, California

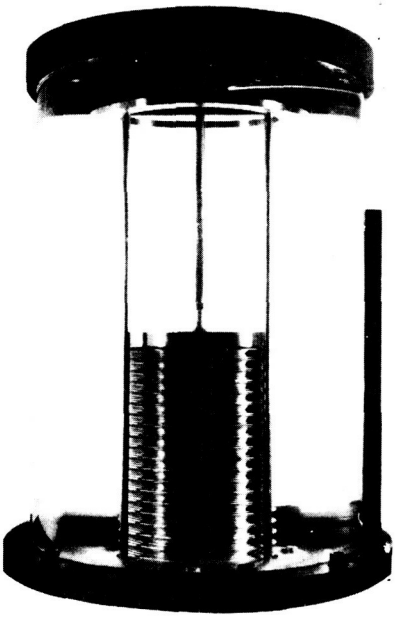

1. **Type of Device:** Metallic Bellows

2. **Description/Application:** For cylindrical propellant tanks

3. **State of Development:** Developed. not qualified

4. **Geometry/Shape:** Multi-convolutions - welded corrugated diaphragms, bellows construction.

Type of Closure: Hemi-spherical

5. **Recommended Materials:** 300 series stainless steels

6. **Weight Comparison:** --

7. **Size Limitations:** Limited by size of welding machines; bellows up to 20 in. diameter can be welded.

Max. Diameter: 20 in. **Max. Volume:** No definite limitations

8. **Characteristics:** --

9. **Environmental Capabilities:** Good

Temperature and Pressure Range: Limited by propellant operating temperature only. Differential pressure should not exceed 50 psi. **Storability:** Good

10. **Method of Operation:** Propellant can be outside or inside the bellows.

11. **Energy/Power Requirements:** Pressure differential of 10 psi required for full-stroke operation.

12. **Cycle Life (Ambient):** 100 cycles minimum

13. **Probable Failure Modes:** Weld failure

14. **Material Properties:** N A

15. **Expulsion Efficiency:** Depends on tank configuration

16. **Volumetric Efficiency:** 98% minimum

17. **Analysis Data:** Flow Characteristics:

ΔP Level = 10 psi max. Response Time = 50 ms

18. **References:**

SUMMARY OF POSITIVE EXPULSION DEVICES

Contractor's Name and Address:

Aerojet-General Corporation
P. O. Box 296
Azusa, California

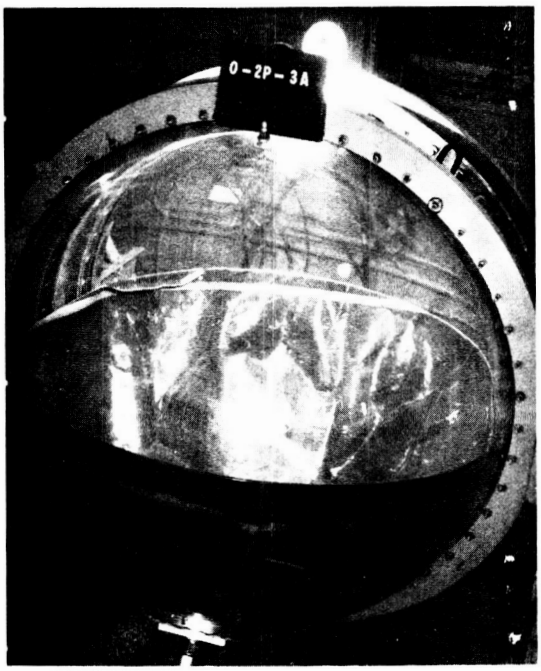

1. **Type of Device:** Teflon Bladder

2. **Description/Application:** System 706 Propellant Tank Expulsion Device

3. **State of Development:** Developed. qualified

4. **Geometry/Shape:** Spherical

5. **Recommended Materials:** Teflon TFE and FEP

6. **Weight Comparison:** --

7. **Size Limitations:** No definite limits

Max. Diameter: see (7) **Max. Volume:** see (7)

8. **Characteristics:** (Material Properties:)

a. Gas and Vapor Transmission Rates - --

b. Permeability - Slight

c. Degradation due to Saturation - Not investigated

d. Radiation Stability - Medium - see published data on Teflon

9. **Environmental Capabilities:** As applicable to Teflon

Temperature and Pressure Range: Max. $\Delta P = 2$ psi, 30° to 200°F **Storability:** Limited

10. **Method of Operation:** Propellant inside bladder

11. **Energy/Power Requirements:** Pressure differential of 1 psia required for full stroke operation.

12. **Cycle Life (Ambient):** 30

13. **Probable Failure Modes:** Pin holes

14. **Material Properties:** Published data on Teflon

15. **Expulsion Efficiency:** Depends on tank and bladder design

16. **Volumetric Efficiency:** 98% min

17. **Analysis Data:** (Flow Characteristics:)

ΔP Level = 1 psi max. Response Time = 30 ms

18. **References:**

SUMMARY OF POSITIVE EXPULSION DEVICES

Contractor's Name and Address:

Bell Aerosystems Company
Buffalo 5, New York

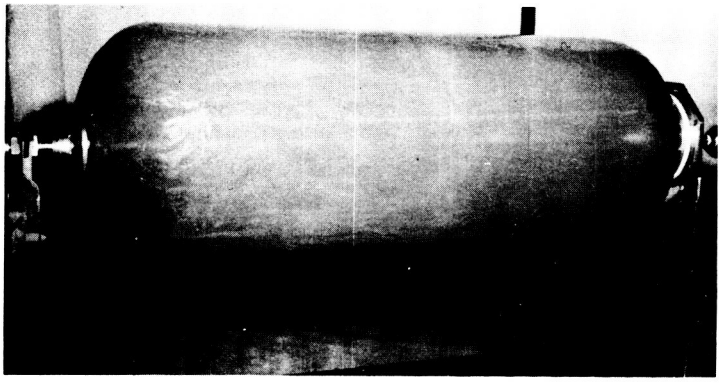

1. **Type of Device:** Collapsing Teflon bladder - seamless construction

2. **Description/Application:** Secondary propulsion system for Agena vehicle

3. **State of Development:** Qualified and flight tested

4. **Geometry/Shape:** Cylindrical with elliptical ends

5. **Recommended Materials:** Teflon TFE/Teflon FEP laminate

6. **Weight Comparison:** Light-weight expulsion device

7. **Size Limitations:** No definite limits have been established

Max. Diameter: See (7) **Max. Volume:** See (7)

8. **Characteristics:** (Low-frequency) Critical during slosh modes with partial loads on longitudinal axis

(High-frequency) Not critical

9. **Environmental Capabilities:**

Temperature and Pressure Range: 0°F - 100°F **Storability:**

10. **Method of Operation:** The propellant inside bladder is expelled as gas pressure is applied between outside of bladder and inside of tank wall causing the bladder to collapse about a central diffuser tube

11. **Energy/Power Requirements:** N/A

12. **Cycle Life (Ambient):** 25 cycles at ambient temp. to 95% of total expulsion PFRT testing (environm cycling from 0°F-100°F) resulted in a proven capability of 10 expulsion cycles to 95 percent.

13. **Probable Failure Modes:** Three corner folds resulting in highly stressed areas causing pin holes

14. **Material Properties:** Long term permeation tests at 70°F indicated that the ullage space would be saturated with MON in 25-30 days. Slight degradation due to saturation. Some radiation degradation at 5×10^5 rads

15. **Expulsion Efficiency:** 98+ percent

16. **Volumetric Efficiency:** 99 percent

17. **Analysis Data:** Excellant compatibility with propellants, seamless construction, readily adaptable to other configurations.

18. **References:** 8101 910 004 - Secondary Propulsion System Liquid Propellant BAC Model 8101 Preliminary Flight Rating Test

SUMMARY OF POSITIVE EXPULSION DEVICES

Contractor's Name and Address

Bell Aerosystems Company
Buffalo 5, New York

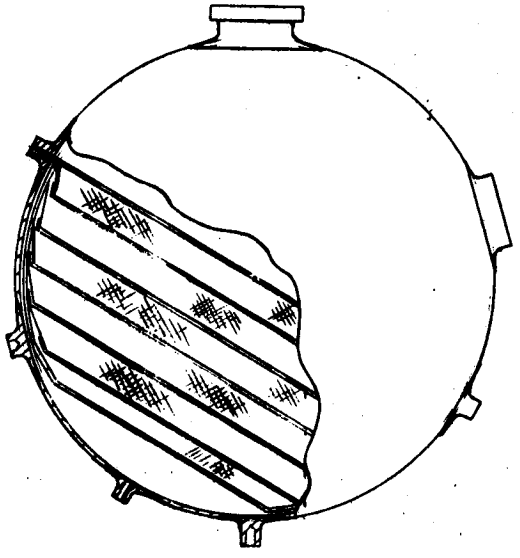

1. **Type of Device:** Surface Force - Propellant Containment, localization and positive expulsion device for reduced or zero-g applications using grids or screens and the principle of liquid surface force phenomenon.

2. **Description/Application:** Screens or grids are employed to control the orientation and expulsion of the propellant in a tank during reduced or zero-g conditions and during an adverse vehicular perbutation, to provide single-phase fluid at the tank outlet. Surface forces at the gas-liquid interface provide the resistance to ullage gas penetration through the screen, thus causing entrapment of the liquid in a containment space. The holding force can be manipulated by the geometry of the interfaces while expulsion is controlled by a multiple screen arrangement.

3. **State of Development:** A feasibility model tank using the surface force concept is being built for test in a zero-g aircraft. Preliminary models, sized for earth-gravity conditions, have been evaluated in the laboratories with excellent results. Work at Bell Aerosystems is being accomplished under Air Force Contract AF04(611)-8200.

4. **Geometry/Shape:** Easily adaptable to any shape, depending on requirements; for example: flats, cones, cylinders, or combinations thereof. (Note pie plate shape in sketch.)

5. **Recommended Materials:** Stainless steel or aluminum alloy

6. **Weight Comparison:** Excellent - screens are light weight

7. **Size Limitations:** None -- may be placed anywhere inside the tank envelope

Max. Diameter: Unlimited **Max. Volume:** Variable, depending on geometry

8. **Characteristics:** Repeated cycle operation possible, volume requirements negligible

Unique Characteristics: No moving parts - no external parts or subsystems necessary.

9. **Environmental Capabilities:** No restrictions, suitable for most propellants either storable or cryo

Temperature and Pressure Range: +150° to -420° F; 10^{-4} to 10^{-7} mm Hg **Storability:** Excellent

10. **Method of Operation:** Device is used for localization of fluid and as an aid to expulsion by controlling location of ullage gas. Actual expulsion of fluid is made by compressed gas in the tank.

11. **Energy/Power Requirements:** None - Pressure drop through screens is less than 1 psi, depending on area of screening and the flow factor.

12. **Cycle Life (Ambient):** Unlimited

13. **Probable Failure Modes:** Weld or bond failure of screen to tank wall joint. Pertubation force higher than capability of screen to contain fluid. Faulty grid mesh has openings larger than anticipated in local areas.

14. **Material Properties:** Screening must be of excellent quality. Weave must show regular pattern to ensure that no opening in the grid pattern exceeds a maximum permissible value.

15. **Expulsion Efficiency:** 99%

16. **Volumetric Efficiency:** Excellent - 95% plus

17. **Analysis Data:** Installation Technique: Earth gravity containment checkout to ensure satisfactory screen fabrication to limit values specified.

18. **References:** Phase I Progress Report - Development of Expulsion and Orientation Systems for Advanced Liquid Rocket Propulsion Systems; Contract AF04(611)-8200; Report No. SSD-TDR-62-

Bell Aerosystems Company.

SUMMARY OF POSITIVE EXPULSION DEVICES

Contractor's Name and Address

Bell Aerosystems Company
Buffalo 5, New York

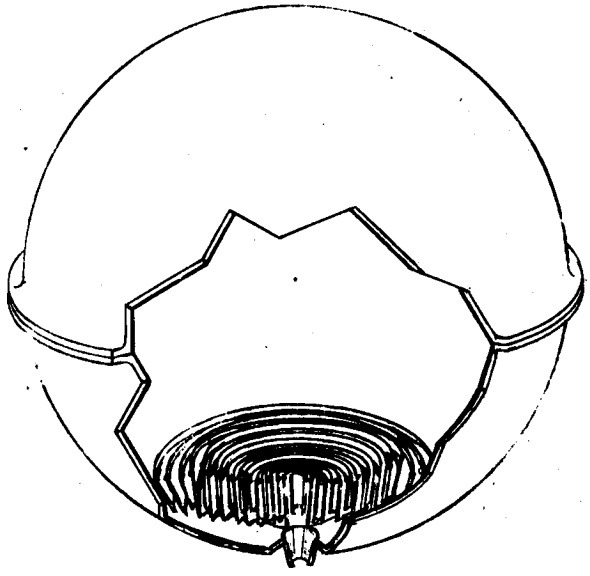

1. **Type of Device:** Dielectrophoresis - Propellant Containment or localization device - suitable for reduced or zero-g applications using the principle of dielectrophoresis phenomemon.

2. **Description/Application:** Involves the action or response of a liquid dielectric when in the presence of a non-uniform field. Concentric, converging conical electrodes electrically isolated and wired for d-c voltage alternately plus/minus are sized by requirements and shaped to be placed inside a tank in the proximity of the tank outlet. Motion of the fluid results from a field-induced pressure differential within the fluid which directs the fluid toward the region of highest field strength and/or toward the tank outlet. The actual pressure developed is a function of the field strength and the dielectric constant of the liquid.

3. **State of Development:** A feasibility model tank using the dielectrophoresis principle is being built for test in a "zero-g aircraft". Preliminary models have been evaluated in the laboratories with satisfactory results. Work at Bell Aerosystems Company is being accomplished under Air Force Contract AF04(611)-8200.

4. **Geometry/Shape:** Can be fabricated in almost any shape that would produce a non-uniform field. An optimum shape would provide highest pressure with the least impressed voltage.

5. **Recommended Materials:** Aluminum alloy electrodes - Teflon insulator and spacer.

6. **Weight Comparison:** Excellent - If necessary, suitable screening material can be substituted for the aluminum alloy plate electrodes; these however, require further study.

7. **Size Limitations:** Internal envelope restriction of the tank.

Max. Diameter: 60 inches **Max. Volume:** depends on requirements

8. **Characteristics:** Repeated cycle operation possible. Volume requirement is relatively small. Accessibility to electrodes is necessary. A high-voltage feed-through terminal is required in the tank shell. A high-voltage power pack is required.

Unique Characteristics: No moving parts.

9. Environmental Capabilities: Most suitable for cryogenic fluids such as hydrogen, oxygen, nitrogen, oxygen difluoride, and diborane having high-resistivity values and, therefore, low power consumption. Not suitable for storable propellants due to relaitvely low resistivity.

9. **Environmental Capabilities:**

Temperature and Pressure Range: 10^{-4} to 10^{-7} mm Hg; $+100^{\circ}$ to -422°F **Storability:** Excellent-Limited by gas and electrical power sup

10. **Method of Operation:** Device is used for location of fluid. Expulsion is made by compressed gas in the tank.

11. **Energy/Power Requirements:** For cryogenic-Low 10^{-1} to 10^{-6} watts d-c voltage 5 to 50 kv~ For storables - High 10^{-1} to 10^{-4} watts.

12. **Cycle Life (Ambient):** Unlimited

13. **Probable Failure Modes:** Loss of power supply, shorting between electrode plates, failure of high voltage feed through terminal at tank shell, change in fluid characterist due to contamination and radiation. Failure of insulator fittings, dislocation of electrode position

14. **Material Properties:** Special material properties not necessary. Use material compatible with propellant, avoid use of dissimilar materials to prevent electrolysis.

15. **Expulsion Efficiency:** 99% plus

16. **Volumetric Efficiency:** 95% plus

17. **Analysis Data:** Installation technique, electrical safety checkout, electrode testing technique for ground containment checkout.

18. **References:** Phase I Progress Report, Development of Expulsion and Orientation Systems for Advanced Liquid Rocket Propulsion Systems; Contract AF04(611)-8200; Report No. SSD-TDR-62- Bell Aerosystems Company.

SUMMARY OF POSITIVE EXPULSION DEVICES

Contractor's Name and Address:

Bell Aerosystems Company
Buffalo 5, New York

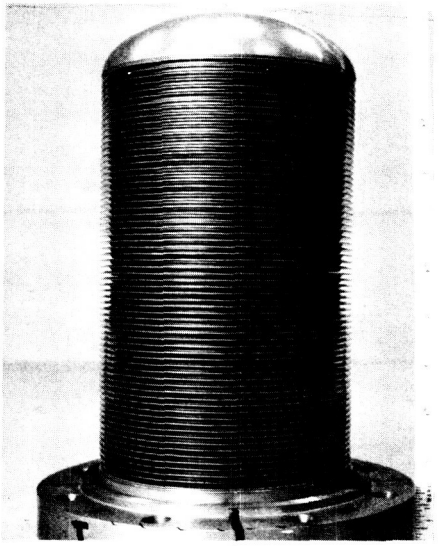

1. **Type of Device:** Metal Welded Bellows (accumulator type)

2. **Description/Application:** Start tank for turbine pump assembly.

3. **State of Development:** Test hardware has proven operational feasibility.

4. **Geometry/Shape:** Nesting ripple diapgragm shape
Fuel - 5-1/4 in. O.D. Oxidizer - 3-3/4 in. O.D.

5. **Recommended Materials:** 347 Stainless Steel - Oxidizer; AM-350 - Fuel

6. **Weight Comparison:**

7. **Size Limitations:**

Max. Diameter: **Max. Volume:**

8. **Characteristics:** ΔP Level - Spring Rate equivalent to ±1 psi

9. **Environmental Capabilities:**

Temperature and Pressure Range: -423° to +600°F
50 psi - ΔP Extended
600 spi - ΔP Nested
Storability: 1 year (min)

10. **Method of Operation:** Unit is pre-charged with N_2 gas. Liquid side is recharged when turbine pump attains operating speed and pressure.

11. **Energy/Power Requirements:** NA

12. **Cycle Life (Ambient):** Design objective - 50,000 cycles
Design requirement - 150 cycles

13. **Probable Failure Modes:** Circumferential fatigue cracks in heat affected zones adjacent to weld.

14. **Material Properties:**

15. **Expulsion Efficiency:** Not a controlling design parameter.

16. **Volumetric Efficiency:** Not a controlling design parameter.

17. **Analysis Data:** Feasibility tests have demonstrated the device to be a reliable multi-cycle devic

18. **References:** No published reports.

SUMMARY OF POSITIVE EXPULSION DEVICES

Contractor's Name and Address

Bell Aerosystems Company
Buffalo 5, New York

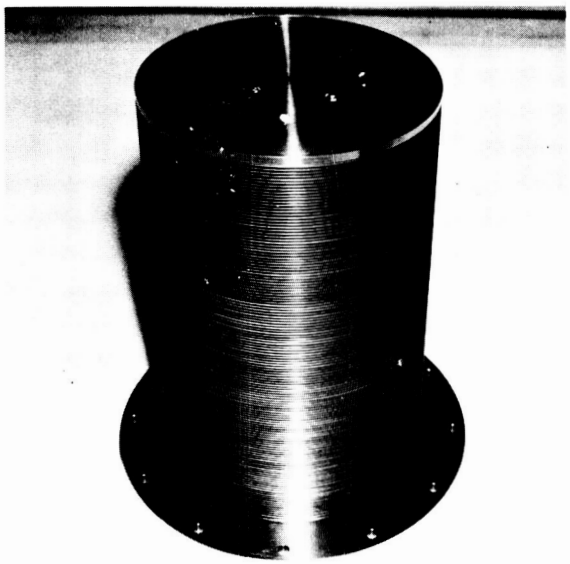

1. **Type of Device:** Metal Welded Bellows

2. **Description/Application:** Main propellant tanks for secondary propulsion system.

3. **State of Development:** Prototype hardware has been fabricated and is undergoing development testing.

4. **Geometry/Shape:** Nesting ripple diaphragm shape - 10 in. O.D.

5. **Recommended Materials:** 347 Stainless Steel

6. **Weight Comparison:**

7. **Size Limitations:**

Max. Diameter: _____ **Max. Volume:** _____

8. **Characteristics:** ΔP Level - Spring Rate to ±2-1/2 psi
Unique Characteristics: Operated with deflections causing plastic deformation of diaphragms.

9. **Environmental Capabilities:**

Temperature and Pressure Range: -423° to +600°F
20 psi - ΔP Extended
200 psi - ΔP Nested
Storability: 1 year (min)

10. **Method of Operation:** Pneumatically actuated through pressure regulator.

11. **Energy/Power Requirements:** NA

12. **Cycle Life (Ambient):** Design objective - 225 cycles.

13. **Probable Failure Modes:** Circumferential fatigue cracks in heat affected zone adjacent to weld

14. **Material Properties:**

15. **Expulsion Efficiency:** 98% plus

16. **Volumetric Efficiency:**

17. **Analysis Data:** Feasibility tests have proven that a predictable cycle life with plastic extension is practical.

18. **References:** No published reports.

SUMMARY OF POSITIVE EXPULSION DEVICES

Contractor's Name and Address

Bell Aerosystems Company
Buffalo 5, New York

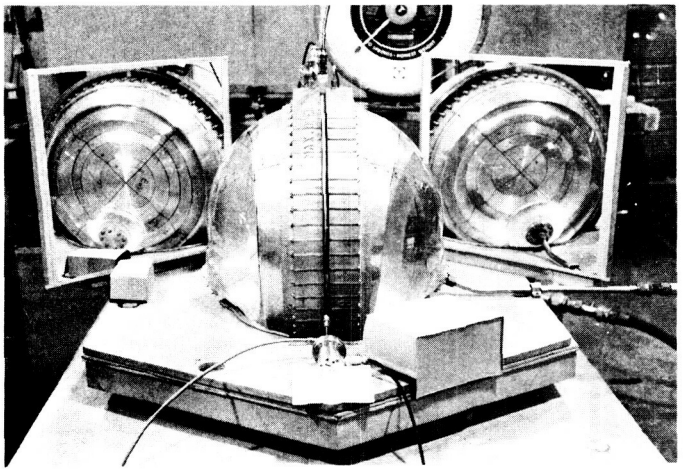

1. **Type of Device:** Convoluted Diaphragm

2. **Description/Application:** The convoluted diaphragm is a rollout single-expulsion device. Fluid is expelled from both sides of the diaphragm as pressure is applied.

3. **State of Development:** Feasibility tests have been conducted with a diaphragm fabricated from 0.040-inch-thick 1100-0 aluminum alloy. Work is being accomplished at Bell Aerosystems under Air Force Contract AF04(611)-8183.

4. **Geometry/Shape:** A series of convoluted rings decreasing in height from outer convolution toward center of diaphragm.

5. **Recommended Materials:** 1100-0 aluminum alloy, 347 stainless steel

6. **Weight Comparison:** Only boiler plate hardware has been designed.

7. **Size Limitations:** Limited only by capability of manufacturing equipment.

Max. Diameter: 54-inch unit has been fabricated **Max. Volume:** 356-gallon unit has been fabricated

8. **Characteristics:**

Low-Frequency: (Slosh) A half-size unit has successfully passed slosh tests (5 to 25 cps)

High-Frequency: To be investigated on half-size (27-in. dia.)

9. **Environmental Capabilities:** Cryogenic capability upper limit a function of material selected.

Temperature and Pressure Range: -423° to +600°F **Storability:** Excellent

10. **Method of Operation:** Pneumatically actuated

11. **Energy/Power Requirements:** NA

12. **Cycle Life (Ambient):** Single-expulsion device.

13. **Probable Failure Modes:** Fatigue cracks due to work-hardening at hinge points.

14. **Material Properties:**

15. **Expulsion Efficiency:** 97% expulslion efficiency is practical

16. **Volumetric Efficiency:** Approximately 91%

17. **Analysis Data:** Excellent characteristics and capability as a single-expulsion device. High expulsion efficiencies can be attained.

18. **References:** (1) Quarterly Report No. SSD-TDR-62-206

(2) Quarterly Report No. RTD-TDR-63-1019

SUMMARY OF POSITIVE EXPULSION DEVICES

Contractor's Name and Address:

Liquid Propulsion Section (No. 384
Caltech Jet Propulsion Laboratory
4800 Oak Grove Drive
Pasadena, California
SY. 0-6811, ext. 1488 or 1403

B

1. **Type of Device:** Mariner A Spacecraft, post-injection propulsion system, propellant-expulsion bladder (cell type); i.e., the fuel is completely encapsulated by the bladder.

2. **Description/Application:** The bladder expels hydrazine from the fuel tank when nitrogen gas, under pressure, is admitted to the ullage space between the fuel tank inner surface and the exterior surface of the bladder.

3. **State of Development:** The bladder successfully performed its function during all developmental testing and is considered flightworthy.

4. **Geometry/Shape:** Spherical

5. **Recommended Materials:** Butyl rubber compounds (selected).

6. **Weight Comparison:**

Item:	Tank	Bladder	Fuel
Weight: (lb)	3.40	0.92	32.1

7. **Size Limitations:** No rigid limit

Max. Diameter: 11.90 inches **Max. Volume:** 880 cubic inches

8. **Characteristics:** See next page

9. **Environmental Capabilities:** The bladder can withstand temperatures and pressures exceeding the operating limits which are listed below:

Temperature and Pressure Range: 32 to 165°F, 0 to 500 psia **Storability:** 9 months plus

10. **Method of Operation:** Pressure-regulated nitrogen gas is admitted to the ullage volume between the exterior surface of the bladder and the interior surface of the propellant tank.

11. **Energy/Power Requirements:** See next page

12. **Cycle Life (Ambient):** Virtually unlimited

13. **Probable Failure Modes:** Not available

14. **Material Properties:** Durable as an automobile tire inner tube

15. **Expulsion Efficiency:** 99% of loaded hydrazine is expelled

16. **Volumetric Efficiency:**

Item:	Tank	Bladder	Fuel
Volume (cubic inches):	1073	28	882

17. **Analysis Data:**

18. **References:**

8. Characteristics: The bladder is not required to expel propellant while in a vibration environment. In the flightready configuration, the bladder must withstand the following vibration without rupture or leakage at the manifold.

Low Frequency:

24 min of ±3 in., 1 to 3 cps and 0.3g 3 to 40 cps

High Frequency:

6 sec at 15g--rms noise
180 sec at 10g--rms noise
360 sec at 4.5g--rms noise and 4.5g--sinusoid
6 sec at 15g--rms noise
255 sec at 1.5g--rms noise

11. Energy/Power Requirements:

$$\Delta P_{N_2} \text{ Reservoir} \approx 1.2 \left[\frac{\text{(Volume of Propellant Expelled) x (Regulated Pressure)}_{\text{Fuel Tank}}}{\text{(Volume of } N_2 \text{ Reservoir)}} \right]$$

SUMMARY OF POSITIVE EXPULSION DEVICES

Contractor's Name and Address:

Liquid Propulsion Section (No. 384)
Caltech Jet Propulsion Laboratory
4800 Oak Grove Drive
Pasadena, California
SY. 0-6811, ext. 1488 or 1403

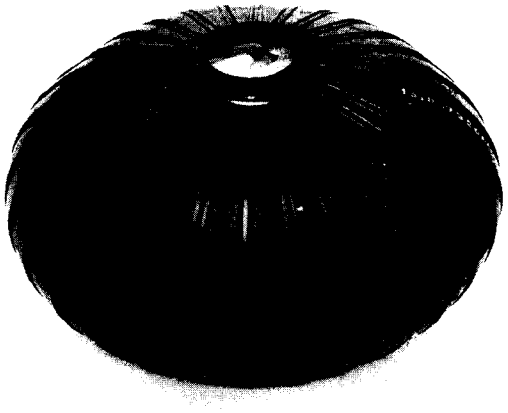

A

1. Type of Device: Ranger 3 – Mariner R Spacecraft, midcourse propulsion system, propellant-expulsion bladder (cell type); i.e., the fuel is completely encapsulated by the bladder.

2. Description/Application: The bladder expels hydrazine from the fuel tank when nitrogen gas, under pressure, is admitted to the ullage space between the fuel tank inner surface and the exterior surface of the bladder.

3. State of Development: The bladder successfully performed its function during Ranger 3 and Mariner R spacecraft flights.

4. **Geometry/Shape:** 1.75/1.00 in. (major diameter/minor diameter) oblate spheroid.

5. **Recommended Materials:** Butyl rubber compounds (selected).

6. **Weight Comparison:**

Item:	Tank	Bladder	Fuel
Weight: (lb)	4.38	0.72	13.5

7. **Size Limitations:** No rigid limit

Max. Diameter: 6.0 inches 10.80 inches **Max. Volume:** 365 cubic inches

8. **Characteristics:** See next page

9. **Environmental Capabilities:** The bladder can withstand temperatures and pressures exceeding the operating limits which are listed below.

Temperature and Pressure Range: 32 to 165° F 0 to 500 psia **Storability:** 3 weeks plus

10. **Method of Operation:** Pressure regulated nitrogen gas is admitted to the ullage volume between the exterior surface of the bladder and the interior surface of the propellant tank.

11. **Energy/Power Requirements:** See next page

12. **Cycle Life (Ambient):** Virtually unlimited.

13. **Probable Failure Modes:** Not available

14. **Material Properties:** Durable as an automobile tire inner tube

15. **Expulsion Efficiency:** 99% of loaded hydrazine is expelled

16. **Volumetric Efficiency:**

Item:	Tank	Bladder	Fuel
Volume (cubic inches):	440	22	371

17. **Analysis Data:**

18. **References:**

8. Characteristics: The bladder is not required to expel propellant while in a vibration environment. In the flightready configuration, the bladder must withstand the following vibration without rupture or leakage at the manifold:

Low Frequency:

24 min of ±3 in., 1 to 3 cps and 0.3g 3 to 40 cps

High Frequency:

6 sec at 15g--rms noise
180 sec at 10g--rms noise
360 sec at 4.5g--rms noise and 4.5g--sinusoid
6 sec at 15g--rms noise
225 sec at 1.5g--rms noise

11. Energy/Power Requirements:

$$\Delta P_{N_2} \text{ Reservoir} \approx 1.2 \left[\frac{(\text{Volume of Propellent Expelled}) \times (\text{Regulated Pressure})_{\text{Fuel Tank}}}{(\text{Volume of } N_2 \text{ Reservoir})} \right]$$

SUMMARY OF POSITIVE EXPULSION DEVICES

Contractor's Name and Address:

Curtiss-Wright Corporation
Wright Aeronautical Division
Wood-Ridge, New Jersey

1. **Type of Device:** Metallic Expulsion Bladder

2. **Description/Application:** R and D on bladder expulsion systems.

3. **State of Development:** In development.

4. **Geometry/Shape:** Cylinder

5. **Recommended Materials:** Aluminum alloy or stainless steel.

6. **Weight Comparison:** Normally, slightly heavier than flexible bladders.

7. **Size Limitations:** Not restricted

Max. Diameter: Not restricted **Max. Volume:** Not restricted

8. **Characteristics:**

9. **Environmental Capabilities:** Basically dependent upon fuel contained.

Temperature and Pressure Range: 400°F Unlimited **Storability:** Good

10. **Method of Operation:** Complete cylindrical bladder with 4 lobe cross-section containing propellants inside and outside. Hot-gas generator used to expel inner propellant which in turn expels outer propellant through bladder.

11. **Energy/Power Requirements:** Hot-gas generator

12. **Cycle Life (Ambient):** Not determined, but low compared to flexible bladder.

13. **Probable Failure Modes:** Bladder failure due to three corner wrinkles.

14. **Material Properties:** Essentially non-permeable to vapor or gas.

15. **Expulsion Efficiency:**

16. **Volumetric Efficiency:** 95%

17. **Analysis Data:**

18. **References:**

SUMMARY OF POSITIVE EXPULSION DEVICES

Contractor's Name and Address

Curtiss-Wright Corporation
Wright Aeronautical Division
Wood-Ridge, New Jersey

1. **Type of Device:** Expulsion Bladder

2. **Description/Application:** R and D on bladder expulsion systems.

3. **State of Development:** Developed

4. **Geometry/Shape:** Cylindrical L/D = 13

5. **Recommended Materials:** Teflon

6. **Weight Comparison:**

7. **Size Limitations:** Not restricted

Max. Diameter: Not restricted **Max. Volume:** Not restricted

8. **Characteristics:**

9. **Environmental Capabilities:** Basically dependent on fuel contained.

Temperature and Pressure Range: **Storability:**

10. **Method of Operation:** Gas applied to external side of bladder, fuel contained inside.

11. **Energy/Power Requirements:** Very low; flexible bladder material.

12. **Cycle Life (Ambient):** Approximately 100 cycles.

13. **Probable Failure Modes:** Bladder pin hole or tear; leak past face seal.

14. **Material Properties:** Permeable to vapors and gas.

15. **Expulsion Efficiency:** 96 to 99.75%

16. **Volumetric Efficiency:** 95%

17. **Analysis Data:** System used with and without central expulsion tube. Expulsion tubes of circular and bourdon tube section.

18. **References:**

SUMMARY OF POSITIVE EXPULSION DEVICES

Contractor's Name and Address:

Hycon Mfg. Company
700 Royal Oaks Drive
Monrovia, California

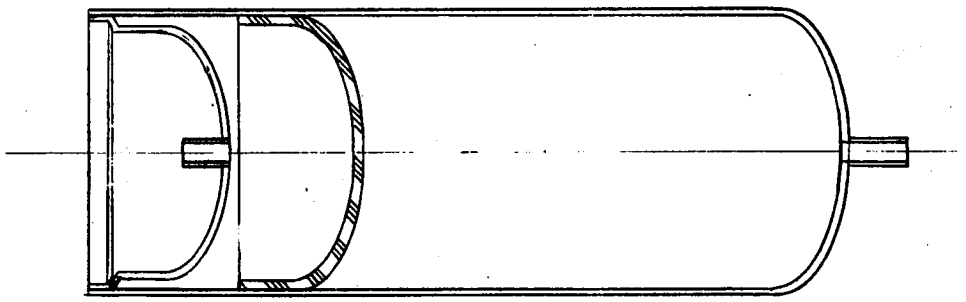

1. **Type of Device:** Positive Expulsion Tank, capable of being fitted in locations not suited for simple cylinders and spheres.

2. **Description/Application:** Primary application is one where a convenient location for a conventional tank is unavailable.

3. **State of Development:** Preliminary design.

4. **Geometry/Shape:** Helix, torroid, sausage, or cylinder.

5. **Recommended Materials:** Steel, aluminum alloy, or titanium alloy.

6. **Weight Comparison:** N A

7. **Size Limitations:** N A

Max. Diameter: N A **Max. Volume:** N A

8. **Characteristics:** Capability of being installed in unusual locations.

9. **Environmental Capabilities:** --

Temperature and Pressure Range: -- **Storability:** --

10. **Method of Operation:** Flexible piston

11. **Energy/Power Requirements:** --

12. **Cycle Life (Ambient):** --

13. **Probable Failure Modes:** --

14. **Material Properties:** --

15. **Expulsion Efficiency:** Greater than 98%

16. **Volumetric Efficiency:** N A

17. **Analysis Data:** The proposed design is based on Freon fluid injection expulsion tanks previously designed for missile thrust vector control systems for Polaris and other experimental missiles.

18. **References:**

SUMMARY OF POSITIVE EXPULSION DEVICES

Contractor's Name and Address:

The Martin Company – Denver Division
Aerospace Division of Martin-Marietta Corp.
P. O. Box 179, Mail No. A-88
Denver 1, Colorado

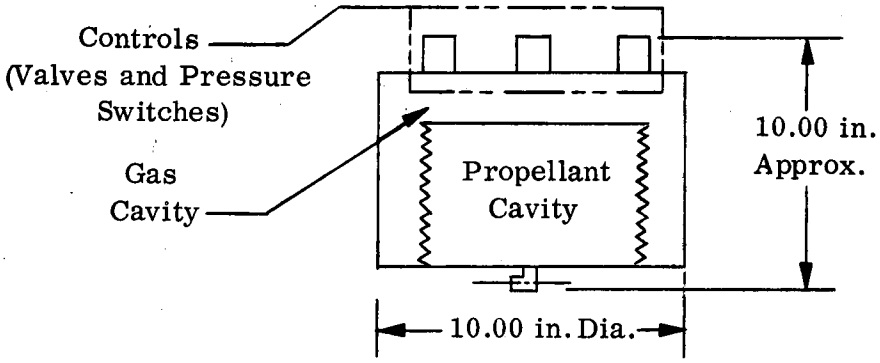

1. **Type of Device:** Pneumatic-Actuated Positive Expulsion Device (Collapsible/expandable metal bellows).

2. **Description/Application:** Auxiliary propellant storage compartment to provide propellant for initial engine start under zero-g conditions.

3. **State of Development:** Prototype Development – Initial acceptance tests completed.

4. **Geometry/Shape:** Collapsible, expandable, metal bellows.

5. **Recommended Materials:** Aluminum alloy or stainless steel.

6. **Weight Comparison:** Assembly weighs 23 pounds (dry) and contains 9 pounds of propellant.

7. **Size Limitations:** None.

Max. Diameter: Not limited **Max. Volume:** Not limited

8. **Characteristics:**
Low Frequency - Hard on bellows
High Frequency - Hard on valves

9. **Environmental Capabilities:** Any, within the properties of the propellants.

Temperature and Pressure Range: +25° to +120°F to 115 psia **Storability:** 2 years

10. **Method of Operation:** (1) Filled by pressurized propellant from external propellant source, (2) Expulsion by high-pressure external pneumatic source.

11. **Energy/Power Requirements:** 1 amp - 28 V dc electrical, 150 psig (min) pneumatic pressure, 70 psia (min) pressurized propellant

12. **Cycle Life (Ambient):** 50 cycles

13. **Probable Failure Modes:** Bellows fatigue

14. **Material Properties:** N A

15. **Expulsion Efficiency:**

16. **Volumetric Efficiency:** 90% (min.)
(volume of expulsion versus total loadable volume)

17. **Analysis Data:** Design intended for long-term storage, with cycling; no organic materials used in construction.

18. **References:** 807-0400020, 807-040030 (Martin Specifications)

SUMMARY OF POSITIVE EXPULSION DEVICES

Name and Address:

NASA Lewis Research Center
21000 Brookpark Road
Cleveland 35, Ohio

1. **Type of Device:** Cryogenic Expulsion Bladder

2. **Description/Application:** This device is a mylar-coated dacron bag capable of expelling liquid nitrogen and possibly liquid hydrogen upon collapse of the bag. The bag is 10 in. in diameter and about 20 in. long.

3. **State of Development:** Research employing different bag materials is in progress.

4. **Geometry/Shape:** Cylindrical bag with elliptical ends.

5. **Recommended Materials:** Mylar-coated dacron cloth worked successfully in this investigation. Other materials are being considered for research.

6. **Weight Comparison:**

7. **Size Limitations:**

Max. Diameter: **Max. Volume:**

8. **Characteristics:**

9. Environmental Capabilities: Seven successful expulsions of liquid nitrogen (-320°F) were made. Six successful expulsions of partly filled bags of liquid helium were made. The apparatus available did not permit complete filling with liquid helium, but the upper portion of the bladder was at a temperature of about -420°F.

9. **Environmental Capabilities:**

Temperature and Pressure Range: -320° to -453°F; 25 to 50 psi pressure drop across system **Storability:**

10. **Method of Operation:** Expulsion accomplished by causing bladder to collapse. Helium gas was used to pressurize bladder.

11. **Energy/Power Requirements:**

12. **Cycle Life (Ambient):** Not definitely known - one bladder has been cycled seven times with liquid nitrogen in bladder and six times with bladder partly filled with liquid helium.

13. **Probable Failure Modes:** Pin holes in bladder wall and failure of the seams.

14. **Material Properties:**

15. **Expulsion Efficiency:** 99%

16. **Volumetric Efficiency:** 99%

17. **Analysis Data:** Tests were run to demonstrate the feasibility of transferring cryogenic fluids by means of an expulsion bag technique. Mylar-coated cacron bags used as a fluid container were found to be flexible enough to collapse at temperatures of approximately -423°F and, thereby, cause expulsion of the fluid. Visual inspection and helium gas pressurization of the bags showed no damage even after repeated cycles.

18. **References:** NASA Technical Note D-849; Transfer of Cryogenic Fluids by an Expulsion-Bag Technique; Paul J. Sirocky; April 1961.

SUMMARY OF POSITIVE EXPULSION DEVICES

Contractor's Name and Address:

United Technology Corporation
P. O. Box 358
Sunnyvale, California

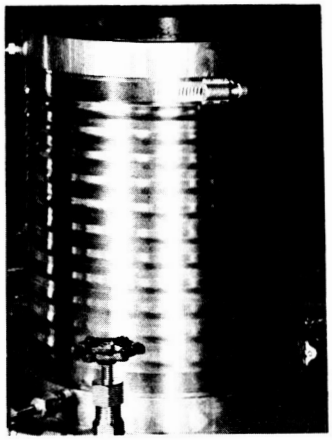

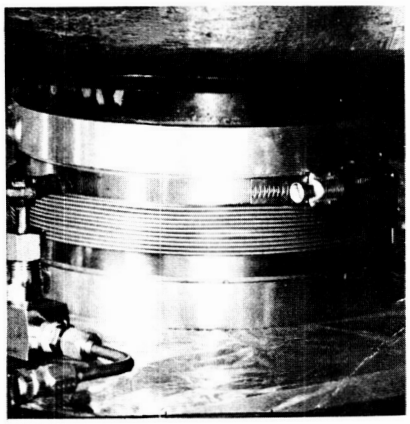

1. Type of Device: Squeeze Tank

2. Description/Application: Thin-walled cylinders (scaleable to capacity requirements) which are longitudinally compressed, expelling propellants for use in liquid rocket engines.

3. State of Development: In-house project funding limited to research.

4. **Geometry/Shape:** 17.4 in. I.D. x 21.0 in. long cylinders

5. **Recommended Materials:** 302 stainless

6. **Weight Comparison:** Component is lightweight, comparable to resilient plastic expulsion components. System weight penalty due to high loading requirements.

7. **Size Limitations:** L/D recommended no greater than 1.2.

Max. Diameter: Not limited **Max. Volume:** Not limited

8. **Characteristics:** Not determined.

9. **Environmental Capabilities:** Limited by material selection, propellant capability, etc.

Temperature and Pressure Range: Standard day (test) 75 psig (test) **Storability:** As above.

10. **Method of Operation:** When longitudinally collapsed, positive expulsion of the propellant is accomplished through one of the end plates.

11. **Energy/Power Requirements:** Actuating force/hydraulic force approximately 1.35

12. **Cycle Life (Ambient):** Only singe-cycle tests carried out. Not recommended for multicycle operation.

13. **Probable Failure Modes:** (a) Joint weld rupture; (b) repeatibility of the desired collapse mode.

14. **Material Properties:**

15. **Expulsion Efficiency:** 81% collapse at force ratio (item 10) of 1.35

16. **Volumetric Efficiency:** Trapped volume/expelled volume = 0.0316

17. **Analysis Data:** System weight penalties probably prohibitive for present generation space systems main propellant tanks. Good for liquid-level sensing. Applicable for attitude control devices, gas generators, APU's, etc.

18. **References:** Technical Report; Results of Squeeze Bottle Test Program; S. A. Martin, UTC; 16 November 1960.

APPENDIX II

SUMMARY OF POSITIVE EXPULSION DEVICES
(Previous Contract NASr-44)

APPENDIX II

SUMMARY OF POSITIVE EXPULSION DEVICES (PREVIOUS CONTRACT NASr-44)

Summarized in this Appendix are designs and design concepts of various zero-gravity positive expulsion devices. These data, as abstracted from the Final Report on Contract NASr-44, will assist the system designer in the selection of an expulsion device to fulfill a particular application. All data are based upon an extensive state-of-the-art survey completed by Bell Aerosystems Company for NASA in March 1962.

The page numbers and reference numbers shown on the Summary Sheets of this Appendix are taken from the NASr-44 Final Report, No. 7129-933003, published by the Bell Aerosystems Company in June 1962. The reader should refer to this unabridged Final Report for detailed information on these expulsion devices.

CONTENTS

(Appendix II)

Page

POSITIVE EXPULSION DEVICES

Controlled Rolling Diaphragm 193
Longitudinal Tank-Type Reversing Diaphragm Longitudinal Tank-Type 195
Convoluted Diaphragm for Spherical Containers 197
Dual Reversing Diaphragm 199
BiConvex Diaphragm 201
Bath-Tub Type Reversing Diaphragm 203
Two-Section Controlled Rolling Diaphragm 205
Multi-Cell Diaphragm Configuration 207
Collapsing Bladder 209
Expanding Bladder 211
Spherical Reversing Bladder 213
3-Cell Collapsing Bladder 215
Preformed 3-Lobe Expanding Bladder 217
Dual Concentric Bladder 219
Piston 221
Floating Piston With Bourrelet 223
Rotating Squeegee Type Device 225
Rotating Squeegee Type Multiple Tube 227
Rotating Squeegee Type Device Diaphragm 229
Twisting Bladder-Uncontrolled 231
Twisting Bladder-Controlled 233
Rotating Tank 235
Capillary Tubes 237
Foam Displacement 239
Roll and Peel Diaphragm 241
Ullage Rockets 243
Trap or Surge Tank 245
Mechanical Bellows 247
Electrostatic Device 249
Pleated Folding Type Bladder 251
Roll Sweep Pleated Bladder 253
Electromagnetic Pump 255
Multiple Exploding Wires 257
Supercritical Systems 259
Wick 261
Channel Accelerator 263

SUMMARY OF POSITIVE EXPULSION DEVICES

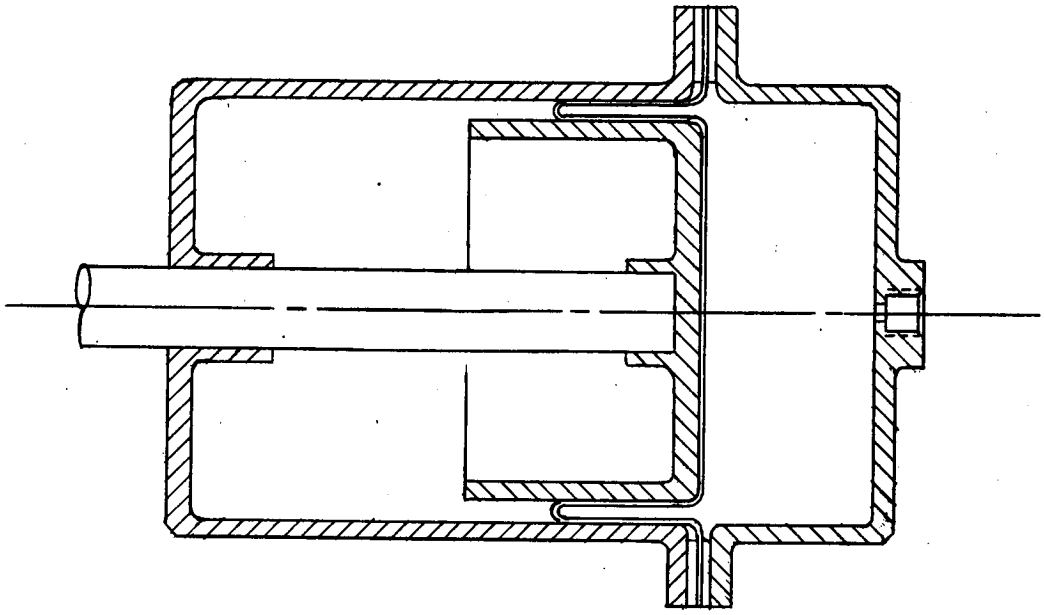

Controlled Rolling Diaphragm

1. **Type of Device:** Controlled Rolling Diaphragm

2. **Description/Application:** A controlled diaphragm is a long-stroke, deep-convolution, constant-area diaphragm which is free positioning in its stroke. The diaphragm is attached to the piston head and, as the diaphragm and piston are moved in the axial direction, the diaphragm will roll off the piston side wall and onto the cylinder side wall, (or in the reverse sequence), with a smooth and continuous frictionless motion.

3. **State of Development:** Similar rolling diaphragms are produced by the Bellofram Corporation, Burlington, Mass., employing fabric and elastomeric materials.

   Feasibility studies performed by Bell Aerosystems Company have indicated that metals can be employed for the thin diaphragm (p.50).

4. **Geometry/Shape:** Ideally suited for circular cylinders with flat heads.

5. **Recommended Materials:**

6. **Weight Comparison:**

7. **Size Limitations:**

Max. Diameter: _____ **Max. Volume:** _____

p. 48

8. **Characteristics:** a) Piston sealing is not desired and associated tolerances on fit and finish are not very important.

b) Larger diameters of piston produce smaller values of circumferential stress in the rolling diaphragm.

c) The skirt on the piston produces a "dead" volume and a decrease in volumetric efficiency.

9. **Environmental Capabilities:**

Temperature and Pressure Range: _____ **Storability:** _____

10. **Method of Operation:**

11. **Energy/Power Requirements:**

12. **Cycle Life (Ambient):**

13. **Probable Failure Modes:**

14. **Material Properties:**

15. **Expulsion Efficiency:**

16. **Volumetric Efficiency:**

17. **Analysis Data:** p. 51

18. **References:** L50, L51

SUMMARY OF POSITIVE EXPULSION DEVICES

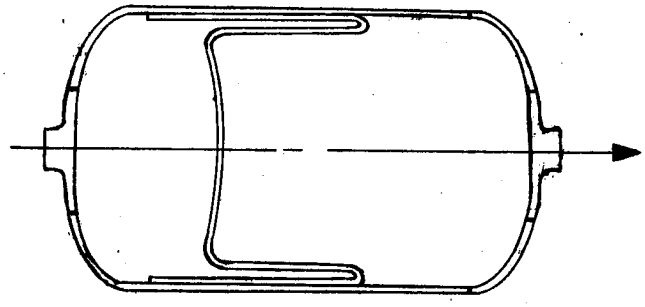

Longitudinal Tank-Type Reversing Diaphragm
Longitudinal Tank-Type

1. **Type of Device:** Reversing Diaphragm (Page 43)

2. **Description/Application:** A longitudinal Tank-Type Reversing Diaphragm is a long-stroke, deep convolution configuration. The diaphragm tends to roll on itself during expulsion. This type of configuration is employed in ejection-type devices, as a self-contained and sealed energy source and as a constant force/stroke buffer.

3. **State of Development:** A device of this type is made by A and I Aircraft Armaments, Inc., Cockeysville, Maryland, and is called Telecartridge.

4. **Geometry/Shape:**

5. **Recommended Materials:**

6. **Weight Comparison:**

7. **Size Limitations:**

Max. Diameter: **Max. Volume:**

8. **Characteristics:** of Device:

a) It is a one-shot device

b) Complete dispensing of material is possible

c) It is recommended as a fast action device.

9. **Environmental Capabilities:**

Temperature and Pressure Range: **Storability:**

10. **Method of Operation:**

11. **Energy/Power Requirements:**

12. **Cycle Life (Ambient):**

13. **Probable Failure Modes:**

14. **Material Properties:**

15. **Expulsion Efficiency:**

16. **Volumetric Efficiency:**

17. **Analysis Data:**

18. **References:**

SUMMARY OF POSITIVE EXPULSION DEVICES

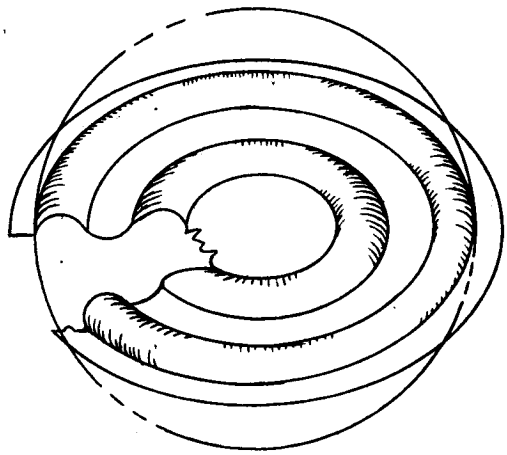

Convoluted Diaphragm for Spherical Containers

1. **Type of Device:** Convoluted Diaphragms (Page 30)

2. **Description/Application:** Convoluted diaphragms have one or more concentric convolutions which are either pressed, formed or spun. Convolutions increase the working stroke of a diaphragm and allow the diaphragm to operate with material flexing, rather than material elongation.

3. **State of Development:**

4. **Geometry/Shape:** Double convoluted diaphragms can be enclosed in a spherical or longitudinal tank configuration, incorporating (Pages 32, 33, 35), a surface of revolution head.

5. **Recommended Materials:** Metals, Plastics, Impregnated Cloth, Elastomers.

6. **Weight Comparison:**

7. **Size Limitations:**

Max. Diameter: **Max. Volume:**

8. **Characteristics:** (Page 31)

a) The device is orientation sensitive with respect to acceleration forces.

b) The use of a double-convoluted diaphragm can be utilized for a bipropellant system within a single tank geometry.

c) A collector tube must be employed between the two tank halves to insure expulsion for a monopropellant system.

d) The volumetric efficiency is dependent upon the convolution design and cycles of operation.

9. **Environmental Capabilities:**

Temperature and Pressure Range: **Storability:**

10. **Method of Operation:**

11. **Energy/Power Requirements:**

12. **Cycle Life (Ambient):**

13. **Probable Failure Modes:**

14. **Material Properties:**

15. **Expulsion Efficiency:**

16. **Volumetric Efficiency:**

17. **Analysis Data:** p. 37

Dynamic Effects p. 42

External closure or tank weights

Construction Material: Metals, Plastics, impregnated cloth, elastomers.

18. **References:**

L50, L51

SUMMARY OF POSITIVE EXPULSION DEVICES

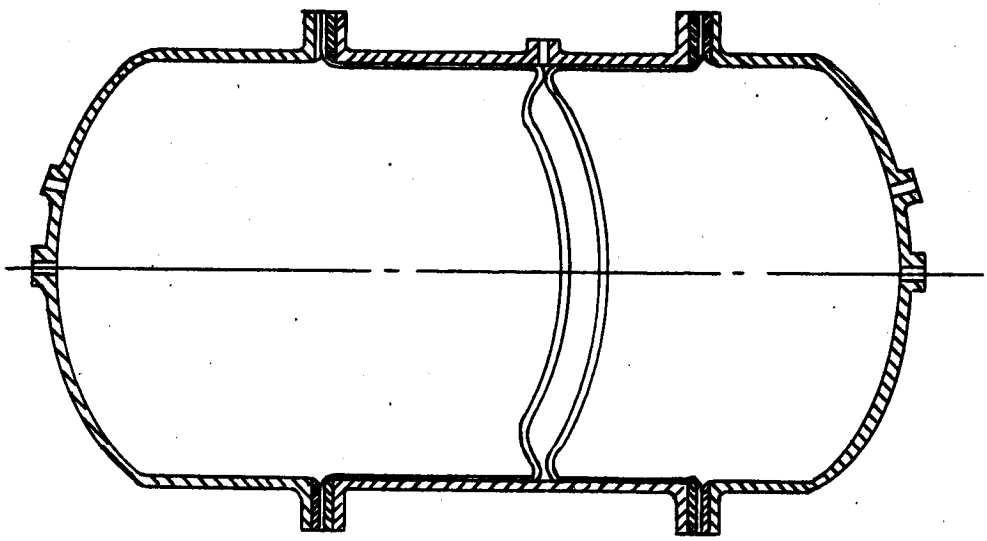

Dual Reversing Diaphragm

1. **Type of Device:** Dual Reversing Diaphragm P. 45

2. **Description/Application:** Two dividing diaphragms are installed within an enclosed shape in such a manner that two fluid-tight volumes are formed.

3. **State of Development:**

4. **Geometry/Shape:** The configuration can be readily enclosed within a longitudinal tank and preferably with surface or revolution heads.

5. **Recommended Materials:**

6. **Weight Comparison:**

7. **Size Limitations:**

Max. Diameter: **Max. Volume:**

8. **Characteristics:** a) The device is suitable for a bipropellant use. p. 45

b) The required volume of each bipropellant can be readily established.

c) Mass ratio flow could be difficult because buckling and rolling of the two diaphragms may not be proportional to each other.

9. **Environmental Capabilities:**

Temperature and Pressure Range: **Storability:**

10. **Method of Operation:**

11. **Energy/Power Requirements:**

12. **Cycle Life (Ambient):**

13. **Probable Failure Modes:**

14. **Material Properties:**

15. **Expulsion Efficiency:**

16. **Volumetric Efficiency:**

17. **Analysis Data:**

18. **References:**

SUMMARY OF POSITIVE EXPULSION DEVICES

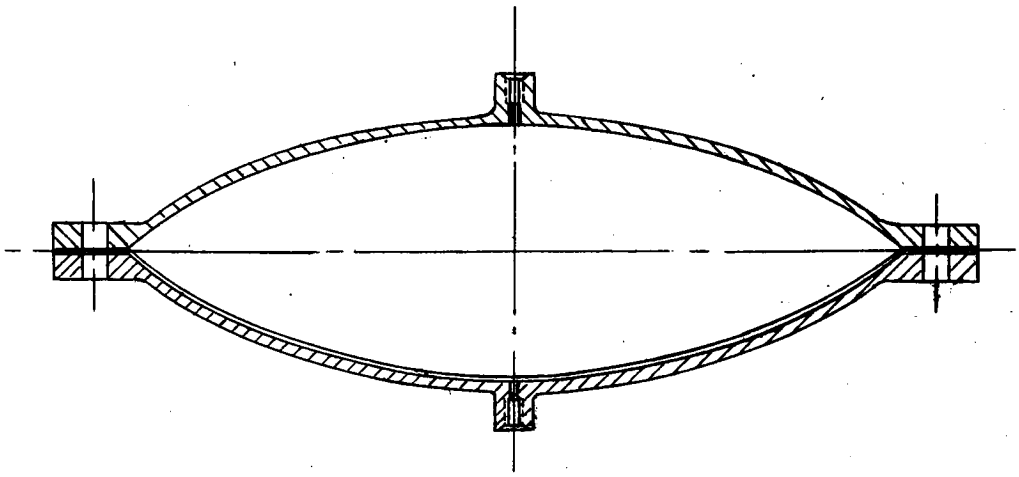

BiConvex Diaphragm

1. **Type of Device:** BiConvex Diaphragm p. 45

2. **Description/Application:** The BiConvex Diaphragm can be either a flat sheet or a shaped configuration to match the inside contour of the BiConvex container. The diaphragm flexes and stretches during operation from one convex head to the other.

3. **State of Development:** The BiConvex Diaphragm is associated with the common and conventional fuel pump employed in automotive power plants. A stainless steel reactor pump of this type configuration has been employed by the Oakridge National Laboratory.

4. **Geometry/Shape:** Spherical caps of relatively shallow shape are usually employed. The inside contour of the container can also be shaped to employ a two-radii contour diaphragm or a free diaphragm which is shaped to match the maximum deflection of a flat circular plate under a normal pressure loading.

5. **Recommended Materials:**

6. **Weight Comparison:**

7. **Size Limitations:**

Max. Diameter: **Max. Volume:**

8. **Characteristics:** a) Repeated cycle operations are possible. p. 43
b) Volume capacity is relatively small.
c) An equatorial ring is required for assembly which induces a weight penalty.

9. **Environmental Capabilities:**

Temperature and Pressure Range: **Storability:**

10. **Method of Operation:**

11. **Energy/Power Requirements:**

12. **Cycle Life (Ambient):**

13. **Probable Failure Modes:**

14. **Material Properties:**

15. **Expulsion Efficiency:**

16. **Volumetric Efficiency:**

17. **Analysis Data:** Two-radii container volumes. p. B-5
Bi-Convex spherical-cap configuration weights. p. B-1

18. **References:** L11

SUMMARY OF POSITIVE EXPULSION DEVICES

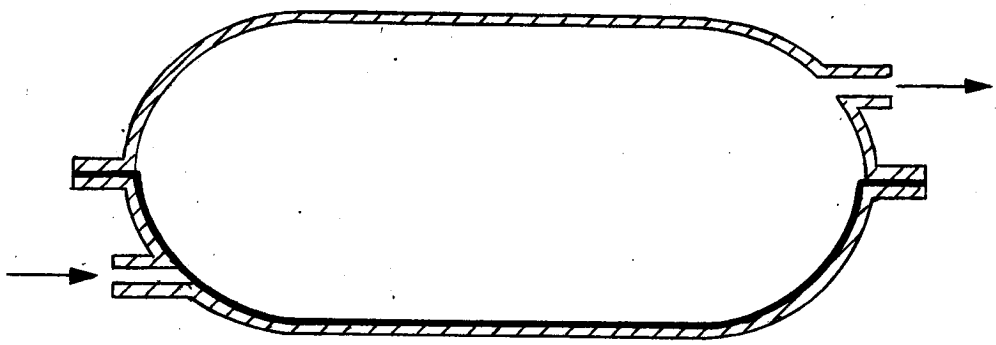

Bath-Tub -Type Reversing Diaphragm

1. **Type of Device:** Bath-Tub -Type Reversing Diaphragm

2. **Description/Application:** The Bath-Tub -Type Reversing Diaphragm can be considered similar to a dished diaphragm. The dish or bath-tub shape increases the allowable stroke which can be twice the dish weight without material stretching. p. 34

3. **State of Development:** Some experimental tests have been performed by the Bell Aerosystems Company on such a diaphragm employing .016- .026 in. 1100-0 aluminum. p. 31

4. **Geometry/Shape:** A longitudinal tank with ellipsoidal heads is most advantageous.

5. **Recommended Materials:**

6. **Weight Comparison:**

7. **Size Limitations:**

Max. Diameter: **Max. Volume:**

8. **Characteristics:** a) Volumetric efficiency is high.
b) An equatorial flange is required for installation and assembly. This induces a weight penalty for the tank.
c) Cycle life is limited for a metallic diaphragm to a maximum of about 3-5.

9. **Environmental Capabilities:**

Temperature and Pressure Range: **Storability:**

10. **Method of Operation:**

11. **Energy/Power Requirements:**

12. **Cycle Life (Ambient):**

13. **Probable Failure Modes:**

14. **Material Properties:**

15. **Expulsion Efficiency:**

16. **Volumetric Efficiency:**

17. **Analysis Data:** p. 76

18. **References:**

SUMMARY OF POSITIVE EXPULSION DEVICES

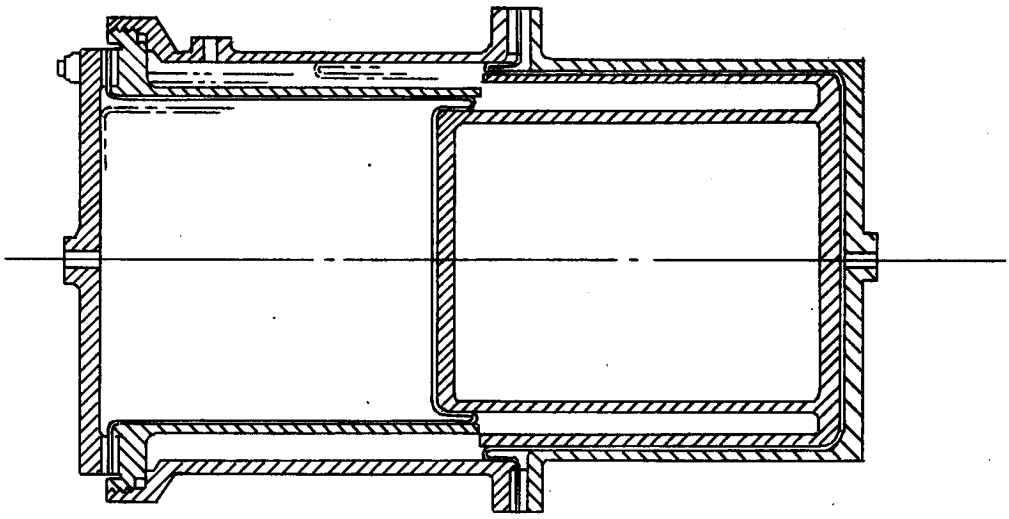

Two-Section Controlled Rolling Diaphragm

1. **Type of Device:** Two-Section Controlled Rolling Diaphragm

2. **Description/Application:** The device is similar to the controlled rolling diaphragm with the exception that dual rolling diaphragms are employed to expel two fluids.

3. **State of Development:** There are several applications involving this type of configuration which are designed and manufactured by Bellofram Corporation, Burlington, Mass.

4. Geometry/Shape: Flat head containers are most suitable.

5. Recommended Materials:

6. Weight Comparison:

7. Size Limitations:

Max. Diameter: Max. Volume:

8. Characteristics: a) Both fluids are sealed from each other by the rolling diaphragm. p. 63
b) Slight misalignment of the two pistons does not affect the operation.
c) Required volume ratios for the bipropellants may not be attainable if near equal volumes are necessary,

9. Environmental Capabilties:

Temperature and Pressure Range: Storability:

10. Method of Operation:

11. Energy/Power Requirements:

12. Cycle Life (Ambient):

13. Probable Failure Modes:

14. Material Properties:

15. Expulsion Efficiency:

16. Volumetric Efficiency:

17. Analysis Data: p. 51

18. References:

SUMMARY OF POSITIVE EXPULSION DEVICES

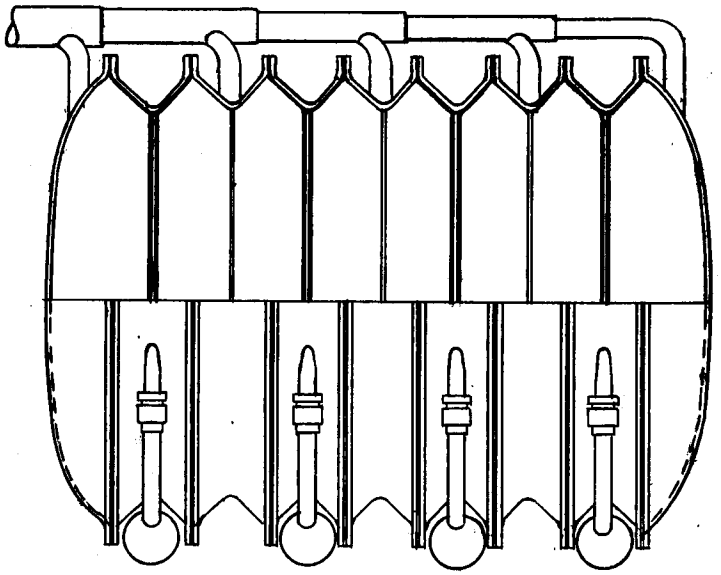

Multi-Cell Diaphragm Configuration

1. Type of Device: Multi-Cell Diaphragm

2. Description/Application: The multi-cell diaphragm configuration is a series of dished diaphragms enclosed within prescribed sections of a container. A common manifold or collector tube is employed to direct the fluid from the numerous dished diaphragm compartments.

3. State of Development:

4. Geometry/Shape:

5. Recommended Materials:

6. Weight Comparison:

7. Size Limitations:

Max. Diameter: Max. Volume:

8. Characteristics: a) Multiplicity of cells increases demand reliability p. 67

b) Installation and assembly of the diaphragm and cells requires considerable welding length.

c) With a relatively small stroke per diaphragm, diaphragm stresses can be reduced and cyclic life increased.

9. Environmental Capabilties:

Temperature and Pressure Range: Storability:

10. Method of Operation:

11. Energy/Power Requirements:

12. Cycle Life (Ambient):

13. Probable Failure Modes:

14. Material Properties:

15. Expulsion Efficiency:

16. Volumetric Efficiency:

17. Analysis Data:

18. References:

SUMMARY OF POSITIVE EXPULSION DEVICES

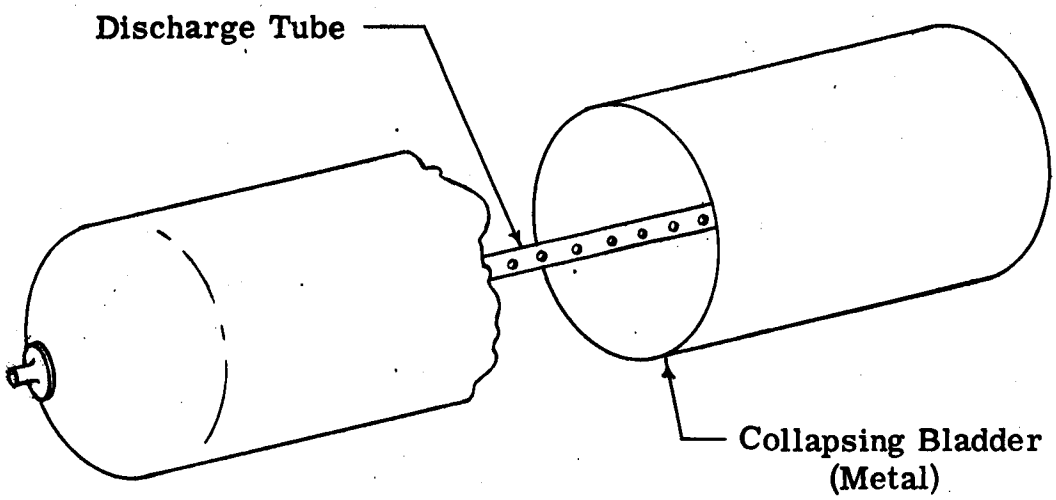

Collapsing Bladder

1. Type of Device: Collapsing Bladder

2. Description/Application: A collapsing bladder which is a flexible container is made to fit the inside smooth contour of a tank. The pressurizing gas is applied external to the bladder causing the bladder to deform and collapse and at the same time forcing the fluid within the bladder to flow out.

3. State of Development: This is the most common device employed today. Such positive expulsion bladders have been designed and developed by the Bell Aerosystems Company for the GAM-63 (Rascal) Air-To-Ground Missile Teflon Bladders were used for the oxidizer and Buna-N rubber over nylon cloth for the fuel. The bladders for the GAM-63 were approximately four feet in diameter.

The feasibility of a collapsing aluminum cylinder bladder for expulsion has also been demonstrated by Bell Aerosystems Company.

4. Geometry/Shape: A bladder can be used in any surface of revolution such as a sphere, cylinder, ellipsoid, torus, etc.

5. Recommended Materials:

6. Weight Comparison:

7. Size Limitations:

Max. Diameter: Max. Volume:

8. Characteristics: a) High rates of flow are possible in expulsion.
b) It is a relatively simple device and dependent on material characteristics, can be utilized for multiple cycles of operation.
c) Compatibility requirements for the propellant and bladder materials imposes a restriction on material selection especially in the plastic and polymer class.

9. Environmental Capabilties:

Temperature and Pressure Range: Storability:

10. Method of Operation:

11. Energy/Power Requirements:

12. Cycle Life (Ambient):

13. Probable Failure Modes:

14. Material Properties:

15. Expulsion Efficiency:

16. Volumetric Efficiency:

17. Analysis Data: p. 76, 104

18. References: L1, L2, L3, L4, L5, L6, L9, L12, L15, L26, L27, L32, L40, L43, L47, L48.

SUMMARY OF POSITIVE EXPULSION DEVICES

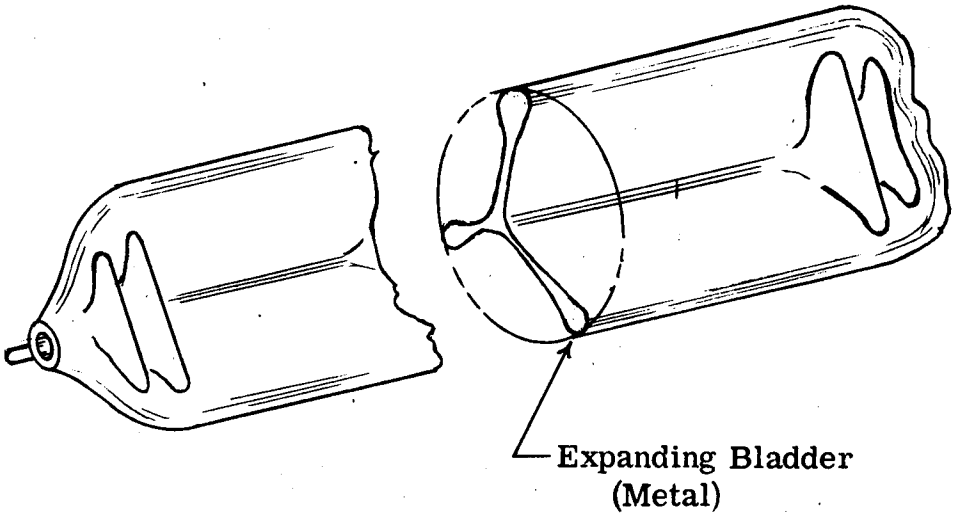

Expanding Bladder

1. Type of Device: Expanding Bladder

2. Description/Application: In an expanding bladder, positive expulsion is achieved by the introduction of a pressurizing gas into the collapsed bladder causing the bladder to expand and forcing the fluid outside the bladder (between bladder and tank shell) to flow out by means of a withdrawal line system. Expanding bladders are also prefolded to minimize creases and to control the expansion.

p. 73

3. State of Development: In-house work has been performed at Bell Aerosystems Company on pre-folding techniques and installations.

4. Geometry/Shape: An expanding bladder can be employed in most any shape that constitutes a surface of revolution.

5. Recommended Materials:

6. Weight Comparison:

7. Size Limitations:

Max. Diameter: Max. Volume:

8. Characteristics: a) Pre-folded and expanded shapes are predictable during the expulsion cycle.
b) Folding techniques for metallic configurations induce finite membrane strains that may limit the geometric shape.

9. Environmental Capabilties:

Temperature and Pressure Range: Storability:

10. Method of Operation:

11. Energy/Power Requirements:

12. Cycle Life (Ambient):

13. Probable Failure Modes:

14. Material Properties:

15. Expulsion Efficiency:

16. Volumetric Efficiency:

17. Analysis Data: p. 76, 104

18. References:

SUMMARY OF POSITIVE EXPULSION DEVICES

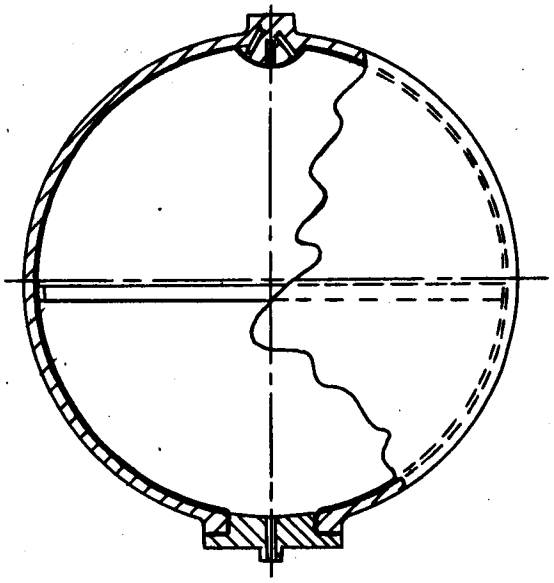

Spherical Reversing Bladder

1. Type of Device: Spherical Reversing Bladder p. 104

2. Description/Application: A ring which is segmented so that it can be folded and inserted through an opening. Holds the bladder against the inner wall of the sphere at the equator. The ring is installed after the insertion of the bladder. As the expulsion cycle progresses, one half of the bladder will collapse and traverse through the tank center and towards the propellant port outlet. At the end of the expulsion cycle, the bladder is folded within itself similar in appearance to two concentric hemispheres.

3. State of Development:

4. Geometry/Shape: The installation of the segmented retainer may limit the contours to be employed.

5. Recommended Materials:

6. Weight Comparison:

7. Size Limitations:

Max. Diameter: Max. Volume:

8. Characteristics: a) Folding and creasing is restricted to one-half of the bladder p. 10
b) A heavy equatorial flange is not required for the assembly of the outer tank.

9. Environmental Capabilties:

Temperature and Pressure Range: Storability:

10. Method of Operation:

11. Energy/Power Requirements:

12. Cycle Life (Ambient):

13. Probable Failure Modes:

14. Material Properties:

15. Expulsion Efficiency:

16. Volumetric Efficiency:

17. Analysis Data: p. 76, 104

18. References:

SUMMARY OF POSITIVE EXPULSION DEVICES

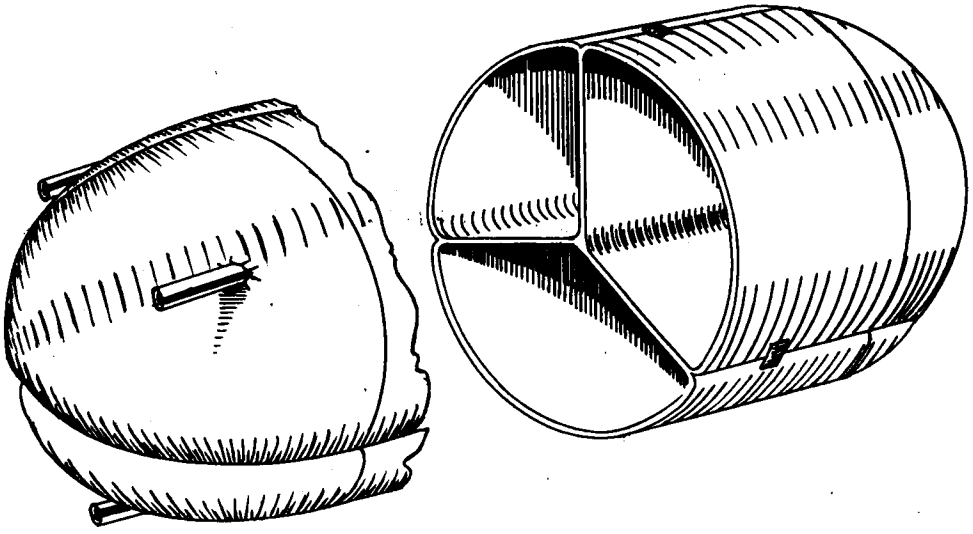

3-Cell Collapsing Bladder

1. Type of Device: 3-Cell Collapsing Bladder

2. Description/Application: The unit constitutes three collapsing bladders housed within a common container. Pressurization gas is introduced at the common apex of the three bladders and the bladders collapse outward against the inside contour of the structural shell.

3. State of Development:

4. Geometry/Shape: A longitudinal tank with ellipsoidal heads or hemispherical heads is desirable

5. Recommended Materials:

6. Weight Comparison:

7. Size Limitations:

Max. Diameter: Max. Volume:

8. Characteristics: a) Creases and folds produced in the bladders are less detrimental than in one large unit. p. 10

b) A weight penalty is involved due to three separate bladders that have common surfaces.

c) Manufacturing and assembly difficulties may be encountered, in a metallic version.

9. Environmental Capabilties:

Temperature and Pressure Range: Storability:

10. Method of Operation:

11. Energy/Power Requirements:

12. Cycle Life (Ambient):

13. Probable Failure Modes:

14. Material Properties:

15. Expulsion Efficiency:

16. Volumetric Efficiency:

17. Analysis Data: p. 76, 104

18. References: L26

SUMMARY OF POSITIVE EXPULSION DEVICES

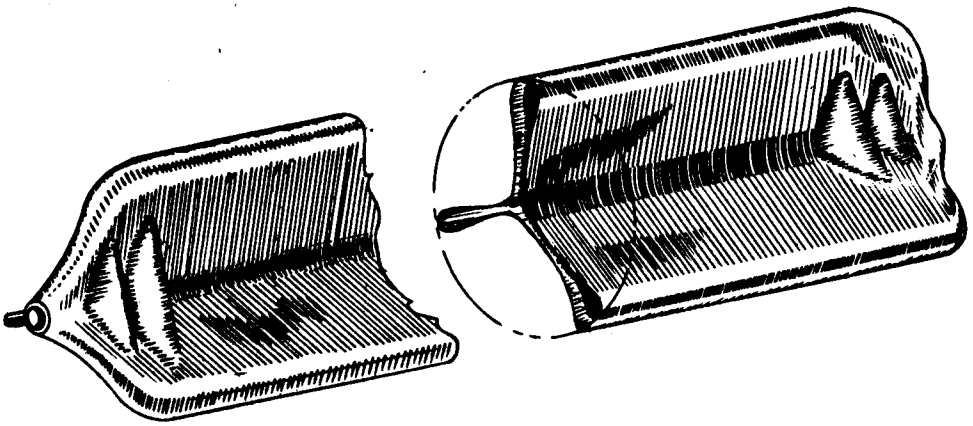

Preformed 3-Lobe Expanding Bladder

1. Type of Device: Preformed 3-Lobe Expanding Bladder

2. Description/Application: The prefolded bladder cross section represents an equal-legged "Y" with each leg enclosing an angle of 120°.

3. State of Development:

4. Geometry/Shape: The ellipsoidal or hemispherical heads should be small in comparison with the total tank length when employing a metallic bladder.

5. Recommended Materials:

6. Weight Comparison:

7. Size Limitations:

Max. Diameter: Max. Volume:

8. Characteristics: a) The shape of the manufactured lobes provides stiffness in handling during assembly. p. 10

b) After snap-through of the bladder during expulsion, the bladder tends to act like a membrane.

9. Environmental Capabilties:

Temperature and Pressure Range: Storability:

10. Method of Operation:

11. Energy/Power Requirements:

12. Cycle Life (Ambient):

13. Probable Failure Modes:

14. Material Properties:

15. Expulsion Efficiency:

16. Volumetric Efficiency:

17. Analysis Data: p. 76, 104

18. References:

SUMMARY OF POSITIVE EXPULSION DEVICES

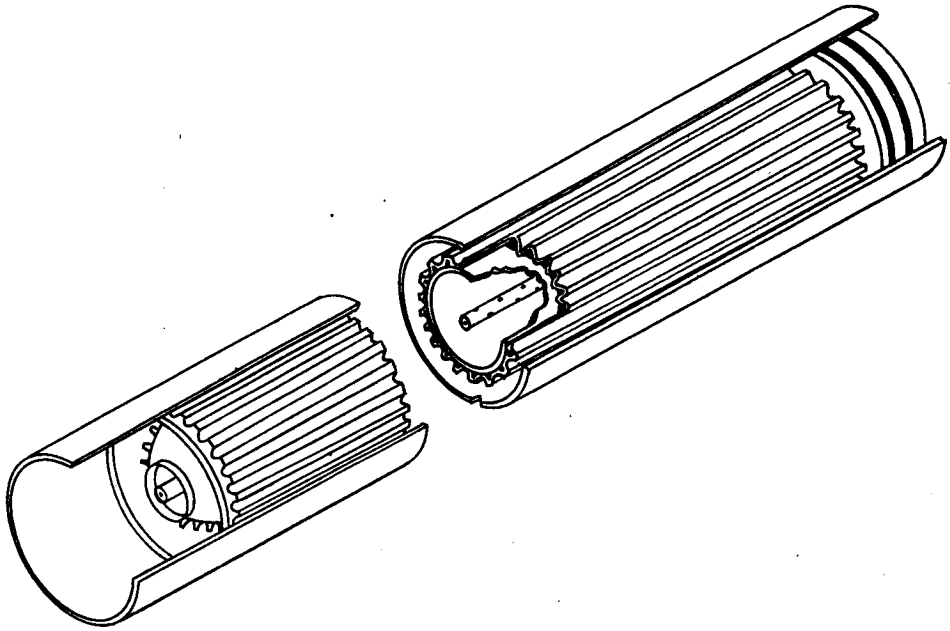

Dual Concentric Bladder

1. Type of Device: Dual Concentric Bladder

2. Description/Application: The device incorporates an expanding and collapsing bladder within our structural container. The inner bladder is a collapsing type unit and the outer bladder is of the expanding type. The latter is a corrugated configuration (equivalent to a prefolded bladder). Pressurizing gas is introduced between the bladders.

3. State of Development: A unit such as this has been built and tested by the U.S. Naval Ordnance Test Station (Reference L14).

4. Geometry/Shape: Long circular cylinders present the best shape.

5. Recommended Materials:

6. Weight Comparison:

7. Size Limitations:

Max. Diameter: Max. Volume:

8. Characteristics: a) Oxidizer and fuel are within one structural enclosure thus utilizing minimum volume or space in vehicle.

b) Fluid mass ratio may pose a problem because of the possible variation in pressures due to the collapsing and expanding bladder configurations.

9. Environmental Capabilties:

Temperature and Pressure Range: Storability:

10. Method of Operation:

11. Energy/Power Requirements:

12. Cycle Life (Ambient):

13. Probable Failure Modes:

14. Material Properties:

15. Expulsion Efficiency:

16. Volumetric Efficiency:

17. Analysis Data: p. 76, 104

18. References: L14, L26.

SUMMARY OF POSITIVE EXPULSION DEVICES

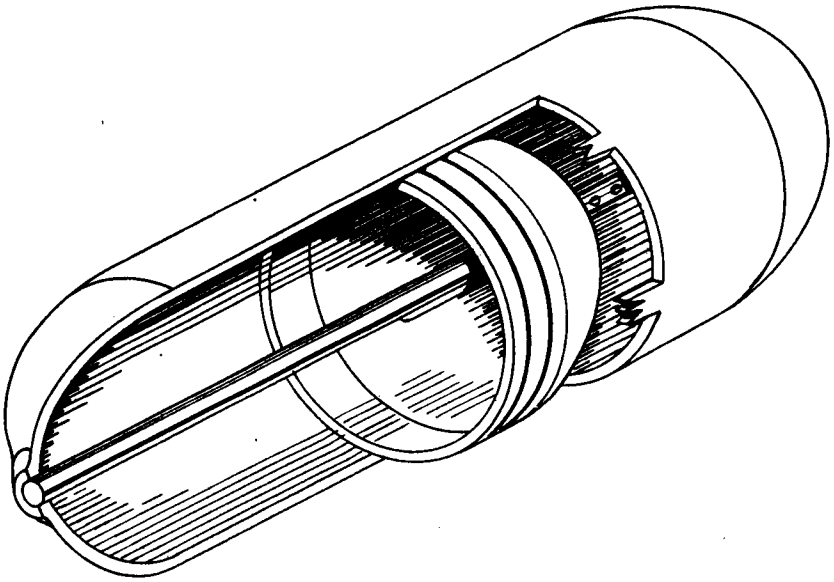

Piston

1. Type of Device: Piston

2. Description/Application: A piston is a sliding member usually a short cylinder moving within a circular cylindrical vessel.

3. State of Development: Units of this type do not require much development and are available commerically. The piston has been demonstrated as an expulsion device in the X1-B airplane.

4. Geometry/Shape: It is restricted to a circular, cylinder. The heads of the cyclinder can be hemspherical, ellipsoid caps, conical or flat.

5. Recommended Materials:

6. Weight Comparison:

7. Size Limitations:

Max. Diameter: Max. Volume:

8. Characteristics: a) The system is reliable and capable of cyclic operation.
b) Fluid flow can be regulated precisely.
c) Sloshing is not present.
d) Close tolerances and smooth machine finishes are required on cylinder and piston.
e) Requires piston sealing and environmental conditions will impose restrictions on seal material.

9. Environmental Capabilties:

Temperature and Pressure Range: Storability:

10. Method of Operation:

11. Energy/Power Requirements:

12. Cycle Life (Ambient):

13. Probable Failure Modes:

14. Material Properties:

15. Expulsion Efficiency:

16. Volumetric Efficiency:

17. Analysis Data:

18. References: L6, L7, L18.

SUMMARY OF POSITIVE EXPULSION DEVICES

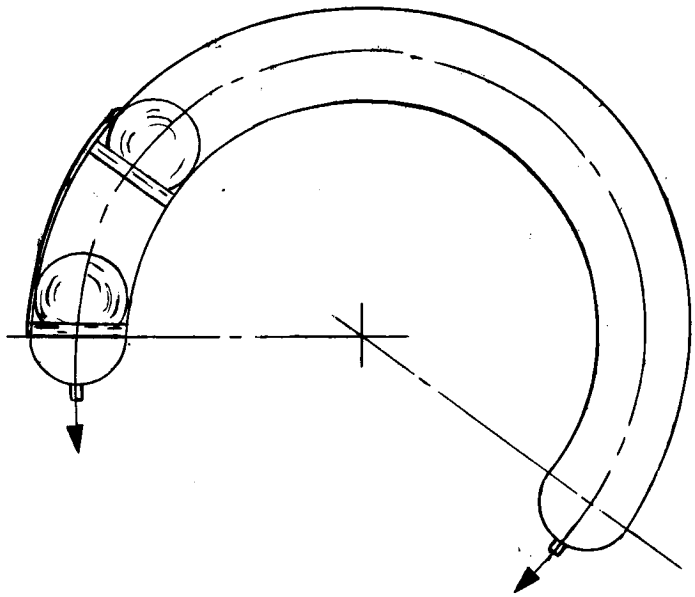

Floating Piston With Bourrelet

1. Type of Device: Floating Piston With Bourrelet (p. 116)

2. Description/Application: The piston resembles a ball or sphere that maintains a press fit in the circular tube. The piston skirt is a bourrelet or ring similar to those employed on artillery shells. The bourrelet provides an interference fit as the piston travels along the tube, expanding the ring.

3. State of Development: A device similar to this has been employed in a flame-thrower (Germany).

4. Geometry/Shape: The fluid container can be any smooth circular shaped cylinder such as a torus or part of a torus, partial ellipse, etc.

5. Recommended Materials:

6. Weight Comparison:

7. Size Limitations:

Max. Diameter: Max. Volume:

8. Characteristics: a) Concentricity or circularity of the tube is not as critical as in the conventiona piston device.

b) Unit is most efficient for continuous operation, and rapid expulsion.

c) The device is a "one-shot" configuration.

d) The pressure differential on the floating piston is relatively high because of the energy required to expand the tube in which it rides and the friction developed due to the sliding action of the bourrelet and ball.

9. Environmental Capabilties:

Temperature and Pressure Range: Storability:

10. Method of Operation:

11. Energy/Power Requirements:

12. Cycle Life (Ambient):

13. Probable Failure Modes:

14. Material Properties:

15. Expulsion Efficiency:

16. Volumetric Efficiency:

17. Analysis Data:

18. References:

SUMMARY OF POSITIVE EXPULSION DEVICES

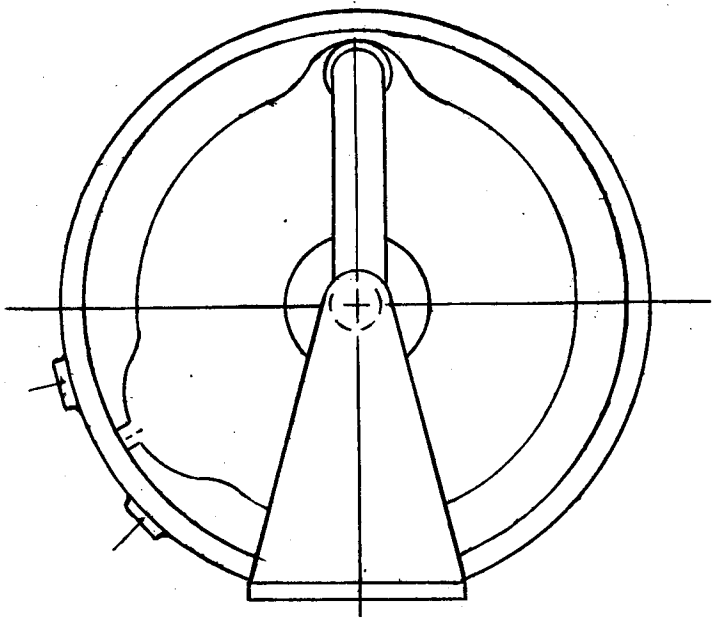

Rotating Squeegee Type Device

1. Type of Device: Rotating Squeegee Type Device Single Tube (p. 117)

2. Description/Application: Fluid transfer is accomplished by means of relatively flexible tube enclosed within a structural body where it is exposed to the squeegee action of a rotor for almost one revolution.

3. State of Development: The squeegee-type principle is employed commercially in pumps. The Randolph Company in Houston, Texas manufacturers such a pump for laboratory and industry.

4. Geometry/Shape: For a rotor sweep, the squeegee tube must be a toroid-shape with a circular cross-section.

5. Recommended Materials:

6. Weight Comparison:

7. Size Limitations:

Max. Diameter: Max. Volume:

8. Characteristics: a) Transfer of slurries or pastes is possible.

b) Volume capacity is limited in comparison with the space required for the over-all device.

c) Complete collapse of the metallic tube, if one is employed (under the rotor), may be difficult to attain.

9. Environmental Capabilties:

Temperature and Pressure Range: Storability:

10. Method of Operation:

11. Energy/Power Requirements:

12. Cycle Life (Ambient):

13. Probable Failure Modes:

14. Material Properties:

15. Expulsion Efficiency:

16. Volumetric Efficiency:

17. Analysis Data:

18. References: L9, L40.

SUMMARY OF POSITIVE EXPULSION DEVICES

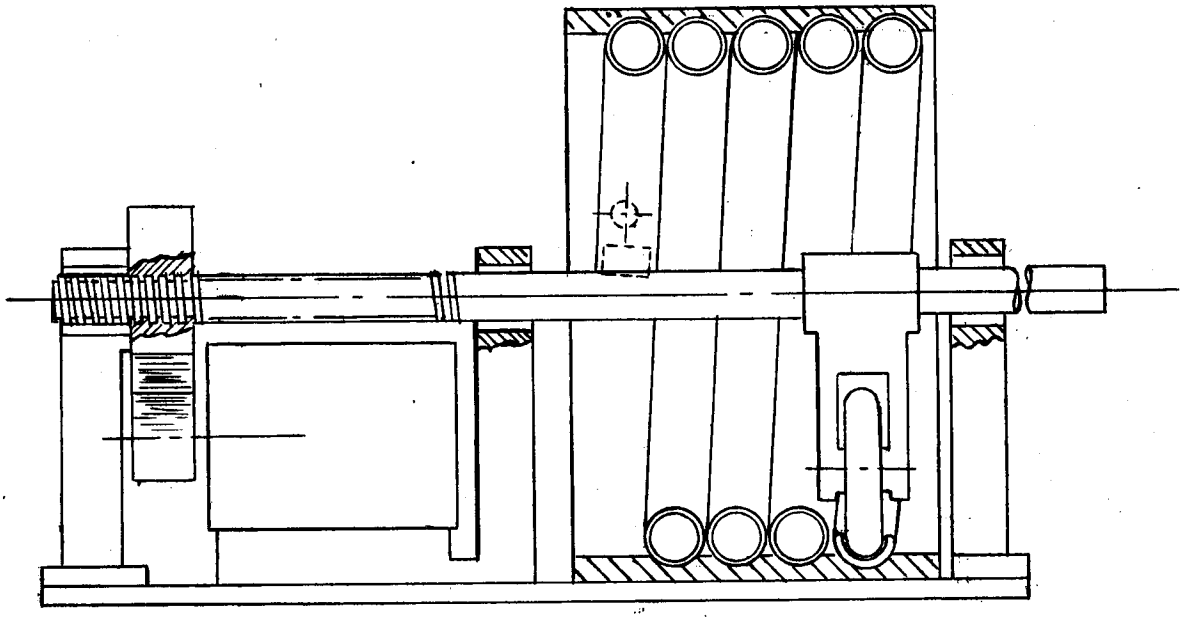

Rotating Squeegee Type Multiple Tube

1. Type of Device: Rotating Squeegee Type Multiple Tube (p. 117)

2. Description/Application: Fluid flow is accomplished by means of collapsing a relatively flexible tube with a rotor or wheel. The tube is wound in a form of a sprial. The rotor motion is made to coincide with the pitch of the tubing so that several revolutions of the rotor can be integrated into the device. As a result, the number of rotor revolutions is dictated by the number of tube coils.

3. State of Development:

4. Geometry/Shape: For minimum weight a circular cross of the squeegee tube is required.

5. Recommended Materials:

6. Weight Comparison:

7. Size Limitations:

Max. Diameter: Max. Volume:

8. Characteristics: a) Volume capacity over a single tube is increased.
b) The device is a "one-shot" unit.

9. Environmental Capabilties:

Temperature and Pressure Range: Storability:

10. Method of Operation:

11. Energy/Power Requirements:

12. Cycle Life (Ambient):

13. Probable Failure Modes:

14. Material Properties:

15. Expulsion Efficiency:

16. Volumetric Efficiency:

17. Analysis Data:

18. References:

SUMMARY OF POSITIVE EXPULSION DEVICES

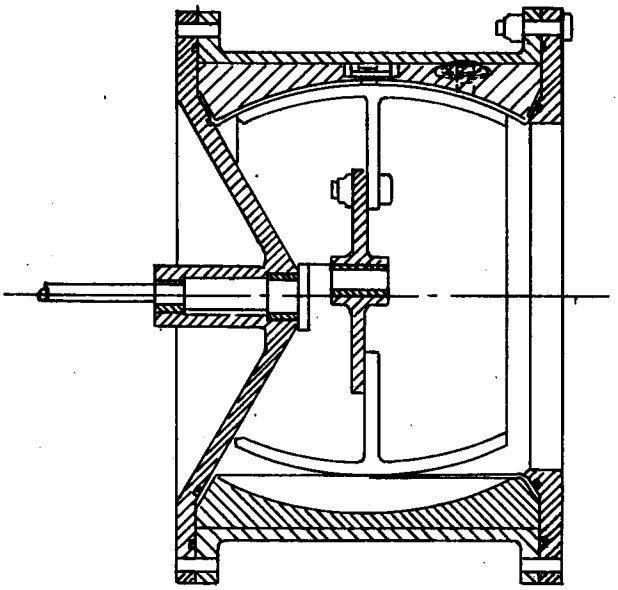

Rotating Squeegee Type Device Diaphragm

1. Type of Device: Rotating Squeegee Type Device Diaphragm (p. 120)

2. Description/Application: Fluid displacement is accomplished by a rotor mounted on an eccentric shaft which rotates within an elastic liner. This creates a progressive squeegee action on the fluid trapped between the liner and the inside of the rigid body block.

3. State of Development: A pump employing this principle is marketed by the Vanton Pump & Equipment Corporation, Hillside, New Jersey.

4. Geometry/Shape:

5. Recommended Materials:

6. Weight Comparison:

7. Size Limitations:

Max. Diameter: Max. Volume:

8. Characteristics: a) The fluid is isolated from the actuating eccentric mechanism and eliminates the need for seals or stuffing boxes.

b) The action of displacement prevents churning and foaming of the fluid.

c) Volume capacity is low.

9. Environmental Capabilties:

Temperature and Pressure Range: Storability:

10. Method of Operation:

11. Energy/Power Requirements:

12. Cycle Life (Ambient):

13. Probable Failure Modes:

14. Material Properties:

15. Expulsion Efficiency:

16. Volumetric Efficiency:

17. Analysis Data:

18. References: a) Roller Diaphragm Pumps, Design News, November 10, 1961. Page 35.

b) L9.

SUMMARY OF POSITIVE EXPULSION DEVICES

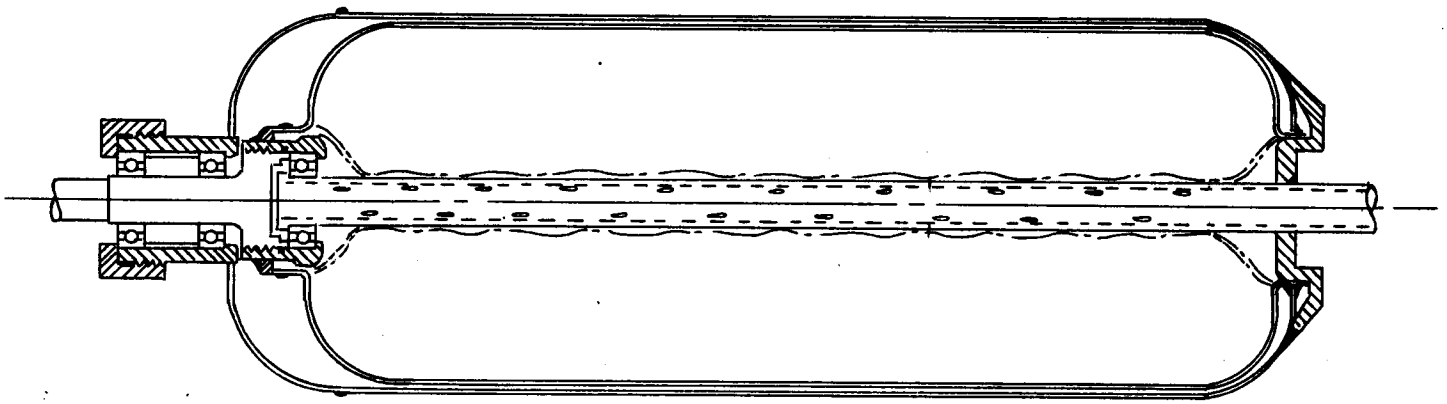

Twisting Bladder - Uncontrolled

1. Type of Device: Twisting Bladder - Uncontrolled (p. 121)

2. Description/Application: In this type of configuration, the fluid is contained within an inner tube whose collapse is initiated and continued by imparting a rotary or twisting motion at its ends. The twisting induces a wrinkling of the tube with a consequent decrease in diameter thus expelling the fluid.

3. State of Development:

4. Geometry/Shape: For torsional buckling and wrinkling, a circular cylinder is desired.

5. Recommended Materials:

6. Weight Comparison:

7. Size Limitations:

Max. Diameter: Max. Volume:

8. Characteristics: a) A flexible material for the fluid container is a prerequisite.
b) Axial and restraint induces considerable tension loads in the fluid shell.

9. Environmental Capabilties:

Temperature and Pressure Range: Storability:

10. Method of Operation:

11. Energy/Power Requirements:

12. Cycle Life (Ambient):

13. Probable Failure Modes:

14. Material Properties:

15. Expulsion Efficiency:

16. Volumetric Efficiency:

17. Analysis Data:

18. References:

SUMMARY OF POSITIVE EXPULSION DEVICES

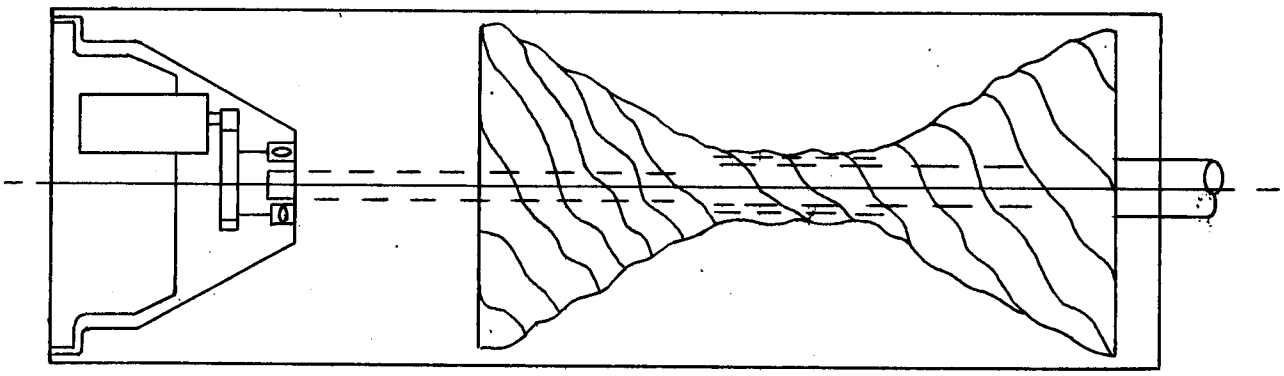

Twisting Bladder - Controlled

1. Type of Device: Twisting Bladder - Controlled (p. 121)

2. Description/Application: The fluid that is contained within the bladder is expelled by means of the collapse of the tube induced by twisting at the ends. The torsion buckles and wrinkles the tube similar to that experienced in the wringing of cloths to expel the water. An axial lead screw is incorporated in the device so that the shortening effect of the bladder is not hampered by any axial restraint. The pitch of the lead screw is made to coincide with the shortening of the tube due to torsion.

3. State of Development:

4. Geometry/Shape: A circular cylinder is most efficient.

5. Recommended Materials:

6. Weight Comparison:

7. Size Limitations:

Max. Diameter: Max. Volume:

8. Characteristics: a) Axial restraint in the twisted bladder is minimized.
b) Volumetric efficiency is not very high.

9. Environmental Capabilties:

Temperature and Pressure Range: Storability:

10. Method of Operation:

11. Energy/Power Requirements:

12. Cycle Life (Ambient):

13. Probable Failure Modes:

14. Material Properties:

15. Expulsion Efficiency:

16. Volumetric Efficiency:

17. Analysis Data:

18. References:

SUMMARY OF POSITIVE EXPULSION DEVICES

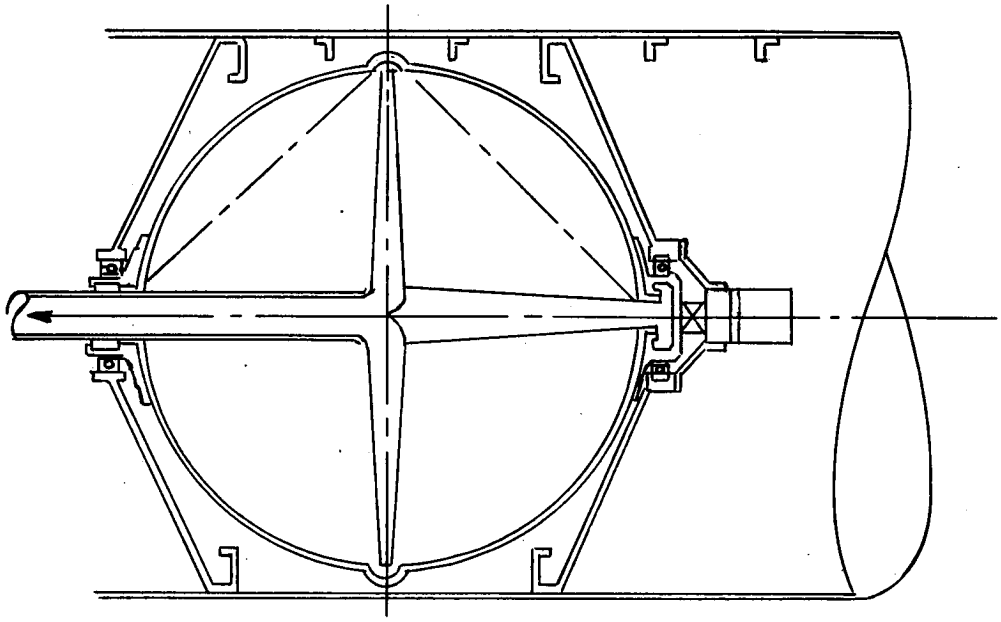

Rotating Tank

1. Type of Device: Rotating Tank (p. 121)

2. Description/Application: In this device, the principles of centrifugal force are utilized to move the fluid. The device is basically an inverted centrifugal pump. Thus, the impeller is stationary and this pump body, in this case the propellant tank, is revolving.

3. State of Development:

4. Geometry/Shape: The application of rotation implies the use of circular bodies.

5. Recommended Materials:

6. Weight Comparison:

7. Size Limitations:

Max. Diameter: Max. Volume:

8. Characteristics: a) Multiple restarts are possible.
b) Gas–liquid separation is an inherent characteristic.
c) Starting or stopping a large rotating mass could produce undesirable end effects.

9. Environmental Capabilties:

Temperature and Pressure Range: Storability:

10. Method of Operation:

11. Energy/Power Requirements:

12. Cycle Life (Ambient):

13. Probable Failure Modes:

14. Material Properties:

15. Expulsion Efficiency:

16. Volumetric Efficiency:

17. Analysis Data:

18. References: L8, L13; L16, L25, L41, L42, L45.

SUMMARY OF POSITIVE EXPULSION DEVICES

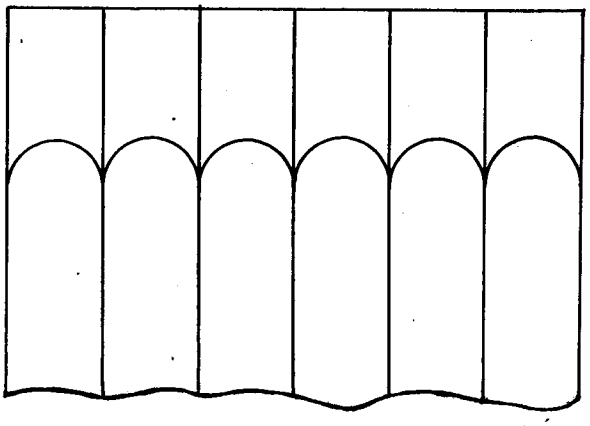

Capillary Tubes

1. Type of Device: Capillary Tubes (p. 125)

2. Description/Application: Capillary tubes consist of parallel bundles of wetted material. The diameter of the capillary tubes is determined by the height of the liquid column to be contained, by admission between capillary and liquid and by the surface tension of the liquid.

3. State of Development: Laboratory experiments are being performed at JPL.

4. Geometry/Shape:

5. Recommended Materials:

6. Weight Comparison:

7. Size Limitations:

Max. Diameter: Max. Volume:

8. Characteristics: a) It is effective in the separation of the entrained gas from this liquid.
b) No outside energy forces are required for operation.
c) Flow resistance of capillary tubes is high.
d) Pumping capacity is small.

9. Environmental Capabilties:

Temperature and Pressure Range: Storability:

10. Method of Operation:

11. Energy/Power Requirements:

12. Cycle Life (Ambient):

13. Probable Failure Modes:

14. Material Properties:

15. Expulsion Efficiency:

16. Volumetric Efficiency:

17. Analysis Data:

18. References: L23, L25, L28, L30, L34, L37, L38, L39, L43.

SUMMARY OF POSITIVE EXPULSION DEVICES

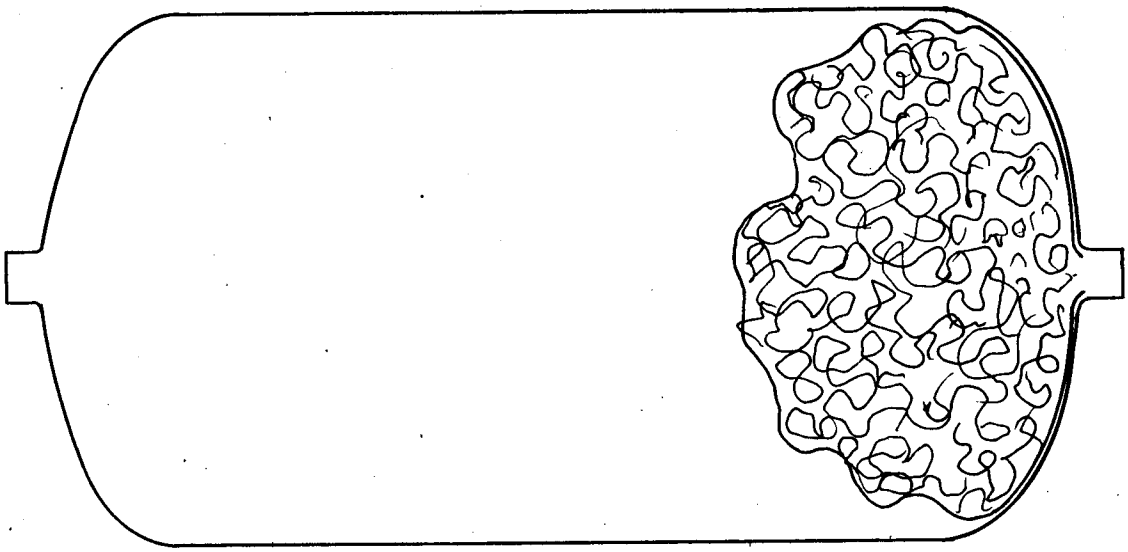

Foam Displacement

1. Type of Device: Foam Displacement (p. 169)

2. Description/Application: A combination of chemicals capable of producing foams which involves the reaction of a plastic resin and blowing agents and/or catalysts displace the fluid in the container.

3. State of Development: Chemicals producing foams from such plastics as vinyls, phenolics, epoxys, polyesters and polyethers are available.

4. Geometry/Shape: Any practical shape of container deserves consideration.

5. Recommended Materials:

6. Weight Comparison:

7. Size Limitations:

Max. Diameter: Max. Volume:

8. Characteristics: a) There are no moving parts within the expulsion device.
b) Compatibility of this foam with the displaced fluid may not be possible.
c) Control of foaming is not precise.
d) In foaming systems there is a built-in heat of reaction and in others heat has to be added to cause foaming.

9. Environmental Capabilties:

Temperature and Pressure Range: Storability:

10. Method of Operation:

11. Energy/Power Requirements:

12. Cycle Life (Ambient):

13. Probable Failure Modes:

14. Material Properties:

15. Expulsion Efficiency:

16. Volumetric Efficiency:

17. Analysis Data:

18. References:

SUMMARY OF POSITIVE EXPULSION DEVICES

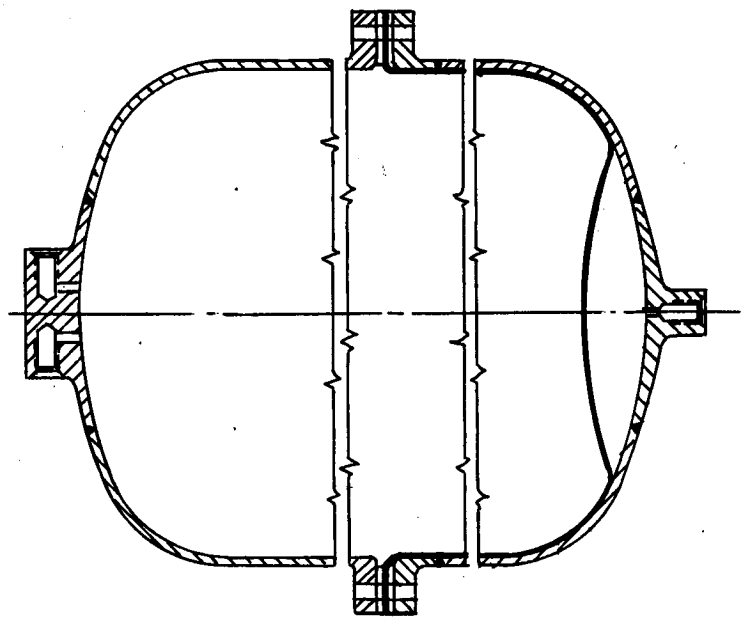

Roll and Peel Diaphragm

1. Type of Device: Roll and Peel Diaphragm (p. 153)

2. Description/Application: The diaphragm is adhesively bonded to the structural wall of the container. The operation of the rolling-type diaphragm is dependent on the ability of the bond to keep the pressurizing gas from coming into contact with the external surface of the unrolled portion of the diaphragm. During the peeling or rolling process, the free surface of the diaphragm increases progressively to a deep convolution.

3. State of Development:

4. Geometry/Shape: Relatively short or small aspect ratio circular cylinders with surface or revolution heads are desirable.

5. Recommended Materials:

6. Weight Comparison:

7. Size Limitations:

Max. Diameter: Max. Volume:

8. Characteristics: a) Random buckling of metallic diaphragm is minimized.
b) Maximum utilization of volume is possible.
c) Device is a "one-shot" configuration.

9. Environmental Capabilties:

Temperature and Pressure Range: Storability:

10. Method of Operation:

11. Energy/Power Requirements:

12. Cycle Life (Ambient):

13. Probable Failure Modes:

14. Material Properties:

15. Expulsion Efficiency:

16. Volumetric Efficiency:

17. Analysis Data: p. 153

18. References:

SUMMARY OF POSITIVE EXPULSION DEVICES

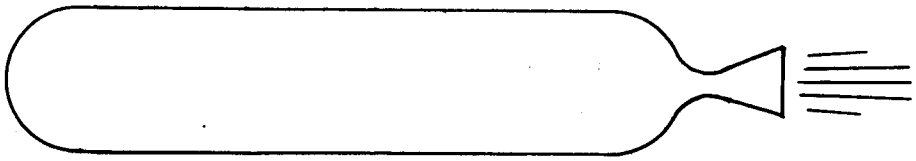

Ullage Rockets

1. Type of Device: Ullage Rockets p. 128

2. Description/Application: The firing of an ullage rocket induces thrust and an associated acceleration. The resulting acceleration or inertia field provides the necessary forces for settling of the fluid at a location within the tank.

3. State of Development:

4. Geometry/Shape:

5. Recommended Materials:

6. Weight Comparison:

7. Size Limitations:

Max. Diameter: Max. Volume:

8. Characteristics: a) For one restart, small solid rockets are satisfactory.

b) Expulsion devices would be required if ullage rockets operate with liquid propellants

c) Gas pressure can be utilized through a nozzle to provide thrust.

9. Environmental Capabilties:

Temperature and Pressure Range: Storability:

10. Method of Operation:

11. Energy/Power Requirements:

12. Cycle Life (Ambient):

13. Probable Failure Modes:

14. Material Properties:

15. Expulsion Efficiency:

16. Volumetric Efficiency:

17. Analysis Data: p. 12

18. References: L37.

SUMMARY OF POSITIVE EXPULSION DEVICES

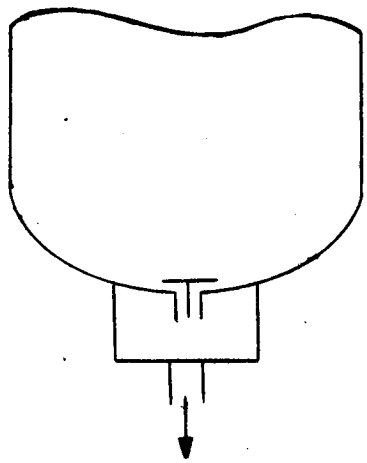

Trap or Surge Tank

1. Type of Device: Trap or Surge Tank p. 132

2. Description/Application: The trap tank is a small tank located at the lower region of a large tank and directly connected to the engine. At engine shut-down, the propellant is automatically trapped in the small tank by appropriate valving. Initial acceleration immediately settles the remaining bulk of main tank propellant thereby sustaining engine operation. The total propellant mass flow continues from the main tank through the trap tank and to the engine for continuous operation.

3. State of Development:

4. Geometry/Shape: The operating pressure will dictate the type of shape to employ in order to minimize weight.

5. Recommended Materials:

6. Weight Comparison:

7. Size Limitations:

Max. Diameter: Max. Volume:

8. Characteristics: a) Tank is refillable during each operation cycle of acceleration.
b) An elaborate plumbing and venting system is required.

9. Environmental Capabilties:

Temperature and Pressure Range: Storability:

10. Method of Operation:

11. Energy/Power Requirements:

12. Cycle Life (Ambient):

13. Probable Failure Modes:

14. Material Properties:

15. Expulsion Efficiency:

16. Volumetric Efficiency:

17. Analysis Data:

18. References:

SUMMARY OF POSITIVE EXPULSION DEVICES

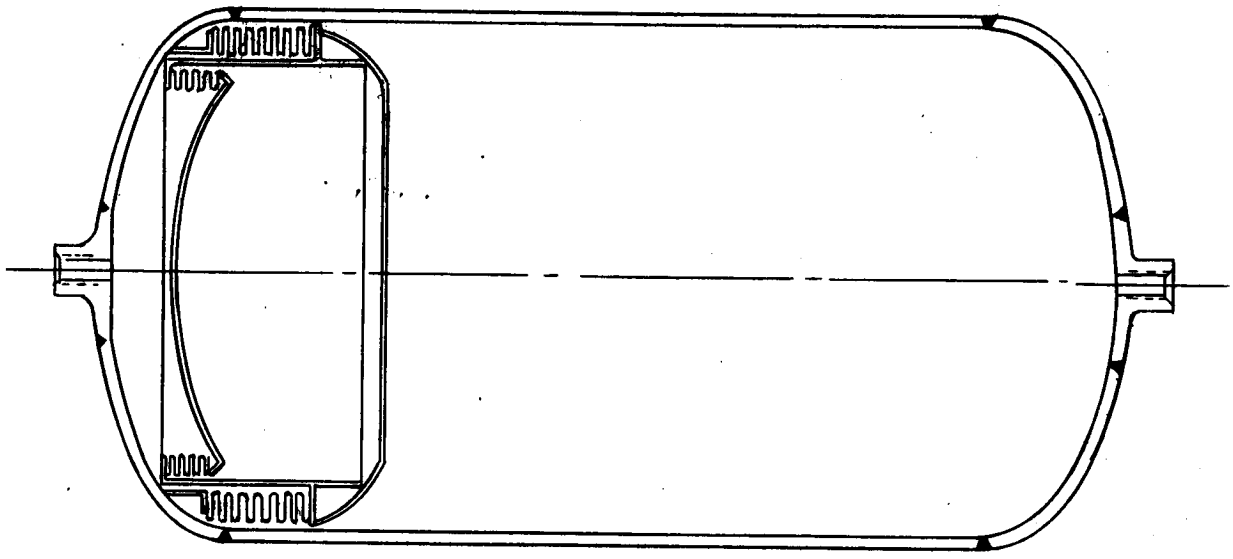

Mechnical Bellows

1. Type of Device: Mechanical Bellows p. 139

2. Description/Application: The bellows are corrugated cylinders which have the ability to perform axially. The flexibility of the bellows is proportional to the number of convolutions and because the radial sides of these corrugations are extremely flexible, bellows possess a high degree of axial freedom of motion.

3. State of Development: Bellows are available commerically and are employed as seals, in pressure instruments, expansion devices, etc.

4. Geometry/Shape: The bellows are rolled formed or welded and encompass shapes such as the "S" shape, double ripple, flat-sided, triangular, toroidal, etc.

5. Recommended Materials:

6. Weight Comparison:

7. Size Limitations:

Max. Diameter: Max. Volume:

8. Characteristics: a) Partial expulsion and cyclic operation is readily available p. 147

b) Contours of corrugations can be varied to achieve desired characteristics.

c) Manufacturing techniques could limit the size, number and type of corrugation.

d) Weight and volume loss due to bellows are detrimental features.

9. Environmental Capabilties:

Temperature and Pressure Range: Storability:

10. Method of Operation:

11. Energy/Power Requirements:

12. Cycle Life (Ambient):

13. Probable Failure Modes:

14. Material Properties:

15. Expulsion Efficiency:

16. Volumetric Efficiency:

17. Analysis Data: p. 140

18. References: L26, L51.

SUMMARY OF POSITIVE EXPULSION DEVICES

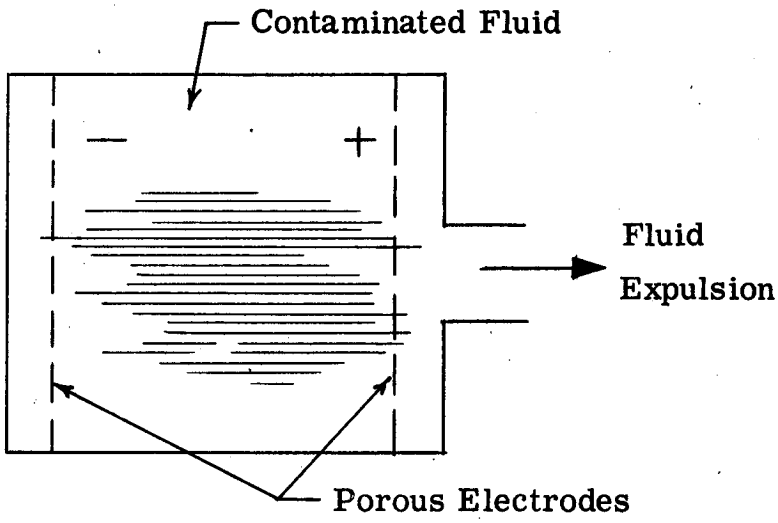

Electrostatic Device

1. Type of Device: Electrostatic Device

2. Description/Application: Fuel is contaminated with negatively charged particles. The electric field moves the particles toward the positive electrode. Neutral fuel is dragged along and ejected with the charged particules.

3. State of Development:

4. Geometry/Shape:

5. Recommended Materials:

6. Weight Comparison:

7. Size Limitations:

Max. Diameter: Max. Volume:

8. Characteristics: a) The chemical properties of the fluid may change due to the high field.

b) Impurities and gas bubbles could change the mobility value of the fluid being pumped.

c) Static charge accumulation may develop which could alter system performanc

d) Cyclic operation is available.

e) Power requirement may be high with respect to power available on board vehicle.

9. Environmental Capabilties:

Temperature and Pressure Range: Storability:

10. Method of Operation:

11. Energy/Power Requirements:

12. Cycle Life (Ambient):

13. Probable Failure Modes:

14. Material Properties:

15. Expulsion Efficiency:

16. Volumetric Efficiency:

17. Analysis Data:

18. References: 4, 5, 6, 7

SUMMARY OF POSITIVE EXPULSION DEVICES

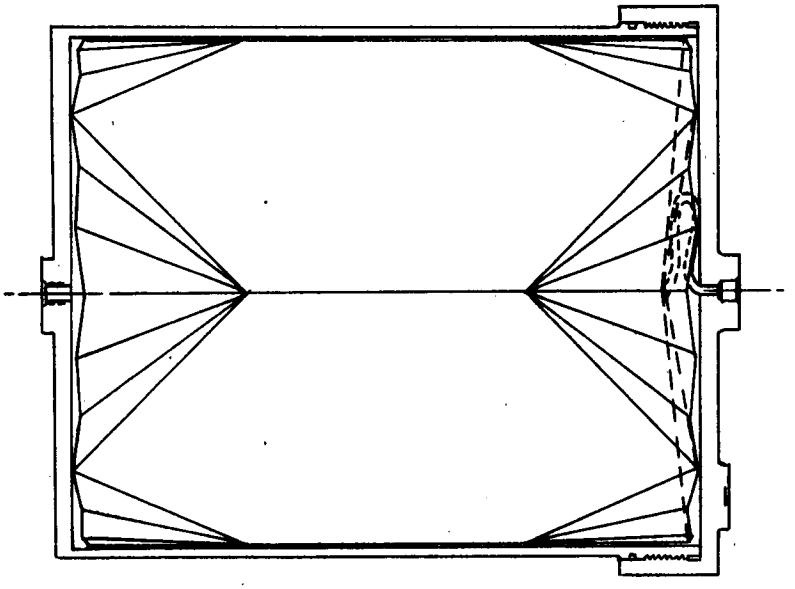

Pleated Folding Type Bladder

1. Type of Device: Pleated Folding Type Bladder p. 149

2. Description/Application: This so called accordian-pleat concept will promote controlled deformation and expansion. The bladder is installed in the pre-folded condition with the propellant between the bladder and the structural container.

3. State of Development:

4. Geometry/Shape: The head shape of the structural container is restricted to a very shallow depth. A flat or conical head is a geometric requirement.

5. Recommended Materials:

6. Weight Comparison:

7. Size Limitations:

Max. Diameter: Max. Volume:

8. Characteristics: a) Single and double folds usually associated with bladders are minimized.
b) Random expulsion cycles are possible.
c) Complete folding of the bladder may introduce ullage volumes larger than other systems.

9. Environmental Capabilties:

Temperature and Pressure Range: Storability:

10. Method of Operation:

11. Energy/Power Requirements:

12. Cycle Life (Ambient):

13. Probable Failure Modes:

14. Material Properties:

15. Expulsion Efficiency:

16. Volumetric Efficiency:

17. Analysis Data:

18. References:

SUMMARY OF POSITIVE EXPULSION DEVICES

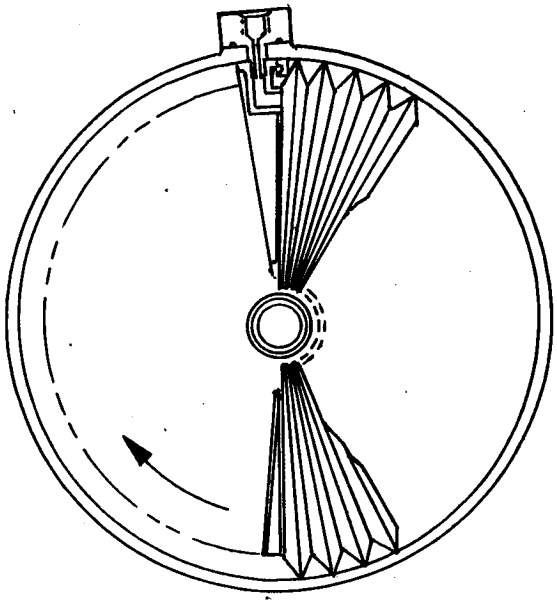

Roll Sweep Pleated Bladder

1. Type of Device: Roll Sweep Pleated Bladder

2. Description/Application: The pleated bladder, whose ends resemble the conventional womens folding fans, rotates about the centerline of the structural container and sweeps approximately 360°. During this rotation, the fluid outside the bladder is expelled by the flat plate and makes up the face of the roll sweep pleated bladder.

3. State of Development:

4. Geometry/Shape: The geometry of the device as well as the operational characteristics of the pleats dictates the use of flat heads.

5. Recommended Materials:

6. Weight Comparison:

7. Size Limitations:

Max. Diameter: Max. Volume:

8. Characteristics: a) The flat heads of the flat sweep plate induce weight penalties.
b) The welding and folding of the pleats introduces fabrication problems.

9. Environmental Capabilties:

Temperature and Pressure Range: Storability:

10. Method of Operation:

11. Energy/Power Requirements:

12. Cycle Life (Ambient):

13. Probable Failure Modes:

14. Material Properties:

15. Expulsion Efficiency:

16. Volumetric Efficiency:

17. Analysis Data:

18. References:

SUMMARY OF POSITIVE EXPULSION DEVICES

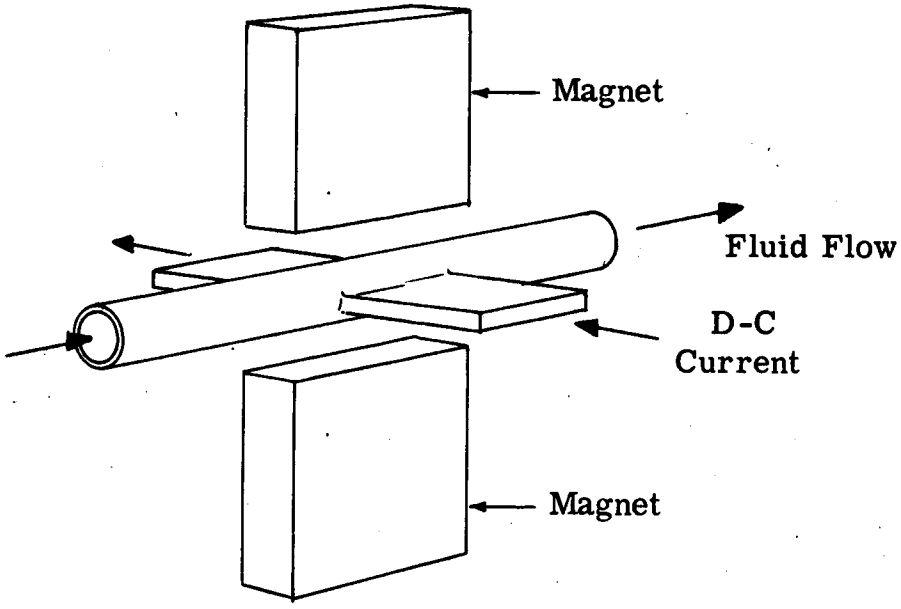

Electromagnetic Pump

1. Type of Device: Electromagnetic Pump p. 161

2. Description/Application: The principle of operation is the so-called motor operation. If a current flows in a conductor which is placed in a magnetic field perpendicular to the current, the conductor will be acted on by a force, normal to both the current and the magnetic field. The conductor in this case is the fluid being pumped and thus the pump works best with high conductivity fluids.

3. State of Development: Such pumps have been developed and built to pump liquid metals, and also relating to nuclear reactors.

4. Geometry/Shape:

5. Recommended Materials:

6. Weight Comparison:

7. Size Limitations:

Max. Diameter: Max. Volume:

8. Characteristics: a) Pump weight is high.

b) Direct current devices are simple and eliminate most of the insulation problems.

c) AC pumps require high voltage and induce insulation problems.

9. Environmental Capabilties:

Temperature and Pressure Range: Storability:

10. Method of Operation:

11. Energy/Power Requirements:

12. Cycle Life (Ambient):

13. Probable Failure Modes:

14. Material Properties:

15. Expulsion Efficiency:

16. Volumetric Efficiency:

17. Analysis Data:

18. References: 18, 19, 20, 21, 22, 23, L19, L23.

SUMMARY OF POSITIVE EXPULSION DEVICES

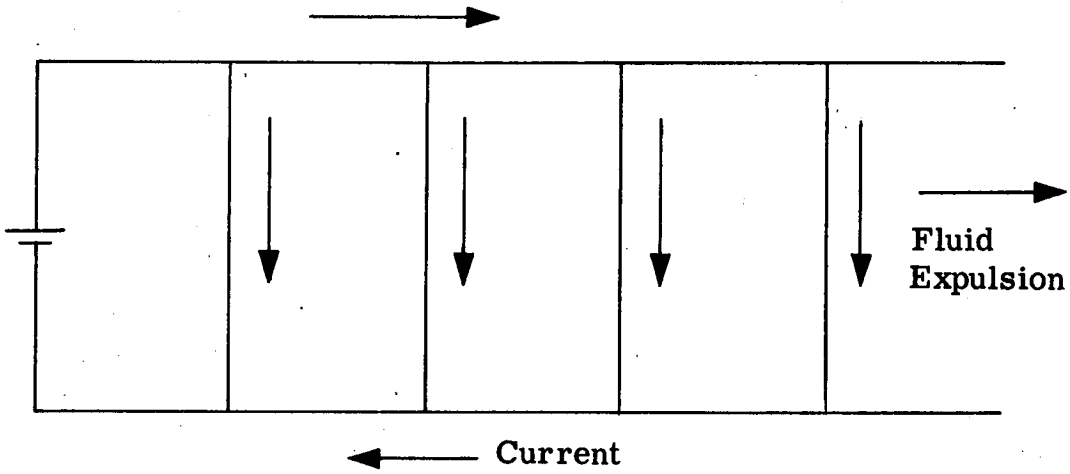

Multiple Exploding Wires

1. Type of Device: Magnetofluid Mechanical Pump Multiple Exploding Wires (p. 162)

2. Description/Application: The wires, I, II, III, & IV are designed such that Wire I explodes first ionizing the fluid in its vicinity, circuital current flow. This magnetic field, coupled with the current density, forces the charged particles out of the tank. Uncharged fuel is also dragged along.

3. State of Development:

4. Geometry/Shape:

5. Recommended Materials:

6. Weight Comparison:

7. Size Limitations:

Max. Diameter: Max. Volume:

8. Characteristics:

9. Environmental Capabilties:

Temperature and Pressure Range: Storability:

10. Method of Operation:

11. Energy/Power Requirements:

12. Cycle Life (Ambient):

13. Probable Failure Modes:

14. Material Properties:

15. Expulsion Efficiency:

16. Volumetric Efficiency:

17. Analysis Data:

18. References: 25, L19.

SUMMARY OF POSITIVE EXPULSION DEVICES

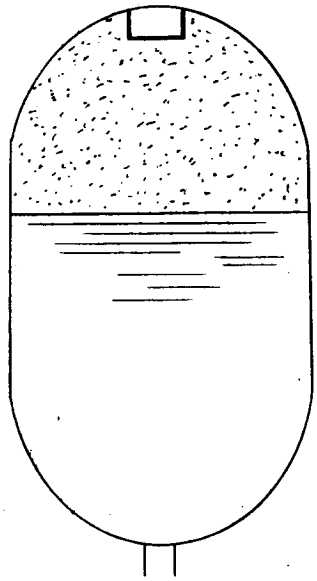

Supercritical Systems

1. Type of Device: Supercritical Systems

2. Description/Application:

3. State of Development: Beech is, at present, performing work on this system.

4. Geometry/Shape:

5. Recommended Materials:

6. Weight Comparison:

7. Size Limitations:

Max. Diameter: Max. Volume:

8. Characteristics: a) A single phase fluid is always present.

b) High required pressures will impose heavier structures.

9. Environmental Capabilties:

Temperature and Pressure Range: Storability:

10. Method of Operation:

11. Energy/Power Requirements:

12. Cycle Life (Ambient):

13. Probable Failure Modes:

14. Material Properties:

15. Expulsion Efficiency:

16. Volumetric Efficiency:

17. Analysis Data:

18. References:

SUMMARY OF POSITIVE EXPULSION DEVICES

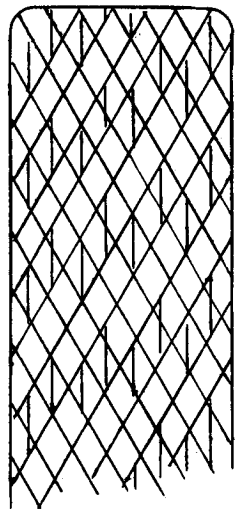

Wick

1. Type of Device: Wick

2. Description/Application: A wick can be considered as composed of randomly oriented capillary tubes of varying lengths and small diameters. The liquid rise in wick materials is similar to that in a capillary tube.

3. State of Development: Laboratory tests are being performed at JPL.

4. Geometry/Shape:

5. Recommended Materials:

6. Weight Comparison:

7. Size Limitations:

Max. Diameter: Max. Volume:

8. Characteristics: a) No vapors or gas bubbles are present.
b) No outside energy sources are required for this natural phenomena.
c) Flow resistance is high.
d) Transport quantity of fluid is low.

9. Environmental Capabilties:

Temperature and Pressure Range: Storability:

10. Method of Operation:

11. Energy/Power Requirements:

12. Cycle Life (Ambient):

13. Probable Failure Modes:

14. Material Properties:

15. Expulsion Efficiency:

16. Volumetric Efficiency:

17. Analysis Data:

18. References: L15, L28, L39.

SUMMARY OF POSITIVE EXPULSION DEVICES

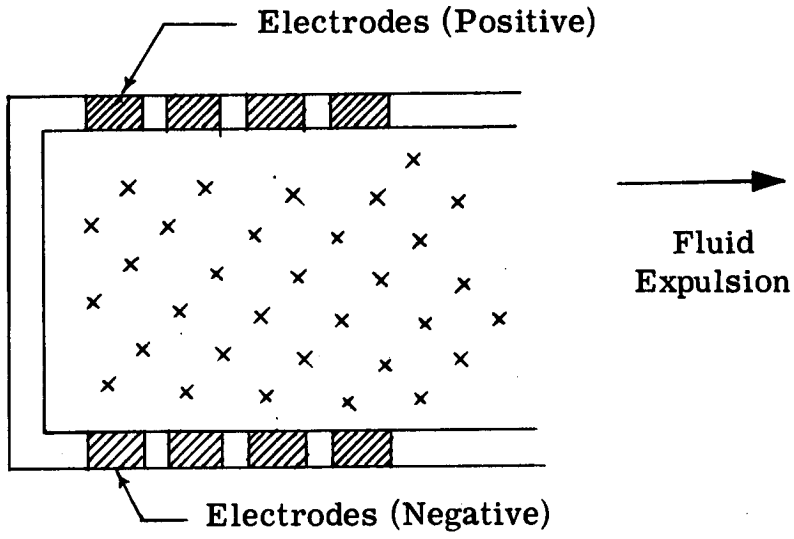

Channel Accelerator

1. Type of Device: Magnetrofluid Mechanical Pump Channel Accelerator p. 163

2. Description/Application: The device utilizes segmented electrodes with an applied magnetic field into and perpendicular to the plane of the sketch shown above. The fluid is partly conductive.

3. State of Development: This is equivalent to a pinch effect engine. It has been discussed in the literature and tested in laboratories.

4. Geometry/Shape: _____

5. Recommended Materials: _____

6. Weight Comparison: _____

7. Size Limitations: _____

Max. Diameter: _____ Max. Volume: _____

8. Characteristics: _____

9. Environmental Capabilties: _____

Temperature and Pressure Range: _____ Storability: _____

10. Method of Operation: _____

11. Energy/Power Requirements: _____

12. Cycle Life (Ambient): _____

13. Probable Failure Modes: _____

14. Material Properties: _____

15. Expulsion Efficiency: _____

16. Volumetric Efficiency: _____

17. Analysis Data: _____

18. References: 27

APPENDIX III

DISCUSSION OF STRUCTURES COMPUTER PROGRAM

APPENDIX III

DISCUSSION OF STRUCTURES COMPUTER PROGRAM

Most of the input parameters are explained by the comments in the program listing. All quantities possessing dimensions, except axial thrust, are input in the dimensional form; i.e., RIN, ROUT, ZRIZE, and THK are in inches; E is lb/in.^{2}.

The axial thrust input as POINIT is a nondimensional form of the total axial thrust force obtained by:

POINIT = 2 π E;THK : TOTAL FORCE/ 12(1-PR^2)

The possible input of T(I,J) allows for continuation of a problem without return to the initial valves. T(I,1) represents the variable β and T(I,2) represents the variable ψ from Equations III and IV of Reference 32.

IBND input is for end boundary conditions:

IBND = 1	Fixed rotation and radial deflection
IBND = 2	Free rotation, fixed radial deflection
IBND = 3	Fixed rotation, free radial deflection
IBND = 4	Free rotation and radial deflection

Geometric information is supplied to the main program by a subroutine, GEOM, which may be changed to suit the bellows geometry under study. There are certain requirements and restrictions involved in the make up of the subroutine, GEOM. The geometry under study must have no points of discontinuity in any bellows leaf except at the juncture with a neighboring leaf. The subroutine is to compute the location of a given number of points in terms of R (the radial distance from the bellows axis) and Z (the vertical distance from some fixed horizontal plane).

The basic differential equations used in the main program are Equations III and IV of Reissner (Reference 32) which are:

$$\underline{\text{III.}} \quad \beta'' + \frac{(r_oD/a_o)'}{(r_oD/a_o)}\beta' - \left[\left(\frac{r_o'}{r_o}\right)^2 - \nu\frac{(r_o'D/a_o)'}{(r_oD/a_o)}\right]\beta$$

$$- \left[\frac{3}{2}\frac{r_o'Z_o'}{r_o^2} - \frac{\nu}{2}\frac{(Z_o'D/a_o)'}{(rD/a_o)}\right]\beta^2 = -\frac{a_o^2}{r_oD}\left\{\psi\sin\phi_o\right.$$

$$\left. - (r_oV)\cos\phi_o - \beta\left[\psi\cos\phi_o + (r_oV)\sin\phi_o\right]\right\}$$

$$\text{IV.} \quad \psi'' + \frac{(r_o/C\alpha_o)'}{(r_o/C\alpha_o)}\psi' - \left[\left(\frac{r_o'}{r_o}\right)^2 + \nu\frac{(r_o'/C\alpha_o)'}{(r_o/C\alpha_o)}\right]\psi$$

$$\left[2\frac{Z_o' r_o'}{r_o^2} + \nu\frac{(Z_o'/C\alpha_o)'}{(r_o/C\alpha_o)}\right]\beta\psi - \nu\frac{Z_o'}{r_o}\beta'\psi =$$

$$\frac{\alpha_o^2 C}{r_o}\left(\beta\sin\phi_o - \frac{1}{2}\beta^2\cos\phi_o\right)$$

$$+\left[\frac{r_o' Z_o'}{r_o^2} + \nu\frac{(Z_o'/C\alpha_o)'}{(r_o/C\alpha_o)}\right](r_oV) + \nu\frac{Z_o'}{r_o}(r_oV)'$$

$$+\left[\frac{(Z_o')^2 - (r_o')^2}{r_o^2} - \nu\frac{(r_o'/C\alpha_o)'}{(r_o/C\alpha_o)}\right]\beta(r_oV) - \nu\frac{r_o'}{r_o}\beta(r_oV)$$

$$-\nu\frac{r_o'}{r_o}\beta(r_oV)' - \frac{\alpha_o}{r_o}(r_o^2 PH)' - \left[\nu\left(\frac{r_o'\alpha_o}{r_o^2} + \beta\frac{Z_o'\alpha_o}{r_o^2}\right) - \frac{\alpha_o C'}{r_o C}\right](r_o^2 PH)$$

The prime denotes differentiation with respect to the parameter ξ, which is directed along the shell midplane. The location of coordinates by the subroutine GEOM, therefore, must be at equal intervals measured in the positive ξ direction. (The positive ξ direction may be assumed as starting at one end of the bellows and progressing along the bellows to the opposite end.)

Computed values of R and Z at each point must be in nondimensional form obtained by division by RIN. For example the (I) point of the first leaf with a straight conical shape may be described by the following statements:

```
R (I)  = RR + (1 .-RR)* X
Z (I)  = ZZ * X
RP (I) = 1.-RR
ZP (I) = ZZ
RPP(I)= o
ZPP(I) = o
```

where RR = ROUT/RIN, ZZ = ZRISE/RIN and X represents the location of the I point as a fraction of the total ξ length of the leaf. (X = 0 at I = 1 and X = 1.0 at I = M + 1.)

At present, the interval spacing must be equal throughout the bellows, which means that the individual leaves must have the same developed length. The subroutine must compute the first and second derivatives of R and Z in terms of ξ . The first and second derivatives of R and Z at the leaf junctures must also be computed by the subroutine. The discontinuity first derivatives have the following notation: RP 21, RP 43, RP 54, RP 65, ZP 21, ZP 32, ZP 43, ZP 54, ZP 65. The discontinuity second derivatives have the following notation: RPP 21, RPP 32, RPP 43, RPP 54, RPP 65, ZPP 21, ZPP 43, ZPP 54, ZPP 65, Between the single-leaf program and the three-convolution program, five different subroutines have been used thus far for GEOM. Obviously, the number of possible leaf geometries is limited only by the imagination of the analyst.

Various output results may occur, depending on the problem and the choice of input loading. If too large a load is used initially, the solution will not converge and the print out will be "(RESF + RESG) exceeds RESMAX." If convergence is not obtained within the designated number of attempts, ITCYCL, the print out will be "ITCNT has exceed ITCYCL." With successful convergence print out will contain the following quantities at each point, selected for print out by KKDEL.

SLONGM and SLATM are radial and circumferential membrane stresses (lb/in.^{2}), positive in tension. SLONGB and SLATB are radial and circumferential bending stresses (lb/in.^{2}), positive when there is tension on the inside surface.

SSHEAR is the transverse shear stress (lb/in.^{2}), positive when the shear acts so as to rotate an element of the shell counterclockwise. DEFLAX and DEFLRD are the axial and radial components of displacement (inches), positive in the positive directions of the coordinate axes, R and Z.

DEFL is the magnitude of the total deflection (inches).

R and Z are the radial and axial coordinates (inches) of the middle surface of the undeformed shell.

The program as shown in the following listing requires an IBM computer equiped with at least 27,000 units of storage. Some slight modification may be required if the machine to be used reads input from cards rather than tape.

```
      DIMENSION A(2,2),B(2,2),C(2,2),D(2),W(2,2),
     1     R1(601,2),T(601,2),TSAVE(601,2),TP(601,1),
     2     R2(601,2),S(601,2),TCALL(601,2),
     3     R(601),RP(601),RPP(601),
     4     Z(601),ZP(601),ZPP(601),AL(601),ALP(601),
     5     P(601),PP(601),PH(601),PPH(601),
     6     QNT(601),VRHO(601),
     7     SLONGM(606),SLATM(606),SLONGB(606),SLATB(606),
     8     SSHEAR(606),DEFLAX(606),DEFLRD(606),DEFL(606),
     9     SMAX(30),RDIMX(30),ZDIMX(30),FLEX(30),NREC(30)
      DIMENSION RDIM(601), ZDIM(601)
      COMMON  R,RP,RPP,Z,ZP,ZPP,RP21,ZP21,RPP21,ZPP21,
     1     RP32,ZP32,RPP32,ZPP32,RP43,ZP43,RPP43,ZPP43,
     2     RP54,ZP54,RPP54,ZPP54,RP65,ZP65,RPP65,ZPP65
     3     ,M,N,M1,M2,M3,M4,M5,M6,M7,M8,M9,M10,N1,QM,H
     4     ,RIN,ROUT,RR,ZZ,ZRISE
      EQUIVALENCE   (R1,SLONGM), (TSAVE,SLATM), (S,SSHEAR),
     1              (R2,SLONGB), (TCALL,SLATB)
      REWIND 3
      NZONE = 6
      T4 = 0.0
    1 READ INPUT TAPE 5, 11, NTRIAL
C     READS NTRIAL,THE NUMBER OF SHELL CONFIGURATIONS TO BE STUDIED
C(SEE1FORMAT 11)
      DO 500 INTR =1,NTRIAL
      SMAX(INTR) = 0.0
      CALL CLOK
      CALL RCLOK(T1)
      READ INPUT TAPE 5,12,RIN,ROUT,ZRISE,E,THK,PR
C     READS RIN,INSIDE RADIUS,ROUT,OUTSIDE RADIUS,ZRISE,ONE HALF
C    1BELLOWS PITCH,E, YOUNGS MODULUS, THK,THICKNESS OF SHELL,
C    2PR,POISSONS RATIO
      READ INPUT TAPE 5, 12, POINIT, PODEL, RHOI, RHODEL,
     1 SLIM,ERRF,ERRG,RESMAX,FAC
C     READS POINIT,INITIAL VALUE OF NONDIMENSIONAL AXIAL THRUST
C    1IN ADDITION TO THAT FROM PRESSURE,PODEL,INCREMEN IN AXIAL
C    2THRUST,RHOI,INITIAL VALUE OF INTERNAL PRESSURE LBS/SQUARE
C    3INCH,RHODEL,INCREMENT IN INTERNAL PRESSURE,SLIM,LIMITING
C    4ALLOWABLE STRESS,ERRF,ALLOWABLE ERROR IN SLOPE VARIABLE,
C    5ERRG,ALLOWABLE ERROR IN STRESS RESULTANT,RESMAX,OVERFLOW
C    6GUARD,FAC,SCALE FACTOR FOR NEW PODEL
      READ INPUT TAPE 5,11,M,ITMAX,ITCYCL ,KK,IBND,KKPRT,
     1 KKDEL,IREG1,IREG2,IPRT
C     READS M,NUMBER OF INTERIOR NODE POINTS PLUS ONE(IN EACH ZONE),
C    1ITMAX,LIMIT ON THE ITERATIONS PERFORMED IN QUEST OF A SOLUTION
C    2FOR A GIVEN P,ITCYCL,LIMIT OF REPEATED ATTEMPTS AT CONVERGEN
C    3CE,WITH NEW PDEL EACH ATTEMPT REDUCED BY FAC, KK=1, NULL START
```

```
C     4FOR T(I,J),KK=2,READS INITIAL T(I,J),IBND,BOUNDARY CONDITION,
C     2KKPRT=0,NO FINAL PRINT OUT OF T(I,J),KKPRT=1,PRINT FINAL
C     3T(I,J),KKDEL,SPACING OF ANSWERS TO BE PRINTED,IREG1,LOWER
C     4LIMIT POINT FOR COMPUTING FLEXIBILITY,IREG2,UPPER LIMIT
C     5POINT FOR COMPUTING FLEXIBILITY,IPRT=0,PRINT OUT ALL CASES,
C     6IPRT=1,PRINT ONLY MAXIMUM FLEXIBILITY CASE
   11 FORMAT (14I5)
   12 FORMAT (8E9.2)
      IF(KKDEL) 854,853,854
  853 KKDEL = M/10
  854 N = NZONE*M + 1
      QM=M
      RR= ROUT/RIN
      ZZ= ZRISE/RIN
      NREC(INTR) = 1
      WRITE TAPE 3, INTR, M, N, IBND, KKPRT, KKDEL,
     1              RIN, ROUT, ZRISE, E, THK, POINIT
C     CONSTRUCT BASIC GEOMETRIC VARIABLES
      M1 = M + 1
      M2 = 2*M + 1
      M3= 3*M + 1
      M4=4*M+1
      M5=5*M+1
      X = 0.
      M6= M1+ 1
      M7=M2+1
      M8 =M3+ 1
      M9=M4+1
      M10=M5+1
      N1 = N-1
      CALL GEOM
      AL21=SQRTF(RP21**2+ZP21**2)
      AL32=SQRTF(RP32**2+ZP32**2)
      AL43=SQRTF(RP43**2+ZP43**2)
      AL54=SQRTF(RP54**2+ZP54**2)
      AL65=SQRTF(RP65**2+ZP65**2)
      DO 704 I=1,N
      AL(I)=SQRTF(RP(I)**2+ZP(I)**2)
  704 ALP(I)=(RP(I)*RPP(I)+ZP(I)*ZPP(I))/AL(I)
      PO = POINIT
      RHO = RHOI
      SQM= SQRTF(12.*(1.-PR**2))
      QQ = SQM*RIN/THK
      GO TO (98,99),KK
   98 DO 2 I=1,N
      P(I)  = 0.0
      PP(I) = 0.0
      PH(I) = 0.0
      PPH(I)= 0.0
      T(1,I)=0.
    2 T(1,2)=0.
      PH21=0.0
      PH32=0.0
      PH43=0.0
```

```
      PH54=0.0
      PH65=0.0
      GO TO 100
   99 READ INPUT TAPE 5, 15, (T(I,1),T(I,2),I=1,N)
   15 FORMAT(5E14.6)
  100 CONTINUE
      ITCONT=0
    4 NCONT=0
      ITXH = 1
      ITXH2= 1
      PBAR = ( ( RHO*CQ) / E) * (RIN/THK)
      PZERO = PBAR * RR * RR / 2.0
      VRHO(1) = 0.0
      P(1) = PZERO + PO
      DO 9 I=1,N
      TCALL(I,1)=T(I,1)
    9 TCALL(I,2)=T(I,2)
    3 DO 7 I=1,2
      S(I,I)=0.
      R1(1,I)=0.
    7 R2(1,I)=0.
  126 IF(RHO) 129,163,129
  129 DO 130 I=2,N1
  130 TP(I,1) = ( T(I+1,1) - T(I-1,1) ) / (2.0*H)
      TP(1,1)  = (  T(2,1) -  T(1,1)   ) / H
      TP(M1,1) = ( T(M1,1) - T(M1-1,1) ) / H
      TP(M2,1) = ( T(M2,1) - T(M2-1,1) ) / H
      TP(M3,1) = ( T(M3,1) - T(M3-1,1) ) / H
      TP(M4,1) = ( T(M4,1) - T(M4-1,1) ) / H
      TP(M5,1) = ( T(M5,1) - T(M5-1,1) ) / H
      TP(N,1)  = (  T(N,1) - T(N-1,1)  ) / H
      DO 132   I=1,N
      QNT(I)=R(I)*(RP(I)+T(I,1)*ZP(I)-.5*RP(I)*T(I,1)**2)
      RP(I) = PBAR * ( RP(I) + T(I,1)*(ZP(I)-.5*T(I,1)*RP(I)) ) * R(I)
      PH(I) = PBAR * ( ZP(I) - T(I,1)*(RP(I)+.5*T(I,1)*ZP(I)) ) / AL(I)
  132 RPH(I)= PBAR * ( (1.0-.5*T(I,1)*T(I,1))*(ZPP(I)-ZP(I)*ALP(I)/AL(I)
     1          ) - T(I,1)*(RPP(I)-RP(I)*ALP(I)/AL(I))
     2           - TP(I,1)* (RP(I)+ZP(I)*T(I,1)) ) / AL(I)
      PH21 = PBAR*( ZP21 - T(M1,1)*(RP21+.5*T(M1,1)*ZP21) ) / AL21
      PH32 = PBAR*( ZP32 - T(M2,1)*(RP32+.5*T(M2,1)*ZP32) ) / AL32
      PH43 = PBAR*( ZP43 - T(M3,1)*(RP43+.5*T(M3,1)*ZP43) ) / AL43
      PH54 = PBAR*( ZP54 - T(M4,1)*(RP54+.5*T(M4,1)*ZP54) ) / AL54
      PH65 = PBAR*( ZP65 - T(M5,1)*(RP65+.5*T(M5,1)*ZP65) ) / AL65
      DO 45  I=2,N
      VRHO(I) = H*PBAR*(QNT(I)+QNT(I-1))/2.0 + VRHO(I-1)
   45 P(I) = PZERO + PO + VRHO(I)
      GO TO (135,57),ITXH
  163 DO 164 I=1,N
  164 P(I) = PO
  135 IBND = IBND
      GO TO (5,8,10,16),IBND
    5 S(1,2)= (-PR*H*P(1)*ZP(1) + H*R(1)*R(1)*AL(1)*PH(1))
```

```
     1          / (R(1) + PR*H*RP(1))
      R2(1,2)= -R(1)/(R(1)+PR*H*RP(1))
      GO TO 10
    8 R1(1,1) = -R(1)/( R(1) - PR*H*RP(1) )
      R2(1,2)=-R(1)/(R(1)+PR*H*RP(1))
      S(1,1)=.5*H*PR*ZP(1)*T(1,1)**2/(R(1)-PR*RP(1)*H)
      S(1,2)=(-PR*H*(ZP(1)*P(1) + T(1,1)*T(1,2)*ZP(1)-T(1,1)*P(1)*
     1RP(1)))/(R(1)+PR*RP(1)*H)
      GO TO 10
   16 R1(1,1)=-R(1)/(R(1)-PR*RP(1)*H)
      S(1,1)=.5*H*PR*ZP(1)*T(1,1)**2/(R(1)-PR*RP(1)*H)
   10 CONTINUE
      MSW=M1
      ISW=1
C     BBGIN INVERSION
      DO 20 K= 2,N1
      IF(K-MSW) 71,72,71
   71 Q1=RP(K)/R(K) - ALP(K)/AL(K)
      Q2=RP(K)/R(K)
      Q3=RPP(K)/R(K) -RP(K)*ALP(K)/(R(K)*AL(K))
      Q4=RP(K)*ZP(K)/R(K)**2
      Q5=ZPP(K)/R(K)-ZP(K)*ALP(K)/(R(K)*AL(K))
      Q6=AL(K)*ZP(K)/R(K)
      Q7=AL(K)*RP(K)/R(K)
      Q8= Q6/AL(K)
      Q9  = ZP(K)/R(K)
      Q10 = RP(K)*AL(K)
      Q11 = AL(K)*R(K)
      A(1,1)=1./H**2 -.5*Q1/H
      A(1,2)=0.
      A(2,1)=0.
      A(2,2) =A(1,1)
      B(1,1)= -2./H**2 -Q2**2 +PR*Q3
      B(1,2)= QQ*Q6
      B(2,1)= -QQ*Q6
      B(2,2)= -2./H**2 -Q2**2 -PR*Q3
      C(1,1)=1./H**2 +.5*Q1/H
      C(1,2)=0.
      C(2,1)=0.
      C(2,2)=C(1,1)
      D(1)=(1.5*Q4-.5*Q5*PR)*T(K,1)**2-QQ*(-P(K)*Q7-T(K,1)*(T(K,2)*Q7+
     1P(K)*Q6))
      D(2) =  -.5*QQ*Q7*T(K,1)*T(K,1) + (Q4+PR*Q5)*P(K)
     1        + PR*Q9*PP(K) - (2.0+PR)*Q10*PH(K) - Q11*PPH(K)
      GO TO 6
   72 GO TO (73,74,75,76,77),ISW
   73 MSW =M2
      ISW=2
      A(1,1)= -1./(AL(M1)*H)
      A(1,2)=0.
      A(2,1)=0.
      A(2,2)=-R(M1)/(AL(M1)*H)
```

```
      B(1,1)=(1./H + PR*RP(M1)/R(M1))/AL(M1)+(1./H-PR*RP21/R(M1))/AL21
      B(1,2)=0.
      B(2,1)=0.
      B(2,2)=(R(M1)/H-PR*RP(M1))/AL(M1)+(R(M1)/H+PR*RP21)/AL21
      C(1,1) = -1.0/(H*AL21)
      C(1,2)=0.
      C(2,1)=0.
      C(2,2)=-R(M1)/(H*AL21)
      D(1)=PR*((-.5*ZP(M1)*T(M1,1)**2/R(M1))/AL(M1)+(.5*ZP21*T(M1,1)**2
     1/R(M1))/AL21)
      D(2) = PR*( (P(M1)*ZP(M1)+T(M1,1)*T(M1,2)*ZP(M1)
     1        -P(M1)*T(M1,1)*RP(M1)) / AL(M1) - (P(M1)*ZP21
     2        +T(M1,1)*T(M2,1)*ZP21-P(M1)*T(M1,1)*RP21) / AL21 )
     3        + R(M1)*(PH21-PH(M1))
      GO TO 6
   74 NSW =M3
      ISW = 3
      A(1,1)=-1./(AL(M2)*H)
      A(1,2)=0.
      A(2,1)=0.
      A(2,2)=-R(M2)/(AL(M2)*H)
      B(1,1)=(1./H+PR*RP(M2)/R(M2))/AL(M2)+(1./H-PR*RP32/R(M2))/AL32
      B(1,2)=0.
      B(2,1)=0.
      B(2,2)=(R(M2)/H-PR*RP(M2))/AL(M2)+(R(M2)/H+PR*RP32)/AL32
      C(1,1) = -1.0/(H*AL32)
      C(1,2)=0.
      C(2,1)=0.
      C(2,2)=-R(M2)/(H*AL32)
      D(1)=PR*((-.5*ZP(M2)*T(M2,1)**2/R(M2))/AL(M2)+ (.5*ZP32*T(M2,1)**2
     1/R(M2))/AL32)
      D(2)=PR*( (P(M2)*ZP(M2)+T(M2,1)*T(M2,2)*ZP(M2)-P(M2)*T(M2,1)
     1        *RP(M2))/AL(M2) - (P(M2)*ZP32+T(M2,1)*T(M2,1)*ZP32
     2        -P(M2)*T(M2,1)*RP32)/AL32 ) + R(M2)*(PH32-PH(M2))
      GO TO 6
   75 NSW=M4
      ISW=4
      A(1,1)=-1./(AL(M3)*H)
      A(1,2)=0.
      A(2,1)=0.
      A(2,2)=-R(M3)/(AL(M3)*H)
      B(1,1)=(1./H+PR*RP(M3)/R(M3))/AL(M3)+(1./H-PR*RP43/R(M3))/AL43
      B(1,2)=0.
      B(2,1)=0.
      B(2,2)=(R(M3)/H -PR*RP(M3))/AL(M3)+(R(M3)/H+PR*RP43)/AL43
      C(1,1) = -1.0/(H*AL43)
      C(1,2)=0.
      C(2,1)=0.
      C(2,2)=-R(M3)/(H*AL43)
      D(1)=PR*((-.5*ZP(M3)*T(M3,1)**2/R(M3))/AL(M3)+(.5*ZP43*T(M3,1)
     1**2/R(M3))/AL43)
      D(2)=PR*( (P(M3)*ZP(M3)+T(M3,1)*T(M3,2)*ZP(M3)-P(M3)*T(M3,1)
```

```
 1        *RP(M3))/AL(M3) - (P(M3)*ZP43+T(M3,1)*T(M3,2)*ZP43
 2        -P(M3)*T(M3,1)*RP43)/AL43 ) + R(M3)*(PH43-PH(M3))
   GO TO 6
76 MSW=M5
   ISW=5
   A(1,1)=-1./(AL(M4)*H)
   A(1,2)=0.
   A(2,1)=0.
   A(2,2)=-R(M4)/(AL(M4)*H)
   B(1,1)=(1./H+PR*RP(M4)/R(M4))/AL(M4)+(1./H-PR*RP54/R(M4))/AL54
   B(1,2)=0.
   B(2,1)=0.
   B(2,2)=(R(M4)/H-PR*RP(M4))/AL(M4)+(R(M4)/H+PR*RP54)/AL54
   C(1,1)=-1./(H*AL54)
   C(1,2)=0.
   C(2,1)=0.
   C(2,2)=-R(M4)/(H*AL54)
   D(1)=PR*((-.5*ZP(M4)*T(M4,1)**2/R(M4))/AL(M4)+(.5*ZP54*T(M4,1)
  1**2/R(M4))/AL54)
   D(2) = PR*( (P(M4)*ZP(M4)+T(M4,1)*T(M4,2)*ZP(M4)-P(M4)*T(M4,1)*
  1        RP(M4))/AL(M4) - (P(M4)*ZP54+T(M4,1)*T(M4,2)*ZP54-P(M4)*
  2        T(M4,1)*RP54)/AL54)+ R(M4)*(PH54-PH(M4) )
   GO TO 6
77 CONTINUE
   A(1,1)= -1.0/(AL(M5)*H)
   A(1,2)=0.
   A(2,1)=0.
   A(2,2)=-R(M5)/(AL(M5)*H)
   B(1,1)=(1./H+PR*RP(M5)/R(M5))/AL(M5)+(1./H-PR*RP65/R(M5))/AL65
   B(1,2)=0.
   B(2,1)=0.
   B(2,2)=(R(M5)/H-PR*RP(M5))/AL(M5)+(R(M5)/H+PR*RP65)/AL65
   C(1,1)=-1./(H*AL65)
   C(1,2)=0.
   C(2,1)=0.
   C(2,2)=-R(M5)/(H*AL65)
   D(1)=PR*((-.5*ZP(M5)*T(M5,1)**2/R(M5))/AL(M5)+(.5*ZP65*T(M5,1)
  1**2/R(M5))/AL65)
   D(2) = PR*( (P(M5)*ZP(M5)+T(M5,1)*T(M5,2)*ZP(M5)-P(M5)*T(M5,1)*
  1        RP(M5))/AL(M5) - (P(M5)*ZP65+T(M5,1)*T(M5,2)*ZP65-P(M5)*
  2        T(M5,1)*RP65)/AL65)+ R(M5)*(PH65-PH(M5) )
 6 W(1,1)=B(1,1)-A(1,1)*R1(K-1,1)
   W(1,2)=B(1,2)-A(1,1)*R1(K-1,2)
   W(2,1)=B(2,1)-A(2,2)*R2(K-1,1)
   W(2,2)=B(2,2)-A(2,2)*R2(K-1,2)
   DET=W(1,1)*W(2,2)-W(1,2)*W(2,1)
   WSAVE=W(1,1)
   W(1,1)=W(2,2)/DET
   W(1,2)=-W(1,2)/DET
   W(2,1)=-W(2,1)/DET
   W(2,2)=WSAVE/DET
   S(K,1)=W(1,1)*(D(1)-A(1,1)*S(K-1,1))+W(1,2)*(D(2)-A(2,2)*S(K-1,2))
```

```
      S(K,2)=W(2,1)*(D(1)-A(1,1)*S(K-1,1))+W(2,2)*(D(2)-A(2,2)*S(K-1,2))
      R1(K,1)=W(1,1)*C(1,1)
      R1(K,2)=W(1,2)*C(2,2)
      R2(K,1)=W(2,1)*C(1,1)
   20 R2(K,2)=W(2,2)*C(2,2)
      IBND = IBND
      GO TO (17,18,49,21),IBND
   17 W(1,1) = 1.0
      W(1,2)=0.
      W(2,1)=R(N)*R2(N1,1)/H
      W(2,2)=R(N)/H -PR*RP(N)+R(N)*R2(N1,2)/H
      GO TO 44
   18 W(1,1) = R(N) + PR*H*RP(N) + R(N)*R1(N1,1)
      W(1,2) = R(N)*R1(N1,2)
      W(2,1) = R(N)*R2(N1,1)
      W(2,2) = R(N) - PR*H*RP(N) + R(N)*R2(N1,2)
      GO TO 44
   49 S(N,1) = 0.0
      S(N,2) = 0.0
      GO TO 46
   21 W(1,1)=0.0
      W(1,2)=1.0
      W(2,1)=-R(N)/H-PR*RP(N)-R(N)*R1(N1,1)/H
      W(2,2)=-R(N)*R1(N1,2)/H
   44 DET = W(1,1)*W(2,2) - W(1,2)*W(2,1)
      WSAVE = W(1,1)
      W(1,1)=W(2,2)/DET
      W(1,2)=-W(1,2)/DET
      W(2,1)=-W(2,1)/DET
      W(2,2)=WSAVE/DET
      IBND = IBND
      GO TO (22,23,46,29),IBND
   22 XXX = P(N)*PR*ZP(N) - R(N)*R(N)*PH(N) + R(N)*S(N1,2)/H
      GO TO 47
   29 XXX=.5*PR*ZP(N)*T(N,1)**2-R(N)*S(N1,1)/H
   47 S(N,1)=W(1,2)*XXX
      S(N,2)=W(2,2)*XXX
      GO TO 46
   23 XX1=-.5*PR*ZP(N)*H*T(N,1)**2+R(N)*S(N1,1)
      XX2 = H*PR*(P(N)*ZP(N)+T(N,1)*T(N,2)*ZP(N)-T(N,1)*P(N)*
     1RP(N))+R(N)*S(N1,2)
      S(N,1)=W(1,1)*XX1+W(1,2)*XX2
      S(N,2)=W(2,1)*XX1+W(2,2)*XX2
   46 CONTINUE
      DO 25 I=1,N
      TSAVE(I,1)=T(I,1)
   25 TSAVE(I,2)=T(I,2)
      T(N,1)=S(N,1)
      T(N,2)=S(N,2)
      DO 30 K=1,N1
      J=N-K
      J1=J+1
```

```
      T(J,1)=S(J,1)-R1(J,1)*T(J1,1)-R1(J,2)*T(J1,2)
   30 T(J,2)=S(J,2)-R2(J,1)*T(J1,1)-R2(J,2)*T(J1,2)
   31 NCNT=NCNT+1
      RESF=0.
      RESG=0.
      DO 32 I=1,N
      RESF = RESF + (T(I,1)-TSAVE(I,1))*(T(I,1) - TSAVE(I,1))
   32 RESG = RESG+(T(I,2)-TSAVE(I,2))**2
      IF(RESF+RESG-RESMAX) 34,35,35
   35 ITXH3 = 1
      GO TO 808
   43 ITXH3 = 2
  808 WRITE OUTPUT TAPE 6,850, INTR,  N,  IBND
      GO TO (835,836),ITXH3
  835 WRITE OUTPUT TAPE 10, 36
      GO TO 37
  836 WRITE OUTPUT TAPE 10,119
   37 WRITE OUTPUT TAPE 10, 371
      WRITE OUTPUT TAPE 6, 419, PO,RHO,RIN,ROUT,ZRISE, THK,E,PR,RESF,
     1       RESG, N, ITMAX, ITCYCL, ITCNT, NCNT
      WRITE OUTPUT TAPE 6,14,(TCALL(I,1),TCALL(I,2),I=1,N )
      ITXH2= 2
      GO TO 809
  850 FORMAT ( 1H1 / 11HO CASE NO.-I3,10X,3HN =,I4,10X,6HIBND =,I2)
  119 FORMAT(30H1 ITCNT HAS EXCEEDED ITCYCL            )
   36 FORMAT (1HO/32HO (RESF + RESG) EXCEEDS RESMAX    )
  371 FORMAT (75H PO,RHO,RIN,ROUT,ZRISE,THK,E,PR,RESF,RESG,N,ITMAX,
     1 ITCYCL,ITCNT,NCNT            )
  419 FORMAT (10E10.4,5I5)
   13 FORMAT  (2F10.5,2F5.1,2E8.2,5I5)
   14 FORMAT(6E20.8)
   34 IF(RESF-ERRF**2) 33,33,39
   33 IF(RESG-ERRG**2) 50,50,39
   39 IF(NCNT-ITMAX) 3,40,40
   40 ITCNT=ITCNT+1
      IF(ITCNT-ITCYCL) 41,43,43
   41 PO =PO - PODEL
      RHO = RHO - RHODEL
      PODEL = PODEL*FAC
      RHODEL = RHODEL*FAC
      DO 42 I=1,N
      T(I,1       )=TCALL(I,1)
   42 T(I,2)=TCALL(I,2)
      PO =PO + PODEL
      RHO = RHO + RHODEL
      GO TO 809
   50 ITXH = 2
      PLAST = PO
      IF (RHO) 126,57,126
   57 IF (KKPRT)  58,59,58
   58 WRITE TAPE 3, (T(I,1),T(I,2),I=1,N)
      NREC(INTR) = NREC(INTR) + 1
```

```
   59 WRITE TAPE 3, PO, RHO, NCNT
      NREC(INTR) = NREC(INTR) + 1
C     COMPUTATION AND PRINT OUT OF STRESSES AND DEFLECTIONS
      L = 0
      DO 200 IP=2,N,M
      IF(IP-M1) 201,201,210
  201 DEFST=0.
      JB=1
      JF= M1
  444 SUM=0.
   61 DO 64 I= JB,JF
      L = L+1
      ZDIM(L) = Z(I)*RIN
      RDIM(L) = R(I)*RIN
      Z1=(T(I,1)*RP(I)-.5*T(I,1)**2*ZP(I))/AL(I)
      Z2 = (T(I,2)*RP(I) + P(I)*ZP(I) + T(I,1)
     1       *(T(I,2)*ZP(I)-P(I)*RP(I))) / R(I)
      IF((JF-I)*(JB-I)) 26,24,26
   24 IF(I-JF)85,84,85
   84 Z3 = ( T(I,2) - T(I-1,2) ) / H + R(I)*AL(I)*PH(I)
      GO TO 86
   85 Z3 = ( T(I+1,2) - T(I,2) ) / H + R(I)*AL(I)*PH(I)
      GO TO 86
   26 Z3 = (T(I+1,2)-T(I-1,2))/ (2.*H) + R(I)*AL(I)*PH(I)
   86 Z4= (ZP(I)-T(I,1)*RP(I))/AL(I)
      F = (-QQ*Z1*AL(I) + (Z2 - PR*Z3)*Z4) / SQM
      DEN=AL(I)*QQ
      SLONGM(L) = E*Z2/DEN
      SLATM(L)  = E*Z3/DEN
      IF ( (JF-I)*(JB-I) )  28,27,28
   27 IF(I-JF)88,87,88
   87 Z5=(T(I,1)-T(I-1,1))/H
      GO TO 89
   88 Z5 = (T(I+1,1) - T(I,1)) / H
      GO TO 89
   28 Z5=(T(I+1,1)-T(I-1,1))/(2.0*H)
   89 Z6= (RP(I)*T(I,1) + .5*ZP(I)*T(I,1)**2) / R(I)
      SLONGB(L) = 6.0*E*(Z5 + PR*Z6)/(SQM*DEN)
      SLATB(L)  = 6.0*E*(Z6 + PR*Z5)/(SQM*DEN)
      SSHBAR(L) = E*( -T(I,2)*ZP(I) + P(I)*RP(I) + T(I,1)*(T(I,2)*RP(I)
     1            + P(I)*ZP(I)) ) / (R(I)*DEN)
      SLONG = ABSF(SLONGM(L)) + ABSF(SLONGB(L))
      SLAT  = ABSF(SLATM(L))  + ABSF(SLATB(L))
      IF (I-IREG1)  801, 94, 94
   94 IF (I-IREG2)   95, 95,801
   95 IF (SLONG - SLAT)  92,92,93
   92 WS = SLAT
      GO TO 799
   93 WS = SLONG
  799 IF (WS - SMAX(INTR))  801,801,800
  800 SMAX(INTR)  = WS
      RDIMX(INTR) = RDIM(L)
```

```
      ZDIMX(INTR) = ZDIM(L)
801   SUM = SUM + F
      DEFLAX(L) = .5*H*THK*SUM + DEFST
      IF (I-JB)  81,82,81
 82   DEFLAX(L) = DEFST
 81   DEFLRD(L) = R(I)*(Z3 - PR*Z2)*THK / (SQM*AL(I))
      DEFL(L)= SQRTF(DEFLAX(L)*DEFLAX(L) + DEFLRD(L)*DEFLRD(L))
      IF (I-JB)  63,64,63
 63   SUM= SUM+F
 64   CONTINUE
      IWS = L + JB -JF
      WRITE TAPE 3,  (RDIM(I1),ZDIM(I1),SLONGM(I1),SLATM(I1),SLONGB(I1),
     1       SLATB(I1),SSHEAR(I1),DEFLAX(I1),DEFLRD(I1),DEFL(I1),
     2       I1=IWS,L,KKDEL)
      GO TO 200
210   IF(IP-M2) 211,211,220
211   DEFST = DEFLAX(L)
      JB=M1
      JA=M2
      PHSV1 = PH(M1)
      PHSV2 = PH(M2)
      PHSV3 = PH(M3)
      PHSV4 = PH(M4)
      PHSV5 = PH(M5)
      RASV1=RP(M1)
      RASV2=RP(M2)
      RPSV3= RP(M3)
      RASV4=RP(M4)
      RPSV5=RP(M5)
      ZASV1=ZP(M1)
      ZASV2=ZP(M2)
      ZPSV3=ZP(M3)
      ZPSV4=ZP(M4)
      ZASV5=ZP(M5)
      RAPS1=RPP(M1)
      RPPS2=RPP(M2)
      RAPS3 = RPP(M3)
      RPPS4=RPP(M4)
      RPPS5=RPP(M5)
      ZAPS1= ZPA(M1)
      ZPPS2=ZPP(M2)
      ZAPS3 = ZPP(M3)
      ZPPS4=ZPP(M4)
      ZPPS5=ZPP(M5)
      ALSV1 = AL(M1)
      ALSV2= AL(M2)
      ALSV3=AL(M3)
      ALSV4=AL(M4)
      ALSV5=AL(M5)
      PH(M1) = PH21
      RA(M1) = RP21
      ZA(M1) = ZP21
```

```
      RPP(M1)=RPP21
      ZPP(M1)=ZPP21
      AL(M1) = AL21
      GO TO 444
  220 IF ( IP - M3) 221,221,230
  221 DEFST = DEFLAX(L)
      JB = M2
      JF = M3
      PH(M2) = PH32
      RP(M2)=RP32
      ZP(M2)=ZP32
      RPP(M2) = RPP32
      ZPP(M2) = ZPP32
      AL(M2)=AL32
      GO TO 444
  230 IF(IP-M4)231,231,232
  231 DEFST = DEFLAX(L)
      JB = M3
      JF=M4
      PH(M3) = PH43
      RP(M3)  = RP43
      ZP(M3)  = ZP43
      RPP(M3) = RPP43
      ZPP(M3) = ZPP43
      AL(M3)  = AL43
      GO TO  444
  232 IF(IP-M5)233,233,234
  233 DEFST=DEFLAX(L)
      JB=M4
      JF=M5
      PH(M4)=PH54
      RP(M4)=RP54
      ZP(M4)=ZP54
      RPP(M4)=RPP54
      ZPP(M4)=ZPP54
      AL(M4)=AL54
      GO TO 444
  234 IF(IP-N)235,235,200
  235 DEFST=DEFLAX(L)
      JB=M5
      JF=N
      PH(M5)=PH65
      RP(M5)=RP65
      ZP(M5)=ZP65
      RPP(M5)=RPP65
      ZPP(M5)=ZPP65
      AL(M5)=AL65
      GO TO 444
  200 CONTINUE
      NREC(INTR) = NREC(INTR) + 1
      IF (SMAX(INTR) - SLIM) 802,803,803
  803 I2 = IREG2 + (IREG2/M) - 1
```

```
      IF(IREG1-1)  823,823,804
804   I1 = IREG1 + (IREG1/M) - 1
      GO TO 824
823   I1 = IREG1
824   FLEX(INTR)= 6.2831852*E*THK*THK*P(1)/(SQM*(DEFLAX(I2)-DEFLAX(I1)))
      ITXH2= 2
      GO TO 809
802   PO =PO + PODEL
      RHO = RHO + RHODEL
      ISAMP   = ISAV
      PH(M1) = PHSV1
      PH(M2) = PHSV2
      PH(M3) = PHSV3
      PH(M4) = PHSV4
      PH(M5) = PHSV5
      RP(M1)  = RPSV1
      RP(M2)  = RPSV2
      RP(M3)  = RPSV3
      RP(M4)=RPSV4
      RP(M5)=RPSV5
      ZP(M1)  = ZPSV1
      ZP(M2)  = ZPSV2
      ZP(M3)  = ZPSV3
      ZP(M4)=ZPSV4
      ZP(M5)=ZPSV5
      RPP(M1) = RPPS1
      RPP(M2) = RPPS2
      RPP(M3) = RPPS3
      RPP(M4)=RPPS4
      RPP(M5)=RPPS5
      ZPP(M1) = ZPPS1
      ZPP(M2) = ZPPS2
      ZPP(M3) = ZPPS3
      ZPP(M4)=ZPPS4
      ZPP(M5)=ZPPS5
      AL(M1)  = ALSV1
      AL(M2)  = ALSV2
      AL(M3)  = ALSV3
      AL(M4)=ALSV4
      AL(M5)=ALSV5
809   CALL CLOK
      CALL RCLOK (T2)
      T3 = T2 - T1
      GO TO (786,789),ITXH2
786   IF (T3 - 5.0)  4,4,789
789   T4 = T4 + T3
500   CONTINUE
      END FILE 3
      REWIND 3
      IF (IPRT)  831,807,831
831   DO 797 I=1,NTRIAL
      IF (FLEX(I))  798,797,798
```

```
  797 CONTINUE
      CALL DUMP     (Z1,AL21,1, NZONE,I1,0, NREC(10),NREC,0,
     1              TP,R1,1, ZZ,R,1)
C     FIND LARGEST FLEX(I),I=1,NTRIAL
  798 BIG = 0.0
      K = 0
      L = 2
      DO 807  K=1,NTRIAL
      IF (BIG - FLEX(K))  806,807,807
  806 BIG = FLEX(K)
      IBIG = K
  807 CONTINUE
      DO 805  K=1,NTRIAL
      IF (IPRT)  833,832,833
  832 IBIG = K
  833 IF (IBIG - K)   811,810,811
  810 L = 1
  811 READ TAPE 3,  INTR, M, N, IBND, KKPRT, KKDEL,
     1              RIN, ROUT, ZRISE, E, THK, POINIT
      NREC(K) = NREC(K) - 1
      GO TO (812,813),L
  812 WRITE OUTPUT TAPE 6, 855, INTR, N, IBND
      WRITE OUTPUT TAPE 6, 856, RIN, ROUT, ZRISE, E, THK
      WRITE OUTPUT TAPE 6, 857,POINIT, FLEX(IBIG), SMAX(IBIG),
     1                     RDIMX(IBIG), ZDIMX(IBIG)
  813 IF (KKPRT)  814,816,814
  814 READ TAPE 3, (T(I,1),T(I,2),I=1,N)
      NREC(K) = NREC(K) - 1
      GO TO (815,816),L
  815 WRITE OUTPUT TAPE 6,858,N,KKDEL,(T(I,1),T(I,2),I=1,N)
  816 READ TAPE 3, PO, RHO, NCNT
      GO TO (817,818),L
  817 WRITE OUTPUT TAPE 6, 861, PO, RHO, NCNT
      WRITE OUTPUT TAPE 6, 91
  818 LL = M+1
      DO 820   K1=1,6
      READ TAPE 3,   (RDIM(I), ZDIM(I), SLONGM(I), SLATM(I), SLONGB(I),
     1       SLATB(I), SSHEAR(I), DEFLAX(I), DEFLRD(I), DEFL(I),
     2       I=1,LL,KKDEL)
      GO TO (819,820),L
  819 WRITE OUTPUT TAPE 6, 860, (RDIM(I), ZDIM(I), SLONGM(I), SLATM(I),
     1       SLONGB(I), SLATB(I), SSHEAR(I), DEFLAX(I), DEFLRD(I),
     2       DEFL(I), I=1,LL,KKDEL)
  820 CONTINUE
      NREC(K) = NREC (K) - 2
      IF (NREC(K))  813,821,813
  821 IF (IPRT) 834,805,834
  834 GO TO (822,805),L
  805 CONTINUE
  822 CALL CLOK
```

```
      CALL RCLOK(T5)
      T4 = T4 + T5 - T2
      WRITE OUTPUT TAPE 6, 788, T4
      CALL EXIT
   91 FORMAT ( 1H0, /
     1        118H0     R              Z              SLONGM        SLATM        SLONG
     1B       SLATB          SSHEAR         DEFLAX         DEFLRD          DEFL
     2  )
  788 FORMAT (13H1     RUN TIME, F7.2, 5H MIN.)
  855 FORMAT ( 12H1  CASE NO.-,I3,10X, 3HN =,I4,10X, 6HIBND =,I2)
  856 FORMAT  ( 1H0,/ 98H0            RIN                        ROUT
     1   ZRISE                    E                        THK        / 6E20.8 )
  857 FORMAT  ( 1H0,/ 98H0          PINI1                        FLEX
     1     SMAX                  RDIMX                    ZDIMX       / 6E20.8 )
  858 FORMAT  (26H0  BETA(I), PSI(I),  I=1, I3,1H,,3I,2H ), / (6E20.8) )
  859 FORMAT  ( 1H0 /  7H0  PO = , E15.8,  /  1H  )
  860 FORMAT  (10E12.4)
  861 FORMAT ( 1H0,/   83H0          PO                          RHO
     1      NCNT                                  / 2E20.8, I14 )
      END
```

APPENDIX IV

OPERATING INSTRUCTIONS FOR BELLOWS-TYPE PERMEATION APPARATUS

APPENDIX IV

OPERATING INSTRUCTIONS FOR BELLOWS-TYPE PERMEATION APPARATUS

In an application where a liquid is transferred by collapsing a flexible bladder containing the liquid, with an inert gas pushing against it, several categories of information are required for engineering design purposes.

First, it is necessary to know how much liquid will be lost due to permeation through the bladder into the gas space between the bladder and confining tank wall. Since the total amount that permeates depends on the area of the bladder that is permeating and on the temperature, these two parameters must be accurately known.

Next, it is necessary to know what quantity of gas will permeate through the bladder and dissolve in the liquid. If a fixed amount of gas is added initially without subsequent make-up, a pressure drop in the tank will result. Again, the area of the bladder that is permeating and the temperature must be known.

Since the bladder is free to collapse to the limiting volume of the incompressible liquid as gas pressure is increased, the pressure across any increment of bladder is limited to the head of liquid above the particular increment.

To eliminate the need for special small-size bladders (at considerable expense), and to eliminate the need for complex piping and valves, while at the same time provide a flexible membrane that will seek the confines of the liquid, the subject apparatus was developed.

This apparatus consists of a stainless steel chamber or body with removable top and bottom covers. A bellows with a low spring constant, 1.5 psi/in. travel (in the existing design) or lower, is fastened at one end to the top cover plate. The other end of the bellows is covered with the test specimen and the bottom cover plate installed. The bellows cavity is filled with the liquid, and gas pressure is admitted to the space outside the bellows and specimen.

Dimensions of the chamber are not critcal although somewhat limited by the bellows size. The volume of the gas space should be kept low to provide a reasonable ratio of surface area of specimen to volume of gas space. The ratio for the apparatus developed at Bell Aerosystems Company is approximately 1 in.$^{-1}$.

The remainder of the apparatus consists of two valves on the gas side, two valves on the liquid side, a pressure pickup on the gas side (pressure gage or pressure transducer can be used), a thermocouple or thermometer well on the liquid side (terminating close to the test specimen, but not touching it), and an analytical

device on the gas side. The analytical device can be a unit constructed as an integral part of the permeation chamber, or simply a gas bottle for drawing of a sample of gas periodically.

The object of the test is to produce a plot of the weight of permeant in the gas side as a function of time. A typical curve is shown here:

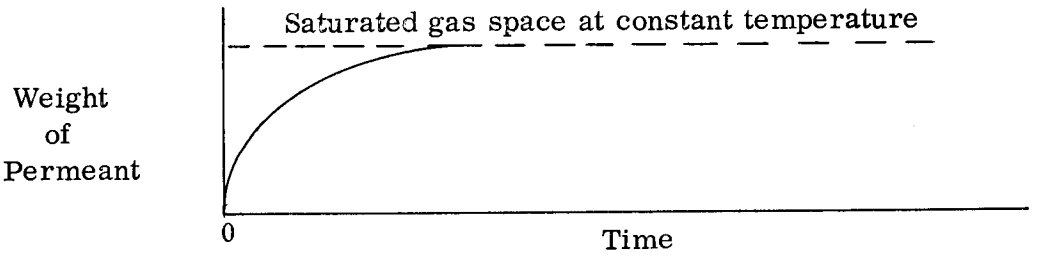

With this curve, one can calculate the amount of liquid that will be lost over any given period of time. The pressure drop that might occur during a test will be a measure of the gas solubility in the permeant.

The sensitivity of the analytical technique employed will determine the accuracy of the shape of the curve during the initial hours of the test, which will also determine whether the curve starts at zero time (or more probably at some time, t).

In regard to the foregoing discussion of surface to volume ratio, if this ratio is of little importance, an alternate design of the chamber can be used. The chamber can be a straight cylinder closed at the bottom (except for pressurizing and purge ports); the inside diameter would be slightly larger than the maximum diameter of the bellows and flanges. The bellows would be bolted to the top cover and this assembly lowered into the "pot" and bolted in place. This type construction would have the advantage of having a simpler seal between the gas and liquid sides, and only one seal to the outside of the chamber.

A. DESCRIPTION OF APPARATUS

Figure IV-1 is a cross-sectioned drawing of the permeation chamber; Figures IV-2 through IV-7 are detailed drawings of the components. Figure IV-8 is a flow schematic of the entire apparatus. The diameter of the specimen exposed to the permeant is 3.9 inches, giving an area of 11.9 square inches. Valves used are 1/8-inch Ideal needle valves. The pressure pickup is a Taber pressure transducer. A high-pressure infrared gas cell is piped into the bottom, or gas side, of the permeation chamber; this cell is designed for the Model 421 Perkin-Elmer Infra-Red Spectrophotometer; Figure IV-9 is a picture of the unit installed on the infra-red instrument for analysis. The tubing is 1/4-inch stainless steel and the fittings are standard AN parts. All materials are stainless steel. The seals are flat teflon gaskets confined between two serrated surfaces.

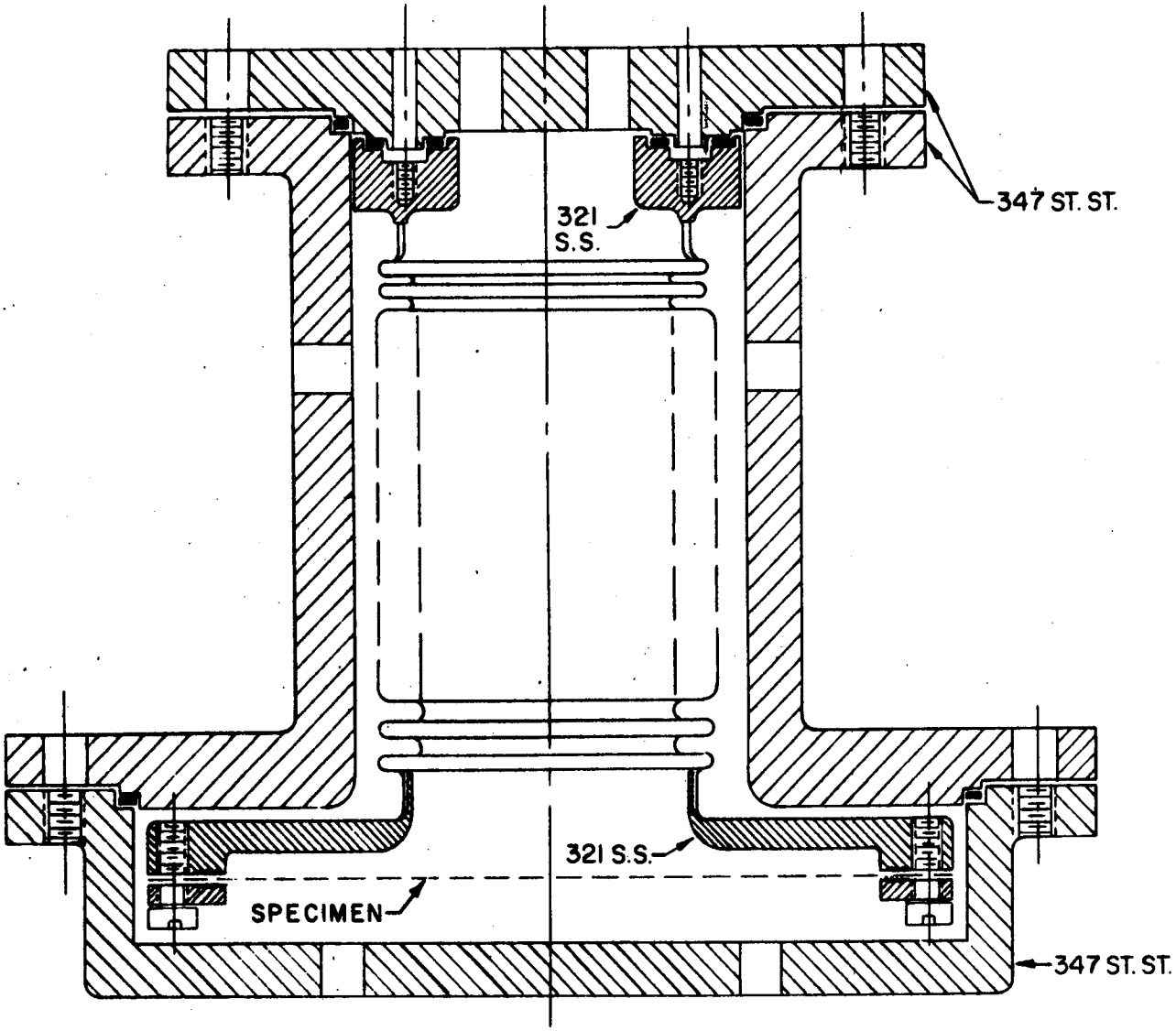

Notes: Approximated Full-Scale.
All Machined Surfaces 63 RMS or Better.

Figure IV-1. Permeability Test Apparatus

Scale 2:1 Approx.
Material: 321 Stainless Steel

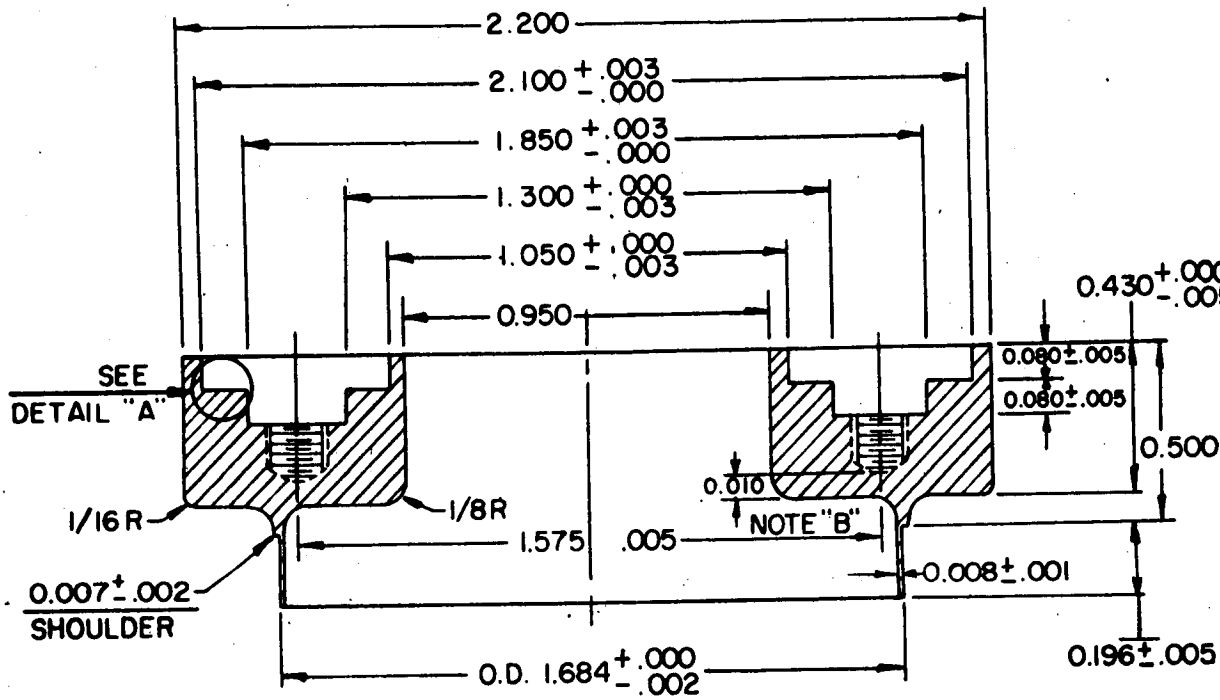

Detail "A"

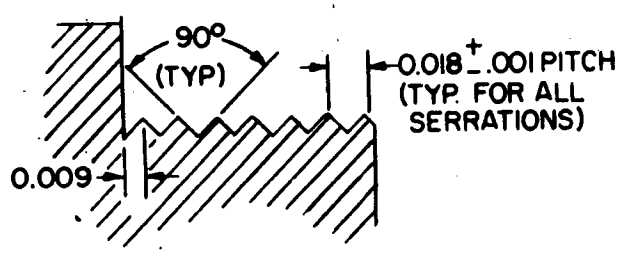

Note "B"
Drill and tap 12 holes
No. 8-36 thread
Leave 0.010 inch well at bottom of hole

Both serrated surfaces controlled to 0.005 inch max. flat crest of serrations in plane which is flat within 0.001 T.I.R. for full diameter

Figure IV-2. Upper Bellows Flange

① 12 holes 8-36 thread
② 12 holes No. 19 drill

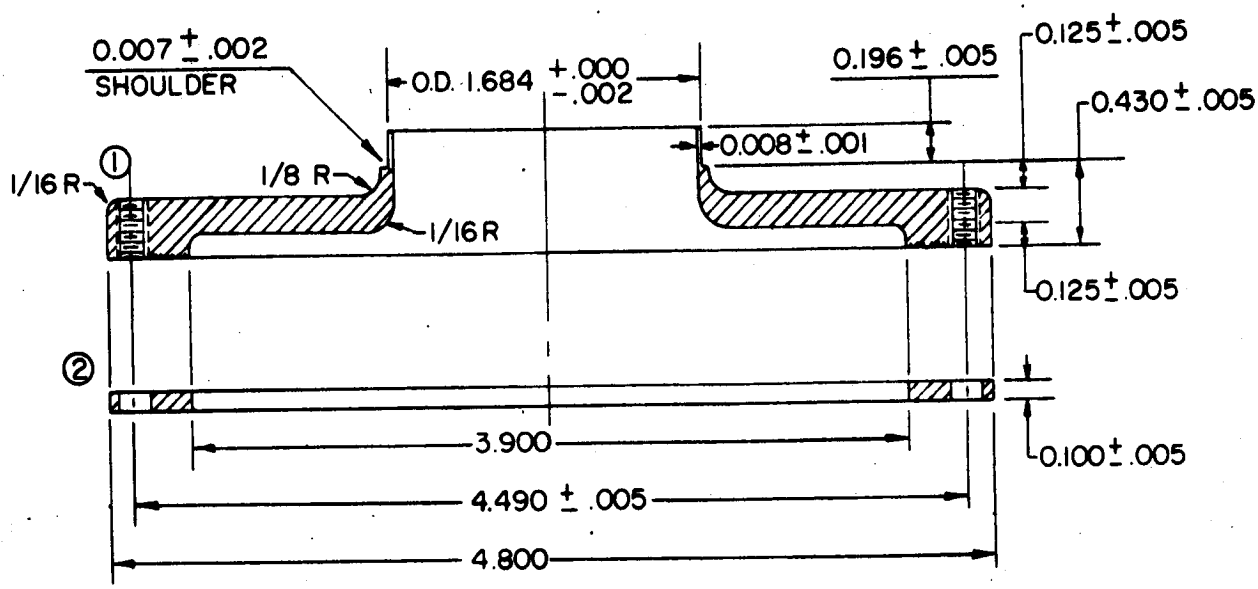

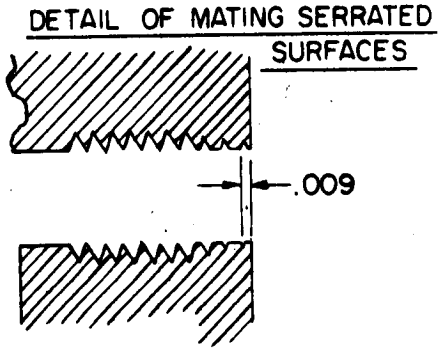

Crest of serrations in plane which is flat within 0.001 T.I.R. for full diameter. Depth of cut for 3rd serration 75% of full cut; for 2nd, 50%; and for first, 25%.

Figure IV-3. Mounting Flange and Supporting Ring

① 2 holes 1/4 in. diameter
② 12 holes No. 19 drill
③ 12 holes 7/32 drill

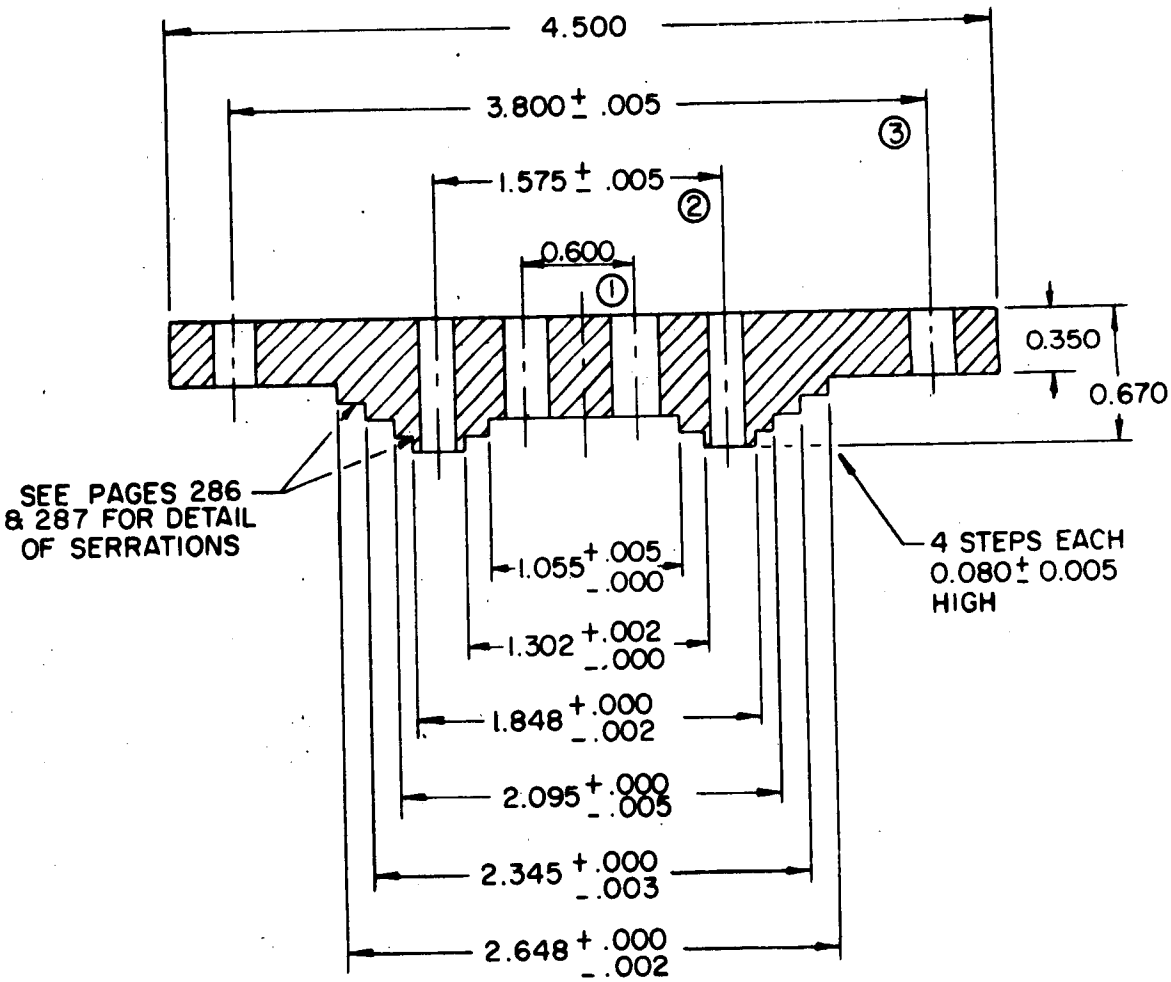

Figure IV-4. Top Cover

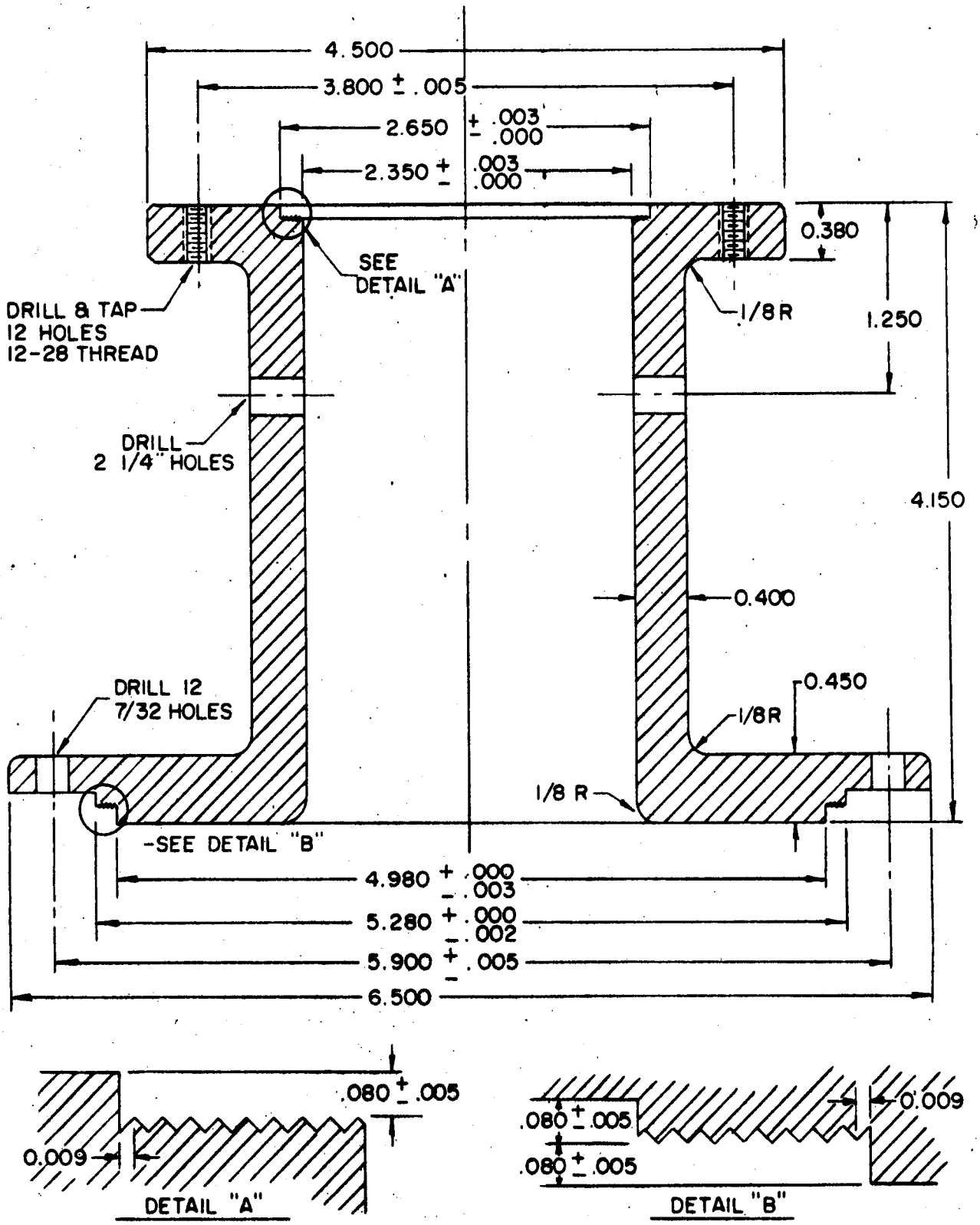

Figure IV-5. Body

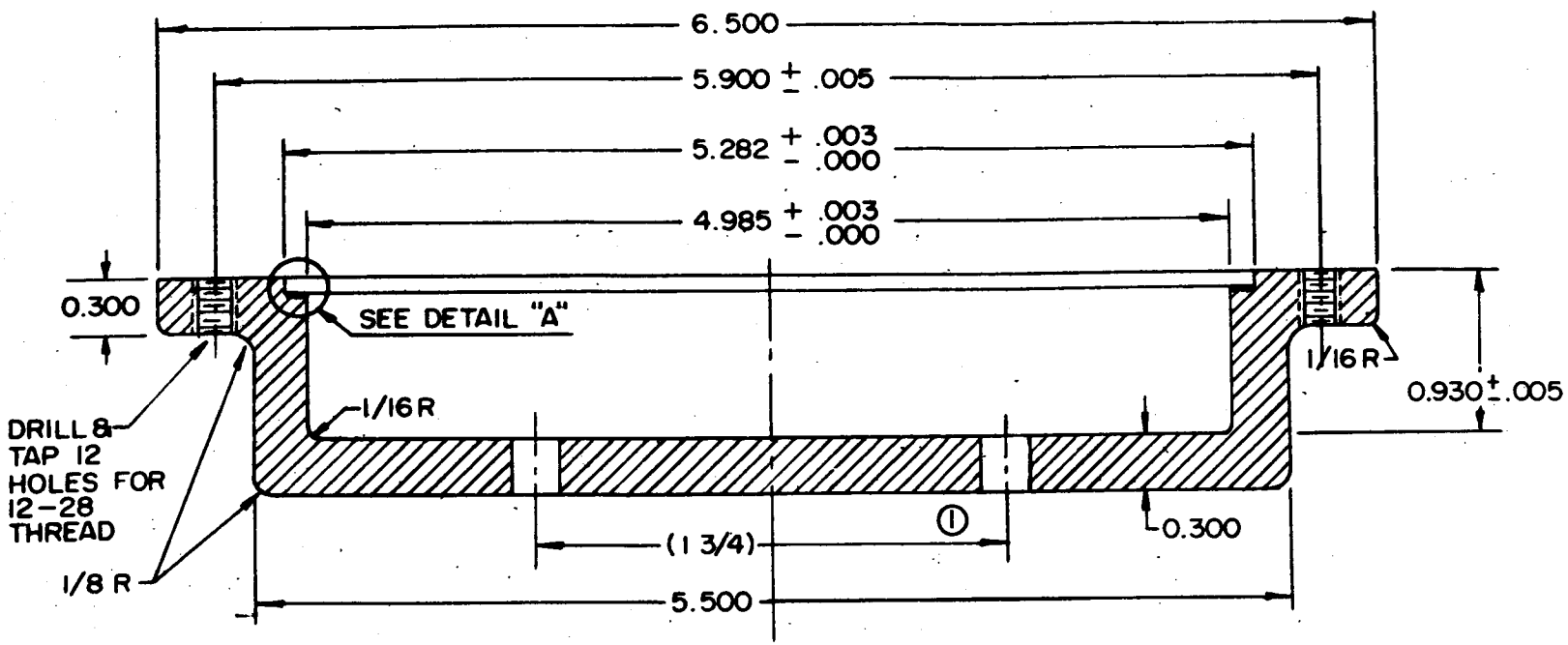

① Drill 2-1/4 in. holes; before drilling contact W.H. Walters for exact distance between holes

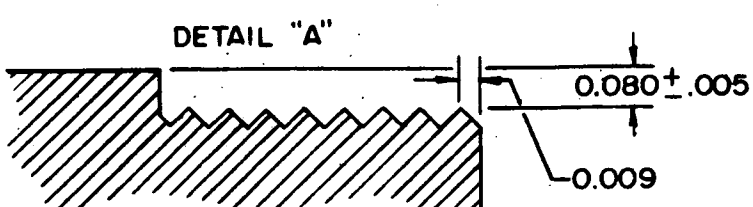

Figure IV-6. Bottom Cover

Make three sets

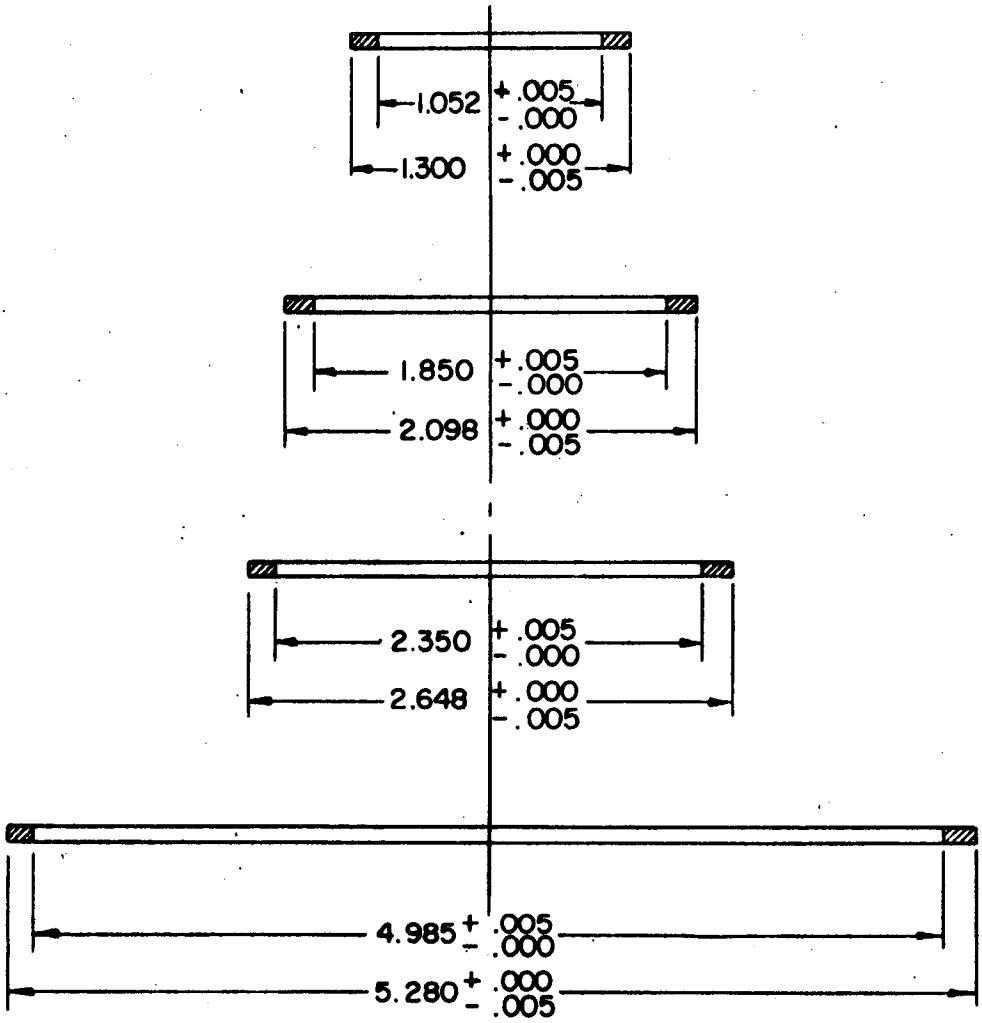

Note: All gaskets 0.060 in. thick teflon

Figure IV-7. Gaskets

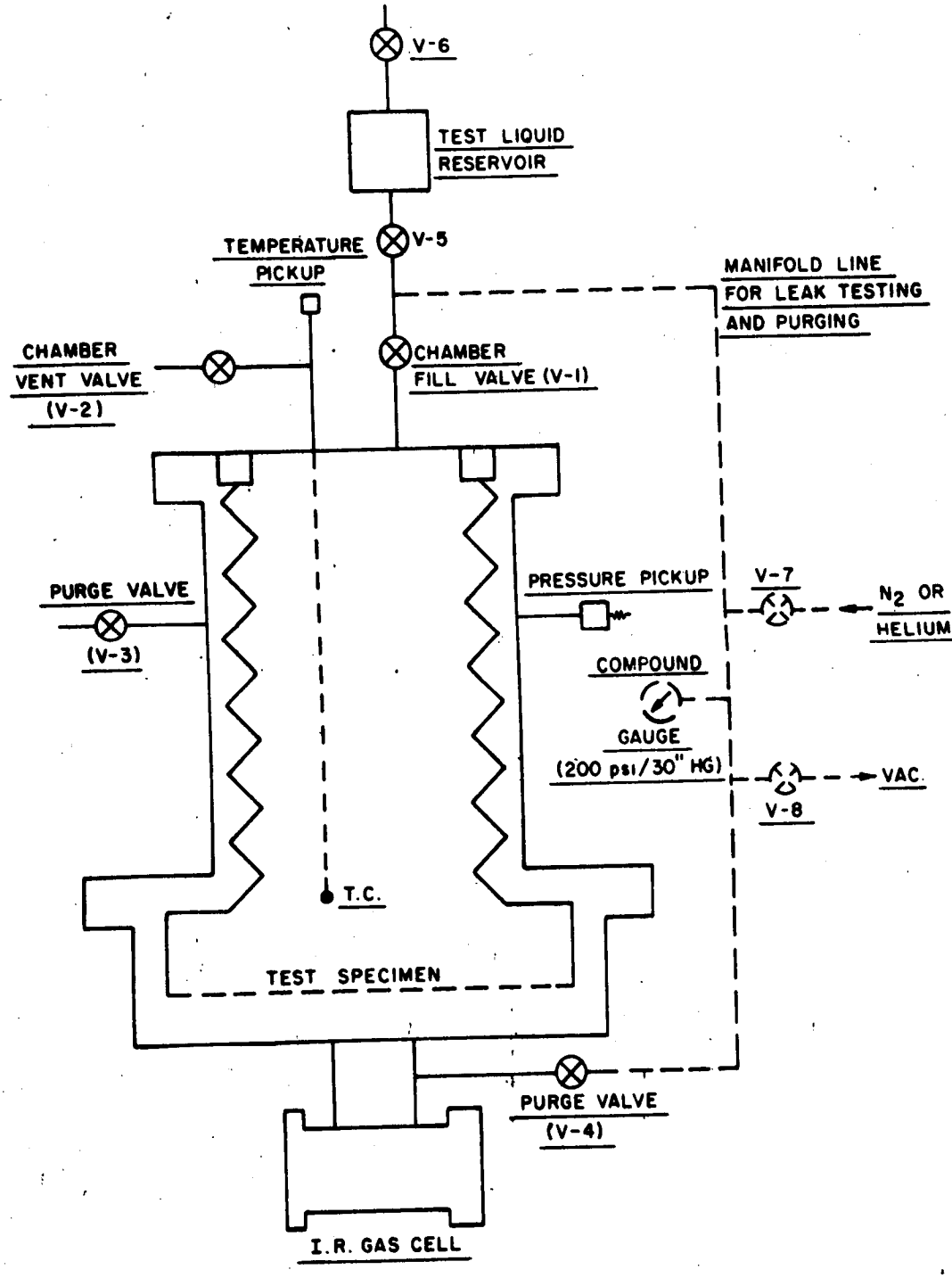

Figure IV-8. Flow Schematic of Permeation Test Apparatus

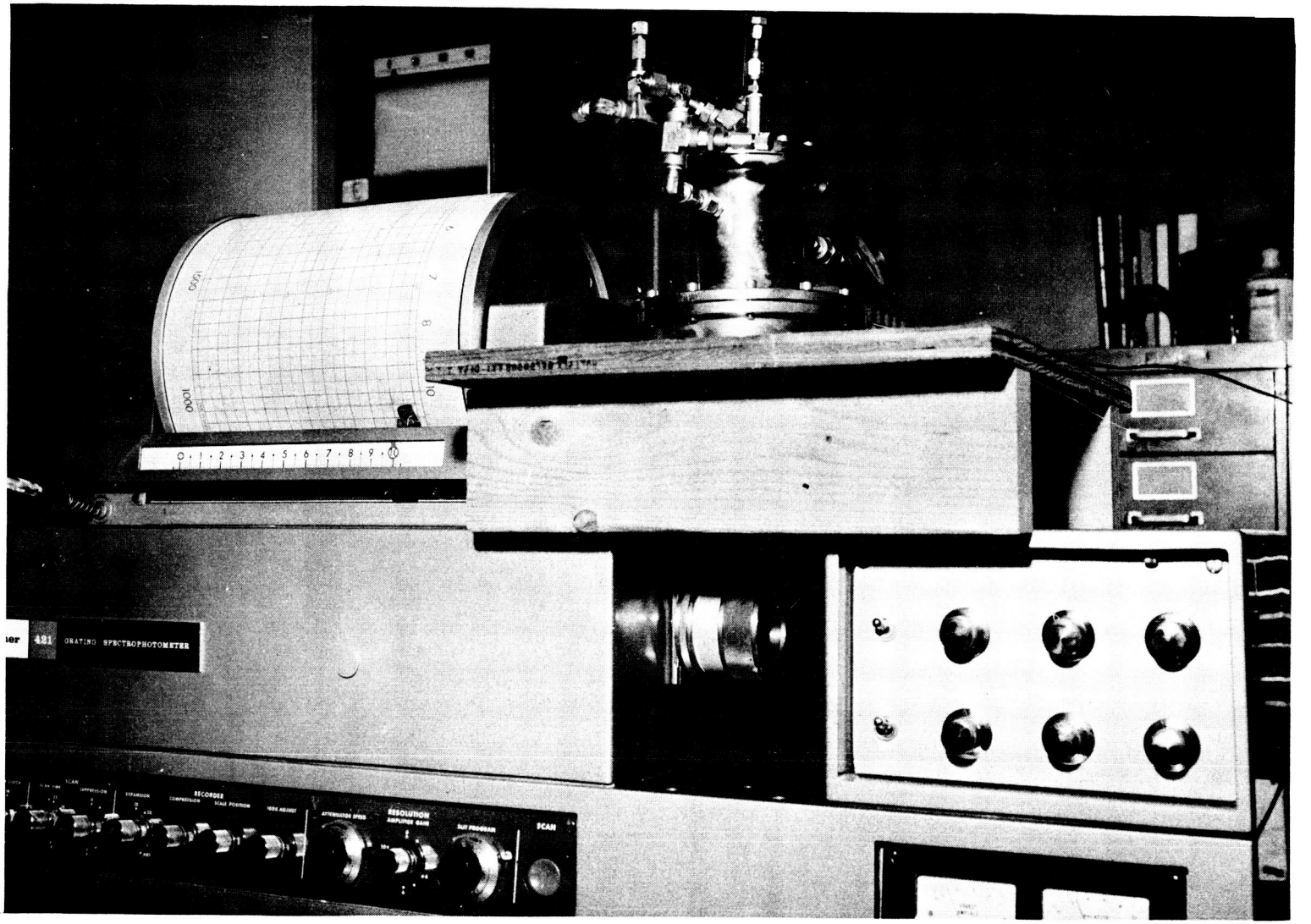

Figure IV-9, Permeability Apparatus Mounted on Infrared Unit

B. CAPABILITIES OF APPARATUS

This apparatus can be used for conducting permeation tests with any chemically compatible combination of liquid permeant, pressurizing gas, and test membrane. The tests can be conducted at any pressure up to the rated pressure of 200 psi and at any suitable temperature within the temperature-pressure restrictions of the test materials.

Following is a list of typical propellants that can be used for tests in subject apparatus. The boiling point of these propellants is given to aid in complying with Step 1 of Paragraph D and Step 1 of Paragraph E of these procedures:

Propellant	Boiling Point
Unsymmetrical Dimethyl Hydrazine (UDMH)	146°F
Hydrazine	236°F
50/50 Blend of UDMH and Hydrazine	146° to 236°F
Hydrogen Peroxide	288°F
Mixed Oxides of Nitrogen (MON)	38° to 40°F
Nitrogen Tetroxide (N_2O_4)	70°F

If it is desired to test pentaborane and other pyrophoric liquids, then special techniques for loading, unloading, etc. will be required.

To conduct tests under temperature-cycling conditions, install the apparatus in an oven capable of temperature-cycling control, e.g., cycle temperature from 0° to 140°F to 0°F in 24 hours. Analysis must be made when temperature is 70°F.

C. ASSEMBLY OF APPARATUS

(See sectional veiw of chamber in Figure IV-1. Also, see Paragraph F on Volume Calibration of Apparatus.)

CAUTION

Before and during assembly, protect and/or handle with care parts with serrated sealing surfaces to avoid any scratches or nicks on these surfaces.

1. Thoroughly clean and dry all components prior to assembly. Disassemble valves for cleaning.

a. Use vapor degreaser for all metal parts except thermocouple and pressure pickup. Wipe thermocouple with clean cloth saturated with methylene chloride.

b. Pressure pick-up will be cleaned by instrumentation personnel.

2. Place gasket in serrated groove on top of chamber body.

3. Carefully place top cover in place and secure. Torque screws to 40 to 42 in.-lb alternating back and forth across diameters until all screws are tight.

4. Install gasket in each serrated groove in small end flange on bellows.

5. Carefully insert small end of bellows assembly into bottom of permeation chamber. Bellows should be compressed so that when small flange is properly seated, large flange will just rest against the bottom of the body when unit is held in an upright position.

6. When flange is properly seated on inside of top cover, install screws through top cover and tighten alternately to a torque of 18 to 20 in.-lb.

7. Cut test specimen from flat sheet stock to a diameter of 4.80 inches. Punch 12 holes (0.166 in. diameter) to coincide with 12 holes on specimen mounting flange. (Use specimen support ring as guide.)

8. Before installing specimen, wipe clean with methyl alcohol, methylene chloride, or some other compatible solvent; use a clean lint-free cloth.

9. Place specimen and support ring on specimen mounting flange insert screws and tighten them alternately to 18 to 20 in.- lb torque.

10. Allow partly assembled apparatus to stand for 24 hours at room temperature and then retorque all screws to values previously stated in Steps 3, 6, and 9.

11. Install thermocouple and valves, V-1 and V-2, in accordance with flow sheet Figure IV-8. Tighten all AN fittings to 135 to 150 in.-lb.

12. Leak test bellows assembly with helium leak detector.

a. Atach helium line to valve V-1 for purging.

b. Open valves V-1 and V-2 and purge inside of bellows with low pressure (0.7 psig max.) helium for 2 to 3 minutes.

c. Slowly close valve V-2 and immediately close valve V-1.

NOTE

Maximum bulge of specimen at center will be 1/8 inch.

d. Move helium sniffer around bellows assembly; note particularly area where specimen is sealed between mounting flange and support ring and where bellows assembly is fastened to top cover. Placing sniffer at either port on side wall of body will indicate whether upper gaskets are sealing. No leakage is permitted around the bellows assembly.

e. Remove helium line and bleed off pressure through valve V-1.

13. After leak test, install gasket in serrated groove in bottom cover.

14. Install bottom cover; install screws and tighten alternately to 40 to 42 in.-lb. Allow unit to stand 24 hours and retorque screws.

15. On one of the two ports on the side of the permeation chamber, attach purge valve V-3, and on the other port attach the pressure pickup.

16. Attach purge valve V-4 to AN tee on bottom cover.

17. Install manifold line between valves V-1 and V-4; line will have a compound gage (200 psi/30 inch Hg vacuum) and two centrally located tee fittings with valve V-7 at inlet to one tee, and valve V-8 at inlet to other tee.

18. Assemble infrared gas cell according to instructions from personnel in Spectrographic Laboratory (or have the laboratory personnel assemble cell).

19. Attach the infrared gas cell to ports on bottom cover. Tighten AN nuts to 135 to 150 in.-lb.

20. Leak testing completely assembled apparatus:

a. Open valves V-1 and V-4.

b. Close valves V-2, V-3, and V-8.

c. Close valve V-7 and attach helium line to valve V-7.

d. Slowly open valve V-7 on manifold line and pressurize both gas side and liquid side simultaneously with helium to a pressure of 185 psig. Allow several minutes to build up pressure.

e. Close valve V-7 on manifold line. Leave valves V-1 and V-4 open.

f. Check for leaks with helium sniffer; no leakage is allowed.

g. Remove helium line and slowly bleed off pressure through valve V-7 on manifold line.

21. Close valve V-7 and attach low pressure nitrogen line to it (0.7 psig max.)

22. Attach vacuum line to valve V-8. (Valves V-1 and V-4 must be open).

23. Slowly open valve V-8 and pull vacuum of 28 to 29 inches Hg or better.

24. Hold vacuum for 10 minutes then close valve V-8.

25. Slowly open valve V-7 and break vacuum with clean, dry nitrogen. Pressurize to 0.5 psig.

26. Close valve V-7 and repeat Steps 23, 24, and 25.

27. Close valves V-1 and V-4 and remove manifold line. (Apparatus will contain slight nitrogen pressure and all valves will be closed prior to loading for test).

D. LOADING APPARATUS WITH TEST LIQUID

1. Soak apparatus and test liquid at a minimum of 5°F below the boiling point of the liquid for at least 1 hour, and maintain temperature during Steps 2 through 6. (Use thermocouple on chamber for temperature indication.)

2. Attach test liquid reservoir to chamber valve V-1. (Reservoir can be attached to chamber prior to temperature soak, and entire system cooled together.)

3. Open reservoir vent valve V-6 and chamber vent valve V-2.

4. Open fill valves, V-1 and V-5 and allow test liquid to flow by gravity into chamber. Loading should be conducted in hood or well ventilated area. (Keep purge valves V-3 and V-4 on gas side closed).

5. When a steady stream of liquid flows from the chamber vent valve, V-2 (collect in suitable container), close V-2, and immediately close chamber fill valve V-1. (See Paragraph G,Safety Notes.)

6. Close valves V-5 and V-6 on reservoir and remove reservoir. Cap AN fittings.

CAUTION

Some liquid may remain between valves V-5 and V-1; protect hands and body. (See Paragraph G, Safety Notes).

7. Attach nitrogen line to purge valve V-3.

8. Add clean, dry nitrogen slowly through purge valve V-3 to a pressure of 185 psig at 70°F, except when loading with MON and N_2O_4, in which case pressurize initially to 125 to 150 psig. (Pressure will increase as temperature rises to test temperature.) When temperature reaches 70°F complete pressurization to 185 psig.

9. Close valve V-3, remove nitrogen line, cap AN fitting, record pressure, and store unit at 70°F for 24 hours.

E. UNLOADING APPARATUS

1. At the conclusion of the test, apparatus may require cooling for unloading; it must be at least 5°F below the boiling point of the liquid prior to unloading.

2. Slowly bleed off gas pressure through purge valve V-3. Do this in hood or well-ventilated area. (See Paragraph G, Safety Notes.)

3. Immediately after gas flow has stopped, open fill and vent valves V-1 and V-2 on liquid side and pour test liquid into suitable container. (See Paragraph G, Safety Notes.)

4. Open all valves: V-1, V-2, V-3, and V-4.

5. Open valve V-7 on manifold line and attach manifold line between valves V-1 and V-4.

6. Attach low-pressure nitrogen line to valve V-7.

7. Purge gas and liquid sides simultaneously with regulated low-pressure (0.7 psig max.) nitrogen for a minimum of 30 minutes. Carefully rotate and tumble while purging to dislodge any trapped liquid. Hot (150° to 180°F) dry nitrogen will accelerate purge process.

8. Remove bottom cover for inspection of specimen and in preparation for next test.

F. VOLUME CALIBRATION OF APPARATUS

The permeant is present on the gas side of the apparatus in the gaseous state. To calculate partial pressures to determine the weight of test liquid that permeated to the gas side, it will be necessary to know the volume of the gas side. Also, knowing the volume of the liquid side, the volume of test liquid loaded into the apparatus will be an indication as to whether the liquid side is completely filled with test liquid.

1. Assemble the apparatus in accordance with Paragraph C, Steps 1 through 6.

2. Install a piece of teflon (10 to 20-mil thick) or rubber (40 to 60-mil thick) in accordance with Paragraph C, Steps 7, 8, and 9. Do not use a specimen to be used for test.

3. Install thermocouple and valves V-1 and V-2 in accordance with Paragraph C, Step 11.

4. The neutral position (unloaded position) of the specimen mounting flange is approximately 1/8 inch below the body flange, when in an upright position. Therefore, install 3 or 4 spacers (0.120 to 0.125-inch thick) around the specimen mounting flange between it and the lower surface of the body flange. Clamp specimen mounting flange to body flange.

5. Fill liquid side completely with water at a measured temperature (e.g., 70°F). Allow water to flow into valve V-1 and out valve V-2 for several minutes to remove any bubbles inside bellows assembly.

6. Remove water line.

7. Carefully pour out water into calibrated container, measure and record volume.

8. Remove clamps and spacers from specimen mounting flange and body flange.

9. Remove diaphragm and replace specimen mounting ring and screws (with end of bellows open).

10. Install bottom cover valves, manifold line, etc. in accordance with Paragraph C, Steps 13 through 17.

11. Close valve V-2. Attach water line to valve V-7 on manifold line. Invert apparatus, and then open valves V-1, V-3, and V-4.

12. Open valve V-7 and fill complete apparatus with water at a known temperature. Allow water to flow out of valve V-4 and uncapped AN fittings on bottom cover for several minutes to remove any air bubbles inside apparatus.

13. When apparatus is filled, shut off water supply and pour out water into calibrated container. Measure and record volume.

14. The difference between the total volume recorded in Step 13 of this paragraph and the liquid-side volume recorded in Step 7 will be the volume of the gas side up to the AN fittings at the infrared gas cell. (The volume of the infrared gas cell will be determined by personnel of the Spectrographic Laboratory or in accordance with their instructions.)

15. Disassemble apparatus, flush parts in methyl alcohol (to remove water), and blow dry with clean nitrogen. Prepare for test in accordance with Paragraph C, Assembly of Apparatus.

G. SAFETY NOTES

1. All propellants listed in Paragraph B are potentially dangerous. Except for hydrogen peroxide, the vapors of these propellants are toxic. The oxidizers will cause severe burns to the skin. The fuels - UDMH, hydrazine, and 50/50 blend - can cause irritation of the skin particularly in tender areas such as eyes, face, and inside of arm.

2. Before handling any test liquid in subject apparatus, consult detailed safety manuals and procedures for the specific liquid.

3. Because of the toxic nature of the propellants listed in Paragraph B, all operations involving these propellants must be conducted in a well-designed laboratory-type fume hood, or in a well-ventilated area.

4. In Step 5 of Paragraph D, and in Step 3 of Paragraph E, the test liquid is to be collected in a suitable container. The suitable container can generally be a beaker, flask, or bottle sitting in the fume hood. In the case of MON, the beaker or flask should be set in an ice bath to keep fumes at a controllable level. Do not flush MON with water but allow it to evaporate.

5. When gas pressure is bled off the apparatus, the port should be directed into the hood and away from the operator.

6. The liquid remaining between valves, V-5 and V-6 (Step 6 of Paragraph D), will amount to 3 to 5 cc; nevertheless, wear protective gloves and hold container under line when AN fittings are opened.

APPENDIX V

GLOSSARY

APPENDIX V

GLOSSARY

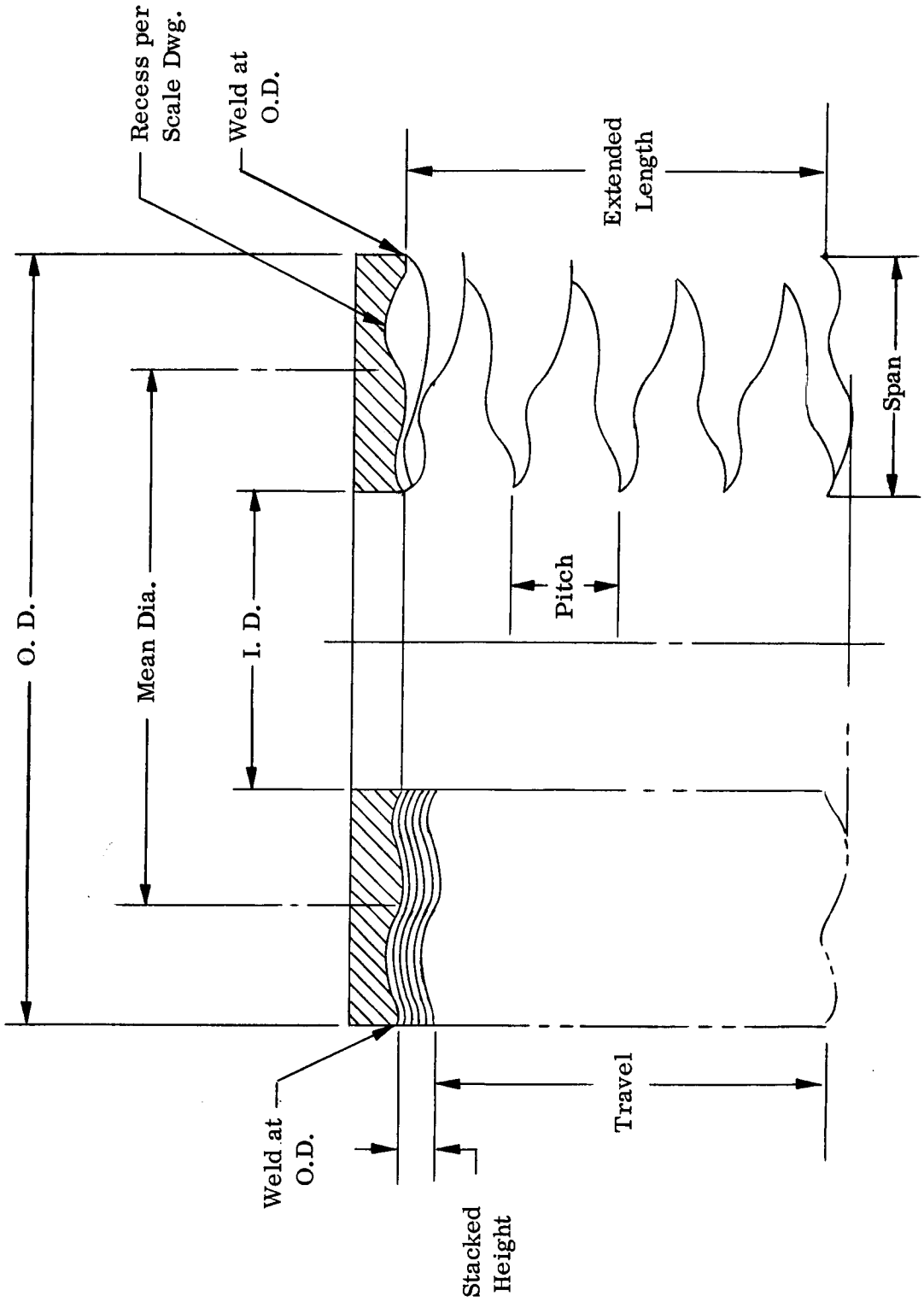

Welded Bellows

ACCORDION MODE: A longitudinal vibration mode characterized by convolution motion parallel to the longitudinal axis of the bellows with little or no bellows head motion.

AREA, EFFECTIVE: That surface on which pressure acts to produce motion of the bellows.

$$\frac{(O.D. + I.D.)^2}{4}$$

BUCKLING: Failure caused by exceeding the critical hoop compression of the bellows.

CONTOURS, BASIC:

Single Sweep 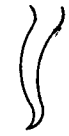

Flat Plate

Torodial (Omega)

Nesting Ripple

CONVOLUTION: Two diaphragms welded together at the I.D.

CORRUGATION: (See Ripple)

DEFLECTION: (See Travel)

DIAMETER, MEAN:	The diameter measured at the midpoint on the span. $\frac{O.D. + I.D.}{2}$	
DIAMETER, OUTSIDE:	(O.D.):	Outside diameter of bellows assembly.
DIAMETER, INSIDE:	(I.D.):	Inside diameter of bellows assembly.
DYNAMIC PRESSURE:		The pressure variation about the absolute static pressure usually associated with the liquid displacement mode.
EFFICIENCY, EXPULSION:		Ratio of loadable volume of propellant to usable volume.
EFFICIENCY, VOLUMETRIC:		Ratio of usable volume to total envelope volume.
ELASTIC STRAIN REGION:		The region over which the bellows can be extended without sustaining a permanent deformation in the convolutions, i.e., region were stress is proportional to strain.
FLEXIBILITY:		Deflection per psi.
FLIP:		Reversal of diaphragm corrugation due to local instability.
GEOMETRIC NONLINEARITY:		The condition in which bellows leaves (diaphragms) are in the elastic strain region during loading and unloading, with the load-deflection relationship following a curved rather than a straight-line path. The geometric nonlinearity region is characterized on the hysteresis loop as being a curved, reversible path.
HEIGHT, STACKED:		Distance from the center of the weld bead on the first convolution (or attachment point) to the center of the weld bead on the last convolution when bellows assembly is nested.
HYSTERESIS:		Area between extension and compression curves of spring rate.

LATERAL MODE:	A vibration mode characterized by a sideward or lateral motion of the bellows. At fundamental or lowest lateral mode the center convolution moves in a direction which is at all times perpendicular to the longitudinal axis of the bellows and the other convolutions are rocking about the longitudinal axis.
LEAF:	(See Diaphragm)
LENGTH, EXTENDED:	Length of bellows measured from center of attachment weld to center of the weld bead on last convolution at full extension.
LENGTH, FREE:	The equilibrium point of the bellows assembly. The length the bellows assumes when not acted upon by an external force.
LENGTH, NESTED:	(See Height, Stacked)
LIFE, CYCLE:	The number of complete expulsion cycles before failure.
LINEAR ELASTIC:	The condition characterized by very small leaf (diaphragm) deflection where the stresses are very small and caused largely by bending action. The diaphragms are obviously in the elastic strain region with the load-deflection relationship following a straight-line path during loading and unloading. The linear elastic region is characterized on the hysteresis loop as being a straight, reversible path.
LINEARITY:	Constant rate of stroke with pressure.
LIQUID DISPLACEMENT:MODE:	A longitudinal vibration mode characterized by both lateral and longitudinal convolution tip motion, along with considerable bellows head motion.

PHYSICAL NONLINEARITY:	The condition resulting when the bellows material is stressed beyond its elastic limit, i.e. into the inelastic or plastic strain regions. The diaphragms are no longer in the elastic strain region and the load-deflection relationships, although following a curved path on the hysteresis loop, differ during loading and unloading, The more the loading is increased beyond the elastic limit the greater the area of the hysteresis loop. The region is characterized on the hysteresis loop as being a curved, irreversible path.
PITCH:	Distance from the center of the weld bead on one convolution to the center of the weld bead on the adjacent convolution. (stroke per convolution).
PITCH, DESIGN:	The maximum pitch at which the bellows assembly will operate reliably for the design cycle life.
PITCH, NESTED:	Distance between the centers of adjacent weld beads in nested (stacked) position.
PLASTIC STRAIN REGION:	The region beyond the elastic strain region in which the bellows sustains appreciable permanent deformation without rupture, i.e., region beyond the yield point.
PLY:	Number of diaphragm thicknesses.
POINT, PIVOT:	(See Free Length)
PRESSURE, DIFFERENTIAL (P):	Pressure differential across bellows.
RIPPLE:	Contour of diaphragm (corrugation). (See Contours, Basic)
RIPPLE, NEUTER:	Diaphragms are fabricated using the same die for better nesting characteristics. This required that free length be set after assembly, normally at one-half of design pitch.

RIPPLE, MIRROR IMAGE: Diaphragms are fabricated from mating dies with preset free length.

SPAN: Width of convolution measured from O.D. to I.D.

$$\frac{O.D. - I.D.}{2}$$

SPRING RATE: The ratio of force to stroke expressed in lb per inch.

STROKE: (See Travel).

TRAVEL: Length of bellows at extension measured from the center of weld bead of end convolution at stacked height to the center of the same weld bead when fully extended to design pitch.

$$(P_d - P_s) \cdot Nc$$

VOLUME: The volume contained within the bellows assembly at design pitch.

$$Vol = \frac{\pi}{4} \cdot D_m^2 (P_s - P_d) \cdot Nc$$

D_m = Mean diameter

P_s = Pitch at stacked height

P_d = Design pitch

Nc = Number of convolutions

DISTRIBUTION LIST FOR BELL AEROSYSTEMS COMPANY
REPORT NO. 8230-933004 - FINAL REPORT ON CONTRACT NAS7-149
STUDY OF ZERO-GRAVITY POSITIVE EXPULSION TECHNIQUES

Copies	Recipient
	NASA Western Operations Office 150 Pico Boulevard Santa Monica, California
1	Office of Technical Information
1	Contracting Officer
1	Patent Office
	NASA Headquarters Washington 25, D. C.
4	Mr. Henry Burlage, Jr. Chief, Liquid Propulsion Systems, RPL
1	Mr. A.O. Tischler Assistant Director for Propulsion, MLP
1	Mr. Richard N. Porter Liquid Propulsion Section Propulsion Division Jet Propulsion Laboratory 4800 Oak Grove Drive Pasadena, California
2	Ames Research Center Moffett Field, California Attn: Technical Librarian
2	Goddard Space Flight Center Greenbelt, Maryland
2	Jet Propulsion Laboratory California Institute of Technology 4800 Oak Grove Drive Pasadena, California
2	Langley Research Center Langley Field, Virginia
2	Lewis Research Center 21000 Brookpark Road Cleveland 35, Ohio
2	Marshall Space Flight Center Huntsville, Alabama
2	Manned Spacecraft Center Houston, Texas
1	Advanced Research Projects Agency Pentagon, Room 3D154 Washington 25, D. C.

Copies	Recipient
1	Aeronautical Systems Division Air Force Systems Command Wright-Patterson Air Force Base, Ohio
1	Air Force Missile Development Center Holloman Air Force Base, New Mexico
1	Air Force Missile Test Center Patrick Air Force Base, Florida
1	Air Force Systems Command, Dyna-Soar Air Force Unit Post Office Los Angeles 45, California
1	Army Ordnance Missile Command Redstone Arsenal, Alabama
1	Armed Services Technical Information Agency Arlington Hall Station Arlington 12, Virginia
1	Arnold Engineering Development Center A.E.O.R. Tullahoma, Tennessee
1	Bureau of Naval Weapons Department of the Navy Washington 25, D.C.
1	Central Intelligence Agency 2430 E Street, N. W. Washington 25, D.C.
1	Headquarters, United States Air Force Washington 25, D. C.
1	Office of Naval Research Washington 25, D. C.
1	Picatinny Arsenal Dover, New Jersey
1	Rocket Research Laboratories Edwards Air Force Base, California
1	U.S. Naval Ordnance Test Station China Lake, California
1	U. S. Atomic Energy Commission Technical Information Services Box 62 Oak Ridge, Tennessee

Copies	Recipient
1	Chemical Propellant Information Agency Johns Hopkins University Applied Physics Laboratory 8621 Georgia Avenue Silver Spring, Maryland
1	Aerojet-General Corporation P. O. Box 296 Azusa, California
1	Aerojet-General Corporation P. O. Box 1947 Sacramento 9, California
1	Aeronutronic A Division of Ford Motor Company Ford Road Newport Beach, California
1	Aerospace Corporation 2400 East El Segundo Boulevard El Segundo, California
1	Arthur D. Little, Inc. Acorn Park Cambridge 40, Massachusetts
1	Astropower, Inc., Subsidiary of Douglas Aircraft Company, Inc. 2968 Randolph Avenue Costa Mesa, California
1	Astrosystems, Inc. 82 Naylon Avenue Livingston, New Jersey
1	Atlantic Research Corporation Edsall Road and Shirley Highway Alexandria, Virginia
1	Beech Aircraft Corporation Boulder Facility Box 631 Boulder, Colorado
1	Bell Aerosystems Company P. O. Box 1 Buffalo 5, New York Attn: Technical Librarian
1	Bendix Systems Division Bendix Corporation Ann Arbor, Michigan
1	Boeing Company P. O. Box 3707 Seattle 24, Washington

Copies	Recipient
1	Convair (Astronautics) Division of General Dynamics Corporation P. O. Box 2672 San Diego 12, California
1	Curtiss-Wright Corporation Wright Aeronautical Division Wood-ridge, New Jersey
1	Douglas Aircraft Company, Inc. Missile and Space Systems Division 3000 Ocean Park Boulevard Santa Monica, California
1	Fairchild Stratos Corporation Aircraft Missiles Division Hagerstown, Maryland
1	General Electric Company Missile and Space Vehicle Department Box 8555 Philadelphia, Pennsylvania
1	General Electric Company Rocket Propulsion Units Building 300 Cincinnati 15, Ohio
1	Grumman Aircraft Engineering Corporation Bethpage, Long Island, New York
1	Kidde Aero-Space Division Walter Kidde and Company, Inc. 675 Main Street Belleville 9, New Jersey
1	Lockheed Aircraft Corporation Missile and Space Division Sunnyvale, California
1	Lockheed Propulsion Company P. O. Box 111 Redlands, California
1	Marquardt Corporation 16555 Saticoy Street Box 2013 - South Annex Van Nuys, California
1	Martin Division Martin Marietta Corporation Baltimore 3, Maryland
1	Martin Denver Division Martin Marietta Corporation Denver, Colorado

Copies	Recipient
1	McDonnell Aircraft Corporation P. O. Box 6101 Lambert Field, Missouri
1	North American Aviation, Inc. Space & Information Systems Division Downey, California
1	Northrop Corporation 1001 East Broadway Hawthorne, California
1	Pratt & Whitney Aircraft Corporation Florida Research & Development Center West Palm Beach, Florida
1	Radio Corporation of America Astro-Electronics Division Defense Electronic Products Princeton, New Jersey
1	Reaction Motors Division Thiokol Chemical Corporation Denville, New Jersey
1	Republic Aviation Corporation Farmingdale Long Island, New York
1	Rocketdyne (Library Dept. 586-306) Division of North American Aviation, Inc. 6633 Canoga Avenue Canoga Park, California
1	Space General Corporation 9200 Flair Avenue El Monte, California

Copies	Recipient
1	Stanford Research Institute 333 Ravenswood Avenue Menlo Park, California
1	TAPCO Division Thompson-Ramo-Wooldridge, Inc. 23555 Euclid Avenue Cleveland 17, Ohio
1	Thiokol Chemical Corporation Redstone Division Huntsville, Alabama
1	Space Technology Laboratories P. O. Box 95001 Airport Station Los Angeles 45, California
1	United Aircraft Corporation East Hartford Plant 400 Main Street Hartford, Connecticut
1	United Technology Corporation 587 Methilda Avenue Sunnyvale, California
1	Vought Astronautics Box 5907 Dallas 22, Texas
1	Stillman Rubber Co. P. O. Box 1097 Culver City, California
1	Hycon Mfg. Co. 700 Royal Oaks Drive Monrovia, California